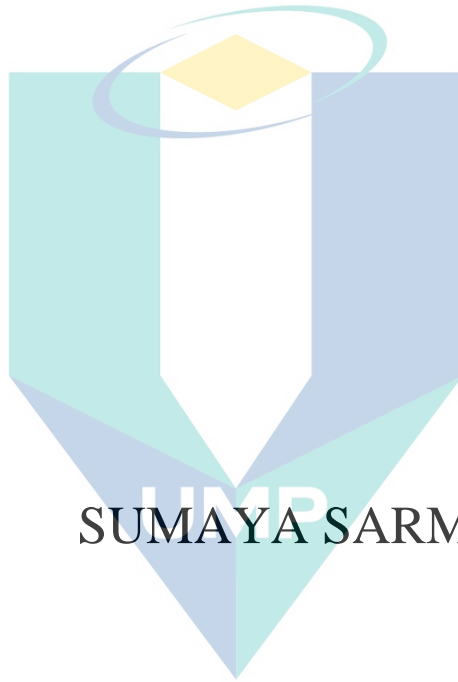


BIO-ELECTROCHEMICAL POWER
GENERATION FROM PETROCHEMICAL
WASTEWATER USING AS SUBSTRATES IN
MICROBIAL FUEL CELL



SUMAYA SARMIN

اونيورسيتي مليسيا قهغ

UNIVERSITI MALAYSIA PAHANG

MASTER OF SCIENCE

UNIVERSITI MALAYSIA PAHANG

UNIVERSITI MALAYSIA PAHANG

DECLARATION OF THESIS AND COPYRIGHT

Author's Full Name : SUMAYA SARMIN

Date of Birth : 3 JANUARY 1990

Title : BIO-ELECTROCHEMICAL POWER GENERATION FROM
PETROCHEMICAL WASTEWATER USING AS
SUBSTRATES INS MICROBIAL FUEL CELL

Academic Session : SEM 2 2019/2020

I declare that this thesis is classified as:

- CONFIDENTIAL (Contains confidential information under the Official Secret Act 1997)*
- RESTRICTED (Contains restricted information as specified by the organization where research was done)*
- OPEN ACCESS I agree that my thesis to be published as online open access (Full Text)

I acknowledge that Universiti Malaysia Pahang reserves the following rights:

1. The Thesis is the Property of Universiti Malaysia Pahang
2. The Library of Universiti Malaysia Pahang has the right to make copies of the thesis for the purpose of research only.
3. The Library has the right to make copies of the thesis for academic exchange.

Certified by:

(Student's Signature)

BP0714519

New IC/Passport Number

Date:

(Supervisor's Signature)

Dr. Md. Maksudur Rahman Khan

Name of Supervisor

Date:

NOTE : * If the thesis is CONFIDENTIAL or RESTRICTED, please attach a thesis declaration letter.

SUPERVISOR'S DECLARATION

We hereby declare that we have checked this thesis and in our opinion, this thesis is adequate in terms of scope and quality for the award of the degree of Master of Science.

(Supervisor's Signature)

Full Name : DR. MD. MAKSUDUR RAHMAN KHAN

Position : PROFESSOR

Date :



(Co-supervisor's Signature)

Full Name : DR. ASMIDA BINTI IDERIS

Position : SENIOR LECTURER

Date :

STUDENT'S DECLARATION

I hereby declare that the work in this thesis is based on my original work except for quotations and citations which have been duly acknowledged. I also declare that it has not been previously or concurrently submitted for any other degree at Universiti Malaysia Pahang or any other institutions.

(Student's Signature)

Full Name : SUMAYA SARMIN

ID Number : MKC18005

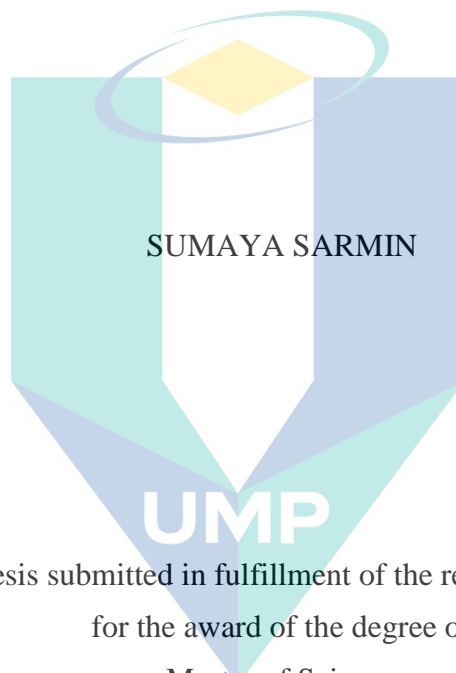
Date :

UMP

اونيورسيتي ملايسيا قهغ

UNIVERSITI MALAYSIA PAHANG

BIO-ELECTROCHEMICAL POWER GENERATION FROM PETROCHEMICAL
WASTEWATER USING AS SUBSTRATES IN MICROBIAL FUEL CELL



Thesis submitted in fulfillment of the requirements
for the award of the degree of
Master of Science

اونيورسيتي ملايسيا قهغ

UNIVERSITI MALAYSIA PAHANG
College of Engineering
UNIVERSITI MALAYSIA PAHANG

AUGUST 2020

ACKNOWLEDGEMENTS

The research presented in this thesis has been carried out at the Faculty of Chemical and Process Engineering Technology, Universiti Malaysia Pahang, Malaysia. The journey of my research would not be possible without the help and support of a number of persons.

At first, I am grateful to my Almighty to give me a chance to finish my degree. Then, I wish to my humble gratefulness and sincere thanks to my honourable supervisor, Professor Dr Md. Maksudur Rahman Khan for his valuable support and guidance throughout the study. Indeed, it was the utmost opportunity for me to get him as my main supervisor. He has always been able to keep on amazing me with his introspective thinking, ideas, and insights. I would also like to give special thanks to my co-supervisor, Dr Amida Binti Ideris and also thankful to Dr Chin Sim Yee for their inspiration and support.

I am highly grateful to the Universiti Malaysia Pahang (UMP), Malaysia, for funding this work under the grant number of RDU 180355. Apart from that, I would like to acknowledge the authority Panching Palm Oil Mill (FELDA), Kuantan, Pahang, Malaysia for their continuous support by giving me anaerobic sludge.

I would like to express my sincere gratitude to Dr Baranitharan Ethiraj for his unconditional support in write-up my thesis as well as research papers. A special thanks also go to Dr Amirul Islam for helping and giving suggestions during experiments and writing paper and thesis. A million thanks should go to Mostafa Tarek and Kaykobad Rezaul Karim for their kind helps and suggestions to conduct my experiments and to write-up my thesis. Special thanks must be given to Fatema Khatun, Mr Ahasanul Karim and Mr Woon Chee Wai for sharing their resources in the lab.

Lastly, I also want to thank my parents, brother, sister, brother-in-law, sister-in-law and my friend for their continuous supports, encouragements and inspiration. It would be really tough to finish my studies without their supports and devotions.

اونيورسيتي ملايسيا فاهغ

UNIVERSITI MALAYSIA PAHANG

ABSTRAK

Air sisa petrokimia (PCW) dari kilang asid akrilik mempunyai permintaan oksigen kimia (COD) yang sangat tinggi kerana adanya asid akrilik (AA) bersama dengan asid organik lain. Rawatan PCW dengan kaedah aerobik dan anaerob konvensional memerlukan tenaga. Namun, perlakuan PCW dengan penjana tenaga serentak dengan menggunakan sel bahan bakar mikroba (MFC) dapat menjadi alternatif yang berpotensi untuk menyelesaikan masalah tenaga dan alam sekitar. Rintangan utama untuk rawatan PCW di MFC adalah mencari inokulum yang sesuai berdasarkan interaksi substrat-inokulum, untuk menguraikan mekanisme pemindahan elektron yang membawa kepada penjana kuasa tinggi serta kecekapan penyingkiran COD yang tinggi. Tujuan kerja ini adalah untuk mengetahui inokulum yang sesuai yang mempunyai sifat elektrogenik dan fermentasi, untuk menjelaskan mekanisme pemindahan elektron dan akhirnya untuk menyiasat kinetik pemindahan caj anod. MFC dikendalikan menggunakan PCW dari loji AA tempatan dan enapcemar anaerob (AS) sebagai biokatalis di mana AS disesuaikan untuk menyiapkan inokulum yang berkesan. Mikrob yang didominasi dikenal pasti yang merangkumi genera elektrogenik iaitu *Pseudomonas aeruginosa* (PA) dan *Bacillus cereus* (BC) bersama dengan metanogenik archea *Methanobacterium* spp. Komponen utama PCW, seperti asid akrilik, asid asetik (ACA) dan dimetil phthalate (DMP) digunakan sebagai makanan bagi MFC untuk menilai interaksi substrat-inokulum. Prestasi MFC dinilai dari segi penjana voltan / arus serta penjana kuasa maksimum menggunakan polarisasi dan kurva kuasa. Vertammetri siklik (CV) dan spektroskopi impedans elektrokimia (EIS) digunakan untuk menjelaskan kinetik pemindahan caj anod dan model Nernst-Monod-Butler-Volmer digunakan untuk mengesahkan dan meramalkan prestasi MFC. Hasil kajian menunjukkan bahawa substrat campuran dengan AS yang disesuaikan dapat menghasilkan daya tinggi (0.78 W/m^3) dibandingkan dengan AA dengan PA (0.24 W/m^3), AA dengan BC (0.22 W/m^3), ACA dengan PA (0.39 W/m^3), ACA dengan BC (0.32 W/m^3), DMP dengan PA (0.24 W/m^3) dan DMP dengan BC (0.21 W/m^3) masing-masing. Data penjana tenaga berkorelasi dengan pola pertumbuhan mikroba yang menunjukkan pembentukan sinergi berdasarkan substrat-inokulum dalam sistem AS yang disesuaikan dengan substrat. Kajian ini selanjutnya diperluas ke PCW sebenar yang menunjukkan bahawa PCW dengan COD awal $45,000 \text{ mg/L}$ dapat menghasilkan ketumpatan daya 850 mW/m^2 (pada kepadatan arus 1500 mA/m^2) menggunakan AS yang diaklimatisasi sebagai biokatalis. Kecekapan penghapusan COD dan kecekapan coulombic (CE) didapati 40% dan 21%, masing-masing setelah 11 hari beroperasi menggunakan COD awal 45000 mg/L . Penyiasatan CV mengesahkan peranan pyocynin dan hydroquinone sebagai ulang-alik elektron. Semasa membandingkan data CV biofilm dan anolit bebas inokulum setelah 11 hari beroperasi, arus puncak redoks tinggi diperhatikan untuk kes terakhir yang menunjukkan dengan jelas peranan utama mekanisme pemindahan caj tidak langsung untuk penjana kuasa menggunakan PCW dan AS yang disesuaikan. Kinetik pemindahan caj dijelaskan dengan menggunakan Tafel slop. Parameter kinetik dinilai dengan pas data kinetik dalam model Nernst-Monod-Butler-Volmar di mana COD eksperimen dan pengeluaran ketumpatan semasa didapati sesuai dengan model yang dicadangkan. Model tersebut dapat digunakan untuk mengoptimumkan prestasi MFC yang diberi makan PCW.

ABSTRACT

The petrochemical wastewater (PCW) from the acrylic acid plant possesses a very high chemical oxygen demand (COD) due to the presence of acrylic acid (AA) along with other organic acids. The treatment of PCW by conventional aerobic and anaerobic methods is energy-intensive. However, the treatment of PCW with concurrent power generation by employing microbial fuel cell (MFC) could be a potential alternative to solve the energy and environmental issues. The main hurdle for the treatment of PCW in MFC is to find out the suitable inoculum based on the substrate-inoculum interaction, to unravel the mechanism of electron transfer leading to the high power generation as well as high COD removal efficiency. The goal of the present work is to find out the suitable inoculum possessing electrogenic and fermentative properties, to elucidate the electron transfer mechanism and finally to investigate the anode charge transfer kinetics. MFCs were operated using PCW from local AA plant and anaerobic sludge (AS) as biocatalyst where AS was acclimatized to prepare effective inoculum. The predominated microbes were identified which include the electrogenic genera namely *Pseudomonas aeruginosa* (PA) and *Bacillus cereus* (BC) along with methanogenic archaea *Methanobacterium spp.* The major constituents of the PCW, such as acrylic acid, acetic acid (ACA) and dimethyl phthalate (DMP) were used as feed for MFC to evaluate the substrate-inoculum interaction. The performance of the MFC was evaluated in terms of voltage/current generation as well as maximum power generation using polarization and power curve. Cyclic voltammetry (CV) and electrochemical impedance spectroscopy (EIS) were employed to elucidate the kinetics of anode charge transfer and Nernst-Monod-Butler-Volmer model was used to validate and predict the performance of MFC. The results revealed that the mixed substrates with acclimatized AS could produce high power (0.78 W/m^3) compared to AA with PA (0.24 W/m^3), AA with BC (0.22 W/m^3), ACA with PA (0.39 W/m^3), ACA with BC (0.32 W/m^3), DMP with PA (0.24 W/m^3) and DMP with BC (0.21 W/m^3) respectively. The power generation data was correlated with the microbial growth pattern which indicated the formation of substrates-inoculum based synergy in the mixed substrate-acclimatized AS system. The study was further extended to the real PCW which demonstrated that the PCW with an initial COD of 45,000 mg/L could generate power density of 850 mW/m^2 (at a current density of 1500 mA/m^2) using acclimatized AS as biocatalyst. The COD removal efficiency and the coulombic efficiency (CE) were found to be 40% and 21%, respectively after 11 days of operation using initial COD of 45000 mg/L. CV investigations confirmed the role of pyocynin and hydroquinone as electron shuttles. While comparing the CV data of the biofilm and the inoculum free anolyte after 11 days of operation, the high redox peak current was observed for the latter case which clearly demonstrated the predominant role of indirect charge transfer mechanism for power generation using PCW and acclimatized AS. The charge transfer kinetics was elucidated using the Tafel slope. The kinetic parameters were evaluated by fitting the kinetic data in Nernst-Monod-Butler-Volmer model where the experimental COD and current density production was found to be in good agreement with the proposed model. The model can be used for optimization of the performance of the PCW-fed MFC. The results of the present study showed that the electrocatalytic activity of anaerobic sludge can be improved by acclimatization which can be effectively used for simultaneous power generation and treatment of PCW.

TABLE OF CONTENT

DECLARATION

TITLE PAGE

ACKNOWLEDGEMENTS **ii**

ABSTRAK **iii**

ABSTRACT **iv**

TABLE OF CONTENT **v**

LIST OF TABLES **x**

LIST OF FIGURES **xi**

LIST OF SYMBOLS **xiv**

LIST OF ABBREVIATIONS **xv**

CHAPTER 1 INTRODUCTION **1**

1.1 Research background 1

1.2 Problem statement 3

1.3 Objectives of the study 5

1.4 Scopes of the study 5

1.5 Significance of the study 6

1.6 Organization of this Thesis 7

1.6.1 Chapter 1 7

1.6.2 Chapter 2 7

1.6.3 Chapter 3 7

1.6.4 Chapter 4 7

1.6.5 Chapter 5 8

CHAPTER 2 LITERATURE REVIEW	9
2.1 Chapter overview	9
2.2 Renewable energy	9
2.3 Petrochemical wastewater (PCW)	10
2.4 Wastewater treatment methods	12
2.4.1 Physical treatment	12
2.4.2 Chemical treatment	13
2.4.3 Biological treatment	18
2.5 Biological treatment of petrochemical wastewater (PCW)	21
2.6 Microbial fuel cell (MFC)	23
2.6.1 The working principle of Microbial fuel cell	23
2.7 Different types of MFC	25
2.7.1 Two-compartments MFC system	25
2.7.2 Single-compartments MFC system	26
2.7.3 Sediment MFC system	27
2.7.4 Upflow MFC system	28
2.8 Advantages and disadvantages of MFC	29
2.9 Effects of operating conditions in MFC	30
2.9.1 Effect of Inoculum	30
2.9.2 Effect of Substrates	32
2.9.3 Effects of pH	37
2.9.4 Effects of operating temperature	38
2.9.5 Effects of external resistance	38
2.10 Factors limiting the energy generation in microbial fuel cell	38
2.10.1 Ohmic losses	40
2.10.2 Activation losses	40

2.10.3	Mass transfer losses	41
2.11	Electron transfer and biofilm formation in MFC	41
2.11.1	Direct electron transfer (DET)	42
2.11.2	Mediated electron transfer	44
2.11.3	Primary and secondary metabolism	45
2.11.4	Biofilm formation mechanism	49
2.11.5	Electrochemical methods	53
2.12	Kinetic study	57
2.12.1	Kinetic model	60
2.13	Summary	65
CHAPTER 3 METHODOLOGY		67
3.1	Introduction	67
3.2	Materials	68
3.2.1	List of chemicals	68
3.3	Inoculum screening and time-course biofilm analysis	68
3.3.1	Sampling of PCW	68
3.3.2	pH measurement	69
3.3.3	COD measurement	69
3.3.4	Sources and acclimatization of inoculums	70
3.3.5	Microbes analysis method by BIOLOG GEN III	70
3.4	MFC Fabrications and operations	71
3.4.1	Electrode preparation	73
3.4.2	Membrane treatment	74
3.4.3	Measurement and analysis	74
3.4.4	COD removal efficiency	74

3.4.5	Scanning electron microscope (SEM) analysis	75
3.4.6	Electrochemical impedance spectroscopy (EIS) analysis	75
3.4.7	Cyclic voltammetry (CV) analysis	76
3.4.8	Cell growth analysis (OD)	76
3.4.9	Liquid sample analysis by high liquid performance spectroscopy (HPLC)	77
3.4.10	Ultraviolet-Visible spectroscopy (UV-Vis)	77
CHAPTER 4 RESULTS AND DISCUSSION		78
4.1	Introduction	78
4.2	Treatment of synthetic wastewater by MFC	78
4.2.1	Effect of substrates	78
4.2.2	Effect of inoculum	81
4.2.3	Time course biofilm formation of synthetic wastewater using SEM	85
4.2.4	Electrochemical impedance spectroscopy of synthetic wastewater	89
4.3	Substrate analysis by HPLC	95
4.4	Treatment of industrial PCW by MFC	96
4.4.1	Effect of initial concentration	96
4.4.2	Polarization behaviour of the MFC	97
4.4.3	Time course biofilm formation of PCW using SEM	98
4.5	Electron transfer mechanism in MFC	100
4.5.1	Cyclic voltammetry	100
4.5.2	Role of both biofilm and metabolite and their effect on MFC performance	107
4.5.3	Electrochemical impedance spectroscopy	110
4.6	HPLC analysis PCW fed MFC	113

4.7	PCW treatment efficiency and comparison of the MFC performance with literature	115
4.8	Kinetic study	118
	4.8.1 The effect of initial COD	123
4.9	Summary	126
CHAPTER 5 CONCLUSION		127
5.1	Conclusion	127
5.2	RECOMMENDATION	128
REFERENCES		130
APPENDIX A COLONY FORMING UNIT AND SEM		165
APPENDIX B PHYLOGENETIC TREE		166
APPENDIX C EIS AND BODE PLOT		167
APPENDIX D HPLC OF DIFFERENT SUBSTRATTES		171
LIST OF PUBLICATIONS		175

اونیورسیتی ملیسیا قهغ

UNIVERSITI MALAYSIA PAHANG

LIST OF TABLES

Table 2.1	The lists of chemicals containing PCW	12
Table 2.2	Different types of petrochemical wastewater treatment using different reactors	22
Table 2.3	The performance of using different types of culture	31
Table 2.4	Different types of substrates used in MFC	33
Table 2.5	Different microbes el	43
Table 2.6	Selection of exogenous redox mediators used for microbial fuel cell	45
Table 2.7	Some common exo-electrogens with their electron transfer mechanism	47
Table 2.8	Selection of extracellular bacterial (endogenous) redox mediators	48
Table 3.1	Chemicals and materials	68
Table 3.2	Different MFCs operational day	72
Table 4.1	Oxidative and reductive peaks with oxidative and oxidative current using PA, BC and acclimatized AS with different substrates	88
Table 4.2	EIS fitting parameters using different substrates at day 11	91
Table 4.3	Redox peaks and current (A) data on different days using PCW	101
Table 4.4	EIS data fitting parameters for DC-MFC	111
Table 4.5	Comparison the performance of PCW with literature	117
Table 4.6	Kinetics parameters	122

اونيورسيتي ملايسيا قهغ

UNIVERSITI MALAYSIA PAHANG

LIST OF FIGURES

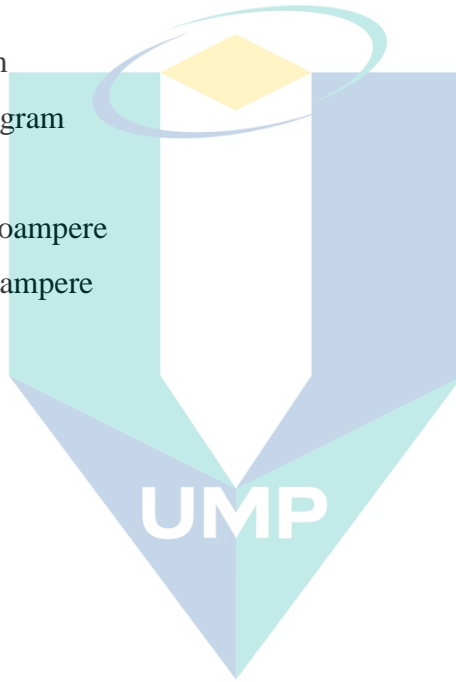
Figure 2.1	Environmental imbalance using fossil fuel	10
Figure 2.2	Petrochemical wastewater treatment plant	11
Figure 2.3	Physical treatment process	13
Figure 2.4	Chemical precipitation process	14
Figure 2.5	Chemical coagulation method	15
Figure 2.6	Chemical oxidation and advanced oxidation	16
Figure 2.7	Ion exchange process	17
Figure 2.8	Biological treatment process	18
Figure 2.9	Aerobic degradation pathway	19
Figure 2.10	Anaerobic degradation pathway .	21
Figure 2.11	Working principle of MFC	24
Figure 2.12	Two chamber MFC	26
Figure 2.13	Air cathode MFC	27
Figure 2.14	Sediment MFC	28
Figure 2.15	Upflow MFC	29
Figure 2.16	Substrates- microbes interaction in MFC for power generation	37
Figure 2.17	Different types of losses in MFC	41
Figure 2.18	Direct electron transfer	43
Figure 2.19	Mediated electron transfer process	44
Figure 2.20	Anaerobic respiration of MFC	48
Figure 2.21	Biofilm formation mechanism	49
Figure 2.22	Polarization curves of MFCs on different days of operation	51
Figure 2.23	Contribution of anode internal resistance of MFCs (R_s represents the solution resistance, R_{ct} represents the charge transfer resistance and R_d represents the diffusion resistance)	52
Figure 2.24	a) Turn-over and b) Non-turn over cyclic voltammetry	54
Figure 2.25	Different types of cyclic voltammetry	55
Figure 2.26	a) EIS plot, b) bode plot and c) phase angle with respect to frequency	56
Figure 2.27	Different types of operational parameters experimental and simulated using Butler-Volmer and Nernst-Monod model	59
Figure 2.28	Power density using Nernst-Monod Model	60
Figure 2.29	Conceptual schematic showing substrate (S) degradation by a primary bacterial cell (X_p) and electron transfer to the anode via reduced (M_{red}) and oxidized (M_{ox}) intracellular mediators.	61

Figure 3.1	Overview of research methodology	67
Figure 3.2	Dual chamber MFC	71
Figure 3.3	MFC glass setup for metabolite analysis	73
Figure 3.4	EIS measurement setup	76
Figure 4.1	Voltage vs time using a) AA (0.5-5 wt%), b) ACA (0.5-5 wt%), c) DMP (0.5-2 wt%) and d) 3 substrates (2:2:0.5 wt%)	79
Figure 4.2	a) Microbial growth and b) power density using AA (2 wt%), ACA (2 wt%), DMP (0.5 wt%) and AA : ACA : DMP (2 : 2 : 0.5 wt%) at day 11	80
Figure 4.3	Polarization and power density curve using a) AA (2 wt%), b) ACA (2 wt%), c) DMP (0.5 wt%), and d) 3 substrates (AA:ACA:DMP=2:2:0.5 wt%) with <i>Pseudomonas aeruginosa</i> (PA), <i>Bacillus cereus</i> (BC), and acclimatized AS at day 11.	82
Figure 4.4	Microbial growth data using a) AA, b) ACA, c) DMP and d) 3 substrates at day 11	83
Figure 4.5	SEM of PA and BC using same wt% a) AA (2 wt%) with PA, b) ACA (2 wt%) with PA, c) DMP (2 wt%) with PA, d) 3 substrates (AA:ACA:DMP = 2:2:0.5 wt%) with PA, e) AA with BC, f) ACA with BC, g) DMP with BC and h) 3 Substrates with BC at day 11	85
Figure 4.6	SEM using a) AA (2 wt%), b) ACA (2 wt%), c) DMP (2 wt%) and d) 3 Substrates (AA:ACA:DMP=2:2:0.5 wt%) with AAS at day 11	86
Figure 4.7	Cyclic voltammetry of a) AA (2 wt%), b) ACA (2 wt%), c) DMP (0.5 wt%) and d) 3 Substrates (AA:ACA:DMP=2:2:0.5 wt%) using PA, BC and acclimatized AS at day 11.	87
Figure 4.8	a) Nyquist plot of different substrates using PA , b) BC and c) Acclimatized AS at day 11	90
Figure 4.9	Bode plot of different substrates using different microbes, a) PA, b) BC and c) acclimatized AS.	93
Figure 4.10	Bode plot of different substrates using different microbes, a) PA, b) BC and c) acclimatized AS.	94
Figure 4.11	Relative concentration, COD vs time using a) Acrylic acid (AA), b) Acetic acid (ACA) and c) Dimethyl phthalate (DMP)	95
Figure 4.12	(a) The current vs. time curves at different initial COD, and (b) Effect of initial COD on microbial growth in MFCs (after 7 days of operation).	96
Figure 4.13	a) The polarization curve, and b) The power curves for MFC	98
Figure 4.14	SEM images on anode electrode at a) Control, b) Day 5, c) Day 8, d) Day 11 and e) Day 16 using PCW (45000 mg/L) with acclimatized AS.	98
Figure 4.15	a) CV at 0 to 48 h (20 mV/s) b) CV at day 5, day 8 and day 11 and day 16 (20 mV/s), c) CV at different scan rates on day 11 and d) Peak current vs. square root of the scan rate on day 11.	100

Figure 4.16	UV-vis of using a) Acclimatized AS, PA and BC with PCW (45000 mg/L), and b) UV-vis of pyocyanin and hydroquinone	103
Figure 4.17	Cyclic voltammetry of supernatant from a) Acclimatized AS, PA and BC fed MFC after 11 days (PCW 45000 mg/L); (b) Cyclic voltammetry of pyocyanin and hydroquinone (CV in glass cell)	104
Figure 4.18	EIS of a) Acclimatized AS, PA, BC with PCW (45000 mg/L) and b) EIS of pyocyanin and hydroquinone	105
Figure 4.19	Bode modulus phase angle vs. log f using a) and b) acclimatized AS, PA, and BC (PCW= 45000 mg/L), c) and d) pyocyanin and hydroquinone	106
Figure 4.20	a) CV of biofilm in microbe-free medium and b) CV of microbe-free supernatant with fresh anode after 16 days of operation at different scan rates.	107
Figure 4.21	a) Current vs. time data, b) Cyclic voltammetry at day 18 and day 24 (20 mV/s)	109
Figure 4.22	Schematic diagram of Electron transfer mechanism in PCW fed MFC	110
Figure 4.23	Nyquist of PCW 45000 mg/L and Acclimatized AS on different days of operation	111
Figure 4.24	a) $-Z'$ vs. log f, and b) phase angle vs. log f using PCW (45000 mg/L) after different days of operation	113
Figure 4.25	(a) Relative concentration vs. time of AA (2 wt%), ACA (2 wt%) and DMP (0.5 wt%) using PCW (45000 mg/L)	114
Figure 4.26	a) COD removal efficiency (%) and CE (%) with respect to time; b) Effect of initial COD on power generation and COD removal efficiency.	116
Figure 4.27	Anode and cathode polarization curve using PCW (45000 mg/L) on different days of operation	119
Figure 4.28	Tafel slope using PCW (45000 mg/L) on different days of operation	120
Figure 4.29	(a) Oxidative value vs time, and (b) Anodic potential and resistance vs time using PCW (45000 mg/L) on different days	121
Figure 4.30	a) Initial COD vs. time (experimental and simulated), b) COD removal rate vs. time, and c) Current density vs. time (experimental and simulated).	124

LIST OF SYMBOLS

P	Power
I	Current
T	Time
R_{ct}	Charge transfer resistance
R_{Ω}	Resistance
W	Watt
V	Volt
g	Gram
mg	Milligram
L	Litre
μA	Microampere
mA	Milliampere



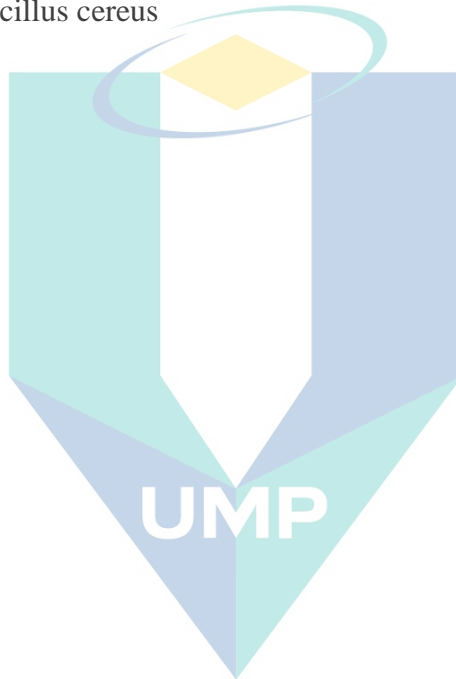
اونيورسيتي مليسيا قهغ

UNIVERSITI MALAYSIA PAHANG

LIST OF ABBREVIATIONS

PCW	Petrochemical wastewater
AA	Acrylic acid
AC	Acetic acid
DMP	Dimethyl phthalate
MFC	Microbial fuel cell
POME	Palm oil mill effluent
AS	Anaerobic sludge
PRW	Petroleum refinery wastewater
DW	Domestic wastewater
SM	Sugercane molasses
SPW	Starch processing wastewater
RS	Rice straw
PA	Pseudomonas aeruginosa
BC	Bacillus cereus
CV	Cyclic voltammetry
CEM	Cation exchange membrane
PEM	Proton exchange membrane
DET	Direct electron transfer
EET	Extracellular electron transfer
EPS	Extracellular polymeric substance
EIS	Electrochemical impedance spectroscopy
SEM	Scanning electron microscope
FTIR	Fourier Transform Infrared
mg/L	Milligram per litre
mV	Millivolt
V	Volt
mA	Milli ampere
mW	Milliwatt
COD	Chemical oxygen demand
CE	Coulombic efficiency
OD	Optical density

PEM	Proton exchange membrane
UV	Ultraviolet
OCV	Open circuit voltage
rpm	Revolutions per minute
PACF	Poly acrylonitrile carbon felt
k Ω	Kiloohm
PA	Pseudomonas aeruginosa
AAS	Acclimatized anaerobic sludge
BC	Bacillus cereus



اونيورسيتي ملايسيا قهغ

UNIVERSITI MALAYSIA PAHANG

CHAPTER 1

INTRODUCTION

1.1 Research background

The present world is confronting with three major inter-connecting issues: energy crisis, environmental pollution, and global warming (Sarmin et al., 2019). Among those, excessive wastewater generation and energy depletion are the most critical issues since those cannot be controlled due to rapid industrialization and population growth (Yin et al., 2020). In past decades, intensive research efforts have been dedicated to find out the alternative renewable energy sources particularly energy generation through the sustainable treatment of wastewater (Islam, Karim, et al., 2019). In that context, renewable energy sources are considered as sustainable as well as carbon neutral substitutes to fossil fuels which are highly needed to relieve the global environmental deterioration and energy crisis (Nassani, Aldakhil, Abro, Zaman, & Kabbani, 2019). According to the European Renewable Energy Council (EREC), around 50% of the global energy supply will be supported by renewable energy in 2040 (Karatayev, Movkebayeva, & Bimagambetova, 2019). Generally, various wastes particularly wastewater contains abundant organic matter. Thus it could be considered as a potential renewable energy reservoir (Crini, Lichtfouse, Wilson, & Morin-Crini, 2019). Although huge efforts have been made in promoting the renewable energy sector, the petro-energy sector continues to stay prominent. These petrochemical industries, in addition to its contribution in the development of the nation by exponential growth produces a massive amount of wastewater which serves as the cause of many environmental problems (Spitz, 2019). Acrylic acid (AA) is one of the major petrochemical products used in the production of acrylic esters, and also a by-product of the petrochemical industry (Zhu et al., 2020). A typical acrylic acid production industry discharges wastewater containing AA, acetic acid (ACA) and dimethyl phthalate (DMP) in a range of 4–15 wt%, 0.5-5 wt% and 0.1-2 wt%. respectively which are usually incinerated in the AA manufacturing plants (M. Ahmad, Kamaruzzaman, & Chin, 2014). Other methods, such as physico-chemical treatment (Goel & Soni, 2019), biological treatment (Mohanakrishna, Abu-Reesh, & Al-

Raoush, 2018) and advanced oxidation process (Varjani, Joshi, Srivastava, Ngo, & Guo, 2019) could not simultaneously solve the energy and environmental issues. Incineration, as a physical method is commonly used for the destruction of waste material, mostly concerning solid or gaseous, dry to semi dry materials with high energy contents where a certain portion of the energy can be recovered (Momayez, Karimi, & Taherzadeh, 2019). However, while it is applied for the destruction of organics in the water body, the process displays a very poor energy recovery efficiency due to the low heating value of the effluent. Additionally, it produces a large amount of greenhouse gases and low-grade heat which poses the threats to the environment (Momayez et al., 2019).

Conventional physico-chemical methods also fall to the same pot as they produce a significant amount of solid waste (Bahri, Mahdavi, Mirzaei, Mansouri, & Haghghat, 2018). On the brighter side, the biological treatment of wastewater requires less energy and thus it is considered as a promising technique for the industrial wastewater treatment (J. Tang, Zhang, Shi, Sun, & Cunningham, 2019). The biological wastewater treatment can be accomplished by aerobic and anaerobic processes. The anaerobic process is preferred over the aerobic due to lower energy consumption, reduced solid's formation, and potential energy recovery (Macarie & technology, 2000). However, Microbial fuel cell (MFC) technology is considered as one kind of biological anaerobic treatment which in contrast to typical bioreactors, can concurrently generate electricity and treat wastewater (Ragab, Elawwad, & Abdel-Halim, 2019). Early reports also demonstrated the successful degradation of AA containing wastewater in anaerobic reactor (L. Zhang, Fu, & Zhang, 2019). The biological treatment of AA containing wastewater with an initial chemical oxygen demand (COD) of 10 - 12 g /L with the use of mixed culture (anaerobic sludge) where the COD removal efficiency was more than 90% (Birjandi, Younesi, Ghoreyshi, & Rahimnejad, 2020). However, there is a problem of using anaerobic sludge as it mostly contained the methanogenic bacteria which decreased the power generation. Hence, the role of acclimation of the microbes is crucial (Yan et al., 2020). Although the acclimatized AS was used as an inoculum for biological treatment, it cannot ensure its performance in the MFC because it requires the electrogen (X. M. Li, Cheng, Selvam, & Wong, 2013). Additionally, it was reported that methanogenic bacteria could suppress the electrogenic bacteria's performance (Raychaudhuri & Behera, 2020a). In that context, the inoculum development for the acrylic acid treatment plant is a critical need to treat and generate electricity by using this kind of wastewater. On the other hand, MFC

performance is generally evaluated in terms of power generation in addition to COD removal efficiency (Marassi et al., 2020).

Moreover, several factors such as type of the substrates, concentration of the substrates (initial COD), pH, temperature, electrode material and biocatalysts influence the performance of MFC (Gadkari, Shemfe, & Sadhukhan, 2019). In recent years, a huge number of papers have been published to optimize the operating conditions of MFCs (Rani, Sharma, & Kumar, 2019; Wu et al., 2019; Y. Zhang et al., 2019). In addition, various kinds of wastewaters have already been tested in MFCs such as food wastewater (Radeef & Ismail, 2019), domestic wastewater (DW) (Corbella, Hartl, Fernandez-Gatell, & Puigagut, 2019), starch wastewater (Cao, Chen, Ray, Le, & Chang, 2019), palm oil mill effluent (POME) (Islam, Ethiraj, Cheng, Yousuf, & Khan, 2017), sugarcane molasses wastewater (SMWS) (S. H. Hassan, Abd el Nasser, & Kassim, 2019), rice straw wastewater (RSWS) (S. H. Hassan et al., 2014) and petroleum refinery wastewater (PRW) (Sevda, Abu-Reesh, Yuan, & He, 2017) in which a variety of inoculums, pure cultures as well as mixed cultures have been used. The composition of the inoculums and its interaction with the substrates as well as electrodes play a major role in generating power from MFC (Xiao, Wu, Huang, & Selvaganapathy, 2020). Besides, for petrochemical wastewater, the initial COD could have adverse effect on the microbial growth (Tan et al., 2020). Hence, there should be a systematic study on the performance of MFC operated with petrochemical wastewater from AA plant to primarily assess the feasibility of the MFC. Additionally, the efficacy of the MFC in terms of power generation depends on the charge transfer efficiency from the microbes to the anode surface (Raghavulu et al., 2012) which has never been addressed for the AA containing wastewater fed MFC. In this context, the present study for the first time reports the potentiality of PCW from AA plant as fuel in MFC for simultaneous treatment and power generation using acclimatized anaerobic sludge (AS).

1.2 Problem statement

Even though enormous efforts have been made in promoting the renewable energy sector, the petro-energy sector continues to stay remarkable. These petrochemical industries, produce a large amount wastewater containing very high COD which requires proper treatments before discharging to the environment. (Arvin, Hosseini, Amin, Darzi, & Ghasemi, 2019). Different conventional technologies, such as coagulation,

flocculation, advanced oxidation process, membrane separation process, adsorption and biological treatment (aerobic and anaerobic process) are most commonly used for the treatment of wastewater and among them the biological treatment is the most promising due to its low energy requirement for the wastewater treatment (Abuabdou, Ahmad, Aun, & Bashir, 2020). Although, previous literature showed that the PCW from AA plant is difficult for biodegradation using anaerobic sludge (AS) (Lixun Zhang et al., 2019), whereas some studies demonstrated the high degradation efficiency of the anaerobic process using acclimatized anaerobic sludge (Ansari, 2019; Smith, 1981). The anaerobic sludge suitable for anaerobic biodegradation could be the potential source of the inoculum to be used in MFC anode (H. Hassan et al., 2018). However, anaerobic sludge are mixed culture microorganisms, mainly methanogens possessing the ability to consume the organics present in the wastewater leading to the production of biogas (Banu, Kavitha, Kannah, Bhosale, & Kumar, 2020). Moreover, the power generation in the MFC depends not only on the biodegradation abilities, but also on the electron generation and transfer abilities of the microbes (Pandit, Chandrasekhar, Jadhav, & Madhao, 2019). Low power generation is the bottleneck of the MFC development while operating with real industrial wastewater such as PCW. The understanding on the interaction of the microbes with different organic substrates present in the complex wastewater is crucial for high power generation in MFC (Anawar & Strezov, 2019). PCW from acrylic acid plant mainly contains acrylic acid, acetic acid and dimethyl phthalate which possess different microbial interactions establishing synergistic or antagonistic effects. The acclimatized AS have never been investigated for simultaneous power generation and treatment of PCW from acrylic acid plant. In this context, a systematic study is required to achieve high power generation in the MFC fed with PCW.

Additionally, the presence of electrogens in the inoculum possessing synergy with other microbes is vital to augment the power generation in MFC. From literature, the mutualistic interaction among co-culture namely, *Pseudomonas aeruginosa* (PA) and *Klebsiella. vericola* (KV) using different substrates was shown, which increased the power generation significantly in the MFC (Islam, Ethiraj, Cheng, Yousuf, & Khan, 2018). On the other hand, the effect of substrate on the pure and mixed culture inoculum plays an important role on the performance of MFC. The synergistic interactions within the microbes especially which are involved in electron transfer could possibly influence this performance of MFCs (T. N.-D. Cao et al., 2019; Sima, Ebadi, Reiahisamani, &

Rasekh, 2019). However, by using the PCW and its constituents individually as substrates in MFC, the study has never been done.

The mechanism of electron transfer is a key information to design the MFC for enhanced power generation. Two specific electron transfer mechanisms such as direct electron transfer and indirect electron transfer have widely been studied in MFC (Louro et al., 2019; Utesch et al., 2019). However, electron transfer mechanism in PCW fed MFC is unknown.

1.3 Objectives of the study

The objectives of the proposed study are summarized as:-

1. To evaluate the potentiality of the acclimatized anaerobic sludge and its electrogen constituents for the treatment of synthetic wastewater.
2. To investigate the performance by using the industrial petrochemical wastewater (PCW) from acrylic acid (AA) plant with acclimatized mixed culture.
3. To elucidate the mechanism and kinetics of electron transfer in petrochemical wastewater fed microbial fuel cell anode.

1.4 Scopes of the study

In order to achieve the objectives (1-3) of this study some important tasks have to be carried out. The basic experiments have been investigated for this research in achieving the goals are projected below:

- I. Anaerobic sludge (AS) from the local palm oil mill was used as the primary source of mixed culture microbes. The anaerobic sludge was acclimatized in microbial fuel cell running with petrochemical wastewater from acrylic acid plant for 11 days with an initial COD of 45000 mg/L. Finally, the predominated microbes namely *Pseudomonas aeruginosa* and *Bacillus cereus* from acclimatized AS were identified and used as an inoculum in the present study.
- II. The main constituents of PCW such as acrylic acid (AA), acetic acid (ACA), and dimethyl phthalate (DMP) were investigated as substrate in MFC using

acclimatized AS which was obtained from petrochemical wastewater. The concentration of AA, ACA, and DMP was (0.5-5 wt %), (0.5-5 wt %) and (0.5-2 wt %) respectively. The performance of the individual substrates in terms of power generation and microbial growth using the above-mentioned concentration was investigated.

- III. A synthetic wastewater was prepared using AA, ACA, and DMP with a composition of 2:2:0.5 wt% (based on individual substrate best performance). The performance of the MFC was evaluated in terms of polarization curve and voltage vs. time. Individual and mixed substrates concentration was determined by using the high performance liquid chromatography (HPLC).
- IV. The performance was observed using the raw PCW with initial COD (100000 mg/L) and to investigate the effect of initial COD, the PCW was diluted with DI water.
- V. The initial COD was varied from 100000-5000 mg/L. The performance was evaluated in terms of current vs. time, polarization curve, microbial growth and COD removal efficiency.
- VI. The time course biofilm formation was visualized by scanning electron microscope (SEM) correlated with the power generation.
- VII. Cyclic voltammetry (CV) and electrochemical impedance spectroscopy (EIS) were done to identify the mechanism of electron transfer.
- VIII. The natural metabolites secreted by the microbes was identified by employing ultraviolet visible spectroscopy.
- IX. The role of biofilm was investigated by using SEM in conjunction with CV and EIS.
- X. The electron transfer kinetics were elucidated by using the Tafel slope analysis. The kinetic model was proposed by using the Butler-Volmer model, Nernst-Monod model, and the kinetics parameters were evaluated.

1.5 Significance of the study

Petrochemical wastewater is a major source of wastewater which is currently incinerated producing low-grade heat energy along with the CO₂ emission. Biological treatment of PCW in MFC producing direct electricity could be an ultimate solution to handle the wastewater. However, the performance of the MFC depends on the substrate-

inoculum interaction which requires to be optimized before using the technology in large scale. In the present work, the potentiality of PCW to be used as fuel in MFC has been evaluated which will give impetus to its further utilization and treatment in bio-electrochemical systems.

1.6 Organization of this Thesis

The content of the present thesis has been divided into five chapters.

1.6.1 Chapter 1

This chapter presents the introduction to the present study. Research background and objectives, problem statement, scopes and significant of the study are described shortly in this chapter.

1.6.2 Chapter 2

This chapter summarizes the different types of wastewater and past treatment methods, past research efforts in the field of MFC, types, advantages, limitations, thermodynamics and different types of losses in MFC. In this connection, the electron transfer mechanism, the role of biofilm, substrates-inoculum also have been discussed in brief.

1.6.3 Chapter 3

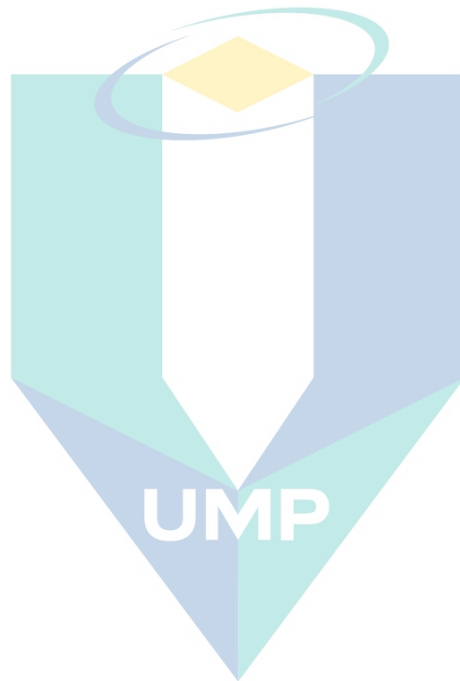
This chapter represents the methodology for the treatment of PCW in this study and preparation of inoculum, sample, measurement, calculation, and analysis. Moreover, the theory and instruments used for the operation of MFC are also considered in this chapter.

1.6.4 Chapter 4

This chapter deals with the performance of the MFC by using acclimatized AS as biocatalyst with PCW. The performance was done using voltage vs. current curve, microbial growth data, polarization, and power curve. The biofilm formation was visualized by Scanning electron microscope (SEM). Electron transfer mechanism and the charge transfer kinetics were performed using CV and EIS. The presence of natural mediators was confirmed using CV, EIS, and ultraviolet visible spectroscopy (UV-vis).

1.6.5 Chapter 5

It includes the Conclusion of the present work are presented in this chapter along with the recommendation for further work.



اونيورسيتي مليسيا قهغ

UNIVERSITI MALAYSIA PAHANG

CHAPTER 2

LITERATURE REVIEW

2.1 Chapter overview

This chapter represents the renewable energy, wastewater and wastewater treatment, past research history connected to MFC, energy existence of microorganisms and the kinetics of electron transfer mechanisms from microorganisms to electrodes are arranged. Besides this, the advantages and disadvantages of MFC also considered. On the other hand, the point about electrodes and substrates are included. The limitations of using other microorganisms and the advantages of using specific microorganisms are discussed too.

2.2 Renewable energy

Fossil fuels have supported the industrialization and economic growth of all the economies in the world over the past century. Dependence on fossil fuels is unsustainable due to pollution and limited availabilities and threaten their utilization as primary energy sources, as go growing environmental concerns (the emission of greenhouse gases and the consequent increase in the average global temperature) with environmental imbalance (Uniyal, Paliwal, Kaphaliya, & Sharma, 2020). The environmental imbalance using fossil fuel presented in Figure 2.1. On the other hand, the use of fossil fuels, particularly oil and gas, has increased and is causing a global energy crisis (Ağbulut, Ceylan, Gürel, & Ergün, 2019). These concerns have catalyzed the development of alternative energy sources. Research is being conducted in a broad range of energy solutions, as only one solution alone will not be able to replace fossil fuels. Many efforts are devoted to developing other electricity production methods. Renewable bioenergy is one possible way to reduce the global warming crisis (Qazi et al., 2019). There are several types of renewable energy sources such as solar energy, wind power, biomass, and geothermal energy are abundant and inexhaustible (Williams, Raimi, Yarwamara, & Modupe, 2019). Among them, the biomass has drawn much attention as a sustainable energy resource due to their capability to generate electricity without creating environmental imbalance (Xue et al., 2020). Two

major biomass types are utilized as energy sources: those that are produced for energy-generating reasons (e.g. corn) and those that are available as waste materials (e.g. wastewater produced from petrochemical industries and sludge from sewerage) (G. D. Saratale, Saratale, Banu, & Chang, 2019). The second type of biomass is considered one of the biomass resources as the petrochemical industry generates a massive amount of wastewater each year (260 million tons) (Leyva-Díaz et al., 2019). This type of wastewater is full of high biomass content which is harmful to the environment. For this reason, petrochemical wastewater treatment is needed before released to the environment in order to prevent water pollution and power generation (Coenen, Martin, & Dahl, 2020).

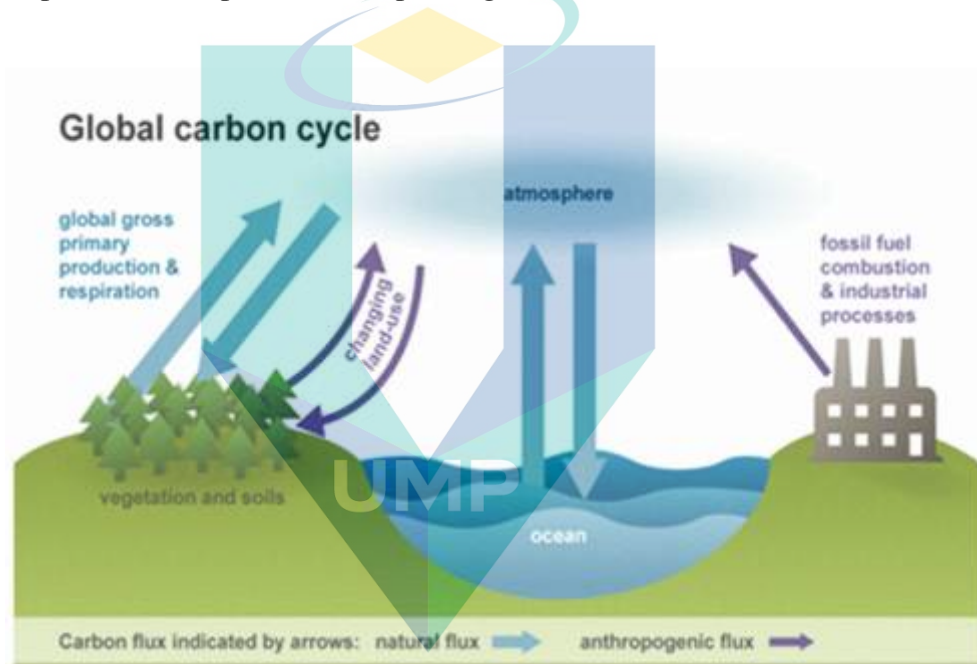


Figure 2.1 Environmental imbalance using fossil fuel

Source: Huppmann et al., (2019)

The detailed description of petrochemical wastewater is given in section 2.3.

2.3 Petrochemical wastewater (PCW)

Petrochemical wastewater contained high polycyclic aromatics, which were very toxic as well as a wide range of contaminants at varying concentrations. For this reason, it was considered as hazardous pollutants on the environment (Bharagava, Saxena, & Mulla, 2020). The overall feature of PCW is given in Figure 2.2.



Figure 2.2 Petrochemical wastewater treatment plant

Source: Behnami, Benis, Shakerkhatibi, Derafshi, & Chavoshbashi, (2019)

The organic pollutants in petroleum refinery wastewater in some refineries showed that the major compounds were different fractions of petroleum aliphatic hydrocarbons (up to C10) and the well-known aromatic compounds such as benzene, toluene, and ethyl-benzene (de Oliveira, Viana, & Amaral, 2020). By using physical treatment showed that the maximum removal for COD and BOD were around 1400-1500 mg/L and 25-30 mg/L, respectively from different sources of petrochemical wastewater and concluded that separation and individual treatment for each source was a good alternative against treatment full quantity after mixing of different sources (Aljuboury, Palaniandy, Abdul Aziz, & Feroz, 2017). Most of them contained Oil and grease, which flow down drain pipes and causing unpleasant odor and corroding as well as are sticky (C. Chen et al., 2015) phenolic compounds, which is dangerous for the environment due to their extreme toxicity and ability to remain for long periods and the nitrogen and sulphur components, which are represented in the form of ammonia and hydrogen sulphide (H₂S), respectively (Jawad & Abbar, 2019). Besides, Naphthenic acids (NAs) are one class of compounds in wastewaters from petroleum industries that are known to cause toxic effects, and their removal from oilfield wastewater is an important challenge for remediation of large volumes of petrochemical effluents in total naphthenic acids (NAs) was estimated to be 2.1-8.8% in a refinery wastewater treatment plant (R. Qin, 2019). The percentage of different chemicals in PCW are given in Table 2.1.

Table 2.1 The lists of chemicals containing PCW

Name of chemicals	Amount (%)
Water	92.69
Acrylic acid	3
Acetic acid	0.2
Dimethyl phthalate	0.2
Formic acid	0.11
Maleic acid	1.38
Benzoic acid	0.05
Diacrylic acid	0.68
Formaldehyde	0.71

Source: Ghimire & Wang, (2018)

2.4 Wastewater treatment methods

The wastewater treatments are divided into three types; physical, chemical and biological. Although, the treatment needed a typical application of the integrated system owing to the difficulty of characteristics of wastewater. Hence, the standard treatment processes need multistage process treatment (Magwaza, Magwaza, Odindo, & Mditshwa, 2020). The main stage formed of pre-treatment, which includes mechanical and physicochemical treatments when compared to the second stage which is the most advanced treatment of the wastewater pre-treatment (Deng, Lin, Cheng, & Murphy, 2019). Based on the literature review conducted, the techniques and methods for petroleum wastewater treatment included physical, chemical, biological treatment processing (Christensen, Keiding, Nielsen, & Jørgensen, 2015). Different types of treatment methods are given in the following section.

2.4.1 Physical treatment

Physical treatment is a process where no biological or chemical changes are carried out and strictly physical properties are used to treat the wastewater. For example, coarse screening to remove larger entrained objects and sedimentation (Olajire, 2020). The physical treatment process is a preliminary treatment stage, which is important to remove suspended solids (SS), immiscible liquids, suspended substances, and solid particles, from wastewater by using coagulation, flocculation, and sedimentation (N. Ahmad, Sultana, Khan, & Sabir, 2020). Sedimentation treatment is a method that is used to separate oil from water. The physical treatment process is presented in Figure 2.3

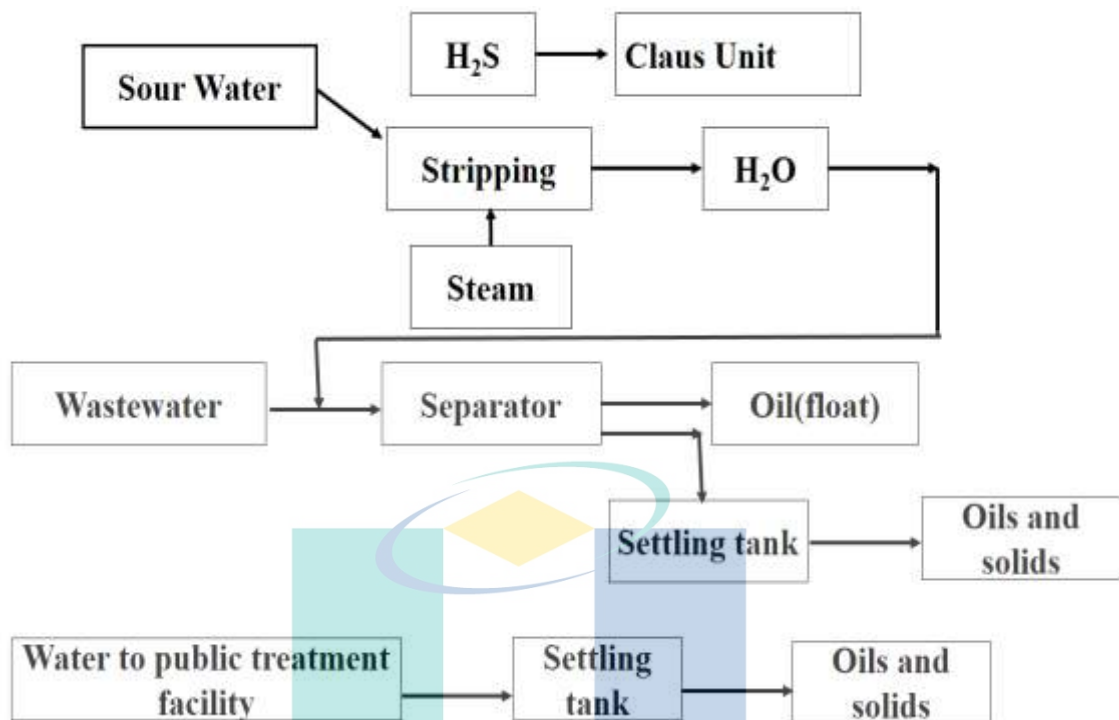


Figure 2.3 Physical treatment process

Source: Azeumo et al., (2019)

From Figure 2.3, it can be seen that the primary treatment of sour water contaminated with oils and solid particles involve the stripping of dissolved H_2S using steam, float/sink density separation for skimming the floating oil, and the settling tanks to separate heavier oil and solids, usually in multiple stages, before the treated water can be directed to public treatment facilities. The secondary treatment uses micro-organisms to further remove organic contaminants.

2.4.2 Chemical treatment

Chemical treatment is a process that is consisted of using some chemical reaction or reactions to develop water quality. A chemical process generally used in many industrial wastewater treatment operations is neutralization (Abbasi, Mirghorayshi, Zinadini, & Zinatizadeh, 2020). Neutralization is a process which is the addition of acid or base to adjust pH levels back to neutrality. The most implemented chemical treatment processes are chemical precipitation, neutralization, adsorption, disinfection (chlorine, ozone, ultraviolet light), and ion exchange (Samer, 2015) which are described by the following processes:

2.4.2.1 Chemical precipitation

Chemical precipitation is the most common method for removing dissolved metals from wastewater solution containing toxic metals. The chemical precipitation process is shown in Figure 2.4.

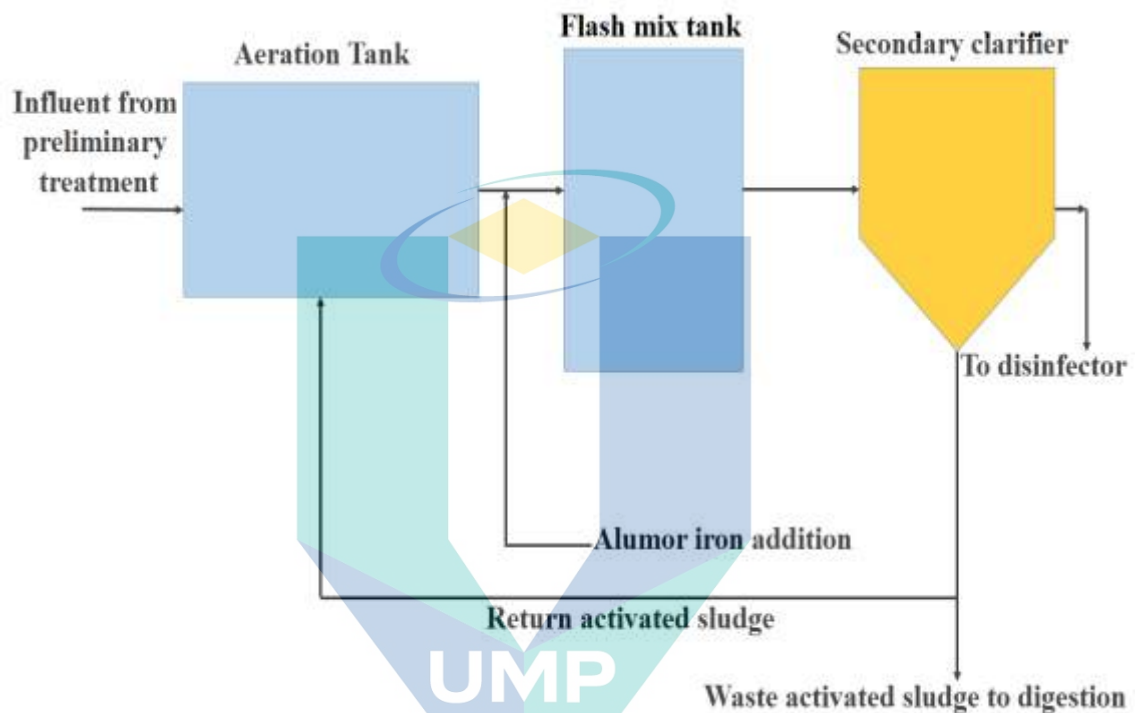


Figure 2.4 Chemical precipitation process

Source: Du, Gao, Ueda, & Kitamura, (2019)

To convert the dissolved metals into solid particle form, influent or a precipitation reagent from preliminary treatment is added to the aeration tank for proper mixing. A chemical reaction, triggered by the reagent, causes the dissolved metals to form solid particles. Filtration can then be used to remove the particles from the mixture which then went to clarifier and finally got the waste sludge (Figure 2.4) (Crini & Lichtfouse, 2019). How well the process works is dependent upon the kind of metal present, the concentration of the metal, and the kind of reagent used. In hydroxide precipitation, a commonly used chemical precipitation process, calcium or sodium hydroxide is used as the reagent to create solid metal hydroxides. However, it can be difficult to create hydroxides from dissolved metal particles in wastewater because many wastewater solutions contain mixed metals (Segundo et al., 2019).

2.4.2.2 Chemical coagulation

This chemical process involves destabilizing wastewater particles so that they aggregate during chemical flocculation. The overall process is shown in Figure 2.5.

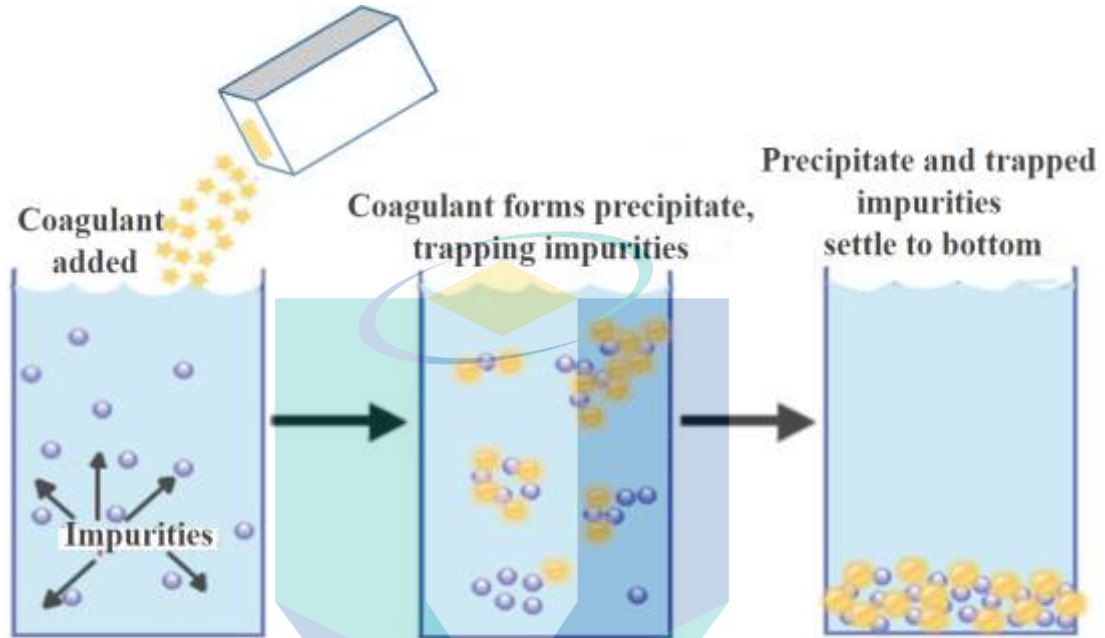


Figure 2.5 Chemical coagulation method

Source: Can, Gengec, & Kobya, (2019)

In this process, fine solid particles dispersed in wastewater carry negative electric surface charges (in their normal stable state), which prevent them from forming larger groups and settling (Y. Zhao, Meng, & Shen, 2020) as shown in Figure 2.5. Chemical coagulation destabilizes these particles by introducing positively charged coagulants that then reduce the negative particles' charge. Once the charge is reduced, the particles freely form larger groups (Bratby, 2016). Next, an anionic flocculant is introduced to the mixture. Because the flocculant reacts against the positively charged mixture, it either neutralizes the particle groups or creates bridges between them to bind the particles into larger groups. After larger particle groups are formed, sedimentation can be used to remove the particles from the mixture (Shankar, Ankur, Bhushan, & Mohan, 2019).

2.4.2.3 Chemical oxidation and advanced oxidation

With the introduction of an oxidizing agent during chemical oxidation, electrons move from the oxidant to the pollutants in wastewater. The pollutants then undergo

structural modification, becoming less destructive compounds. Alkaline chlorination uses chlorine as an oxidant against cyanide (McQuillan, Stevens, & Mumford, 2020). However, alkaline chlorination as a chemical oxidation process can lead to the creation of toxic chlorinated compounds, and additional steps may be required. Advanced oxidation can help to remove any organic compounds that are produced as a by-product of chemical oxidation, through processes such as steam stripping, air stripping, or activated carbon adsorption (J. Yu et al., 2020). The whole process is shown in Figure 2.6.

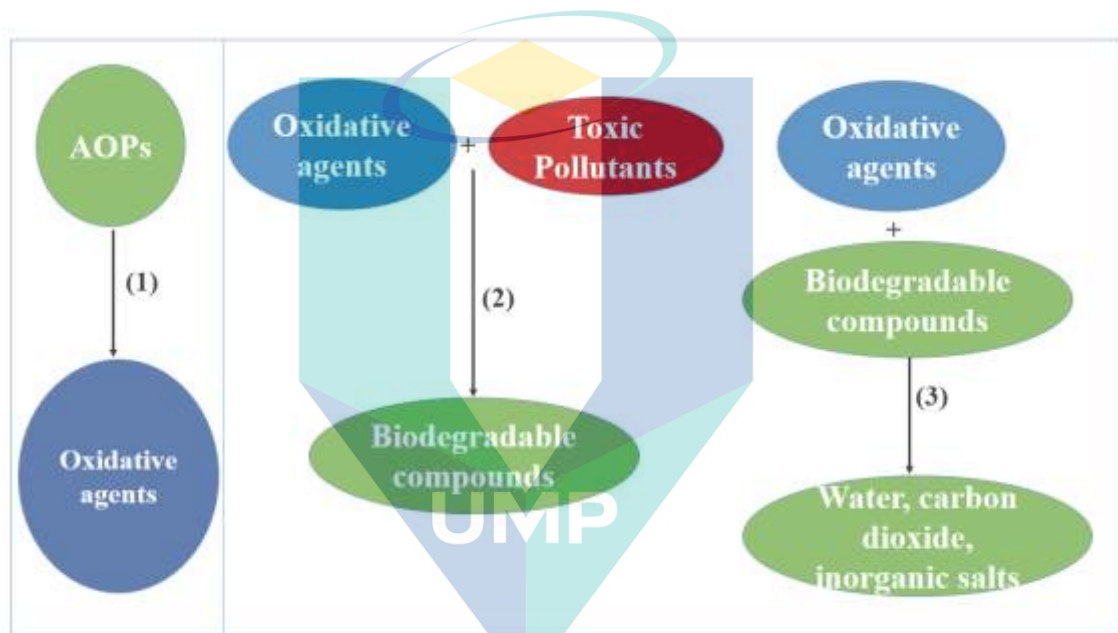


Figure 2.6 Chemical oxidation and advanced oxidation

Source: Gautam, Kumar, & Lokhandwala, (2019)

From Figure 2.6, it can be seen that three steps happen in this process. Firstly, the formation of strong oxidants (e.g. hydroxyl radicals). Secondly, the reaction of these oxidants with organic compounds in the water producing biodegradable intermediates. And finally, the reaction of biodegradable intermediates with oxidants referred to as mineralization (i.e. production of water, carbon dioxide and inorganic salts) (Gounden & Jonnalagadda, 2019).

2.4.2.4 Ion exchange

When water is too hard, it is difficult to use to clean and often leaves a grey residue. An ion - exchange process, similar to the reverse osmosis process, can be used to soften the water (E. Liu, Lee, Ong, & Ng, 2020). The ion exchange process is shown

in Figure 2.7. The ion exchange process occurs between a solid (resin or a zeolite) and a liquid (water) from Figure 2.7.

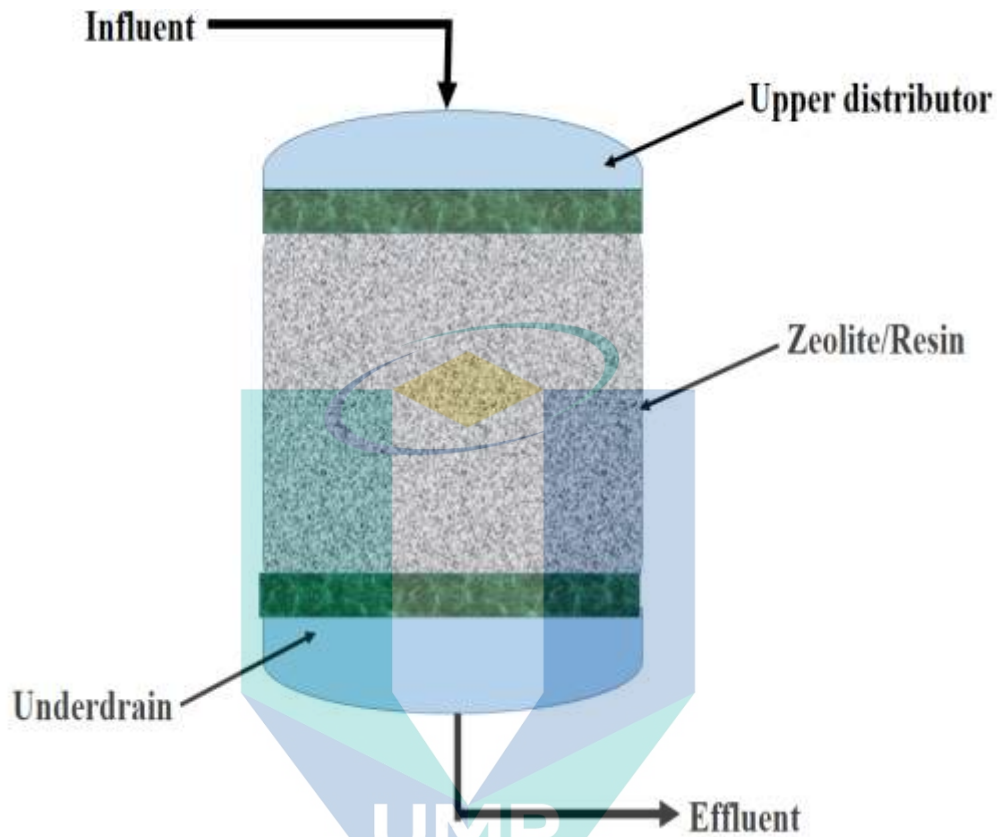


Figure 2.7 Ion exchange process

Source: C. Zhao et al., (2019)

In the process, the less desired compounds are swapped for those that are considered more desirable. These desirable ions are loaded onto the resin material. In the exchange of cations during water treatment, positively charged ions that come into contact with the ion exchange resin are exchanged with positively charged ions available on the resin surface, usually sodium (Ploetz, Engelke, Lächelt, & Wuttke, 2020). In the anion exchange process, negatively charged ions are exchanged with negatively charged ions on the resin surface, usually chloride. Various contaminants-including nitrate, fluoride, sulfate, and arsenic can all be removed by anion exchange. These resins can be used alone or in concert to remove ionic contaminants from the water (Hitam & Jalil, 2020) (Figure 2.7). On the other hand, in the ion exchange process, calcium and magnesium are common ions that lead to water hardness (Dong et al., 2019). To soften the water, positively charged sodium ions are introduced in the form of dissolved sodium chloride salt or brine. The hard calcium and magnesium ions exchange places with

sodium ions, and free sodium ions are simply released in the water. However, after softening a large amount of water, the softening solution may fill with excess calcium and magnesium ions, requiring the solution to be recharged with sodium ions and finally got effluent (Sarode et al., 2019).

2.4.3 Biological treatment

Biological wastewater treatment is shown in Figure 2.8.

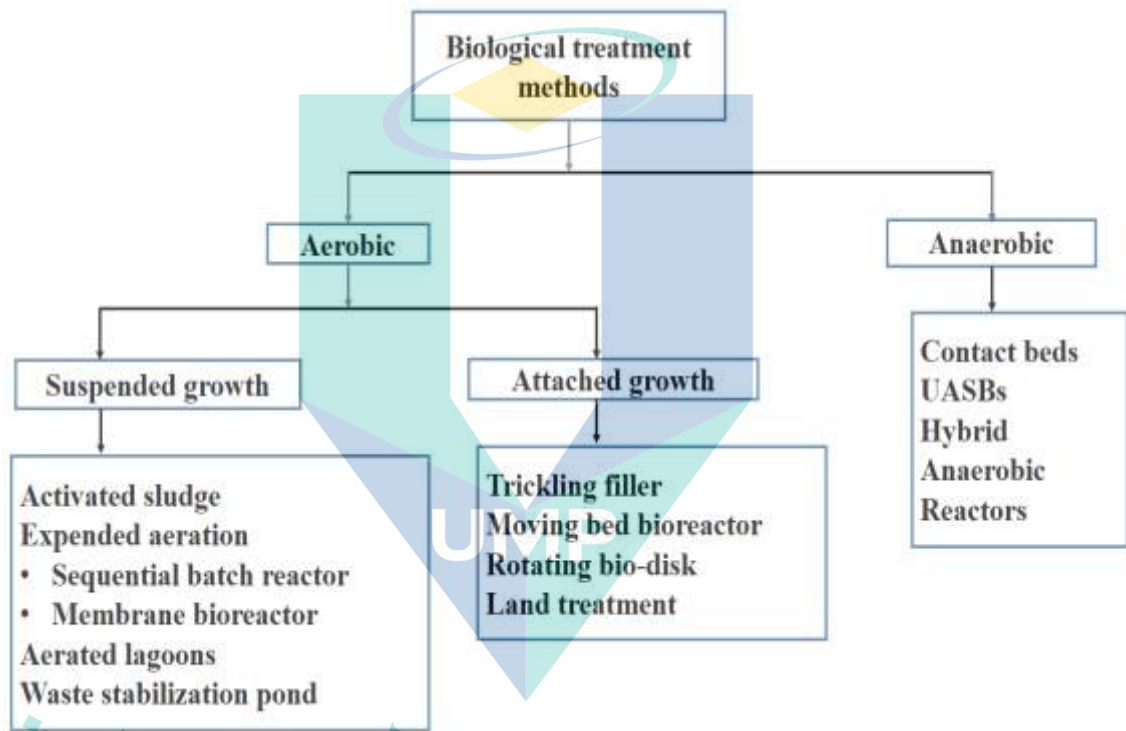


Figure 2.8 Biological treatment process

Source: Celenza, (2019)

It is often called as a secondary treatment process which is used to remove any contaminants that leftover after primary treatment. Chemical treatment of wastewater makes use of chemicals to react with pollutants present in the wastewater and whereas biological treatment uses microorganisms to degrade wastewater contaminants (Ansari, 2019). This treatment relies on bacteria, nematodes, algae, fungi, protozoa, rotifers to break down unstable organic wastes using normal cellular processes to stable inorganic forms (Sobczyk, 2019). Generally, biological treatment methods can be classified into two types such as aerobic and anaerobic methods, based on the availability of dissolved oxygen from Figure 2.8. In anaerobic systems, the products of chemical and biochemical

reactions produce colors and odors in water. Thus, oxygen availability was important in water to reduce colors and odors (J. Song et al., 2020).

2.4.3.1 Aerobic degradation

Aerobic degradation is presented in Figure 2.9. In Aerobic degradation, bacteria that thrive in oxygen-rich environments break down and digest waste (Ohki & Rich, 2020).

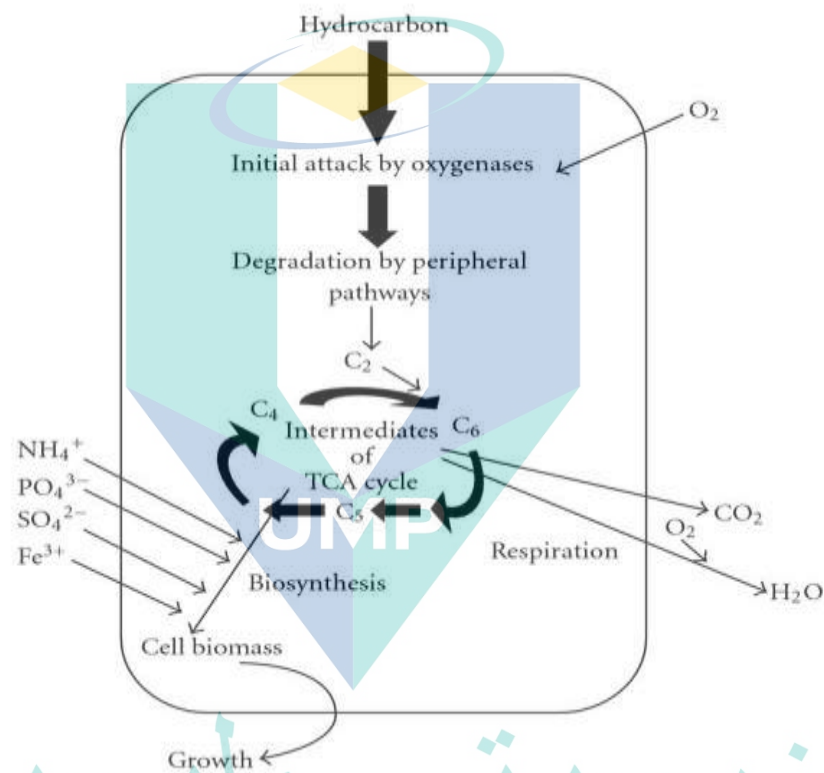


Figure 2.9 Aerobic degradation pathway

Source: Ebenau-Jehle, Soon, Fuchs, Geiger, & Boll, (2020)

During this oxidation process, contaminants and pollutants are broken down into CO_2 , water, nitrates, sulfates, and biomass (microorganisms). In the conventional aerobic system, the substrate is used as a source of carbon and energy (Figure 2.9). It serves as an electron donor, resulting in bacterial growth (X. Chen, 2020). The extent of degradation is correlated with the rate of oxygen consumption, as well as the previous acclimation of the organism in the same substrate (Rivett & Sweeney, 2019). Co-enzymes primarily involved in the process are di- and mono-oxygenises. The latter enzyme can act on both aromatic and aliphatic compounds, while the former can act only on aromatic compounds.

Another class of enzymes involved in aerobic degradation is the peroxidases, which have been receiving attention recently for their ability to degrade lignin (Sheldon & Brady, 2019).

2.4.3.2 Anaerobic degradation

In the anaerobic process, the complex organics are first broken down into a mixture of volatile fatty acids (VFAs), mostly acetic, propionic, and butyric acids. This is achieved by "acidogens," a consortium of hydrolytic and acidogenic bacteria (L. N. Nguyen, Nguyen, & Nghiem, 2019). The VFAs are in turn converted to CO₂ and methane which is shown in Figure 2.10 by acetogenic (acetogens) and methanogenic (methanogens) bacteria, respectively (Aquino, Araújo, Passos, Curtis, & Foresti, 2019).

In the absence of oxygen, close-knit communities of bacteria cooperate to form a stable, self-regulating fermentation that transforms organic matter into a mixture of methane and CO₂ (Figure 2.10). The amount of methane gas produced varies with the amount of organic waste fed to the digester and the operating temperature (Moscoviz, Quéméner, Trably, Bernet, & Hamelin, 2020). Anaerobic digestion occurs in six main stages (A. Kumar & Samadder, 2020):

- i. Hydrolysis of complex organic biopolymers (proteins, carbohydrates, and lipids) into monomers (amino acids, sugars, long chain fatty acids) by hydrolytic bacteria (group I) (acidogens)
- ii. Fermentation of amino acids and sugars by hydrolytic bacteria (group I)
- iii. Anaerobic oxidation of volatile fatty acids and alcohols by heteroacetogenic bacteria (group II)
- iv. Anaerobic oxidation of intermediary products such as volatile fatty acids by heteroacetogenic bacteria (group II)
- v. Conversion of hydrogen to methane by methanogenic bacteria utilizing hydrogen (group IIIA)
- vi. Conversion of acetate to methane by methanogenic bacteria utilizing acetate (group IIIB)

The hydrolysis of undissolved carbohydrates and proteins follows separate paths. The heteroacetogenic bacteria grow in close association with the methanogenic bacteria during the final stages of the process. The reason for this is that the conversion of the

fermentation products by the heteroacetogens is thermodynamically possible only if the hydrogen concentration is kept sufficiently low. This requires a close symbiotic relationship among the classes of bacteria (Gupta & Shukla, 2020).

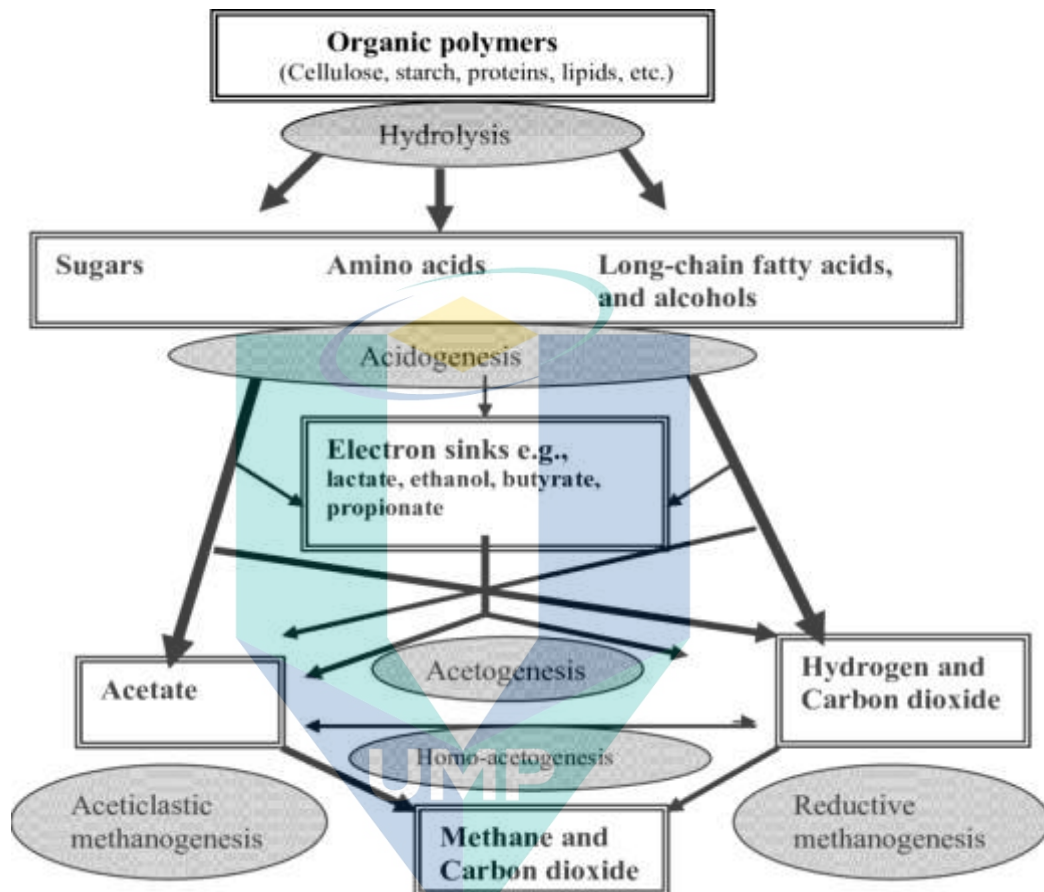


Figure 2.10 Anaerobic degradation pathway

Source: Harder, Marmulla, & Lipids, (2020)

2.5 Biological treatment of petrochemical wastewater (PCW)

Biological treatment incorporates actions of different microbes to eliminate organics and stabilize hazardous pollutants in petrochemical wastewater (Ghimire & Wang, 2018). Stringent environmental standards and recycling of water for reuse have shifted focus to biological treatments because of its cost and pollutant removal efficiency (Cai et al., 2020). As the nature of petrochemical wastewater is very complex, biological treatment to remove pollutants still has challenges despite immense potentials. Complex structures of aromatic, polycyclic, and heterocyclic ringed chemicals are known to be restraint to biological degradation (X. Dai, Chen, Yan, Chen, & Guo, 2016). However, recent research activities have produced notable removal percentages of pollutants from

petrochemical wastewater (Jamaly, Giwa, & Hasan, 2015). Anaerobic digestion has the advantages of producing methane as a renewable energy, requiring less space and having lower sludge generation than aerobic process (Yao et al., 2020). A literature review of anaerobic digestion on the petrochemical wastewater is given in Table 2.2. Petrochemical wastewater treated in anaerobic baffled reactor (ABR), sequence batch, and up-flow sludge blanket reactor (UASB) was commonly applied (T. Wang et al., 2020). It shows that organics in the petrochemical wastewater could be partially anaerobically digested at a removal efficiency depending on the chemical constituents, reactor type, operational conditions (temperature, loading rate, etc.), and wastewater sources (Bakraoui et al., 2020). COD removal efficiency is used here as a general parameter to assess the performance of different systems. Crude oil extraction of light, medium, and heavy petroleum wastewater treatment by different anaerobic digestion systems at mesophilic or thermophilic conditions showed that in batch test over 56–71% COD removal was achievable at thermophilic condition (Baker, Mohamed, Al-Gheethi, & Aziz, 2020) (Table 2.2), while UASB system can achieve over 93% COD removal at mesophilic conditions for wastewater from light petroleum extraction (Table 2.2).

Table 2.2 Different types of petrochemical wastewater treatment using different reactors

Wastewater	Initial COD (mg/L)	Microbes	Treatment system	Pollutants monitored, COD	Removal efficiency (%)	Ref.
Crude oil extractions	2000	Anaerobic sludge	Batch reactor	COD	70	(Kul & Nuhoglu, 2020)
	2200	Anaerobic sludge	UASB	COD	62	(Y. Zhang, Guo, Zhang, & Liu, 2020)
Crude oil extractions	3500	Activated sludge	Batch reactor	COD	70	(Eljamal et al., 2020)
Crude oil extraction	4000	Anaerobic sludge	UASB	COD	23	(Wei, Jin, & Zhang, 2020)
of light petroleum	3400	Anaerobic sludge	Batch reactor	COD	86	(Bakraoui et al., 2020)
Heavy oil refinery	1234	Activated sludge	UASB	COD	62	(W. Wang, Yao, & Yue, 2020)

It seems light petroleum extraction wastewater was generally easily degradable (over 71–93% removal) compared to the medium and heavy oil extraction wastewater. The setup of plug flow pattern and granular sludge application in UASB might also enhance the interaction between wastewater and organisms, giving higher efficiency. The removal efficiency decreases as the loading rate increases, indicating the inhibition effects to the organisms (L. He et al., 2017). Medium- and heavy oil-produced wastewater treatment efficiency was relatively low. Batch system gives generally a better treatment efficiency for these two wastewaters at about 50–60% removal (Table 2.2), while UASB shows low efficiency at around 20–30% removal efficiency. The effects of toxic chemicals in the wastewater and high content of large organic molecules can be the reason for low efficiency (Bolognesi, Ceconet, & Capodaglio, 2020).

2.6 Microbial fuel cell (MFC)

MFC is defined as bio-electrochemical reactor that can convert chemical energy stored in wastewater organic components into electrical energy with the catalysis of microorganisms (Mathuriya, Hiloidhari, Gware, Singh, & Pant, 2020). The electro-active microorganisms that responsible for substrate oxidation and electron transfer are the key component of MFC, which makes it different from the traditional chemical fuel cells (Srivastava, Yadav, et al., 2020). It can be accomplished when microorganisms change from natural soluble electron acceptor to an insoluble electron acceptor. Electron transfer to an electrode may occur directly or through mediators. Thereafter, the electrons will pass through the circuit containing resistor and get reduced by the final electron acceptor at the cathode (Shaw et al., 2020).

2.6.1 The working principle of Microbial fuel cell

The Microbial fuel cell is operated through bio-electrochemical reactors arranged to use bacteria, which generates, entity and grows in an exo-electrogenic biofilm, as the biocatalysts to transfer organic and inorganic matter, substrates will present in a solution, through the oxidation-reduction reaction and at the same time generate electricity. Thus, chemical energy is converted to electrical energy with the help of microorganisms (Nael Yasri, Edward PL Roberts, & Sundaram Gunasekaran, 2019). Basically, MFC is describes as bio-electrochemical reactor that can transforms chemical energy accumulated in wastewater organic materials into electrical energy with the catalysis of

microorganisms (Ghangrekar & Neethu, 2020). The microorganisms that are in charge of for the oxidation of substrate and electron transfer are the main elements of MFC, which makes it completely different from the conventional chemical fuel cells (D. Liu et al., 2020). MFCs can also be referred to as a bio-electrochemical electrical device that changes biochemical energy of organic compounds to electrical energy, through the catalysis of microorganisms (Hernandez & Osma, 2020). The working principle of the microbial fuel cell is given in Figure 2.11.

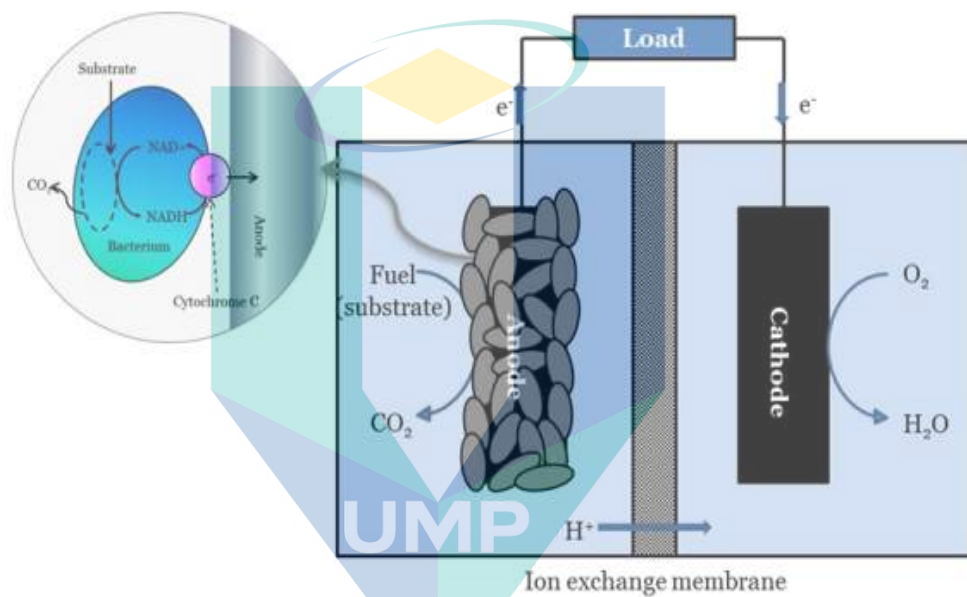


Figure 2.11 Working principle of MFC

Source: Q. Luo, An, & Wang, (2019)

The microbial fuel cell typically consists of two chambers: an anaerobic anode chamber or anode and an aerobic cathode chamber or cathode (Figure 2.11). This chamber is divided by an ion - exchange membrane (PEM), which is leak-proof but grants proton migration between the two chambers. Each chamber is connected by an electrode that means of a circuit so that the collection, transfer, and release of electrons is possible (Pandey et al., 2016). The oxidation-reduction reaction appears in the anode (negative beam), where the anaerobic living bacteria can oxidize with the solid electrode, while saving energy, by oxidizing organic or inorganic matter from the anode solution, and extracts protons, electrons and off-gas containing mainly carbon dioxide (Brocker, 2020). Next, the bacteria discharge new electrons first to the anode electrode and then, they are moved to the cathode electrode through the external circuit. The electron that transfers to the anode electrode may be either direct or indirect. At the same time, the protons that

obtain from the oxidation reaction transfer to the cathode, through the solution and from the one side of the proton exchange membrane (Moradi et al., 2020). When the electrons go to the cathode electrode, they are fully prepared to participate in the reduction reaction that occurs in the aerated cathode (positive beam). Thus, in aerobic conditions the, in maximum cases, dissolved oxygen (DO) keeps an important role of the terminal electron acceptor of the overall fuel cell reaction, and so it can reduce the combination between the electrons and the received protons, already present in the cathode solution, to form water. Catalysts are frequently used in the cathode to perform the reactions (Shabani et al., 2020). According to Ohm's law: $V = I R$ where I is the current through the conductor which unit is ampere, V is the potential difference measured across the conductor which unit is volt, and R is the resistance of the conductor which unit is ohm, a resistor is important between the positive and the negative pole. MFC cathodes have different structures and different fluid options (Hacker & Sumereder, 2020).

2.7 Different types of MFC

2.7.1 Two-compartments MFC system

In general, this configuration has an anodic and a cathodic chamber separated by a PEM that facilitates proton transfer from the anode to cathode with simultaneous prevention of oxygen diffusion into the anode. Therefore, this configuration is generally used for waste treatment with simultaneous power generation (Noori, Vu, Ali, & Min, 2020). The two-chamber MFC is presented in Figure 2.12. From Figure 2.12, it can be seen that both the anode and cathode are different compartments separated but also connected to each other through a proton exchange membrane (PEM), which mainly acts as a proton transfer medium to complete the circuit between the two chambers (Figure 2.12) (Asensio et al., 2017). This completes the reaction process and prevents anode from coming into direct contact with oxygen or any other oxidizers. They typically run in a batch mode often with a chemically defined medium such as glucose or acetate solution to produce higher energy power output and can be utilized to give power in many inaccessible conditions. Moreover, in the double chamber, MFC, the relatively long distance of electrodes can decrease MFC performance due to an elevation of internal resistance (Yousefi, Mohebbi-Kalhari, & Samimi, 2020).

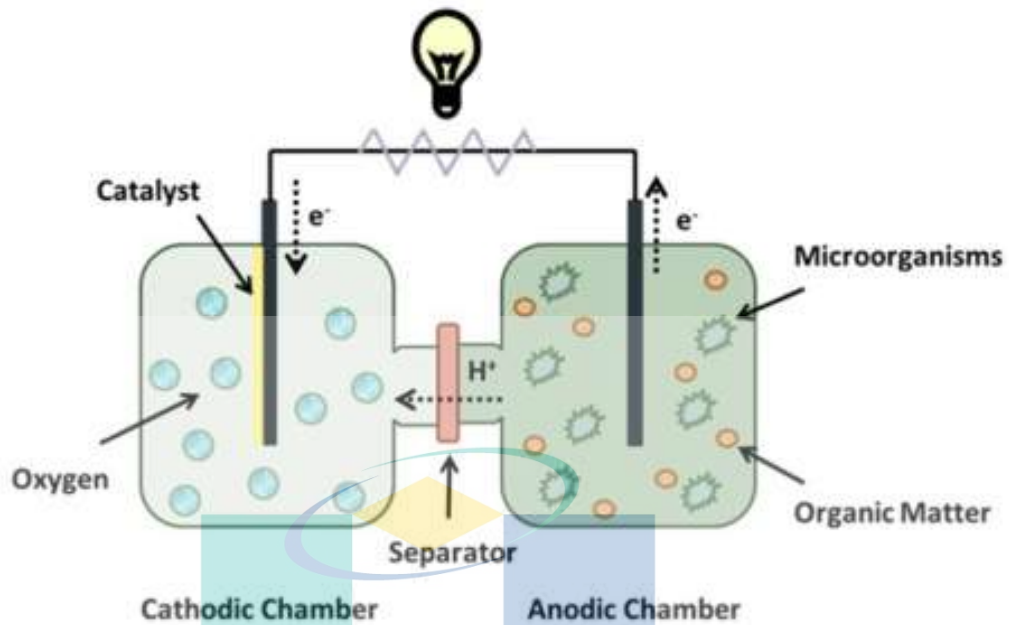


Figure 2.12 Two chamber MFC
 Source: R. Patel, Deb, Dey, & Balas, (2020a)

2.7.2 Single-compartment MFC system

Due to their complex designs, two-compartment MFCs are difficult to scale-up even though they can be operated in either batch or continuous mode. The air-cathode MFC is shown in Figure 2.13. From Figure 2.13, it can be seen that air-cathode MFC typically possess only an anodic chamber without the requirement of aeration in a cathode chamber. One compartment MFC consisting of an anode in a rectangular anode chamber coupled with a porous air-cathode that is exposed directly to the air as shown in Figure 2.13. Protons are transferred from the anolyte solution to the porous air-cathode (Halim, 2019). This type of MFC configuration attracted researcher's attention due to several advantages such as the simple nature of the operation, decrease in internal resistance, enhanced oxygen reduction rate on the cathode, increased proton diffusion and reduced electrode spacing. The limited requirement of regular changing of oxidative media and aeration makes this configuration more adaptable (Noori, Vu, et al., 2020).

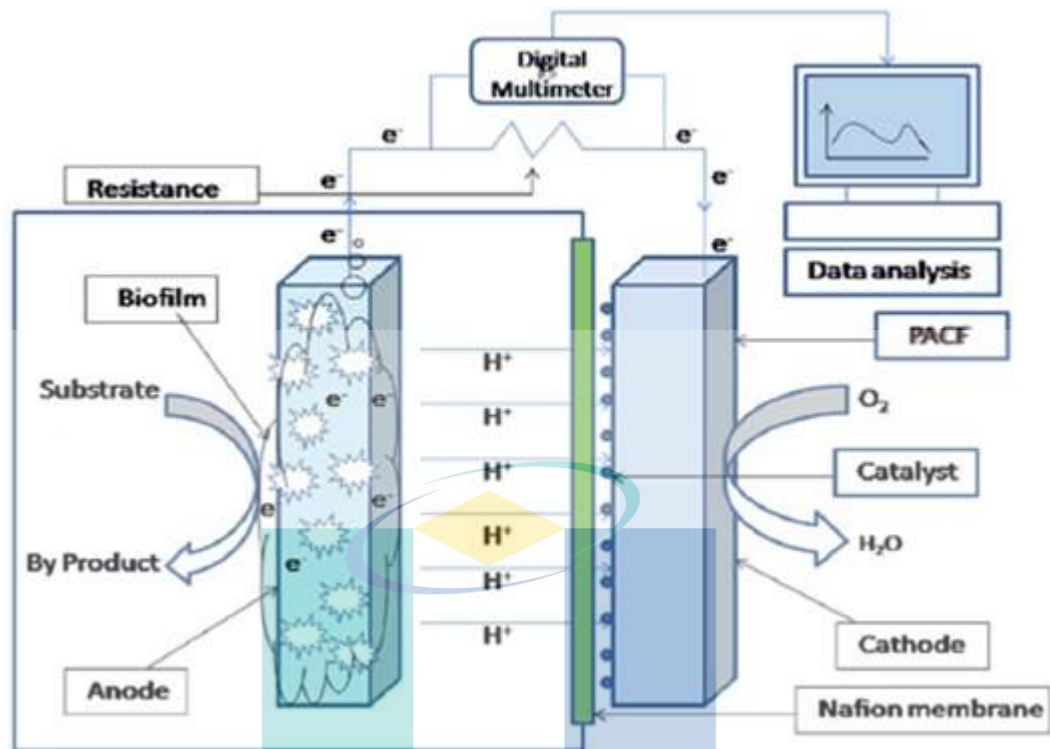


Figure 2.13 Air cathode MFC

Source: H. Wang et al., (2019)

2.7.3 Sediment MFC system

Sediment MFC is presented in Figure 2.14. From Figure 2.14, it can be seen that in the case of marine or sediment environments, a voltage gradient survives across the water–sediment interface obtaining from sedimentary microbial activity. A fuel cell making up of an anode inserted in marine sediment and a cathode in overlying seawater can easily use this voltage gradient to generate electricity (Pushkar & Mungray, 2020). The power generation that obtains from at least two anode reactions: oxidation of sediment sulfide (a by-product of microbial oxidation of sedimentary organic carbon) and oxidation of sedimentary organic carbon catalyzed by colonizing the anode microorganisms (Bagchi & Behera, 2020). This system is identified by a low voltage and power fabrication. Arends showed that a Plant-MFC could offer the prospect to steer and control the sediment redox potential and thus abate undesirable processes such as methylation of metals and emissions of methane. Moreover the plant-MFC produced sustainable power up to 330 W/ha from the oxidation of the plant-derived compounds. Mitigation of methane emissions from wetland has been hypothesized in various reports but never been studied thoroughly yet (Arends, 2013).

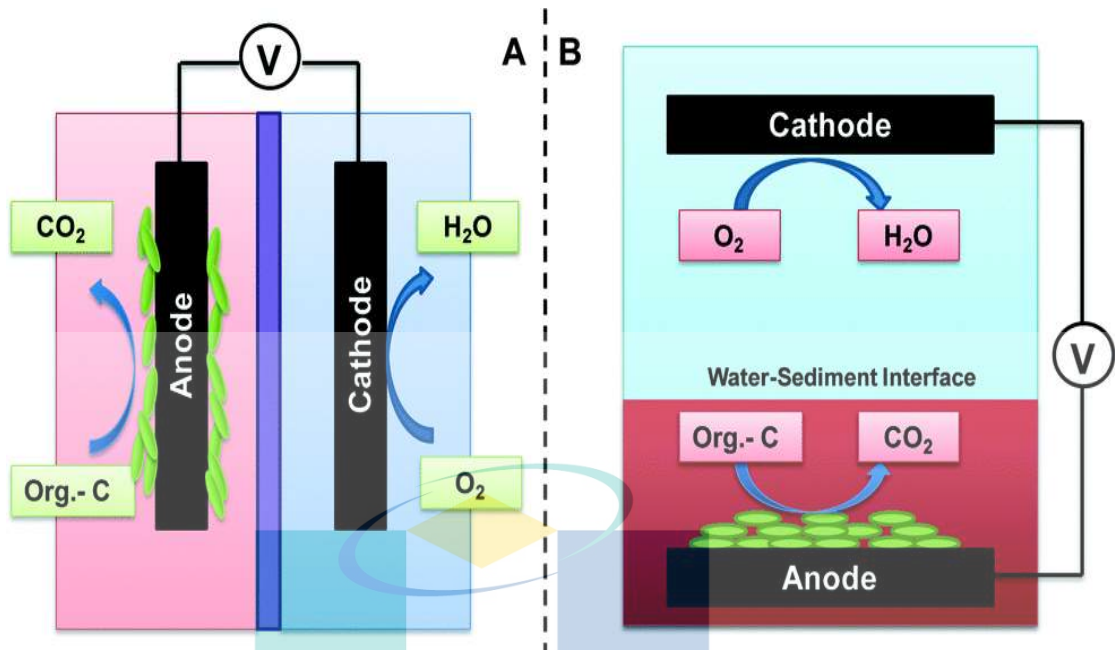


Figure 2.14 Sediment MFC
Source: Sudirjo, Buisman, & Strik, (2019)

2.7.4 Upflow MFC system

The upflow microbial fuel cell (UMFC) is presented in Figure 2.15 which was invented in 2006. From Figure 2.15, it can be seen that the system formed of an U-shaped cathode inside the anode chamber and produced a maximum volumetric power of 29.2 W/m³ with a volumetric loading rate of 3.40 kg COD/(m³/day) and an operating temperature of 35 °C. The upflow MFC mainly comprised of a plastic cylinder with carbon fiber brush electrodes, and glasswool/bead layers separator between anode and cathode compartments. An external column PBR was coupled with the upflow MFC, in which the effluent from the cathode compartment of the up flow MFC was continuously pumped into the column PBR. Continuous illumination was provided to the microalgal culture and a purge of CO₂ (effluent of MFC) and air mixture gas. The Coulombic efficiency was decreased from 51.0% to 10.6% with the increase in the volumetric loading rate from 0.57 to 4.29 kg COD/(m³/day). Besides this, the lab-scale UMFC maintained soluble chemical oxygen demand (COD) removal efficiencies exceeding 90% and volatile fatty acid concentrations of ~40 mg/L, giving information about efficient wastewater treatment (Z. He, Wagner, Minteer, & Angenent, 2006).

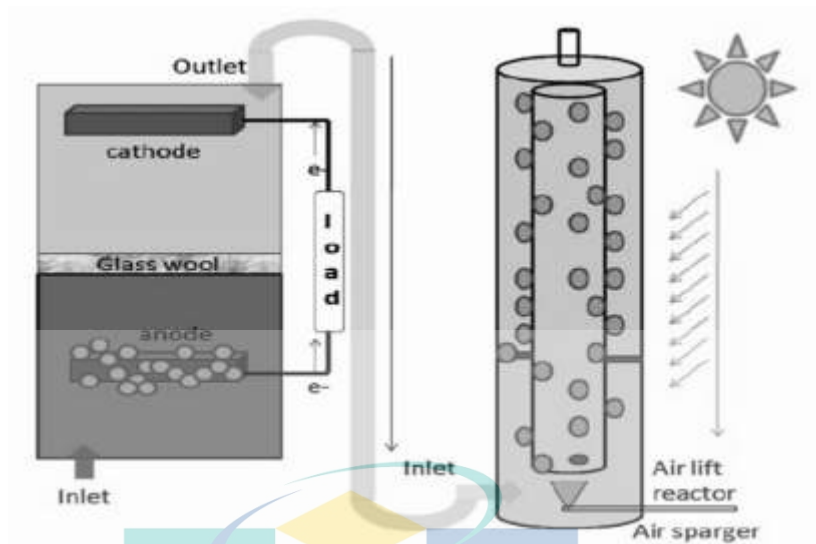


Figure 2.15 Upflow MFC

Source: Z. He et al., (2006)

2.8 Advantages and disadvantages of MFC

The reason that leads the research on MFCs is that MFC has operational and functional advantages over the current technology used for obtaining energy from organic matter. First of all, MFC has the potential to directly convert the substrate into electricity that provides high conversion efficiency (Sarmin et al., 2019). Secondly, MFCs can operate at room temperature and also even at low temperatures which separates the MFC from all existing bioenergy processes (B. Yu et al., 2020). Thirdly, an MFC does not require gas treatment because the off-gases of MFCs are enriched in CO₂ and normally have no useful energy content. Moreover, MFCs do not require any energy input for aeration provided the cathode is passively aerated (M. Li et al., 2019). Lastly, MFCs have the potential for widespread application in locations that lacked of electrical infrastructures and also to fulfill the increasing demands upon energy requirements of the world (Ram, Aghahosseini, & Breyer, 2020). However, at the present stage, full-scale implementation of MFCs for wastewater treatment is not straightforward because certain economic and technological problems need to be resolved. Firstly, in the field of wastewater treatment, the main challenges for commercializing scalable MFCs are developing materials that are cost-effective, efficient in power generation and identifying architectures that can be used at a larger scale (Gajda, Greenman, & Ieropoulos, 2018). According to Gao et al. reported that MFCs sizes have been tested at the scale of several litres or more, reported volumetric power densities were generally low (Gao et al., 2020). There are still many factors hidden behind that directly related to the low power density

generation from MFC and more study needs to be carried out in the future in order to increase the efficiency of the MFC and commercialize it one day.

2.9 Effects of operating conditions in MFC

2.9.1 Effect of Inoculum

Primarily, the performance of MFC increased with time; but after certain days of operation, the performance started deteriorating especially while operated with real wastewater (Linfang Zhang et al., 2019). There are several reasons such as electrode fouling and membrane blockage, which have been reported as predominant reasons for the decrease in a current generation (Giwa, Dindi, & Kujawa, 2019). Besides few studies reported that the fall in current generation occurred due to the thickness of the biofilm because it could affect the diffusion of substrates into the biofilm resulted in the formation of two layers (outer and inner) in the biofilm (Le & Nunes, 2016). Islam et al. told that the bacteria can easily form thin biofilm within 3 days of MFC operation and the cells then increase continuously and form an ineffective multilayer biofilm (Islam, Ethiraj, et al., 2017). In microbial fuel cell (MFC), the electroactive microorganisms can convert energy present in organic compounds directly into the electricity by utilizing electron transferring capability towards the anode electrode (S. Sarkar, 2020). Recently, a number of pure cultures such as *Aeromonas* sp., *Bacillus* sp. (Islam, Ethiraj, et al., 2017), *Escherichia* sp. (V. B. Wang et al., 2015), *Enterobacter* sp., *Geobacter* sp., *Klebsiella* sp. (Islam, Karim, et al., 2017), *Pseudomonas* sp., *Rhodospirillum rubrum* sp., *Shewanella* sp. (V. B. Wang et al., 2015), have been used as anode bio-catalyst in MFCs to investigate their capability of electricity generation and wastewater treatment. In most studies, the pure cultures achieved satisfactory power generation while simple substrates (glucose, acetate etc.) were used as nutrients (Islam et al., 2020). However, the pure culture is not considered as effective inoculum for wastewater fed MFC because most of the pure cultures are not capable of utilizing complex substrates (Islam et al., 2020). Therefore, very low power generation is achieved by MFCs while real wastewater used as substrates (Choudhury, Ray, Bandyopadhyay, & Bhunia, 2020). In contrast, the mixed cultures are considered robust inoculum as they are more tolerant to the extreme environmental conditions, able to accommodate wide range of substrates, available in nature (*i. e.* wastewater, soil, and so on), applicable in large scale, and highly efficient in the secretion of different hydrolytic enzymes to degrade complex biomass (Mudhoo, Ramasamy, Bhatnagar, Usman, & Sillanpää, 2020). However, in most cases, mixed cultures could not

achieve significant performance due to the irreversible relationships between or within microorganisms (Khaneghah et al., 2020).

The inter-microbial interactions within microbes play a crucial role to determine evolutionary relationship within the microbes in a microbial community, with system properties, particularly the dynamics and stability of the entire microbial communities (Sundarraman et al., 2020). In the past few years, the use of synergistic microbial consortia in MFCs has renewed attention because the synergistic interaction between microbes enabled degradation capability in wide range substrates (B. Zhang et al., 2020).

There are various types of inoculum used in MFC such as pure culture, and mixed culture. MFCs use microorganisms as biocatalysts to oxidize the organic matter and transfer electrons via substrate oxidation to the anodic surface for bio-electricity production (Aarthy, Rajesh, & Thirunavoukkarasu, 2020). The performance of using different type's culture is presented in the Table 2.3.

Table 2.3 The performance of using different types of culture

Substrate	Inoculum	Electrode materials	Power density using pure culture (1)	Power density using pure culture (2)	Power density using co-culture (1 and 2)	Ref.
Lactate	<i>S. oneidensis</i> (1) and <i>E. coli</i> (2)	Carbon felt	0.3 $\mu\text{A}/\text{cm}^2$	0.28 $\mu\text{A}/\text{cm}^2$	2 $\mu\text{A}/\text{cm}^2$	(La, Jeon, Sang, Yang, & Cho, 2017)
Xylose	<i>S. oneidensis</i> (1) and <i>E. coli</i> (2)	Carbon cloth	92.8 mW/m^2	91.76 mW/m^2	728 mW/m^2	(F. Li et al., 2017)
Artificial wastewater	<i>G. sulfurreducens</i> (1) and <i>E. coli</i> (2)	Nickel wire	128 mW/m^2	56 mW/m^2	63 mW/m^2	(Koo & Jung, 2019)
Glycerol	<i>P. aeruginosa</i> (1) and <i>E. aerogens</i>		2.25 mW/m^2	1.92 mW/m^2	0.72 mW/m^2	(Temple & O'Donnell, 2020)

From the Table 2.3, it can be seen that among the inoculums, the co-culture inoculum of *S. oneidensis* (*Shewanella oneidensis*) and *E. coli* (*Escherichia coli*) (MFC_{SE}) showed synergistic interaction between the microbes resulting in drastic increased in the performance of MFC. The synergistic interaction between *S. oneidensis* and *E. coli* is also reported by the literature. Yadav and his co-workers observed that the syntrophic co-culture of *S. oneidensis* and *E. coli* showed better decolorization efficiency (80%) and

reduction of pollution parameters (COD 73% and BOD 62%) than the mono cultures (Yadav & Chandra, 2015). In another study, Patel et al. reported that two co-cultures composed of *S. oneidensis*, *E. coli*, and *Enterobacter cloacae* resulted in H₂ yield up to 3.0 mol/L of glucose (S. K. Patel et al., 2014). Apart from that, several studies have reported that the synergism between G⁺ and G⁻ within the MFC environment (X.-Q. Lin, Li, Liang, Nan, & Wang, 2019). For example, the role of a phenazine electron shuttle has been verified in an earlier MFC study where it was observed to increase the current generation in co-cultures of *Brevibacillus sp.* and *Enterococcus sp.* with *Pseudomonas spp.* (D. Liu et al., 2020). These studies determined that the G⁺ were able to use electron shuttles (mediators) produced by *Pseudomonas sp.* the combination of both bacteria being the more successful one. Moreover, Read et al. reported that the power output of co-cultures Gram- positive *Enterococcus faecium* and Gram-negative *Pseudomonas aeruginosa*, increased by 30-70% relative to the single cultures (D. Liu et al., 2020).

2.9.2 Effect of Substrates

In MFCs, the substrate is regarded as one of the most important biological factors affecting electricity generation (Xin et al., 2020). A great variety of substrates can be used in MFCs for electricity production ranging from pure compounds to complex mixtures of organic matter present in wastewater. The objective of the various treatment processes is to remove pollutants from waste streams before their safe discharge to the environment (Kaur, Marwaha, Chhabra, Kim, & Tripathi, 2020). In the last century, the activated sludge process (ASP) has been the mainstay of wastewater treatment. However, it is a very energy-intensive process and according to an estimate, the amount of electricity needed to provide oxygen in ASPs in the USA is equivalent to almost 2% of the total US electricity consumption (Sala-Garrido & Molinos-Senante, 2020). At the same time, the addition of a second treatment step changes the status of several streams generated in the wastewater treatment of agro-industry from “waste” to “raw material” which can eventually be utilized for the production of specific chemicals or energy (L. C. Rodrigues et al., 2020). Moreover, the emphasis of today’s waste management is on reuse and recovery of energy, which has led to new views on how these streams can be dealt with. Table 2.4 presents a comprehensive list of substrates that have been used in MFC studies. It is difficult from literature to compare MFC performances, due to different operating conditions, surface area and type of electrodes and different microorganisms involved (Xin et al., 2020). From Table 2.4, it can be seen that the starch with mixed culture showed better performance than others. Besides, starch is the most common simple substrates which are easily degraded by the microbes. So that the performance increases.

Table 2.4 Different types of substrates used in MFC

Type of substrate	Concentration (mg/L)	Source of inoculum	Type of MFC	Power density (mA/cm ²)	Reference
Acetate	1000	Acclimatized AS	Cube shaped one-chamber	0.8	(Sawalha, Maghalseh, Qutaina, Junaidi, & Rene, 2020)
Arabitol	1220	Acclimatizd AS	One-chamber MFC	0.68	(Elmaadawy et al., 2020)
Azo dye with glucose	300	Mixed culture	One-chamber air-cathode	0.09	(Q. Dai, Zhang, Liu, Huang, & Li, 2020)
Carboxy methyl cellulose	1000	Co-culture	Two-chamber	0.05	(Borciani et al., 2020)
Cellulose particles	4000	Pure culture	U-tube MFC	0.02	(El Chakhtoura, 2011)
Corn stover biomass	1000	Domestic wastewater	One-chamber	0.15	(B.-M. An, Seo, Hidayat, & Park, 2020)
Cysteine	385	Anaerobic sludge	Two-chamber	0.0186	(Korshunov, Imlay, & Imlay, 2020)
1,2 Dichloroethane	99	Acclimatized anaerobic sludge	Two-chamber	0.008	(Kundu & Dutta, 2018)
Ethanol	1000	Anaerobic sludge	Two-chamber	0.025	(L. Feng, Liu, Zhang, Li, & Wu, 2020)
Farm manure	3000	Self build up of anaerobic environment	One reactor vessel	0.004	(S. Singh & Chakraborty, 2020)

Type of substrate	Concentration (mg/L)	Source of inoculum	Type of MFC	Power density (mA/cm ²)	Reference
-------------------	----------------------	--------------------	-------------	-------------------------------------	-----------

Table 2.4 Continued

Type of substrate	Concentration (mg/L)	Source of inoculum	Type of MFC	Power density (mA/cm ²)	Reference
Furfural	6800	Acclimatized anaerobic sludge	One-chamber air-cathode	0.17	(Sheng, Tan, Zhou, & Xu, 2020)
Galactitol	1220	Acclimatized anaerobic sludge	One-chamber air-cathode	0.78	(Allam, Elnouby, El-Khatib, El-Badan, & Sabry, 2020)
Glucose	2000	Mixed Culture	Air cathode	0.70	(Adeel et al., 2020)
Glucuronic acid	2000	Mixed bacterial culture	One-chamber air-cathode MFC	1.18	(Q. Yuan, Liu, & Song, 2020)
Lactate	1800	Pure culture	Two-chambered MFC	0.005	(Obata et al., 2020)
Phenol	400	Mixed culture	Two chambered MFC	0.1	(N. Khan, Anwer, Ahmad, Sabir, & Khan, 2020)
Propionate	530	Anaerobic sludge	Two-chambered MFC	0.035	(Birjandi et al., 2020)
Starch	10000	Mixed culture	Two-chambered MFC	1.3	(Allam et al., 2020)
Brewery wastewater	2240	Anaerobic sludge	One-chamber air-cathode MFC	0.2	(Mahmoudi, Mousavi, & Darvishi, 2020)

Table 2.4 Continued

Type of substrate	Concentration (mg/L)	Source of inoculum	Type of MFC	Power density (mA/cm ²)	Reference
Chocolate industry wastewater	1459	Activated sludge	Two-chambered MFC	0.302	(Ramadan, Abd-Alla, & Abdul-Raouf, 2020)
Domestic wastewater	600	Anaerobic sludge	Two-chambered MFC	0.06	(Ramadan et al., 2020)
Food processing wastewater	1672	Anaerobic sludge	Two-chambered MFC	0.05	(Kaur et al., 2020)
Meat processing wastewater	1420	Anaerobic sludge	One-chamber (28 mL) MFC	0.115	(J. Li, Ziara, Li, Subbiah, & Dvorak, 2020)
Paper recycling wastewater	2452	Anaerobic sludge	One-chamber MFC	0.25	(Nannan Zhao, Treu, Angelidaki, & Zhang, 2019)
Swine wastewater	8320	Anaerobic sludge	One-chamber MFC	0.015	(Kaur et al., 2020)
Synthetic wastewater	510	Anaerobic sludge	Dual chamber MFC	0.008	(Chakraborty, Das, Dubey, Ghangrekar, & Physics, 2020)
Wastewater amended with acetate	1600	Anaerobic sludge	Submersible MFC	0.08	(Obata et al., 2020)

2.9.2.1 Substrate-inoculum relation in MFC

In MFCs, the substrate is one of the most important factors affecting electricity generation because of serving as a nutrient and energy source for the growth of microorganisms involved. To date, in the most of the MFC studies have been used pure compounds such as glucose (Karekar, Srinivas, & Ahring, 2019), ethanol (Saputra, Amri, Marshall, & Gostomski, 2019) and cysteine (Ivase, Nyakuma, Oladokun, Abu, & Hassan, 2020) as an amino acid for electricity generation. In addition to pure compounds, MFCs can generate electricity directly from various complex substrates such as domestic wastewater (Corbella et al., 2019), ocean sediments (Pushkar & Mungray, 2020) and various industrial wastewater such as starch processing wastewater (Haldar, Manna, Sen, Bhowmick, & Gayen, 2019), beer brewery wastewater (Werkneh, Beyene, & Osunkunle, 2019). In order to capture electrical energy from wastewater, a better understanding is needed on how the operating conditions of the system affect microbial communities (particularly exoelectrogenic populations), current densities, and recovery of the substrates as current. The complex mixture of organics presented in most wastewater streams suggests that diverse microbial communities are needed to oxidize the organic matter since many exoelectrogenic bacteria can only utilize a limited range of substrates (Bolognesi et al., 2020). In addition, it is also necessary to understand the bacterial community and dominant species contributing to exoelectrons transfers in the anode biofilm in order to obtain better performance from an MFC (Inohana, Katsuya, Koga, Kouzuma, & Watanabe, 2020). The substrates-microbes interaction in MFC for power generation is presented in Figure 2.16. The power production in the MFCs can be also dependent on the presence of specific strains. For example, *Shewanella oneidensis* consistently produces power densities that are much lower than mixed culture communities in MFCs (Y. Cao et al., 2019b). Thus, based on 16S rDNA sequencing analysis, it is important that the bacterial consortia and pre-dominant species vary with operational conditions, such as inoculum and substrate type (Hanchi, Mottawea, Sebei, & Hammami, 2018). There is little information on how the operational environment affects community structure and system performance for this bio-electrochemical system. For example, diffusion of oxygen into the anode chamber can affect power generation in an MFC (S.-S. Wang, Sharif, Cheng, & Wang, 2019), and presumably the microbial community structure.

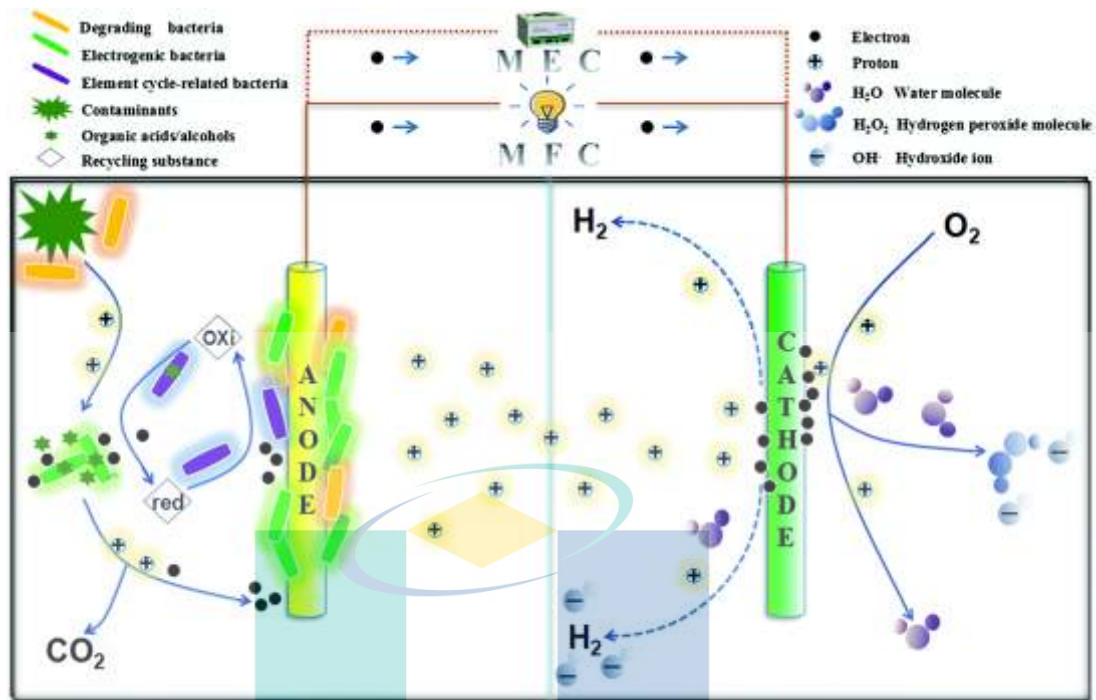


Figure 2.16 Substrates- microbes interaction in MFC for power generation
 Source: Chiranjeevi, Yeruva, Kumar, Mohan, & Varjani, (2019)

Community analysis of MFC biofilms shows that there is no single emergent microorganism in the bacterial communities developing on the anode. Because, there are several different bacteria capable of electricity production in respect to the range of operating conditions, system architectures, electron donors and electron acceptors at the cathode (Tahir et al., 2019). Finally, from the above discussion, it is clear that the interaction between microbes and substrates for better electricity generation.

2.9.3 Effects of pH

It is known that most of the bacteria can grow around pH a value of 6.5-7.0. However, each microbial species has its own pH range for the best growth (W. Song et al., 2019). Zeppilli et al. described that the optimum pH for methanogenic archaea was 6.6–7.5 (Zeppilli et al., 2020). By another study, Yuan et al. (2015) observed that the dominant genus responsible for fermentation usually grows between pH 4 and 10 (Y. Yuan et al., 2015). For instance, the microorganisms such as *Clostridium*, *Ruminococcaceae*, *Actinomyces*, *Tetrasphaera*, and *Zoogloe* grow at pH 4, while *Alcaligenes*, *Anaerolinea*, and *Paludibacter* grow well at or near pH 10. However, the ratio of co- culture and mixed culture inoculum composition can be severely affected by

the varying pH and that in turn influences the performance of MFCs (Vrancken, Gregory, Huys, Faust, & Raes, 2019).

2.9.4 Effects of operating temperature

Operating temperature becomes an important factor to consider when commercializing MFC technology. Unlike a laboratory environment with controlled temperature, MFCs in a real-world application will be exposed to a wide and variable range of operating temperature thus the effect of this parameter on MFC performance (S. Li & Chen, 2018). The majority of MFC research has been conducted under ambient temperature and performance reduction was observed when the operating temperature decreased (Abo-Zahhad et al., 2020). On the other hand, increasing the operating temperature had a positive effect on the current generation (Radwan & Mahrous, 2019). However, it seems that MFCs can be quite tolerant with temperature variation; a recent study demonstrated that a mixed culture anode biofilm inoculated from wastewater can adapt to temperature fluctuations within a temperature range between 0 °C to 45 °C (Krishna, Swathi, Hemalatha, & Mohan, 2019).

2.9.5 Effects of external resistance

In electronics, it is well known that the maximum power transfer (MPT) can be achieved when the external resistance (R_{EXT}) is matched with the internal resistance (R_{INT}) of a system, which is known as Jacobi's law (Jiseon You, 2016). Thus, selecting an external resistor corresponding to the R_{INT} is critical when maximizing power output. For an MFC using organic matter as fuel, external resistance also affects the microbial metabolism in terms of coulombic efficiency (Babanova et al., 2020). Furthermore, in long-term operations, R_{EXT} affects the structure of the anode biofilm. Several studies have shown that electroactive species could be selected by controlling the R_{EXT} during the maturing period (Pasternak, Greenman, & Ieropoulos, 2018). These studies reported that R_{EXT} has a great influence on the length of maturation, suppression of methanogenic growth, morphology and EPS content of anode biofilm.

2.10 Factors limiting the energy generation in microbial fuel cell

The MFC performance depends on different important factors; such as obstacles to electron transfer through the biofilm, ion migration between the anode and cathode,

biofilm formation and maintenance diffusion problems concerning the substrate and reactants, and the kinetics of cathode reaction (Mani, 2019). This is known as internal resistance. The MFC cell voltage is acquired by the difference value between the cathode and anode equilibrium potentials, which is also determined as the theoretical cell voltage or open cell voltage (equation 2.1).

$$OCV = E_{cathode} - E_{anode} \quad 2.1$$

The practical cell voltage is a voltage that achieved by considering the over-potential losses. These losses are two main types such as i) the over-potentials of the anode and the cathode (equation 2.2) (Mani, 2019),

$$\Delta E_{\eta} = \Sigma \eta_{cathode} - \Sigma \eta_{anode} \quad 2.2$$

ii) The ohmic voltage losses of the system (equation 2.3) (Höflinger, Hofmann, & Geringer, 2019).

$$\Delta E_{\Omega} = I \Sigma R_{\Omega} \quad 2.3$$

Moreover, the real cell voltage is the value of the OCV subtracted of the over-potentials and ohmic losses (equation 2.4) (Toghyani, Afshari, & Baniasadi, 2019).

$$\Delta E = OCV - \Delta \Sigma \eta - \Delta E_{\Omega} \quad 2.4$$

where, OCV is open circuit potential (V), E_{anode} is anode potential (V), ΔE is real cell voltage (V), $E_{cathode}$ is cathode potential (V), η_{anode} is anode overpotential (V), $\eta_{cathode}$ is cathode overpotential (V), ΔE_{η} is overpotential difference between anode and cathode (V), ΔE_{Ω} is ohmic voltage losses. The total over-potential (TOP) of an electrode can be classified into two types, i.e. i) the activation, ii) concentration over-potentials. If there is no discrimination necessary, the total over-potential losses can be calculated as the difference between the electrode potential under consideration (E) and the equilibrium potential (E_e) in equation 2.5 (Chmielowiec, 2019).

$$\eta_{electrode} = E - E_e \quad 2.5$$

where, $\eta_{electrode}$ is the difference between equilibrium potentials, E is electrode potentials, E_e is equilibrium potentials. In some cases, it is useful to analyze the over-potentials to understand how they are influencing the MFC performance and try to minimize them.

2.10.1 Ohmic losses

Electron flow is hindered by the resistance of the electrode material which brings an ohmic loss to the cell. If the conductivity is high and the contact losses, travel distance inside the electrode are low then higher will be the electron conduction and lower will be the ohmic loss (Hu, Zhang, Komini Babu, Kongkanand, & Litster, 2019). Moreover, for each negative charge transferred to the anode, an equivalent amount of positive charges requires to flow to the counter electrode. The ions experience the resistance when pass through the electrolyte is also a part of ohmic losses to the reactor. For the better transfer of ions, the conductivity, distance between the electrodes, the buffer capacity of the electrolyte are of utmost importance. There are many techniques available to characterize the ohmic losses (region B of Figure 2.17) (Pedersen, 2019). Plotting polarization curve, current interrupt method or electrochemical impedance spectroscopy, can determine the ohmic losses in the microbial fuel cell.

2.10.2 Activation losses

To initiate the transfer of electrons from microorganisms to the electrode or to the final electron acceptor, the energy barrier requires to be overcome and that causes voltage loss or activation overpotential (I. Chakraborty, S. Sathe, C. Khuman, & M. Ghangrekar, 2020). Activation losses are characterized by an early sudden decrease of the cell voltage at the commencement of the electricity production (region A of Figure 2.17). When the current steadily increases, the other losses such as ohmic losses and mass transfer losses turn into proportionally more significant. To attain low activation losses the following need to be done such as (i) improving the electrode catalysis, (ii) increasing the electrode surface area, (iii) increasing the operating temperature and for microbial catalysis, enriching the biofilm on the electrode surface (Zago et al., 2020). It is assumed that microbes can lower the activation loss through catalysis and also increases the metabolic energy by optimizing their electron transfer mechanisms (PrévotEAU, Carvajal-Arroyo, Ganigué, & Rabaey, 2020).

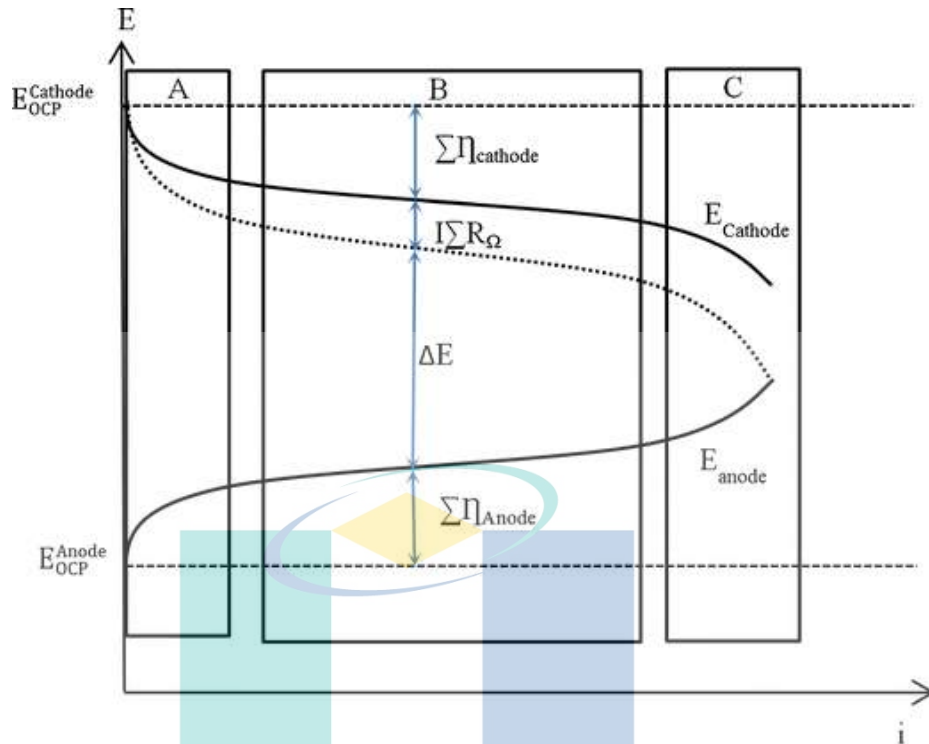


Figure 2.17 Different types of losses in MFC
 Source: Mahadevan, Gunawardena, & Fernando, (2014)

2.10.3 Mass transfer losses

The supply of enough substrate to the biofilm on the anode surface and electron acceptor to the cathode surface equal to the rate of the current generation is vital to maintain the current generation (Xin et al., 2020). Moreover, during the fuel cell process waste products such as protons or oxidized intermediates accumulates in the biofilm which should not be allowed because this might alter the redox conditions and hinder the metabolic activity of the biofilm (H. Chen, Dong, & Minteer, 2020). Inadequate mass transfer of substrate or electron acceptors to the anode or cathode leads to mass transfer or concentration losses (Srivastava, Abbassi, Yadav, Garaniya, & Jahromi, 2020). Usually, mass transfer losses are characterized by a sharp decrease in the voltage in the polarization curve near to the maximum current densities (Figure 2.17). Besides that, poor transfer protons from anode to cathode may cause a pH gradient which can seriously influence the MFC performance (Do et al., 2020).

2.11 Electron transfer and biofilm formation in MFC

Since electrodes are solid entities that cannot penetrate the bacterial cells, a major requirement is that electrons are to be transferred from the inside of the microbial cell

membrane to its outside either via the physical transfer of reduced compounds, or via electron hopping across the membrane using membrane-bound redox enzymes (T. H. T. Nguyen, Lee, Kim, Nam, & Kim, 2020). For an efficient electron transfer the linking species must fulfil the following requirements (D. Wang et al., 2020):

(i) It must be able to physically contact the electrode surface.

(ii) It must be electrochemically active, i.e., it must possess a low oxidation overpotential at given electrode surfaces.

(iii) The standard potential of the linking species should be as close to the redox potential of the primary substrate as possible, or must at least be significantly negative to that of the oxidant (usually oxygen).

2.11.1 Direct electron transfer (DET)

The direct electron transfer requires that the microorganisms possess membrane-bound electron transport protein relays that transfer electrons from the inside of the bacterial cell to its outside, terminating in an outer membrane (OM) redox protein that allows the electron transfer to an external, solid electron acceptor (a metal oxide or an MFC anode) (Alvarado, Behrens, & Josenhans, 2020). C-type cytochromes especially evolved with sediment inhabiting metal reducing microorganisms such as, *Geobacter*, *Rhodospirillum rubrum*, and *Shewanella* that, in their natural environment, often have to rely on solid terminal electron acceptors like iron (III) oxides (Na Zhao, Ma, Song, Xie, & Wang, 2019). In the case of these organisms, the MFC anode can conveniently resume the role of the solid electron acceptor. As mentioned, the DET via outer membrane cytochromes requires the physical contact (adherence) of the bacterial cell and of the cytochrome to the fuel cell anode, with the consequence that only bacteria in the first monolayer at the anode surface are electrochemically active (Aiyer, 2020a). Besides, recently it has been demonstrated that, e.g., some *Geobacter* and the *Shewanella* strains can evolve electronically conducting molecular pili (nanowires) that allow the microorganism to reach and utilize more distant solid electron acceptors (Michelson, Alcalde, Sanford, Valocchi, & Werth, 2019), These pili also allow the organisms to use an electrode that is not in direct cell contact as its sole electron acceptor which is shown in Figure 2.18. The pili are connected to the membrane-bound cytochromes, via which the electron transfer

to the outside of the cell is accomplished. The formation of such nanowires may allow the development of thicker electroactive biofilms and thus higher anode performances (Logan, Rossi, & Saikaly, 2019). It is reported in the literature that ten-fold increases in fuel cell performance upon the nano-wire formation of *Geobacter sulfurreducens*. The DET from living bacteria to an electrode has been clearly identified and the redox potential of the involved species has been undertaken (Aiyer, 2020a). Thus, at the open circuit, however, the redox potential of a metabolizing anaerobic bacterial culture will shift considerably towards negative potentials due to the strong shift of the concentration term of the Nernst equation towards the reduced species (Aiyer, 2020a).

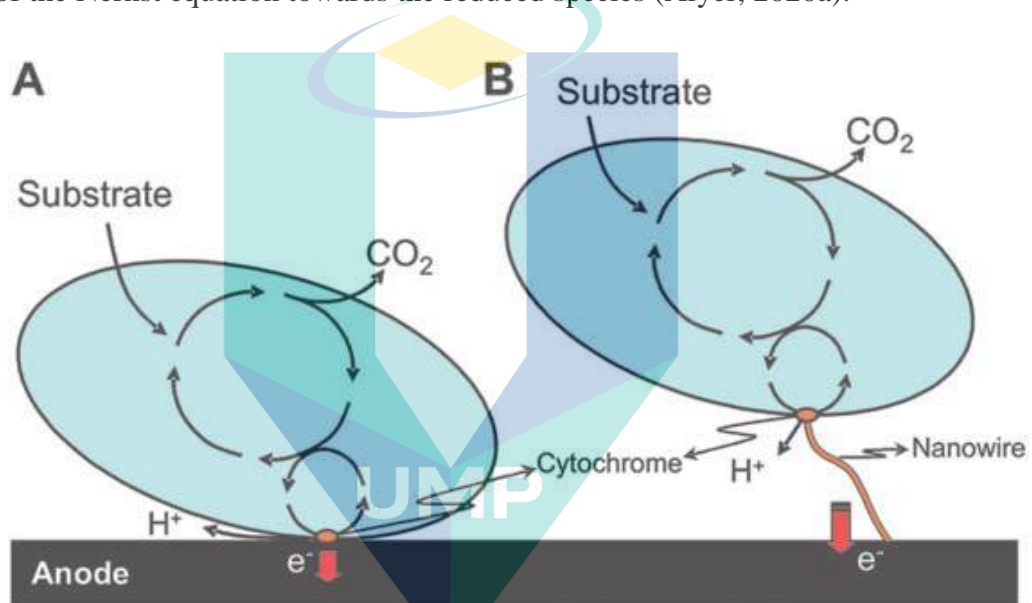


Figure 2.18 Direct electron transfer

Source: S. Qin et al., (2019)

Thus, the open circuit potential may not be equal to the formal potential of the cytochrome based electron transfer. The potential values provided in Table 2.5.

Table 2.5 Different microbes el

Bacterial strain	E'/V ^a
<i>Shewanella putrefaciens</i> IR-1	0.01
<i>Shewanella putrefaciens</i> MR-1	-0.02
<i>Shewanella putrefaciens</i> SR-1	-0.01
<i>Aeromonas hydrophila</i> PA 3	0
<i>Clostridium</i> sp. EG 3	0

Source: Chung, Gwak, Moon, Rho, & Ryu, (2020)

The redox potential of the different bacterial species is virtually identical, with a mean value of 0 V and the shape of the cyclic voltammograms is very similar for all

species. The redox activity to the electron mediation via outer membrane cytochromes, which are believed to be responsible for the DET (Krishna et al., 2019). The assumption is supported by the measurement of washed and freshly re-suspended bacterial cells, which should exclude the presence of bacterial mediators. Since the DET via bacterial nanowires (Figure 2.18 B) is reported to proceed via the membrane-bound cytochromes it will, for the following considerations, be assumed that the same standard redox potentials apply for the cytochrome and nanowire-based electron transfer (Lovley & Walker, 2019).

2.11.2 Mediated electron transfer

MET mechanisms represents an effective means to wire the microbial metabolism to a fuel cell anode which is shown in Figure 2.19.

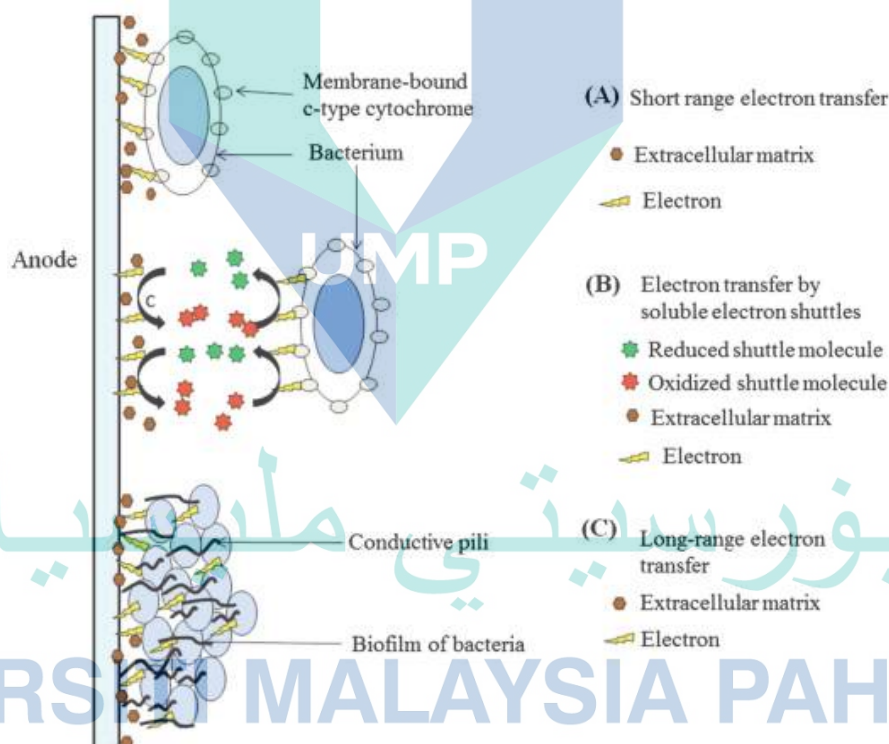


Figure 2.19 Mediated electron transfer process

Source: Choi & Sang, (2016)

Although, DET is the choice for an efficient current generation in MFCs mediated electron transfer (MET) is also important in MFC in terms of current and power densities, MET via exogenous (artificial) redox mediators (Samer, 2015). A large number of compounds, the majority based on phenazines, phenothiazines, phenoxazines, and

quinones were investigated for their suitability and behavior as MFC mediators (D. Liu et al., 2020), (Table 2.6). An interesting spin-off of these studies was the research into so-called gastrobots (or ecobots), i.e., MFC powered robotics systems.

Table 2.6 Selection of exogenous redox mediators used for microbial fuel cell

Redox mediator	Redox potential E ⁰ /V
Neutral Red, Safranin, Phenazine ethosulfate	-0.32, -0.29, 0.06
New Methylene Blue Toluidine Blue O Thionine Phenothiazinone	-0.02, 0.03, 0.06, 0.13
Resorufin, Gallocyanine	-0.05, 0.02
2-Hydroxy-1,4-naphthoquinone Anthraquinone-2,6-disulfonate	-0.14 -0.18

Source: Wu, Sun, Chua, & Zhou, (2020)

The greatest disadvantage of the use of exogenous redox mediators is, beside the usually low current densities (10–100 mA /cm²), the necessity of a regular addition of the exogenous compound, which is technologically unfeasible and environmentally questionable and leads to the general abandonment of the approach.

2.11.3 Primary and secondary metabolism

The characterization of the electron transfer mechanisms requires a differentiation of the species involved in the electron transfer by means of their origin and relevance for the microbial metabolism for primary and secondary metabolites, i.e., products of the primary and secondary metabolism, respectively (H. Chen et al., 2020). Primary metabolites are compounds that are essentially connected to microbial metabolism. They are similar in all groups of living organisms and the major products of catabolic substrate degradation, such as fermentation products and reduced electron acceptors (Prakasham & Kumar, 2019). Secondary metabolites, on the other hand, are usually not directly connected to the main metabolic pathways. Microorganisms, as well as, all higher organisms produce a great variety of these compounds. They may be specific for a certain organism and may serve very different purposes, such as intercellular communication, antibiotics, etc. (Beran, Köllner, Gershenzon, & Tholl, 2019).

2.11.3.1 MET via secondary mediators

Often microorganisms grow under conditions in which neither soluble electron acceptors are available nor solid electron acceptors are in direct reach (for DET). For example, when a thick biofilm, where, e.g., oxygen diffusion into the depth of the film is limited and the cell is not in direct contact with a solid electron acceptor. On the other hand, the microorganism may either use externally available (exogenous) electron shuttling compounds like humic acids or metal chelates or can itself even produce low-molecular, electron shuttling compounds via secondary metabolic pathways such as pyocyanin and 2-amino-3-carboxy-1,4-naphthoquinone, ACNQ (Table 2.6) (Cheeseman et al., 2020). Very different microbial strategies for such mediated transfer exist, and the reader may be referred to as an excellent already reported by literature (Chevrette et al., 2020). The mediator serves as a reversible terminal electron acceptor, transferring electrons from the bacterial cell either to a solid oxidant (the MFC anode) or into aerobic layers of the biofilm, where it becomes re-oxidized and is again available for subsequent redox processes. One molecule can thus serve for thousands of redox cycles (Krishnaraj & Sani, 2019). Consequently, the production of small amounts of these compounds (directly in the anodic biofilm) enables the organism to dispose of electrons at sufficiently high rates. Especially in batch cultures, these redox mediators effectively facilitate the electron transfer and increase the efficiency of the current generation. The theoretical energy efficiency of the current generation. The identification of the extracellular electron shuttling compounds appears to be highly challenging, and so far, only the involvement of pyocyanin and phenazine-1-carboxamide, produced by *Pseudomonas aeruginosa* in the electron transfer to an MFC anode has been proved (S. Rana, Singh, & bin ab Wahid, 2019). Further, it has been reported by the literature that quinone-type redox shuttles support the long distance electron transfer of *Shewanella* species like *Shewanella oneidensis* (Conley & Gralnick, 2019) to electrodes or to solid electron acceptors like Fe^{3+} oxide involving DET via c-type cytochromes and electronically conducting nanowires (Michelson, Alcalde, Sanford, Valocchi, Werth, et al., 2019). Table 2.7 provides an overview of the energy efficiency of the bacterial MET.

Table 2.7 Some common exo-electrogens with their electron transfer mechanism

Microbes	Power density	Proteins involved in electron transfer	Reference
<i>Shewanella oneidensis</i>	3000 mW/m ²	Riboflavin, flavins,	(Y. Yang, Jiang, Liu, & Si, 2020)
<i>Geobacter metallireducens</i>	40 mW/m ²	OmcB, OmcE and c-Type cytochromes,	(X. Liu, Ye, Xiao, Rensing, & Zhou, 2020)
<i>Thermincola ferriacetica</i>	12,000 mA/m ²	-	(Atiénzar Fernández, 2020)
<i>Rhodopseudomonas Palustris</i>	2720 mW/m ²	Anthra quinone-2,6-disulfonate, c-Type cytochromes	(Soundararajan et al., 2019)
<i>Desulfovibrio alaskensis</i>	-	Tetraheme cytochrome C3, transmembrane complexes (QrcA)	(Semkiw, Brown, & Wall, 2014)
<i>Pseudomonas aeruginosa</i>	4310 mW/m ²	Phenazine-1-carboxamide, Pyocyanin,	(S. Sarkar, 2020)
<i>Klebsiella pneumonia</i>	199 mA/m ²	2,6-di-tert-butyl-p-benzoquinone	(Islam et al., 2020)

Note: Units of volume power density are presented in W/m³, units of surface power density are presented in mW/m², and units of current density are mA/m².

It has been argued, this high efficiency may be confined to batch systems, whereas in open (flow) systems a steady loss of mediators may occur, leading to a decreasing value of n and thus to a decreasing coulombic and energetic efficiency. However, recent studies suggest that such losses may be low due to a confinement of the redox shuttles within the biofilm via electrostatic forces (Manyi Sun, Ren, Li, Lu, & Ding, 2019). The production of these electron shuttling compounds is, however, probably energetically expensive leading to additional biological losses.

2.11.3.2 MET via primary mediators

In contrast to the secondary metabolites, the production of reduced primary metabolites is closely associated with the oxidative substrate degradation (Chomel et al., 2016). Naturally, the total amount of reduction equivalents produced matches the amount of oxidized metabolites (Figuroa et al., 2018). To be utilizable as a reductant for anodic oxidation the metabolite has to fulfil certain requirements. Its redox potential should be as negative as possible and it must be accessible for electrochemical oxidation under MFC conditions (H. Xu et al., 2020). The lists of primary mediators with redox potential is presented in Table 2.8.

Table 2.8 Selection of extracellular bacterial (endogenous) redox mediators

Name	Redox potential, E ⁰ /V
Phenazine-1-carboxamide	-0.115
Pyocyanin (phenazine)	-0.03
2-Amino-3-carboxy-1,4-naphthoquinone (ACNQ)	-0.071

Source: Zheng et al., (2020)

However, the utilization of anaerobic respiration for MFC operation shown in Figure 2.20. In principle, any terminal electron acceptor that has a redox potential sufficiently negative to that of the oxygen electrode, that is reversibly oxidizable, and that is soluble in water in its reduced and oxidized form, can be utilized to establish the anodic electron transfer in a MFC (Sevda et al., 2020).

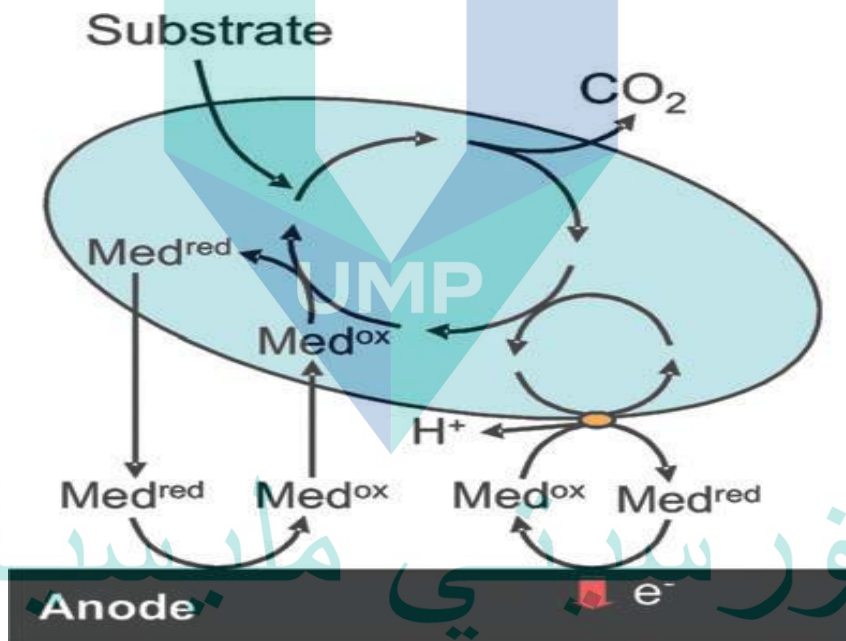


Figure 2.20 Anaerobic respiration of MFC

Source: S.-W. Li, Zeng, & Sheng, (2017)

As described in Table 2.8, the standard potential of Fe³⁺/Fe²⁺ is too positive for an anodic redox mediator. However, the redox potential of the Fe³⁺/Fe²⁺ couple can be significantly shifted towards negative values via the preferable complexation of Fe³⁺ with respect to Fe²⁺ (e.g., with humic acids), which may allow the use of the Fe²⁺/Fe³⁺ system for MFC electron mediation. With a biological standard potential of 0.22 V, the sulfate/sulfide redox couple is thermodynamically the most suitable system and sulfate reduction

is a common respiratory path amongst anaerobic bacteria, (Bagetta, Cosentino, Corasaniti, & Sakurada, 2016) and especially in waste water based MFCs and benthic fuel cells (Kubota et al., 2019) sulfide oxidation represents an important electron transfer mechanism. Further, many sulfate reducers cannot completely degrade the substrate, which further lowers the energetic yield. Additionally, the electrochemical re-oxidation of sulfide to sulfate is difficult, since metallic electrodes are easily poisoned by sulfide due to its strong and often irreversible adsorption. Also, the electrochemical oxidation is usually hampered by the formation of solid sulfur, inhibiting further oxidation (Garcia-Segura et al., 2020).

2.11.4 Biofilm formation mechanism

Biofilm is composed of a variety of biomolecules associated with extra polymeric substances (EPS) or matrices. Generally, biofilm microorganisms are capable to adhere with each other or onto the surface through the secretion of EPS (Karygianni, Ren, Koo, & Thurnheer, 2020). The self-assembled microbial communities are capable of optimizing their functions and regulate various metabolic activities in favor of the enclosed microbial clumps. A series of gene expressions are involved to regulate the formation, multiplication, and dispersal of the mature biofilms. The overall biofilm formation is shown in Figure 2.21.



Figure 2.21 Biofilm formation mechanism

Source: Fuqua, Filloux, Ghigo, & Visick, (2019)

2.11.4.1 Importance of biofilm formation on MFC performance

Generally, the biofilm formation is detrimental since it causes bio-fouling on membrane bioreactors (MBR) as well as in other biological wastewater treatment systems. However, unlike other processes, in MFCs, biofilm is considered as the powerhouse due to the presence of high cell density through which predominant electron transfer occurs with minimum diffusion path (Y. Li et al., 2020). Therefore, the matured biofilm that inevitably formed on the anode surface during MFC operation is considered as a predominant source of electrons (B. Wang, Liu, Zhang, & Wang, 2020). In MFCs, it is imperative if electro-active biofilms are produced having the ability to transfer electrons to the electrode through the metabolism of microbes (Noori, Bhowmick, et al., 2020). Biofilms are very important in wastewater treatment processes, soil and plant ecology (K. L. Rana, Kour, Yadav, Yadav, & Saxena, 2020). In the case of microbial fuel cell technology, the electrical current generated by an anodic biofilm containing EAB typically increases with the amount of active biomass attached to the electrode (J. Y. Chen, Xie, & Zhang, 2019). The mechanism of coordination among cells and intracellular components during electron transfer through a multilayer/thick biofilm and at the interface between anode and biofilm interface remains unresolved (Hou et al., 2020). Little has been reported on how the inefficient layer of biofilm can interrupt the charge transport to the electrodes, and its effect on the catalytic current generation (Ameen, Alshehri, & Nadhari, 2019). However, the mechanism of coordination among cells and cellular components during transport of electrons through a thick biofilm and at the anode/biofilm interface remains unresolved (Czerwińska-Główka & Krukiewicz, 2020).

Electroactive biofilm with higher electron discharging capability is an important factor for enhancing the performance of MFCs (Sravan, Chatterjee, Hemalatha, & Mohan, 2019). Therefore, the metabolic status of cells within anode biofilms is crucial for understanding the functioning of MFCs and developing strategies to optimize their power generation (Chiranjeevi & Patil, 2020). For example, the viable biocatalyst density particularly the ratio of live and dead cells within the biofilm is a unique feature of MFC which mainly affects its power generation (Geng et al., 2020). Although research on MFCs has experienced significant development in recent years, still numerous studies are reporting unstable and deteriorated performance of MFCs during long-term operation, especially those fuelled with real wastes (Velvizhi et al., 2020). The polarization curve

related to this is shown in Figure 2.22. Munjal et al. reported that the performance of MFCs was varied with the changes in biofilm properties. Initially (day 1 to day 3), a very less number of cells were colonized on the anode surface resulting in a very low power generation. However, between the 3rd day to 7th day, rapid biofilm growth occurred which resulted in a significant improvement in the performance (Munjal et al., 2020). Thereafter, a sudden and noticeable drop in the performance of MFC was seen, and a subsequent drop in the polarization performance beyond two weeks of operation. In another study, the biofilm properties were identified as a key factor for the current generation. The higher current density was observed while the biofilm was completely viable (based on using live/dead stains) whereas dead cell accumulation on the biofilm resulted in lower current densities (B. Wang et al., 2020). On the other hand, Sun et al. observed minimal diffusion resistance for initial biofilms, where charge transfer resistance was predominant (J.-Z. Sun et al., 2015) (Figure 2.22). However, the diffusion resistance increased over time due to an increase in the thicknesses of inert biofilm whereas a minimum resistance was observed when the live layer predominated within the biofilm (Liao, Li, & Tjong, 2020).

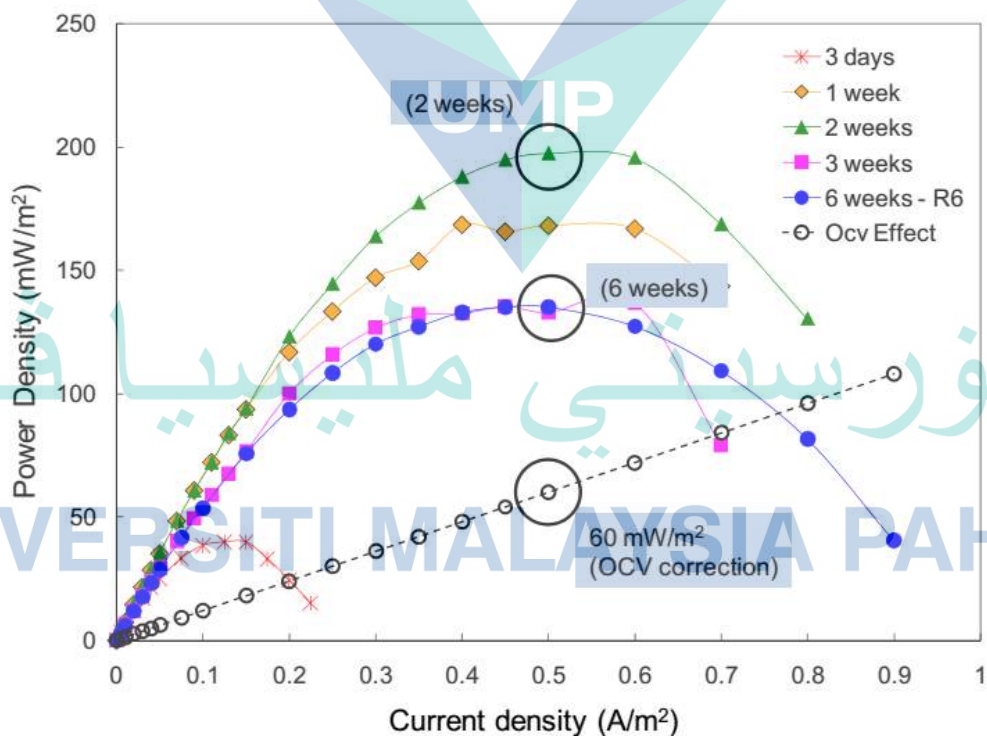


Figure 2.22 Polarization curves of MFCs on different days of operation

Source: Radeef & Ismail, (2019)

Thus, it can be concluded that from their study, the formation of multilayer biofilm on the anode electrode surface over time is accounted for the higher diffusion as well as charge transfer resistance (Tahir et al., 2020). It has been reported that the metabolic status of biofilms such as conductivity, rates, and dimension of substrates and end products can affect the bacterial growth in thick electrogenic biofilms (Chiranjeevi & Patil, 2020). The anode resistance is shown in Figure 2.23.

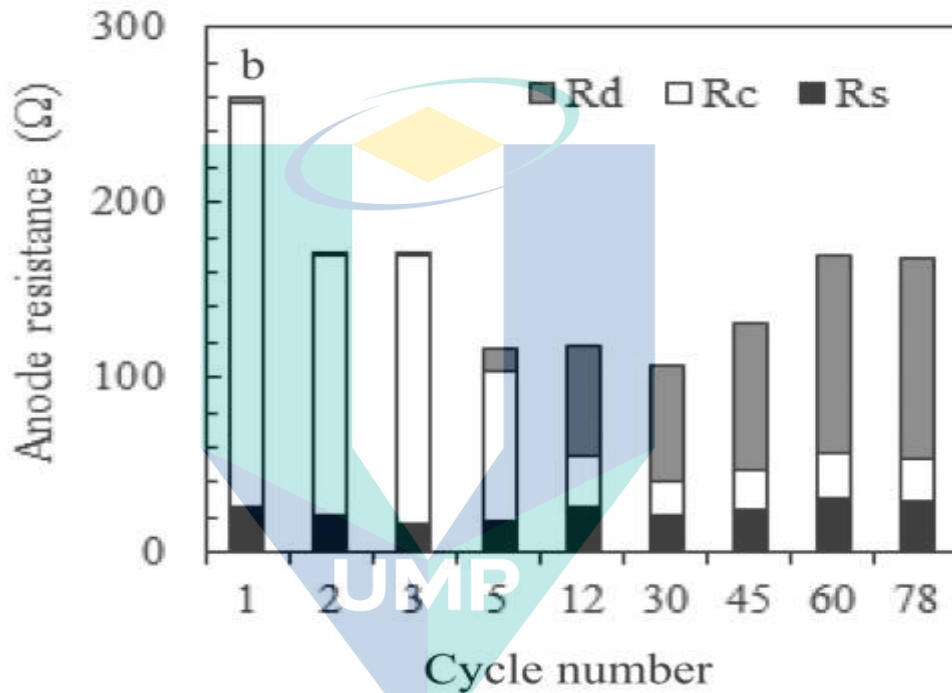


Figure 2.23 Contribution of anode internal resistance of MFCs (R_s represents the solution resistance, R_{ct} represents the charge transfer resistance and R_d represents the diffusion resistance)

Source: Haavisto et al., (2019)

Therefore, the optimal biofilm thickness by removing cell clogging is exigent to vitalize the biofilm for allowing efficient electron transport as well as substrate access (Chiranjeevi & Patil, 2020). Recent studies reported that only a few microorganisms are capable of long-distance electron transfer through the biofilms (Chiranjeevi & Patil, 2020; J. Liu et al., 2020). Long-range extracellular electron transfer (EET) can be occur through the thick biofilm at distances of 10 or even 100 μ distant from the surface of the electrode . As of now, two competing models have been reported for long-distance EET, such as metallic-like conductivity (MLC) and electron hopping (EHM) through the electrically conductive biofilms (Z. Yang & Yang, 2020). According to the EHM, the electrons are relayed through the biofilm by electron tunneling using mediators positioned in the exo-

polymer matrix and also on the nanowire. However, in MFC, electron transport occurs by delocalized electrons in the network of nanowire inside the biofilm (Raychaudhuri & Behera, 2020b). However, evidence in the literature suggests that some biofilms, especially *Shewanella oneidensis* produce the requisite components for both mechanisms (D. Sarkar, Poddar, Verma, Biswas, & Sarkar, 2020). Microorganisms even with electron-conducting pili could not be able to achieve high performance while operating with real wastewater which might be due to the inability of those microorganisms to utilize complex substrates (Nozhevnikova et al., 2020). Islam et al. reported the time-course formation of biofilm in the POME driven MFCs (Islam et al., 2016). It was shown that the efficient biofilm could be formed in 7-14 days of operation and thereafter the power generation was dropped due to the accumulation of dead cells in the biofilm. The efficient biofilm formation was evidenced by lower charge transfer and mass transfer resistances compared to those after 16 days of operation (Islam, Karim, et al., 2019). In order to produce constant power in the MFC few techniques were proposed where the intermittent biofilm removal by ultrasound or flow-induced shear stress methods demonstrated very promising results (Islam et al., 2016).

2.11.5 Electrochemical methods

2.11.5.1 Cyclic voltammetry

Cyclic voltammetry (CV) is a standard tool in electrochemistry and has regularly been exploited to study and to characterize the electron transfer interactions between microorganisms or microbial biofilms and microbial fuel cell anodes (Caizán-Juanarena et al., 2020). CV experiments are generally performed in the absence of a substrate (non-turnover conditions) in order to observe the redox compounds confined inside the biofilm (Ruiz et al., 2020) (Figure 2.24). In theory, each redox compound that is electrochemically accessible to the electrode is oxidised and then reduced during the backward and forward scans, which results in one pair of oxidation and reduction current peaks (Figure 2.24). Cyclic voltammetry performed when the substrate is present in solution, so-called “catalytic” CV, generates typical sigmoidal shape voltammograms showing a potential-independent maximum current at high potentials (Figure 2.24a-b). The limiting catalytic current is not necessarily controlled by the diffusion of the substrate. The impact of the various possible limiting factors, acetate diffusion to the cells,

proton extraction from the biofilm, electron transport inside the biofilm, and metabolic rate, has been analysed in-depth with a *G. sulfurreducens* bioanode by associating a rotating disk electrode with the numerical interpretation of the data (B. Wang et al., 2020). The most common objective of a catalytic CV is to assess the performance of bioanodes at a steady-state. This is the reason why low scan rates are used, most often around 1 mV/s. Occasionally, slower scan rates can be found (Trifonov, 2020). A transient CV in catalytic conditions has been rarely exploited so far, although it should be a powerful tool for fundamental investigations. For instance, a high potential scan rate (100 V/s) used with a *Shewanella* bioanode in catalytic conditions has allowed the contribution of the outer-membrane cytochromes to be clearly evidenced (Jung, Lee, Park, & Kwon, 2020).

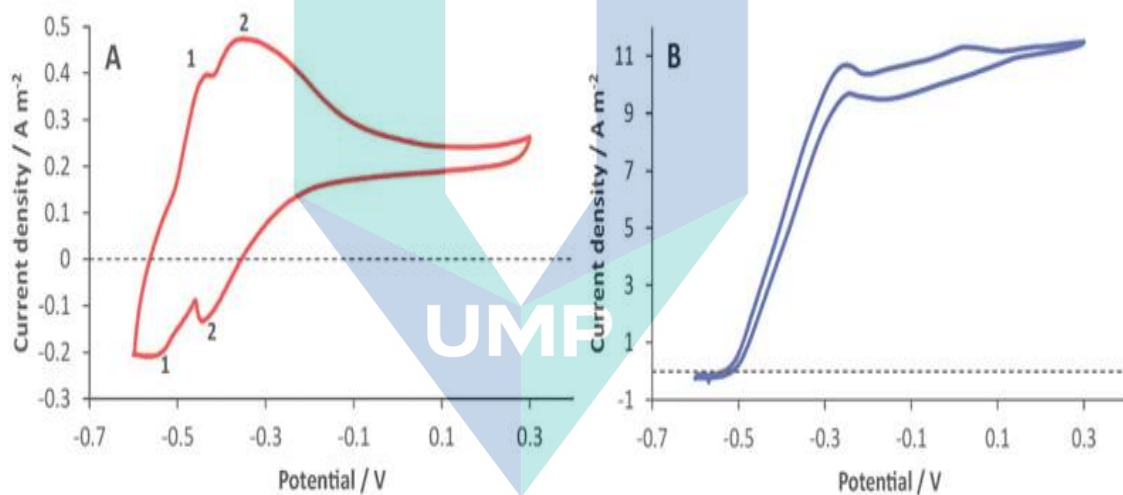


Figure 2.24 a) Turn-over and b) Non-turn over cyclic voltammetry

Source: Modestra & Mohan, (2019)

The different types of CV are shown in Figure 2.25. From Figure 2.25, it can be seen that different types of CV observed using different substrates and microbes which present different types of redox peaks at different positions. The presence of a redox peak in MFC demonstrated that different microbes was not able to secrete electron shuttling mediators. Usually, yeast cell produces very small power attributed to its cytochrome based electron transfer and it is relatively less effective than the naturally produced electron shuttle or pili. The redox potential of different microbes at the different position can be due to different types of mediator secreted by the microbes (S. Zhang et al., 2020). The difference between the two peak potentials of the CV gives an idea of the effects of

the diffusion rates of the analytes. Also, the reversible, irreversible, and quasireversible nature of the system can be found using the ratio of the anodic and the cathodic peak currents (J. Liu et al., 2020). If the said ratio is equal to 1, it means both the anodic and the cathodic peak currents are the same, and it tells about the reversible nature of the system. If the said ratio is not equal to 1, then it tells about the quasireversible nature of the system, whereas the system can be said to be irreversible when its oxidized or reduced product is not reversible. The current peaks are basically obtained, since the CV is taken in a situation in which the solution is kept unstirred; otherwise the peak current may be replaced by the limiting current (X. Liu et al., 2020).

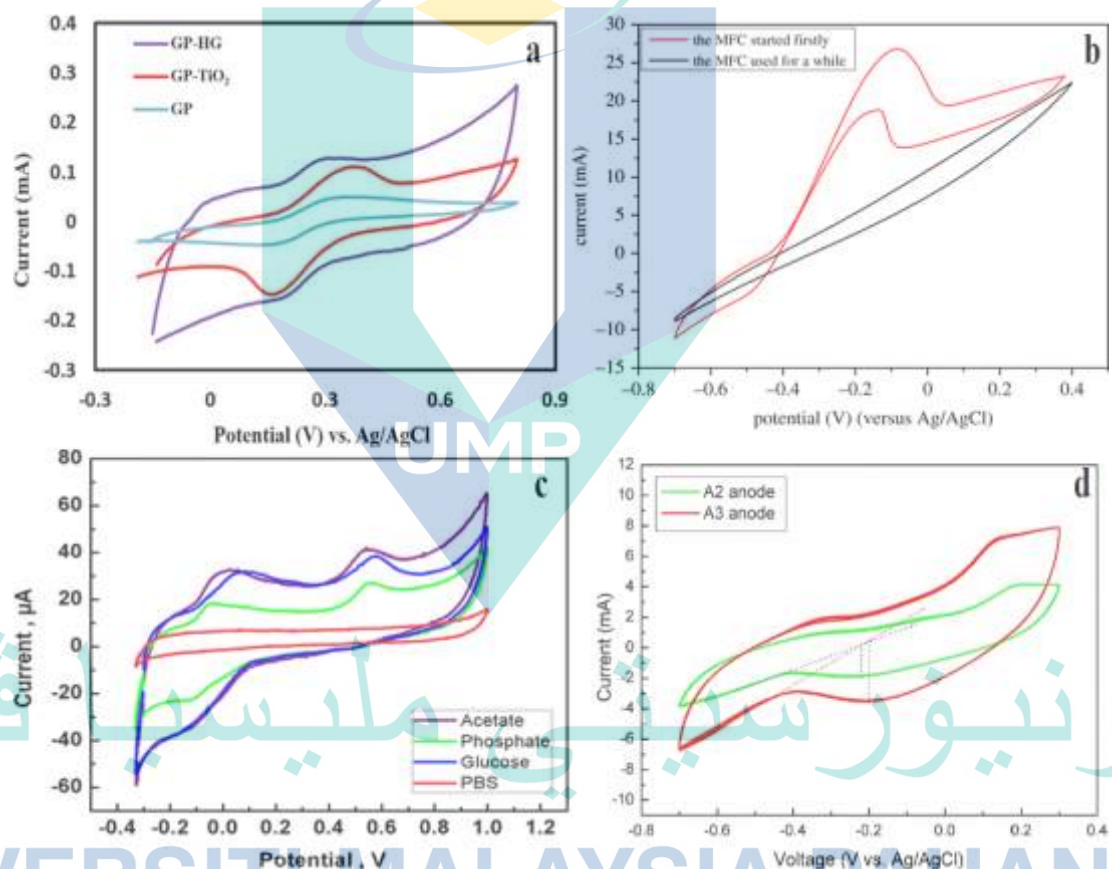


Figure 2.25 Different types of cyclic voltammetry

Source: Khater, El-Khatib, & Hassan, 2018; Khirul, Wang, & Lim, 2020; Ma et al., 2018; J.-Z. Sun et al., (2015)

2.11.5.2 EIS

EIS measurement is a fairly simple procedure that is conducted using instruments such as potentiostats that have EIS functions. An MFC can be connected to a potentiostat in either a three-electrode mode or a two-electrode mode, depending on the purpose of the measurement (N. Khan et al., 2020). The three-electrode mode is used to analyze an

individual electrode. The anode or cathode is used as the working electrode, while the other electrode functions as a counter electrode (Logan et al., 2018). The third lead is attached to a reference (10 mV amplitude) is applied during the measurement to stimulate the current response from the MFC without affecting its performance. The Nyquist plot and frequency vs. Z and phase angle are presented in Figure 2.26. Figure 2.26 shows a complex plane plot for the anode of the MFC (the cathode impedance can be measured and explained in a similar way as the anode) (Yousefi, Mohebbi-Kalhari, & Samimi, 2019). It expresses the impedance with a real part (plotted on the X-axis) and an imaginary part (plotted on the Y-axis that is negative) as a semicircle. Each point on the complex plane plot represents the impedance at a certain frequency. The impedance at the high frequency limit is the ohmic resistance R_s and the diameter of the semicircle is R_p which is the polarization resistance (or charge transfer resistance), which is affected by the kinetics of the electrode reactions. A shortcoming of the complex plane plot is that

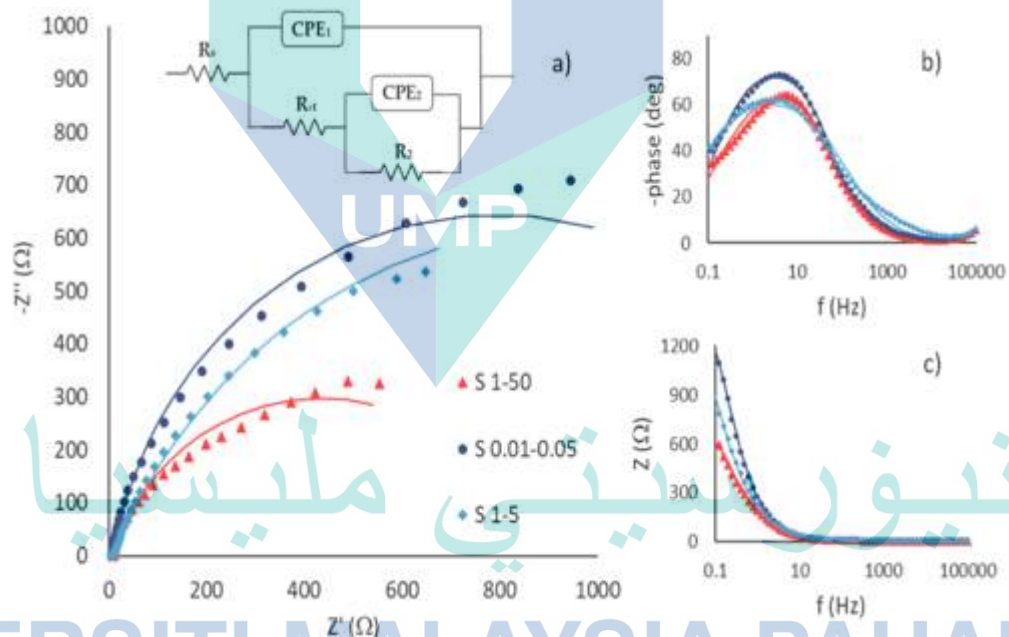


Figure 2.26 a) EIS plot, b) bode plot and c) phase angle with respect to frequency
Source: Fu et al., (2020)

that it does not show the values of the frequency of the applied ac signal and the phase angle. The Bode plot, on the other hand, shows the information of impedance, frequency and phase angle is shown in Figure 2.26. The low- and high-frequency data can be easily determined from the plot, representing R_p+R_s and R_s , respectively. The difference between the low- and high frequency data is R_p . A phase angle of -90° and an impedance slope of -1 indicate a pure capacitance, however under actual conditions both

resistances and capacitances are present and thus the phase angle usually has values between 0 and -90° . Accurate results are obtained by fitting the impedance data to an appropriate equivalent circuit (EC). ECs consist of common electric elements, such as resistors, capacitors and inductors. A simple EC used for describing the electrochemical properties of the MFC is shown in Figure 2.26, which has elements: R_s is ohmic resistance, R_a is anodic polarization resistance, R_c is cathodic polarization resistance and C is capacitance. The sum of R_a , R_c and R_s will be R_{in} . R_a in parallel with C represents the anode. A constant phase element (CPE) usually substitutes the capacitance in ECs because of the inhomogeneous conditions (e.g. electrode roughness, coating, and distribution of reaction rate). ECs can become more complicated by adding more elements with multiple sets of R–C (time constants), according to the complexity of the system (D. R. Rodrigues, Olivieri, Frago, & Lemos, 2019). One or two time constants are usually sufficient to interpret the impedance data for most cases in MFC studies. EIS can determine the values of R_{in} and the contribution of its components. In a tubular air-cathode MFC, it was found that 51.1% of R_{in} was the ohmic resistance, while the charge transfer resistance contributed 22.6% and the rest was due to diffusion effects (J. Liu, Vipulanandan, & Yang, 2019).

2.12 Kinetic study

Microbes in the anode of MFC have the ability to oxidize organic compounds from wastewater and produces an electrical current out of the electrons from those organic compounds (Logan et al., 2019). Moreover, information about the anode-potential losses that occur at the biofilm created by microbes is limited, even though describing these losses is important for understanding the rate of the current generation. Most of the literature on MFC describes current density as a function of potential and correlate this relationship to a bio-electrochemical process (Min Sun, Zhai, Mu, & Yu, 2020). If the microorganisms produce electron shuttles their redox potential can be studied by CV. The kinetics response of electron supply to anode potential is defined by mass transport processes and Butler-Volmer equation (Logan et al., 2019). The equation is given in equation 2.6:

$$I = -I_0 \exp\left[nF(1 - \alpha)(E_{anode} - E_{interface})\right] / RT \quad 2.6$$

where, I_0 is the exchange current density (A / m^2), α is the electron-transfer coefficient or the symmetry coefficient for the anodic or the cathodic reaction, E_{anode} is

the anode potential (V), and $E_{interface}$ is the standard potential (V) of the reaction occurring at the anode interface.

Some microbes species, such as *Shewanella* and *Geobacter*, can transfer electrons through solid conductive matrices that they produce. Production of a conductive matrix also seems to extend to other microorganisms and metabolic interactions (Chiranjeevi & Patil, 2020). The solid conductive matrix creates an electrical connection between the anode and microbes, who take advantage of this to respire electrons to the anode. Though the solid conductive matrix is directly connected to the anode and acts as a conductor, it is considered as an extension of the anode itself (Aiyer, 2020b). Moreover, the biofilm containing a solid conductive matrix a “biofilm anode” (Mai, Yang, Cao, Zhang, & Zhuang, 2020). Since microbes using a biofilm anode are directly connected to the anode, their response is directly coupled to bacterial kinetics. Bacterial kinetics are modelled by the Monod relationship which captures simply the complexity of reversible and irreversible reactions that compose bacterial metabolism (J. Zhao et al., 2020). The most widely used model is the Monod model (equation 2.7) (P. Xu, 2020), in which a single substrate limits the growth of the bacteria. The Nernst-Monod model also accounts for the effects of the potential difference in microbial growth (equation 2.8).

$$r = r_{max} \times \left(\frac{S}{K_s + S} \right) \quad 2.7$$

$$r = r_{max} \times \frac{C}{K_s + S \left(\frac{1}{1 + \exp \left[\frac{-nF}{RT} \right]} \right)} \quad 2.8$$

Here, r is the substrate utilization rate of the substrate (g/L/d), r_{max} maximum substrate utilization rate (g/L/d), S is the substrate concentration (g/L), K_s is the half-saturation coefficient constant (g/L), η is the anodic overpotential (V), F is the Faraday constant (96485 J/K./mol), R is the gas constant (8.314 J/K/mol) and T is the temperature (298 K). Different types of simulated graphs using Nernst-Monod model is presented in Figure 2.27. Figure 2.27 presents reaction rate, concentration, pH, overpotential with respect to time. So, from Figure 2.27, it can be seen that at different current density the reaction rate, concentration and overpotential. This types of operational parameters better fitted using Butler-Volmer and Nernst-Monod model. On the other hand, Lee, et al adopted the Monod model to estimate the kinetic parameters for the growth of *S.*

putrefaciens bacteria in leachate-fed reactors (T. Liu, 2020). The K_s value of bacteria in the leachate-fed MFC reactor was 214 mg/L, with a growth yield coefficient of around 0.65. Peng, et al considered the substrate inhibition and adopted four different models to estimate the kinetic parameters of substrate degradation on the relationship between substrate concentration and the substrate degradation rate, power density, and output voltage in an anodic denitrification MFC (AD-MFC) (Peng, Cao, Xie, Duan, & Zhao, 2020).

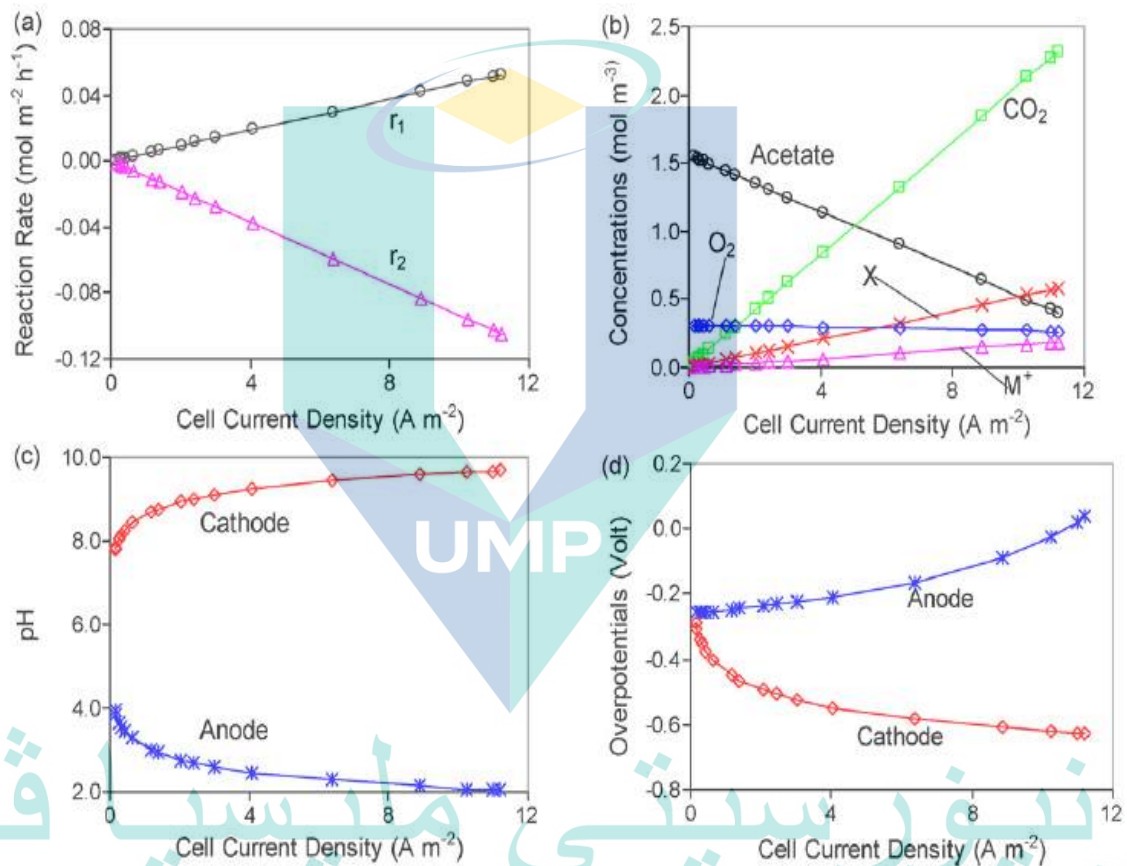


Figure 2.27 Different types of operational parameters experimental and simulated using Butler-Volmer and Nernst-Monod model

Source: R. Patel, Deb, Dey, & Balas, (2020b)

The Nernst-Monod model was found to be the best model to fit the substrate degradation in the AD-MFC. The critical inhibitory concentration of COD was found to be approximately 20 g/L. Liu, et al also adopted the Monod model to fit the performance of the acetate/butyrate-fed MFCs. The graph using Nernst-Monod model is given in Figure 2.28. From Figure 2.28, it can be seen that the model fitting showed the maximum power densities were 661 mW/m² for an acetate-fed MFC and 349 mW/m² for a butyrate-fed MFC; the K_s value was around 141 mg/L and 93 mg/L for the acetate-fed and

butyrate-fed MFC; respectively (Do et al., 2020). For PCW-fed MFCs, studies on the kinetics of petrochemical wastewater degradation and electricity generation are still needed. The kinetics parameters will be informative to optimize MFC design and performance.

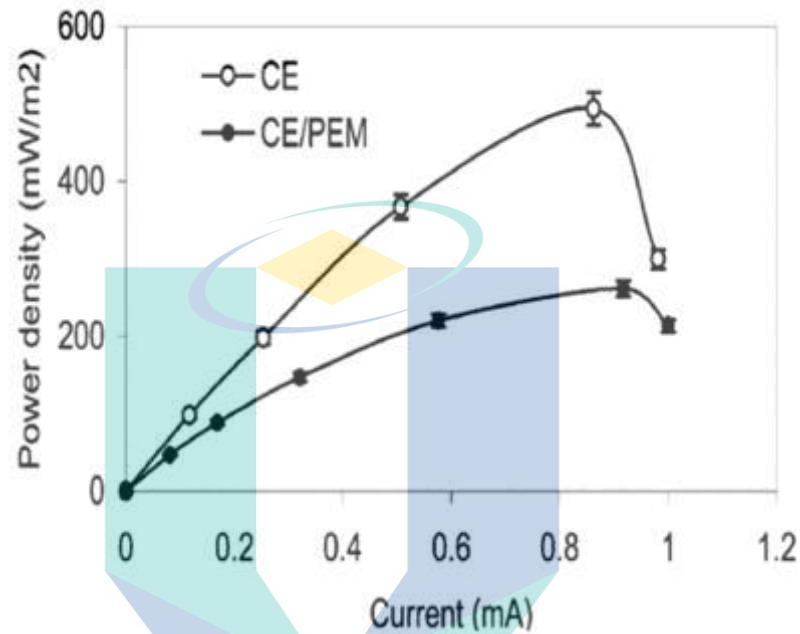


Figure 2.28 Power density using Nernst-Monod Model

Source: J. Zhao et al., (2020)

2.12.1 Kinetic model

Different types of equations were used for kinetic study using PCW with different concentrations which are discussed details in section 0. The kinetic model equation was fitted using polymath software 6.1.

2.12.1.1 Mass balance

The primary microbial population X_p consumes the substrate (S) and, in this process, the oxidized form of the intracellular mediator (M_{ox}) is also converted into its reduced form (M_{red}). This reduced intracellular mediator transfers the electron to the anode and also releases a proton as it regains its oxidized form. A conceptual schematic of this process is described in Figure 2.29. Meanwhile, the secondary microbial population X_s also consumes the substrate but does not release any free electrons which can be intercepted by the intracellular mediators. Considering a fed-batch operation, the

rate of change of substrate and biomass concentrations can be expressed as follows (Gadkari, Shemfe, & Sadhukhan, 2019):

$$\frac{dS}{dt} = -q_p X_p - q_s X_s \quad 2.9$$

$$\frac{dX_p}{dt} = -\mu_p X_p - K_{dp} X_p \quad 2.10$$

$$\frac{dX_s}{dt} = -\mu_s X_s - K_{ds} X_s \quad 2.11$$

where, S represents the substrate concentration (g/L), X is the microbial concentration (g/L), q_p is the substrate consumption rate (d^{-1}), μ is the microbial growth rate (d^{-1}) and K_d is the microbial decay rate (d^{-1}). The subscripts 'p' and 's' represent the primary and secondary microbial populations respectively. The intracellular mediator exists in either oxidized (M_{ox}) or reduced form (M_{red}), however the total mediator

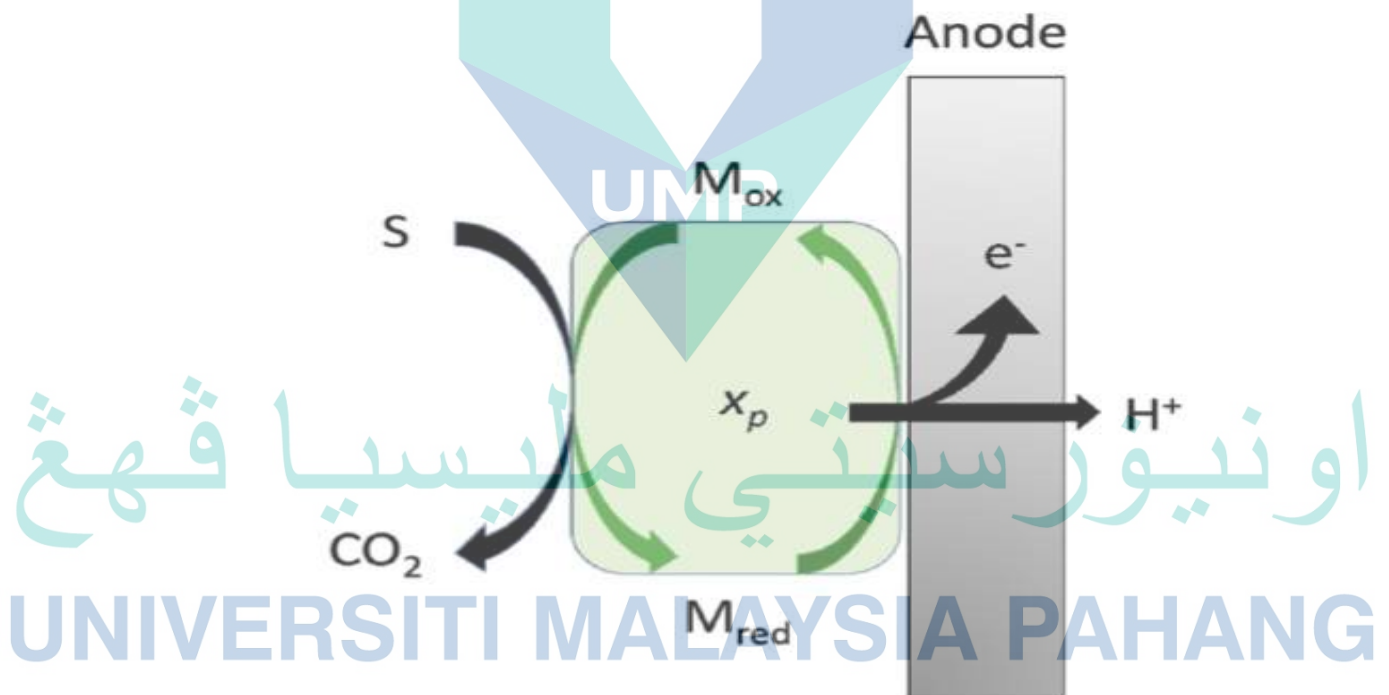


Figure 2.29 Conceptual schematic showing substrate (S) degradation by a primary bacterial cell (X_p) and electron transfer to the anode via reduced (M_{red}) and oxidized (M_{ox}) intracellular mediators.

Source: Gadkari, Shemfe, & Sadhukhan, (2019)

concentration M_{total} remains constant, and can thus be expressed as (Pinto, Srinivasan, Manuel, & Tartakovsky, 2010):

$$M_{total} = M_{ox} + M_{red} \quad 2.12$$

The transfer of electrons from intracellular mediator to anode and then further to cathode, results in current generation. The rate of change of the oxidized mediator concentration is described as follows:

$$\frac{dM_{ox}}{dt} = -Mq_p + \frac{\gamma}{Vx_p} \left(\frac{I_{MFC}}{mF} \right) \quad 2.13$$

where, Y is the dimensionless mediator yield, I_{MFC} is the MFC current (A), m is the number of electrons transferred per mol of mediator, F is the Faraday constant (A s/mol), V is the working volume of the anode chamber, and γ is the molar mass of the mediator (g/mol). The substrate consumption rate by the primary microbial population and the corresponding microbial growth rate are dependent on both the oxidized mediator concentration and the substrate concentration, and are thus described using the multiplicative Monod kinetics. On the other hand, the substrate consumption rate by the secondary bacteria and the corresponding microbial growth rate are only limited by the substrate concentration, and are represented using standard Monod kinetics. The substrate consumption and growth rates are described as follows (Pinto, Srinivasan, Escapa, & Tartakovsky, 2011):

$$q_p = q_{maxp} \left(\frac{S}{K_{S_p} + S} \right) \left(\frac{M_{ox}}{K_M + M_{ox}} \right) \quad 2.14$$

$$\mu_p = \mu_{maxp} \left(\frac{S}{K_{S_p} + S} \right) \left(\frac{M_{ox}}{K_M + M_{ox}} \right) \quad 2.15$$

$$q_s = q_{maxp} \left(\frac{S}{K_{S_s} + S} \right) \quad 2.16$$

$$\mu_s = \mu_{maxs} \left(\frac{S}{K_{S_s} + S} \right) \quad 2.17$$

where, K_S and K_M are the Monod half saturation coefficients for the substrate and mediator respectively (g/L), q_{max} and μ_{max} represent the maximum substrate consumption rate and maximum growth rate respectively (d^{-1}).

2.12.1.2 Ohm's law and voltage losses

The standard electrode potentials determine the maximum theoretical voltage that can be generated from the MFC. However there are activation, concentration and ohmic

voltage losses in the system. Accounting for these over-potential losses and the internal & external resistance, the current generated in the MFC can be expressed using Ohm's Law as follows (X.-C. Zhang & Halme, 1995):

$$I_{MFC} = \frac{E_{OCV} - \eta_{act} - \eta_{conc}}{R_{ext} + R_{int}} \quad 2.18$$

where, E_{OCV} is the open circuit voltage (V), R_{ext} and R_{int} are the external and internal resistance in the electrochemical cell, η_{act} and η_{conc} represent the activation and concentration over-potentials (V). A constant supply of intracellular electron transfer mediators is assumed, which undergo transformation between reduced and oxidized forms as they transfer electrons to the anode. Thus the major limiting factor influencing the voltage losses at the anode is the substrate concentration. The concentration over-potential at the anode can therefore be expressed as a function of initial substrate concentration (S_{in}) and the dynamic substrate concentration (S), as follows (De Schampelaire, Rabaey, Boeckx, Boon, & Verstraete, 2008):

$$\eta_{conc} = \frac{RT}{mF} \ln\left(\frac{S_{in}}{S}\right) \quad 2.19$$

Microbes in the anode of MFC have the ability to oxidize organic compounds from wastewater and produces an electrical current out of the electrons from those organic compounds. Moreover, information about the anode-potential losses that occur at the biofilm created by microbes is limited, even though describing these losses is important for understanding the rate of current generation (Anawar & Strezov, 2019). Most of the literatures on MFC describe current density as a function of potential and correlate this relationship to a bio-electrochemical process. If the microorganisms produce electron shuttles their redox potential can be studied by CV (Anawar & Strezov, 2019). The kinetics response of electron supply to anode potential is defined by mass transport processes and Butler-Volmer equation. The equation is given in below (Garcia, Laurens, & Panin, 2019):

$$I = -I_0 \exp[nF(1 - \alpha)(E_{anode} - E_{interface})]/RT \quad 2.20$$

where, I_0 is the exchange current density (A/m^2), α is the electron-transfer coefficient or the symmetry coefficient for the anodic or the cathodic reaction, E_{anode} is the anode potential (V), and $E_{interface}$ is the standard potential (V) of the reaction

occurring at the anode interface. Activation over-potential represents losses due to the slow electrochemical kinetics, and can be expressed by the following equation (Gadkari, Shemfe, & Sadhukhan, 2019):

$$\eta_{act} = \frac{RT}{\beta m F} \sin^{-1} \left(\frac{I_{MFC}}{A_n i_0} \right) \quad 2.21$$

where, T is the system temperature (K), R is the universal gas constant (J/mol/ K), β is the charge transfer coefficient, A_n is surface area of anode (m^2), and i_0 is the exchange current density (A/m^2). It has been shown that increase in organic substrate concentration increases the ionic strength of the anolyte, which helps in improving the open circuit voltage and reducing the internal resistance of the cell (Y. Feng, Wang, Logan, & Lee, 2008; Oliveira, Simões, Melo, & Pinto, 2013; Velvizhi & Mohan, 2012). These correlations can be used to further improve the model efficacy by incorporating dynamic expressions for open circuit voltage and internal resistance as a function of substrate concentration:

$$E_{OCV} = E_{min} + (E_{max} - E_{min}) e^{\frac{-1}{kr_1 s}} \quad 2.22$$

$$R_{int} = R_{min} + (R_{max} - R_{min}) e^{\frac{-1}{kr_2 s}} \quad 2.23$$

where, E_{min} and E_{max} represent the lowest and the highest observed open circuit voltage in the system, R_{min} and R_{max} represent the lowest and the highest observed internal resistance in the system. kr_1 and kr_2 are constants [g/L] which determine the slope of the curve. Similar expressions have been previously derived by Pinto et al. (Pinto et al., 2010), considering open circuit voltage and internal resistance to be a function of anodophilic microorganisms.

MFC performance is typically assessed based on the maximum voltage that can be generated and the substrate or COD removal efficiency. In addition to these two, Coulombic efficiency (ε_E) is another important performance indicator and determines the electron recovery of the system. It represents the ratio of the total number of electrons recovered at the anode and the maximum number of electrons that could have been recovered if all the consumed substrate contributed to current generation. In the present analysis, the MFC is assumed to be operating in fed-batch mode and thus ε_E can be expressed as (Gadkari, Shemfe, & Sadhukhan, 2019)

$$\varepsilon_E = \frac{M_0 \int_0^t I_{MFC} dt}{FbV\Delta S} \quad 2.24$$

where, M_0 is the molecular weight of oxygen, b is number of electrons exchanged per mole of oxygen and ΔS is the change in substrate (COD) concentration over time t .

2.13 Summary

Biological treatment of petrochemical wastewater has widely been investigated. For biological treatment, the role of fermentative bacteria is well defined where maximum degradation of the organics are required. In contrast to biological treatment, the microbial fuel cell can simultaneously treat the wastewater along with the electricity generation where the presence of electrogenic microbes is crucial. Electrogenic microbes are kind of microorganism which can not only to degrade the organics but also simultaneously produce the electricity. The widely known electrogens such as *Pseudomonas aeruginosa* (PA), *Bacillus cereus* (BC), *Klbesiella variicola*, *Geobacter spp.* are capable of producing high power using simple substrates such as glucose, acetate etc. (Islam et al., 2018; Sarmin et al., 2019). Most of the electrogens capable of direct electron transfer to the electrode via electron conducting pili demonstrated poor survivability in the complex wastewater. On the other hand, PA, BC were found in the biofilms of the MFCs operated with anaerobic sludge as biocatalyst. These microbes were reported to transfer electrons via direct (cytochrome-based) or indirect (metabolite based) mechanisms. The interaction of the microbes present in the mixed culture inoculum with specific substrates from complex wastewater can produce synergistic or antagonistic effects. The microbes possessing synergistic capability in terms of substrates-inoculum interaction are essential in MFC where different types of substrates and microbes play the important role. Hence, the substrates containing in real wastewater also play a vital role where certain microbes grow very fast and some microbes grow very slowly. Thus, the interaction of the microbes with different organic substrates present in complex wastewater could be the key point for high power generation in MFC. Additionally, to enhance the power generation, it is crucial to include electrogens in the inoculum possessing synergy. There are few studies shown this kind of mutualistic interactions using POME, however study on PCW (or with the constituents of the PCW) is very rare. Additionally, acclimatization of the inoculum in the complex substrate is proven to be an effective strategy to increase the efficiency of the biological reactors as well as the MFCs. More specifically, for MFCs the presence of

methanogenic bacteria is detrimental which suppresses the current generation in the MFCs and the problem can be alleviated through acclimatization in MFC. There was no systematic study that could explore the way of acclimatization of the anaerobic sludge to produce effective inoculum for MFC fed with PCW where the power generation along with high wastewater treatment efficiency is required.

Biofilm on the anode is considered as the power house of the MFCs. Biofilm is a complex network of microbes which can be adhered through the extracellular matrix on the electrode surface. Most of the literature described the mechanism of electron transfer through biofilm. Hence some studies reported the time-course formation of efficient biofilm where the live cells outnumbered the dead cells. However with time the accumulation of the dead cells in the vicinity of the surface of the electrodes can severely deteriorate the performance of MFC (Islam et al., 2016). The biofilm functions as the facilitator as well as a barrier for the electron shuttles to contact with the electrode surface due to mass transfer effects. In this case, the role of indirect and direct electron transfer is very important to be determined to enhance the power generation of the MFCs. The study on the electron transfer mechanism in the MFCs are mainly focussed with single substrate-microbe systems. There are very few studies explored the electron transfer mechanism in the complex wastewater fed MFCs (Islam et al., 2020; Islam, Karim, et al., 2017). In few studies it was shown that the periodic removal of the biofilms could enhance the MFC power generation significantly through indirect electron transfer mechanisms (Koók et al., 2019; Zou, Qiao, Zhong, & Li, 2017). It was demonstrated that the lowering of the charge transfer and mass transfer resistances were crucial in the augmentation in MFC power generation. In that context, the electron transfer mechanism along with the charge transfer kinetics in PCW fed MFC needs to be investigated.

UNIVERSITI MALAYSIA PAHANG

CHAPTER 3

METHODOLOGY

3.1 Introduction

The overview of the chapter is presented in Figure 3.1.

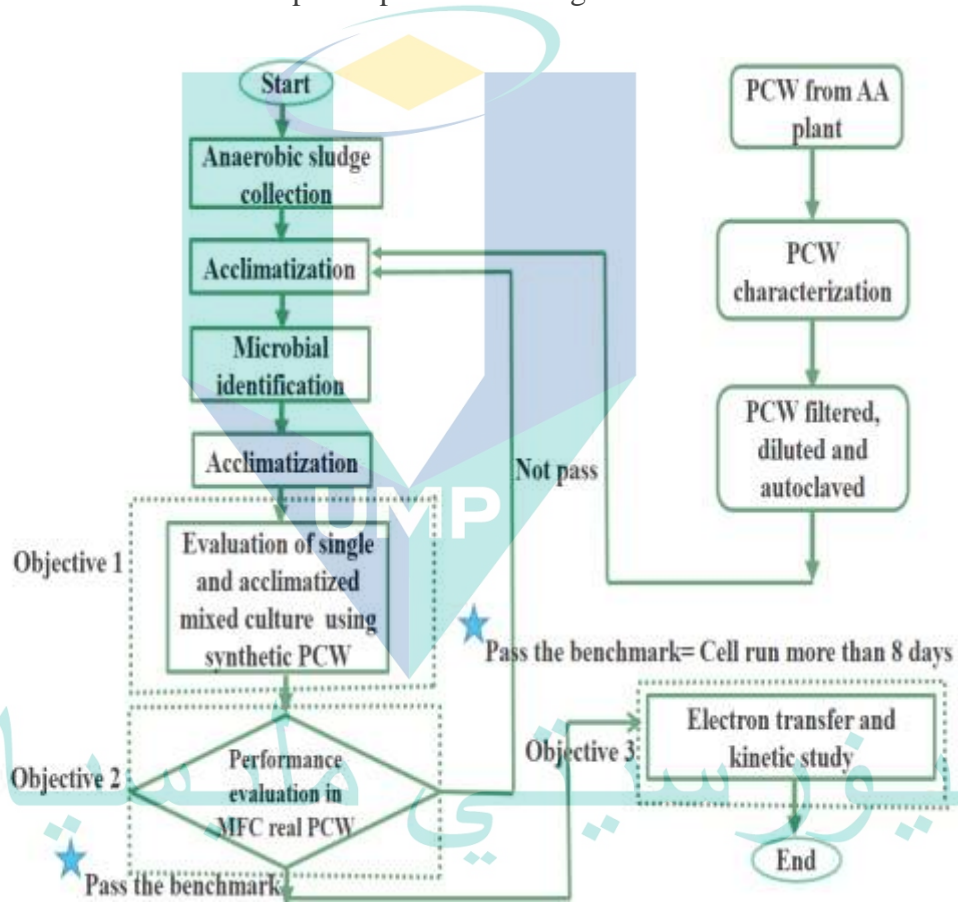


Figure 3.1 Overview of research methodology

The Biolog GEN III method was used for microbial identification and the information about construction and operation of MFCs, measurement, COD removal efficiency, coulombic efficiency, sampling and inoculum preparation have been provided in this chapter. Besides that, the biofilm characterization by field emission scanning electron microscope, cell viability count and electrochemical methods (CV and EIS) are provided. The metabolite analysis by UV-Vis method in the co-culture system is also

included. Moreover, the kinetic study was done by poly-math in order to optimize the operational parameters (i.e pH, initial COD, inoculum composition and time cycle) for maximizing the performance of co-culture inoculated MFCs has been provided in this chapter.

3.2 Materials

3.2.1 List of chemicals

The chemicals and materials used for this study were purchased from Sigma-Aldrich scientific chemicals (Table 3.1). The raw PCW was collected from the local acrylic acid plant and the anaerobic sludge was collected from the Panching Palm oil mill effluent (FELDA), Kuantan, Pahang, Malaysia and stored in refrigerator at 4 °C. The distilled water and deionized water were obtained from the Bioprocess laboratory of University Malaysia Pahang (UMP).

Table 3.1 Chemicals and materials

Chemicals and materials	Source
Ethanol	Sigma-Aldrich
Ag/AgCl electrode	Sigma-Aldrich
HEPES buffer (pH 6.8)	Sigma-Aldrich
MgCl ₂	Sigma-Aldrich
NH ₄ Cl	Sigma-Aldrich
Urea	Sigma-Aldrich
K ₂ HPO ₄	Sigma-Aldrich
KH ₂ PO ₄	Sigma-Aldrich
KMnO ₄	Sigma-Aldrich
CaCl ₂	Sigma-Aldrich
KCl	Sigma-Aldrich
Glutraldehyde	Sigma-Aldrich

3.3 Inoculum screening and time-course biofilm analysis

3.3.1 Sampling of PCW

Petrochemical wastewater (PCW) was obtained from a local acrylic acid plant. The samples were collected before the effluent discharge into the mixing pond at about 80-90 °C. The wastewater sample was filtered by Whatman no.1 filter paper for the removal of suspended particles and stored at 4 °C in order to prevent self-deteriorations. The palm oil mill effluent anaerobic sludge (POME AS) was collected from bottom

sampling port of the running anaerobic digester of palm oil mill while the municipal wastewater (MWW) sludge was collected from drainage discharge point of Kuantan city, Malaysia (*Latitude* DMS: 3°48'45.36"N. *Longitude* DMS: 103°22'19.21"E) and immediately stored at 4 °C.

3.3.2 pH measurement

The wastewater pH was measured throughout most of the experiment. The measurement was made using a standard pH meter on the soluble wastewater analyte samples before preservation.

3.3.3 COD measurement

COD measurement was done in this study followed by Islam et al. (Islam, Ethiraj, et al., 2017). At first, preserved samples were diluted with deionized water. Following dilution, triplicate 2.5 mL volumes of each wastewater sample were added to 10 mL COD digestion vials. A set of COD calibration standards using synthetic and real PCW were prepared at 0, 25, 50, 100, 200, 300, 400, 600, 800, and 1000 mg COD/L, and 2.5 mL of each standard was added to 10 mL COD digestion vials. If the previous COD digestion had used the exact same batch of reagents, only a 0 and a 1000 COD calibration standards were prepared to confirm the previous calibration curve. If confirmed, the previous calibration curve was re-used. The mixtures were added with 3.5 mL of the sulphuric reagent and 1.5 mL of the chromatic reagent were added to each digestion vial. Once the COD reagents were added, the vials were capped, shaken and placed in a block heater to be digested for 3 hours at 150°C. Following digestion, the vials were allowed to cool before being cleaned with ethanol and tissues. Optical density measurements at a wavelength of 600 nm were recorded for each sample and standard using a spectrophotometer (DR-2800 Portable Data logging Spectrophotometer, Germany) followed by Islam et al. (Islam, Ethiraj, et al., 2017). The COD values were obtained by reading the calibration curve. Subsequently, the solution with raw PCW was put into the spectrophotometer to read the amount of COD present in raw PCW. Similarly, the amounts of COD present in other diluted samples were measured.

3.3.4 Sources and acclimatization of inoculums

The POME anaerobic sludge (AS) used as inoculum in MFCs. The sludges were filtered using Whatman no. 1 filter paper and the filtrate was removed. The acclimatization of AS was carried out by operating an MFC fed with 35 mL of PCW and 5 mL of AS as inoculums, where the initial COD of PCW was maintained at 50000 mg/L. The MFC was operated for 10 days. After 10 days of operation, 5 mL of anolyte was collected from the upper layer of liquid and centrifuged at 6500 rpm for 6 min for the collection of cell pellets/biomass. The pellets were washed using AA free medium (0.1 g NaHCO₃, 0.1 g NaH₂PO₄, 0.05 g KCl, 0.25 g NH₄Cl, 0.5 mL of the mineral mixture and 0.5 mL of the vitamin mixture) (Saïen & Nejati, 2007), and re-suspended into sterile water. The final inoculum was prepared by mandating an optical density (OD) of 0.3. The predominated microbes in that acclimatized inoculum were identified by using BIOLOG GEN III analysis.

3.3.5 Microbes analysis method by BIOLOG GEN III

Once the pure cultures screened through the spread plate technique, the genus and species of microbes were determined using the BIOLOG GEN III test (Biolog Inc., United States). In the BIOLOG GEN III test, the carbon consumption tests were carried out with the obtained microbes under the anaerobic conditions. The Biolog micro-plate consists of 96 wells for source utilization assay while 23 wells for chemical sensitivity determination assays. Tetrazolium redox dye was used to colorimetrically indicate the resistivity or sensitivity to the chemicals. The isolated microbial colonies were pre-cultivated on Tryptic soy agar (TSA) plates and thereafter incubated for 24 h at 33°C. The colonies consisting 3 mm diameter were picked up using cotton tipped inoculator swab from the agar. Thereafter, the agar plates comprising pure cultures immediately released the bacteria into the inoculating fluid (IF) and stirred with the cotton swab to obtain a uniform cell suspension and then all wells filled with 100 µl of cell suspension and incubated at 33 °C for 36 h. Finally, colourless wells were observed while inoculated due to the utilization of carbon sources, causing the reduction of the tetrazolium redox dye. The micro-plates were read using BIOLOG's microbial identification system software after the incubation and based on match, species level identification of the isolate was made. The predominated microorganisms were found as *Pseudomans aeruginosa* and *Bacillus cereus*. To investigate the performance of PA and BC, the pure cultures were

collected from the FTKKP laboratory. The phylogenetic tree of the microbes are presented Appendix A2.

3.4 MFC Fabrications and operations

The DC-MFC setup was assembled as shown in Figure 3.2. In brief, the experiments proceed with cubic chambers made of plexi-glass (Sunny Scientific, Shanghai, China) with an external dimension of 8.3 cm × 8.3 cm × 8.3 cm.

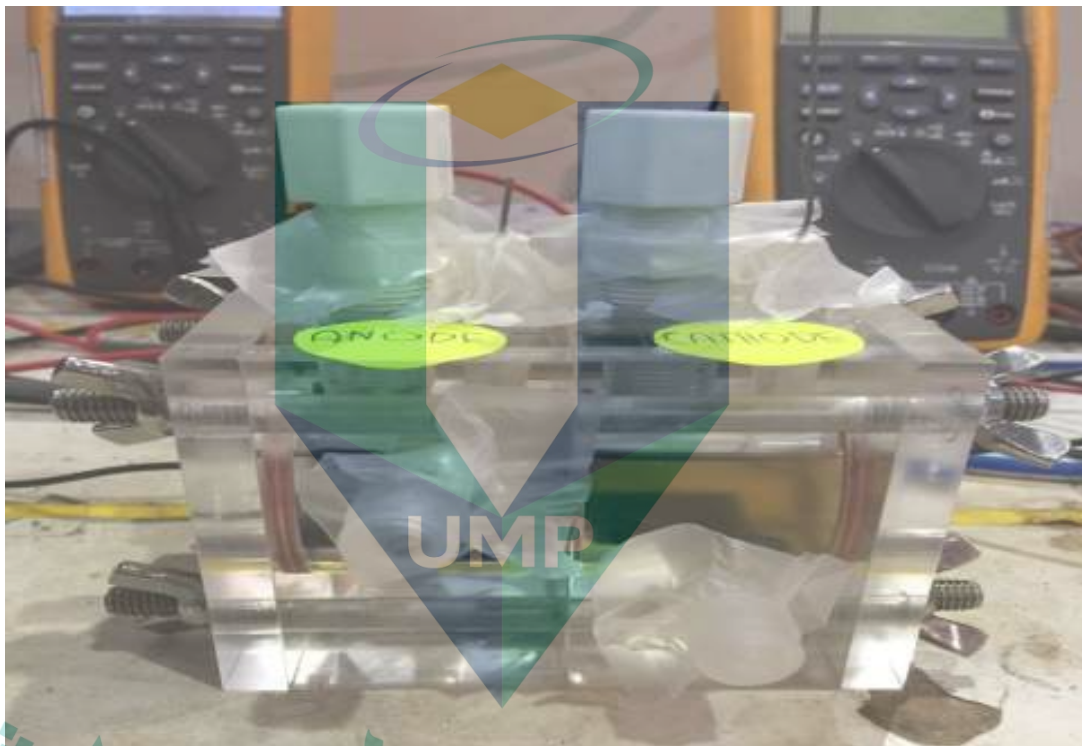


Figure 3.2 Dual chamber MFC

The working volume for anode and cathode was 40 mL. Polyacrylonitrile coated carbon felt (3 cm × 2 cm) was used as the electrode material for all experiments. The electrodes were pre-treated with HCl solution (1 mol/L) and successively washed with DI water. The two chambers were separated by Nafion117 membrane (Dupont Co., Wilmington, DE) which was pre-treated with H₂SO₄ solution (1 mol/L) at 80 °C for 2 h followed by washing with de-ionized water at the same temperature for 1.5 h and stored in deionized water at room temperature before using. Finally, the electrodes were connected with titanium wires and both chambers were tightly held together with screws in order to prevent leakage. The anode chamber was filled with 35 mL substrate (50% PCW) in accordance to the following compositions: NaHCO₃ (8 mg), NH₄Cl (4 mg), CaCl₂ (0.52 mg), MnCl₂·4H₂O (0.044 mg), CoCl₂·2H₂O (0.02 mg), and CO (NH₂)₂ (20

mg) and Na₃PO₄ (20 mg). The anolyte was inoculated with 5 mL of the acclimatized culture and the anode chamber was purged with N₂ for 15 min. Thereafter, the anode chamber was sealed properly for the maintenance of the anaerobic conditions. The KMnO₄ solution (0.1 mol/L) was used as the catholyte for all DC-MFC experiments.

The different MFCs were operated for different days regarding on experimental purposes (MFC₁ run to collect the predominated microbes for the whole experiment, MFC₂-MFC₂₇ were run for 16 days due to MFC performance, MFC₂₈-MFC₂₉ were run for metabolite identification) are presented in Table 3.2 at 1 kΩ of external resistance.

Table 3.2 Different MFCs operational day

Name	Substrates	Inoculum	Operational day
MFC ₁	PCW (45000 mg/L)	AS	10
MFC ₂	AA (0.5 wt%)	Acclimatized AS	16
MFC ₃	AA (1 wt%)	Acclimatized AS	16
MFC ₄	AA (2 wt%)	Acclimatized AS	16
MFC ₅	AA (3 wt%)	Acclimatized AS	16
MFC ₆	AA (5 wt%)	Acclimatized AS	16
MFC ₇	ACA (0.5 wt%)	Acclimatized AS	16
MFC ₈	ACA (1 wt%)	Acclimatized AS	16
MFC ₉	ACA (2 wt%)	Acclimatized AS	16
MFC ₁₀	ACA (3 wt%)	Acclimatized AS	16
MFC ₁₁	ACA (5 wt%)	Acclimatized AS	16
MFC ₁₂	DMP (0.5 wt%)	Acclimatized AS	16
MFC ₁₃	DMP (1wt%)	Acclimatized AS	16
MFC ₁₄	DMP (2wt%)	Acclimatized AS	16
MFC ₁₅	AA:ACA:DMP	Acclimatized AS	16
MFC ₁₆	AA:ACA:DMP	Acclimatized AS	16
MFC ₁₇	AA:ACA:DMP	Acclimatized AS	16
MFC ₁₈	AA (2 wt%)	<i>Bacillus cereus</i>	16
MFC ₁₉	ACA	<i>Bacillus cereus</i>	16
MFC ₂₀	DMP	<i>Bacillus cereus</i>	16
MFC ₂₁	AA	<i>Pseudomonas aeruginosa</i>	16
MFC ₂₂	ACA	<i>Pseudomonas aeruginosa</i>	16
MFC ₂₃	DMP	<i>Pseudomonas aeruginosa</i>	16
MFC ₂₄	PCW (5000 mg/L)	Acclimatized AS	16
MFC ₂₅	PCW (10000 mg/L)	Acclimatized AS	16
MFC ₂₆	PCW (26000 mg/L)	Acclimatized AS	16
MFC ₂₇	PCW (45000 mg/L)	Acclimatized AS	16
MFC ₂₈	PCW (75000 mg/L)	Acclimatized AS	10
MFC ₂₉	PCW(100000 mg/L)	Acclimatized AS	10

Apart from this, again glass cell MFCs were run for doing the CV and EIS from supernatant got from above mentioned MFCs in Table 3.2. For this after MFC operation the samples were collected from anode electrode and the samples filtered and taken in glass cell which is shown in Figure 3.3. The glass cell MFC consists of two electrodes. One is anode and another one cathode.

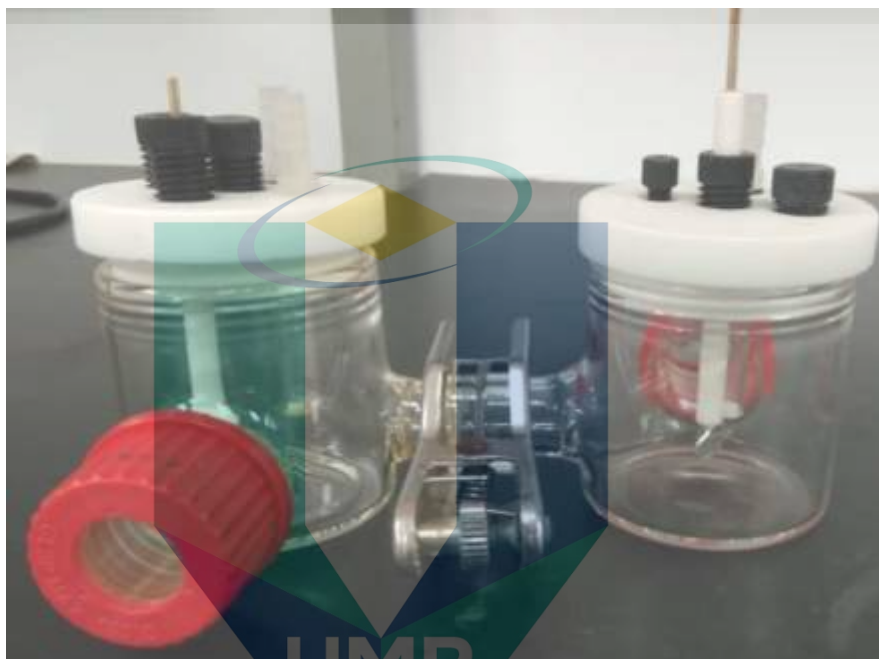


Figure 3.3 MFC glass setup for metabolite analysis

The supernatant was taken in anode electrode (40 mL) and another one is cathode which was filled with catholyte (40 mL 0.1M KMnO_4). The working and reference electrodes were connected with the anode electrode and the counter electrode was connected with the cathode electrode. Thereafter, it was connected to the power supply and connected with the potentiostat and the required CV and EIS were then taken.

3.4.1 Electrode preparation

PACF (Poly acrylonitrile carbon felt) was used as anode and cathode electrodes in all the experiments. Equal size of PACF (3 cm \times 2 cm) was used as an electrode in the compartment of dual chamber MFC. PACF (Shangai sunny scientific, China) was washed with DI water to remove impurities sticking onto them. After that, PACF was drenched in 70% ethanol solution for about 10 minutes then poured away the ethanol and kept the PACF on aluminum foil in the oven for 15 minutes to dry. Finally, after drying PACF

was connected with copper wire. The electrodes were cleaned with 1.0 M NaOH followed by 1.0 M HCl after each experiment and stored in distilled water before use.

3.4.2 Membrane treatment

The Nafion 117 Membrane (Dupont Co. USA) was used as a proton exchange membrane (PEM) and to separate the anode and cathode compartment of the double chamber MFC. The Nafion membrane was cut in the dimension of about 6.5 cm × 6 cm and soaked in a beaker containing 250 mL de-ionized (DI) water. Then, 8 mL of HCl was pipetted and added into the DI water to form an acidic solution for the acid treatment of the membrane to remove any organic impurities (Islam et al., 2020). The membrane in the acidic solution was heated at 100 °C for an hour and cooled down to room temperature. After that, the solution was kept overnight then poured away the solution leaving only the membrane inside the beaker and subsequently membrane was washed several times with DI water before use.

3.4.3 Measurement and analysis

Polarization measurements were performed at regular intervals (15 min) to estimate the power production of MFC at various external resistances ranging from 50 to 20,000 Ω using an external resistor. The voltage data were taken using a digital multimeter with a built-in data logger (Fluke 289 true RMS industrial logging digital multimeter, USA) after it reached the stable value for obtaining the polarization curves. Power density normalized by volume (P , W/m³) was calculated using the following equation (equation 3.1) (Sarmin et al., 2019):

$$P = \frac{UI}{v} \quad 3.1$$

where, v is the volume of the MFC (m³), U is the voltage of the cell (V) and P is the power density (W/m³), and I is the current (A).

3.4.4 COD removal efficiency

COD is used as a measure of the oxygen requirement of a sample that is susceptible to oxidation by the strong chemical oxidants. It is always used to measure the number of organic compounds in water. Most applications of COD are to determine the

number of organic pollutants found in water or wastewater. Indirectly, COD has become a useful measure of water quality. The basis for the COD test is to fully oxidize all organic compounds to carbon dioxide with a strong oxidizing agent under acidic conditions. The amount of oxygen required to oxidize an organic compound to carbon dioxide, ammonia, and water is given by the equation 3.2. The COD was determined using a digestive solution (0- 1500 mg/L range; Hach, USA) and measured using a COD reactor (HACH DRB 200, USA). The COD removal efficiency (η) was calculated using equation (equation 3.2) (Sarmin et al., 2020):

$$\eta = \frac{COD_i - COD_t}{COD_i} \times 100\% \quad 3.2$$

where, COD_i is the initial COD (mg/L) of the anode chamber and COD_t is the COD of the anode chamber at any time.

3.4.5 Scanning electron microscope (SEM) analysis

Biofilm formation on the anode electrode was visualized using SEM (JEOL JSM7800F microscope, 5 kV) at various time intervals of the MFC experiments. The small sections of the anodes were cut off from the anode compartment and rinsed using sterile water. Subsequently, it was soaked in a beaker containing the anaerobic solution of glutaraldehyde (3%). The samples were then washed twice with 0.1 M phosphate buffer and dehydrated successively at various ethanol concentrations for about 10 minutes. After that, the samples were dried and coated with platinum to a thickness of 10 nm. Finally, the specimens were observed by SEM.

3.4.6 Electrochemical impedance spectroscopy (EIS) analysis

The schematic diagram of the EIS measurement system has been presented in Figure 3.4. EIS is a well-known non-destructive electrochemical technique for analyzing bio-electrochemical reactions on electrodes, internal resistances, biofilm development and studying the mass transfer resistance due to the diffusion limitations of the reactants (N. Khan et al., 2020). EIS was employed to measure the MFC anode internal resistances, and the measurement was conducted using a potentiostat (PARSTAT 2273, USA) at the open circuit potential in a frequency of 100 kHz to 50 mHz with the anode as the working electrode, the cathode as the counter electrode, and saturated Ag/AgCl (1.0 M KCl) electrode as the reference electrode.

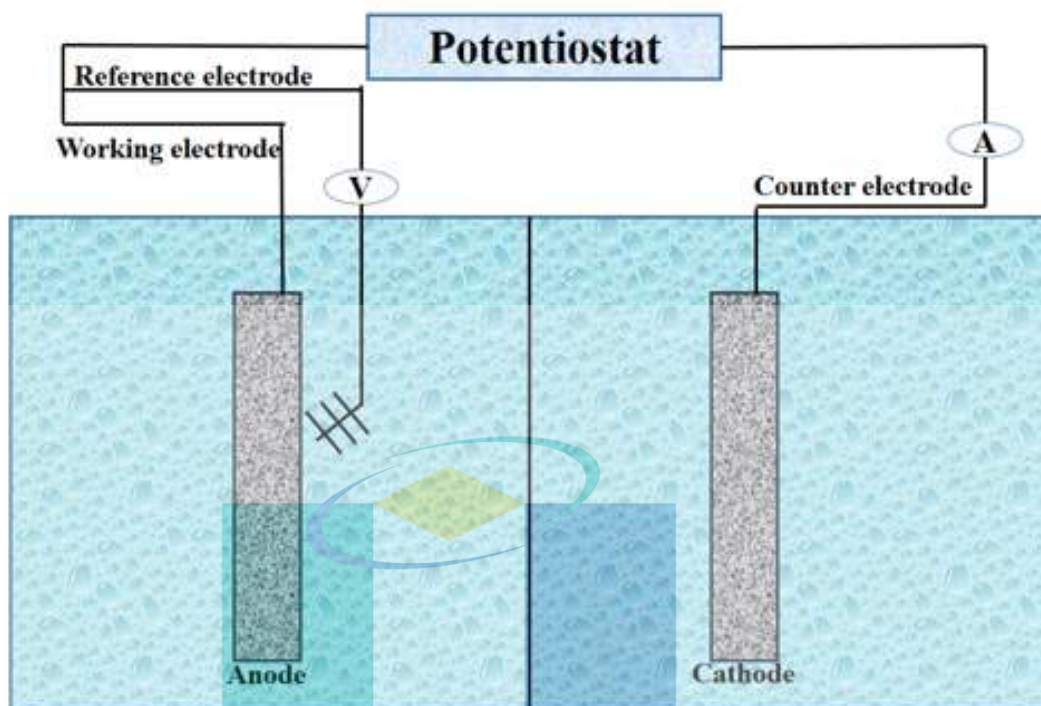


Figure 3.4 EIS measurement setup

3.4.7 Cyclic voltammetry (CV) analysis

CV was used to examine the catalytic behaviour of the MFCs. The CV analysis aids in characterizing the electron transfer interactions between the biofilm (biocatalyst) and the anode electrode of the MFC. Moreover, it helps to reveal the precise role of redox mediators, cytochromes and pili in the electrochemical reactions (Mancilio et al., 2020). The CV was performed using an electrochemical system, PARSTAT 2273, USA. A three electrode system was applied to collect the CV data where anode and cathode were used as working and counter electrodes respectively. The Silver/Silver chloride (1.0 M KCl) electrode was disinfected using 70% ethanol (Sigma) and used as a reference electrode. Moreover, the reference electrode was placed closer to the anode surface during the CV operation. The CV was performed at a scan rate of 30 mV/s in the potential range of +1.0 to -1.0 V and before each measurement; nitrogen gas was purged for about 15 min.

3.4.8 Cell growth analysis (OD)

To observe the growth profile, the sample was prepared using wastewater and microbes. The fixed amount of wastewater with microbes was prepared and kept in an

incubator shaker at 37 °C. After a fixed time later, the optical density of the sample was measured using UV 2600, Shimadzu spectrophotometer at 600 nm.

3.4.9 Liquid sample analysis by high liquid performance spectroscopy (HPLC)

The High-performance liquid chromatography (Agilent 1200 series, USA) with an organic acid column (Aminex HPX-87H, bio-rad, USA), operated with 6 mM H₂SO₄. HPLC was used to identify and quantify compounds from the substrates. Before starting the analysis, the samples were taken with additional H₂SO₄ (5 M H₂SO₄, 100 µL/mL of the reaction mixture). The temperature of the process was controlled 60 °C for 35 min and the flow rate was 0.5 µL/min (G. D. Saratale et al., 2019). To measure the initial and final concentration of AA, ACA, and DMP in synthetic wastewater, HPLC was done. For this, 3 MFCs were ran using 2 wt% of AA, ACA and 0.5 wt% of DMP as substrates with acclimatized AS for 16 days. The sample was collected from each MFC set-up before treatment, on day 5, 8, 11 and 16 respectively. Thereafter, the supernatant was filtered to avoid contamination and did the HPLC. The HPLC data of AA, ACA and DMP and the calibration curve are presented in A3. Finally, the relative concentration of these 3 substrates was calculated using initial and final concentration from the area and correlated with COD with time which is present in Figure 4.11a-c.

3.4.10 Ultraviolet-Visible spectroscopy (UV-Vis)

UV visible was used to analyse the microbial growth and metabolite analysis by using UV 2600, Shimadzu spectrophotometer. The capacity for keeping the sample area was smaller than 2 cm. All measurements were conducted at room temperature using a 1-cm path length cuvette. Prior to recording the spectrum of each sample the spectrometer was zeroed to account for any stray light. To avoid the effect of in homogeneities in the suspending medium, the background spectrum was taken using the respective suspending media from the batch utilized in the preparation of the original sample (Sarmin et al., 2019)(sterilized deionized water). For metabolite analysis. It was run at the range of 200-800 nm.

CHAPTER 4

RESULTS AND DISCUSSION

4.1 Introduction

This chapter presents the performance of the MFC generating energy from synthetic and real petrochemical wastewater using targeted acclimatized microorganisms. Besides, the mechanism of electron transfer from the systems and charge transfer kinetics of microbes are also discussed. The biofilm characterized by several techniques such as SEM, CV, and EIS analysis is also presented. In addition, the electron transfer kinetics also discussed using polymath software.

4.2 Treatment of synthetic wastewater by MFC

4.2.1 Effect of substrates

MFCs were run for 16 days under the load of 1 k Ω external resistance. The voltage data was recorded on a daily basis using AA (0.5-5 wt %), ACA (0.5-5 wt %), DMP (0.5-2 wt %) and their mixed performance (AA: ACA: DMP = 2:2:0.5 wt %) respectively with using targeted acclimatized AS and then the results presented in Figure 4.1a-d. From Figure 4.1a-d, it was observed that all substrates showed a similar trend in voltage generation although their initial value was different. As can be seen from Figure 4.1a-d, the voltage generation increased until the 11th day of operation indicating the presence of a higher concentration of microbes in the cell. Thereafter, it started declining and then it reached a minimum value after 16 days of operation which can be due to the multiple biofilm formation constituting a large percentage of dead cell (Islam, Ethiraj, et al., 2017). In the case of AA, starting with 0.5-2 wt%, the maximum voltage generation (0.027 V) was obtained using 2 wt% (0.029 V). However, for the higher concentration of AA (3-5 wt %), initially, the voltage generation was higher and then goes down. Also, a similar trend was found with the ACA, at 2 wt%, it also shows the maximum voltage (0.033 V) and for 3-5 wt%, initially, the voltage was higher and then goes down. At 3-5 wt%, the deactivation of both AA and ACA can be due to the fact that at higher concentration

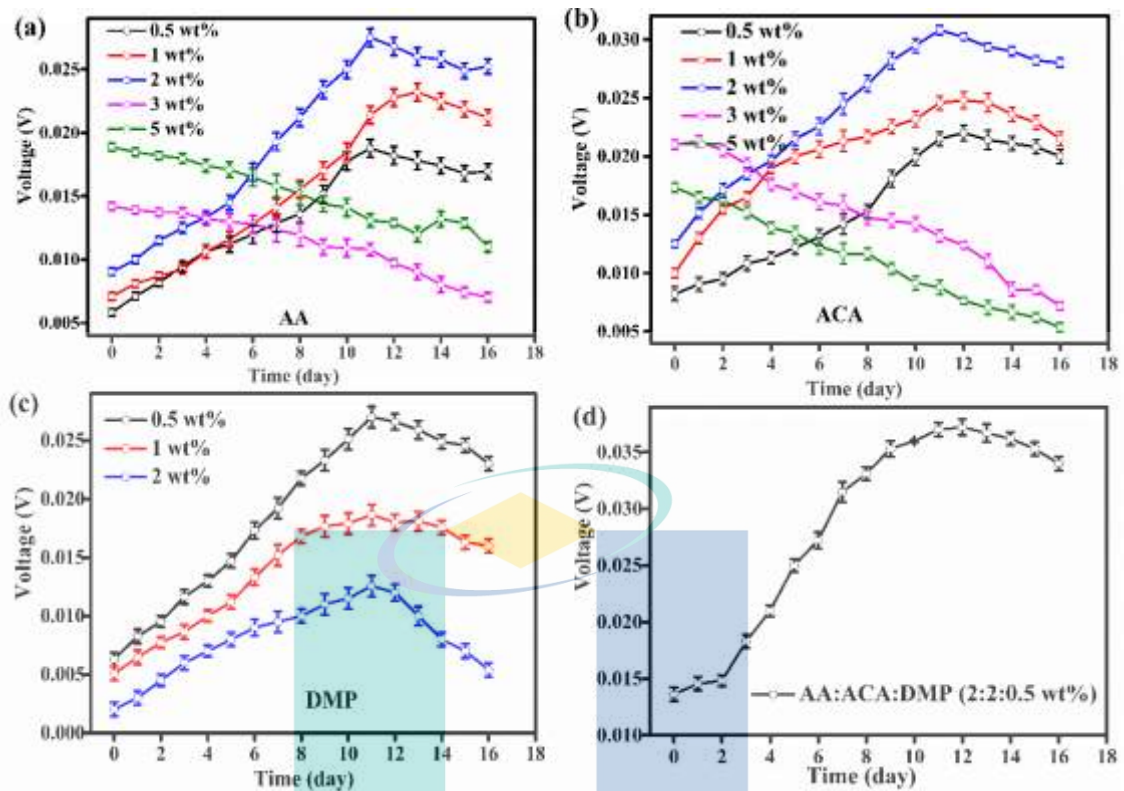


Figure 4.1 Voltage vs time using a) AA (0.5-5 wt%), b) ACA (0.5-5 wt%), c) DMP (0.5-2 wt%) and d) 3 substrates (2:2:0.5 wt%)

microbes cannot survive (Sarmin et al., 2019). Besides, the constant open circuit voltage (OCV) was achieved earlier with lower outputs, due to limitation in consuming carbon content in the substrate at a higher concentration by a microorganism resulted in substrates inhibition effect with lower performance (Bajpai, 2019). On the other hand, better performance for AA and ACA at lower concentration which might be due to the fact that all carbon sources available in the substrate solution at low concentrations which degraded fast in a shorter time resulted in better voltage and power generation (Barhoumi et al., 2017). However, with the DMP, 0.5 wt% shows the highest performance (0.026 V) whereas, with the increase of initial concentration (1 and 2 wt%), the voltage generation drops. The use of a lower concentration of DMP was proved by the literature (Cong, Liu, Wang, & Chai, 2020). The successful degradation of DMP using anaerobic reactor was showed by Liang et al. where they reported more than 99% of DMP (1500 mg/L) and 93% of chemical oxygen demand (COD) were effectively removed in a UASB reactor at an 8-h hydraulic retention time. In their study, they also showed that at higher concentrations, DMP showed cell deactivation which can be due to the longer ester chains and this chain hinders the hydrolytic enzymes from binding to the phthalates and thereby inhibits their hydrolysis (Liang, Zhang, Fang, & He, 2008). While comprising among 3

single substrates, although ACA, shows similar trend like AA, its overall voltage generation (0.030 V using 2 wt%) was higher than the AA (0.027, 2 wt%) and DMP (0.026 V, 0.5 wt%). The result is also consistent in terms of microbial growth and the maximum power density, where the acetic acid-fed-MFC showed the highest microbial growth and power density (1.1 and 0.058 W/m³ using 2 wt%) followed by acrylic acid (0.9 and 0.048 W/m³ using 2 wt%) and dimethyl phthalate (0.5 and 0.025 W/m³ using 0.5 wt%) from Figure 4.2a-b.

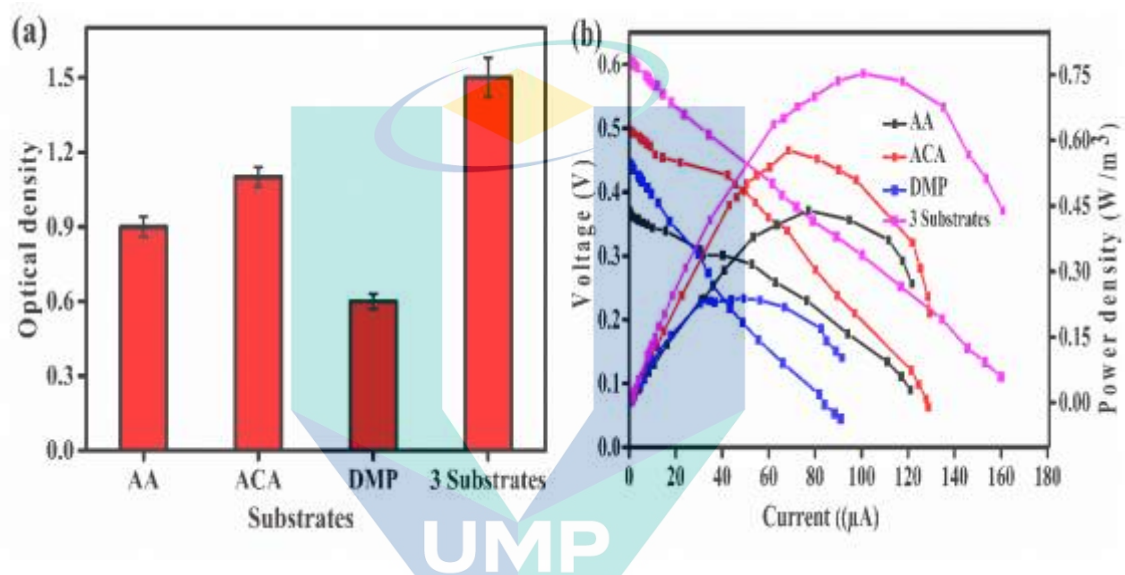


Figure 4.2 a) Microbial growth and b) power density using AA (2 wt%), ACA (2 wt%), DMP (0.5 wt%) and AA : ACA : DMP (2 : 2 : 0.5 wt%) at day 11

It can be due to the simplicity behaviour of ACA than AA and DMP. The result is consistent with previous results where acetate produces more electricity generation than other substrates, because of relatively simpler degradation pathways that could have less energy loss resulted in power production (power output) (Garba, Sa'adu, & Dambatta, 2017). Liu et al. also reported that the power generated with acetate (506 mW/m², 800 mg/L) was up to 66% higher than that produced with butyrate (305 mW/m², 1000 mg/L) (Nael Yasri, Edward PL Roberts, & Sundaram Gunasekaran, 2019).

Although AA and DMP showed lower performance than ACA, but when these three substrates were mixed (AA: ACA: DMP= 2: 2: 0.5 wt%) as synthetic wastewater, the voltage, microbial growth and power generation after 11 days of operation were found as 0.038 V, 1.5 and 0.078 W/m³ respectively which was significantly higher than single substrates from Figure 4.1d and Figure 4.2a-b. The results suggest the inoculum-

substrates based synergy while using mixed substrates with acclimatized AS (H.-T. Song et al., 2016). Initially, all cells started with a similar optical density of 0.3 from Figure 4.2a and then actually when the three substrates mixed with acclimatized AS, their survivability in terms of microbial growth was higher that might be responsible for the higher voltage and power generation. In mixed substrates with a mixed culture, the versatility or specificity of the bacteria for substrate utilization happened fast because of the availability of microbes and substrates (Kitzinger et al., 2019). In other words, it can be said that, the existence of unique versatile electrogenic microbes in acclimatized sludge that can degrade various substrates depending on its growth condition in that environment (R. G. Saratale et al., 2017). The result is consistent with the literature where the electricity generation using mixed substrates, such as acetate, glucose, cysteine, ethanol, and wastewaters with mixed culture showed better performance (Islam, Ethiraj, et al., 2017; Schneider et al., 2020).

4.2.2 Effect of inoculum

The effect of pure culture inoculums were evaluated for maximum power generation using different substrates, such as AA, ACA, DMP and synthetic wastewater and the performance was compared with the acclimatized anaerobic sludge as inoculum. The performance of MFCs was evaluated after 11 days of operations and presented in Figure 4.3a-d. From Figure 4.3a-d, it can be seen that in case of AA, PA showed better performance (0.24 W/m^3) than BC (0.22 W/m^3). However, when the acclimatized sludge was used, then the power generation was significantly higher (0.35 W/m^3). Similar performance was observed for the ACA and DMP driven MFC where the performance in the acclimatized AS was used the maximum power generation was 0.56 W/m^3 and 0.27 W/m^3 respectively. In contrast, when 3 substrates were used, it showed the same trend. However, the maximum power generation of 0.78 W/m^3 was obtained using acclimatized AS which might be due to the mutualistic interaction or synergistic interaction between the microbes and it permitted degradation ability in wide variety of substrates with concurrent power generation (Tyagi, Liu, Poh, & Ng, 2019). The mutualistic interaction in the co-culture comprising *Pseudomonas aeruginosa* (PA) and *Klebsiella. vericola* (KV) using POME substrate was shown by Islam et al. (Islam et al., 2018). It was shown that the microbes produced different fermentative products while simultaneously produced specific electron shuttle compounds responsible for enhanced power generation

(Islam et al., 2018). In another study, Islam et al. reported that *Pseudomonas aeruginosa* and *Enterobacter aerogene* as co-culture showed a electron shuttle based synergy by different metabolic pathways in the glucose environment (Islam et al., 2020).

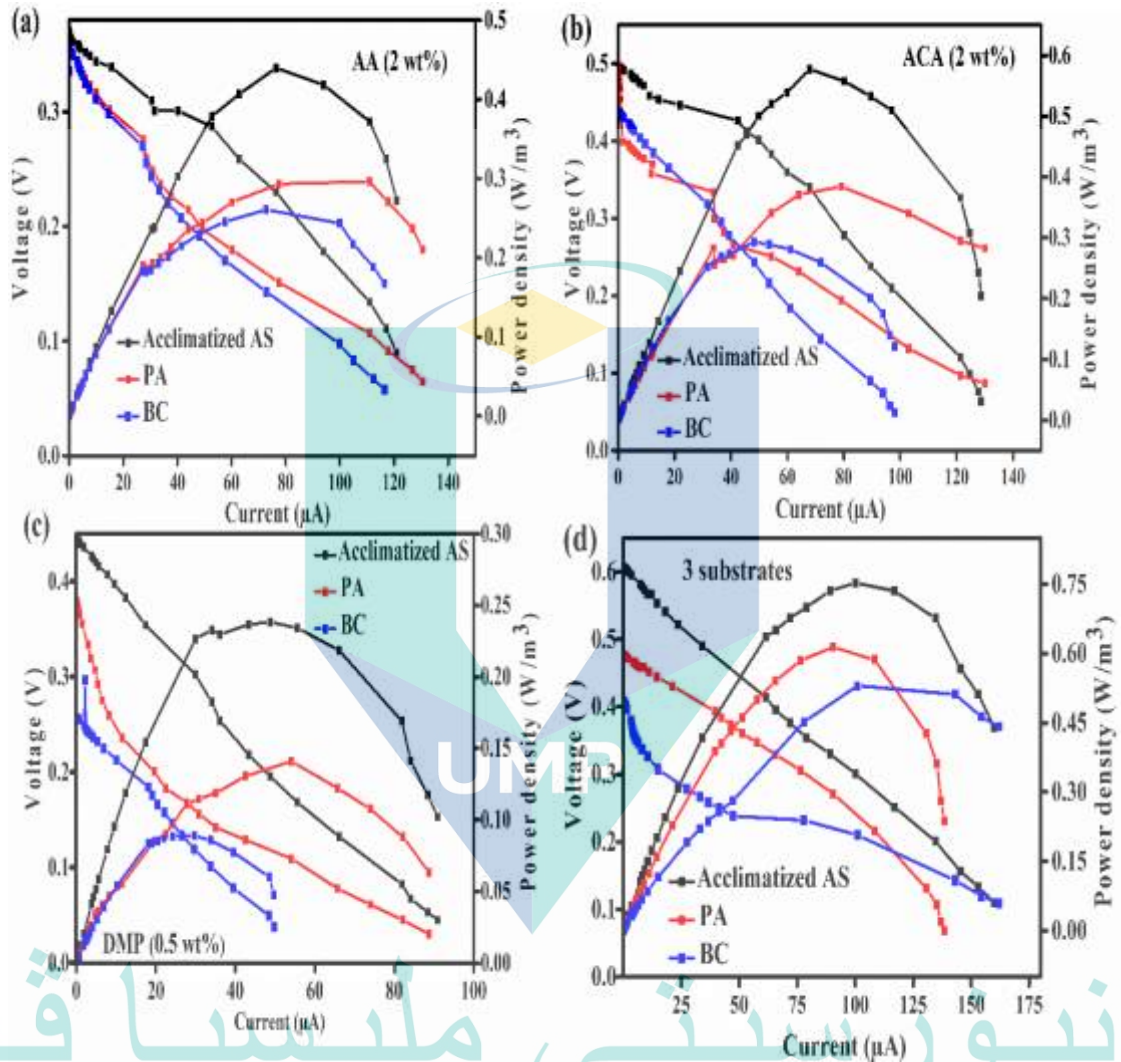


Figure 4.3 Polarization and power density curve using a) AA (2 wt%), b) ACA (2 wt%), c) DMP (0.5 wt%), and d) 3 substrates (AA:AC:DMP=2:2:0.5 wt%) with *Pseudomonas aeruginosa* (PA), *Bacillus cereus* (BC), and acclimatized AS at day 11.

The power generation data is also consistent with the microbial growth data. The microbial growth in the bulk was analyzed after 11 days of operation and the data is presented in Figure 4.4a-d. From Figure 4.4a-d, it can be seen that the bulk microbe density for the acclimatized AS driven MFCs was significantly higher compared to the PA and BC driven MFCs indicating that most of the microbes were activated at this

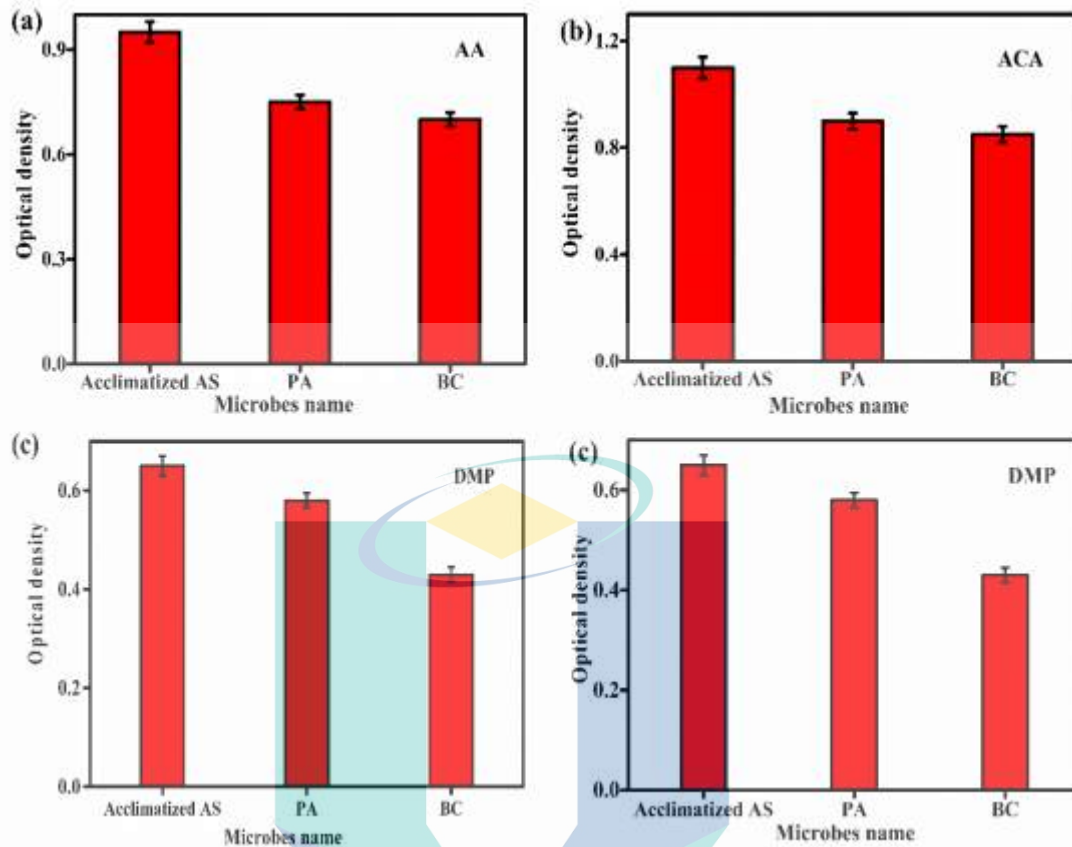


Figure 4.4 Microbial growth data using a) AA, b) ACA, c) DMP and d) 3 substrates at day 11

condition resulted in higher electron transfer efficiency with higher power generation (Basile & Ghasemzadeh, 2020). In contrast, while the comparison between PA and BC, PA showed better performance (0.25, 0.32, 0.2 and 0.5 W/m³ using AA, ACA, DMP and 3 substrates) than the BC (0.2, 0.25, 0.15 and 0.41 W/m³ using AA, ACA, DMP and 3 substrates) from Figure 4.3a-d. It indicated that as PA producing endogenous electron shuttle that directly involved in electron transfer from cells to the anode easily resulted in bioelectricity improvement in PA-inoculated MFC with higher power generation (Y. Cao et al., 2019a). On the other hand, single culture microorganism showed the poor performance also showed by several studies (Q. An, Cheng, Wang, & Zhu, 2020; Licandro et al., 2020). Actually, the performance of wastewater fed MFCs severely depends on the substrate utilization capability and the electrogenic properties of microbes (F. Zhao, Heidrich, Curtis, & Dolfing, 2020). In MFCs, it is well known that PA is a model organism for mediated electron transfer and it can produce four different types of electrochemically active pyocyanin which contains higher electron transfer efficiency compare to other mediators (Y. Cao et al., 2019c).

On the other hand, BC also can produce the metabolite. So, the presence of both known electrogenic properties of PA and BC in acclimatized AS enhanced the power generation (Mani, 2019). Some studies showed a drastic increase in power generation using defined acclimatized AS and co-culture in pure/simple substrate fed MFCs (V. Kumar, 2015; Xia et al., 2019) where they showed the better performance was obtained due to the presence of PA and BC. Haq and his co-workers observed that the syntrophic co-culture of *Bacillus subtilis* and *Klebsiella pneumonia* showed better decolorization efficiency (80%) and reduction of pollution parameters (COD 73% and BOD 62%) than the mono cultures (Haq & Raj, 2020). In another study, Patel and his co-workers reported that two co-cultures composed of BC, *Enterobacter cloacae*, and *Klebsiella sp.* resulted in H₂ yield up to 3.0 mol/L of glucose (El-Mokadem, El-Leboudy, & Amer, 2020). Apart from that, several studies have reported that the synergism between G⁺ and G⁻ within the MFC environment (Islam et al., 2020; Soukup et al., 2016). For example, the role of a phenazine electron shuttle has been verified in an earlier MFC study where it was observed to increase the current generation in co-cultures of *Brevibacillus sp.* and *Enterococcus sp.* with *Pseudomonas sp.* (X.-Q. Lin et al., 2019). These studies determined that the G⁺ were able to use electron shuttles (mediators) produced by *Pseudomonas sp.* the combination of both bacteria being the more successful one. Moreover, Read et al. reported that the power output of co-cultures Gram positive *Enterococcus faecium* and Gram-negative PA, increased by 30-70% relative to the single cultures (Hanchi et al., 2018). Islam et al. also reported that the addition of BC in the AS substantially enhanced the electrochemical activity of mixed cultures (Islam, Ethiraj, et al., 2017). The results of their study suggest that the incorporation of microorganisms possessing electrogenic and anti-methanogenic properties in acclimatized AS promotes the formation of electroactive biofilm and maximizes the power generation of MFC by suppressing the methanogenesis. So, in the present study due to the presence of double electrogen microbes such as PA and BC in acclimatized AS are responsible for the highest power density than pure cultures. Therefore, it can be concluded that the understanding of interactions between the microbes is exigent to get deeper insight into their performance in real wastewater fed MFCs.

4.2.3 Time course biofilm formation of synthetic wastewater using SEM

A biofilm is defined any group of microorganisms in which cells stick to each other's or onto a surface and these adherent cells become embedded within a slimy extracellular matrix that is composed of extracellular polymeric substances (EPS) (Mahamuni-Badiger et al., 2020). The biofilm formation capability of microbes (BC and PA) using different substrates at day 11 was visualized by SEM analysis as shown in Figure 4.5a-h.

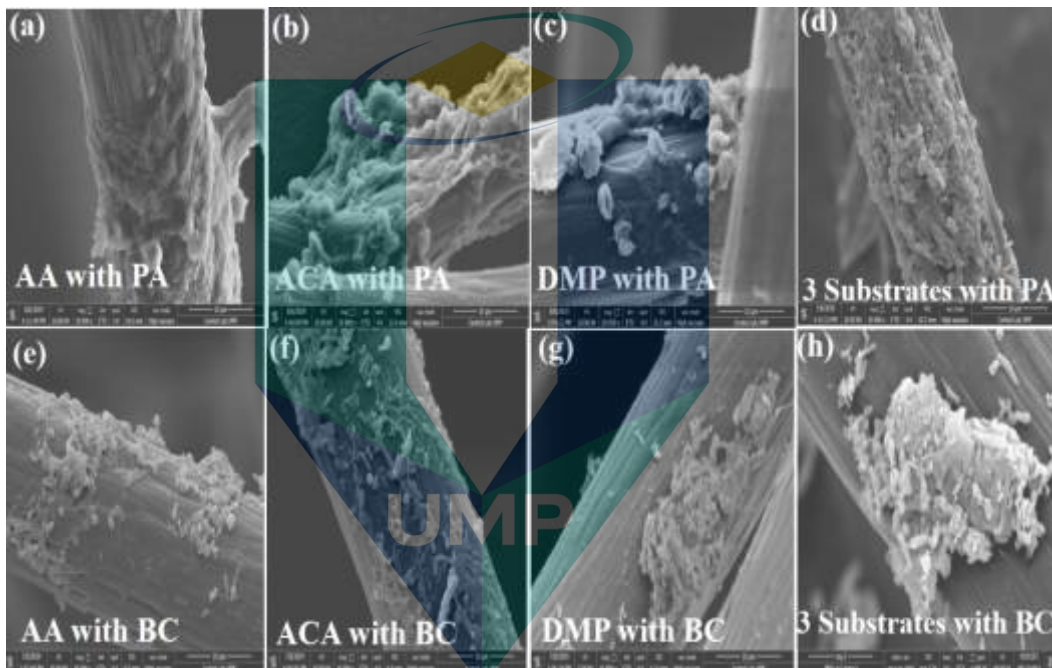


Figure 4.5 SEM of PA and BC using same wt% a) AA (2 wt%) with PA, b) ACA (2 wt%) with PA, c) DMP (2 wt%) with PA, d) 3substrates (AA:ACA:DMP = 2:2:0.5 wt%) with PA, e) AA with BC, f) ACA with BC, g) DMP with BC and h) 3 Substrates with BC at day 11

On the other hand, the biofilm formation using acclimatized AS with different substrates are given in Figure 4.6a-d. From Figure 4.5a-d and Figure 4.6a-d, it can be seen that more effective biofilm formation was observed using acclimatized AS than single microbes (Figure 4.5a-h). On the other hand, effective biofilm means the dense as well as compact biofilm consisting of a higher number of active cells on the electrode surface (Elbourne et al., 2020). On the other hand, substrates can keep role on biofilm formation and there is an interconnection between substrates and biofilm (Fei et al., 2020). Generally, biological colonization is a complex dynamic, depending on both substrates and environmental factors. Usually, the influence of the latter is stronger, but when light, relative humidity and temperature do not represent limiting factors, physicochemical

characteristics of substrates become crucial drivers of the assembly of microbial communities (De Natale et al., 2020). Moreover, species composition may also vary in biofilm growing very close to each other, and, apparently, in the same chemical and physical conditions, suggesting the involvement of species interactions and stochasticity in the community assembly process (Caruso, 2020). Thus, colonization can strongly depend on the organism that establishes the first firm relationship with the substrate, conditioning the subsequent steps of the biofilm consolidation. Community-level interactions are unique to each structured community of microorganisms, and strongly intertwined with the architecture of the biofilm (De Corato, 2020). At a fundamental level, spatial interactions among microorganisms forming biofilms on monuments can often explain important attributes of biofilms and are well documented (Gallego-Cartagena et al., 2020). Actinobacteria and filamentous Cyanobacteria, for example, often grow in a close association, sometimes establishing a direct cell-to-cell contact and some other times sharing a matrix of extracellular polymeric substances (EPS) (Caruso, 2020).

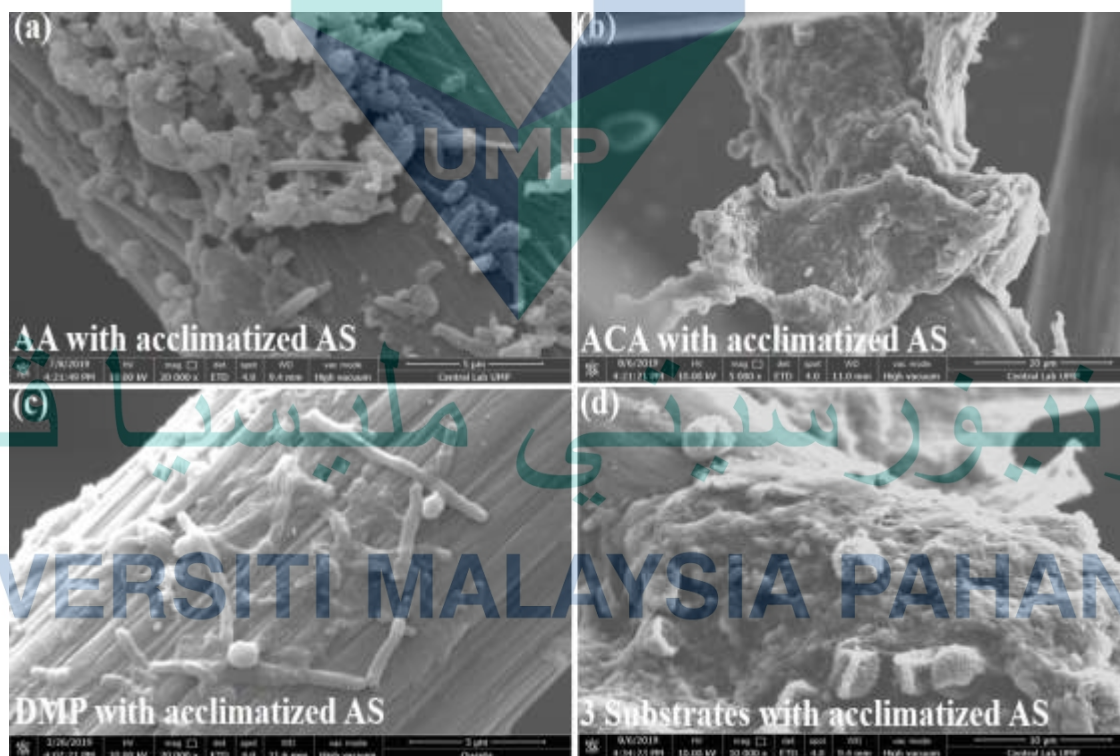


Figure 4.6 SEM using a) AA (2 wt%), b) ACA (2 wt%), c) DMP (2 wt%) and d) 3 Substrates (AA:ACA:DMP=2:2:0.5 wt%) with AAS at day 11

Such matrix represents at the same time the adhesion agent used by organisms to remain anchored to the substrate and the common ground that connects them. It also has

a potential role in modulating chemical signals at the base of microorganisms' interactions (Cullen et al., 2020). In case of mixed substrates with mixed culture, due to above mentioned factors effective biofilm formed (K. Dai, Zhang, Zeng, & Zhang, 2020). The result is also consistent with the power generation and microbial growth where mixed substrates showed better power generation and higher microbial growth (Figure 4.3a-b Figure 4.4a-d).

The CV data were recorded The CV data were recorded after inoculation 11th day of operation using PA, BC and acclimatized AS using different substrates is presented in Figure 4.7a-c.

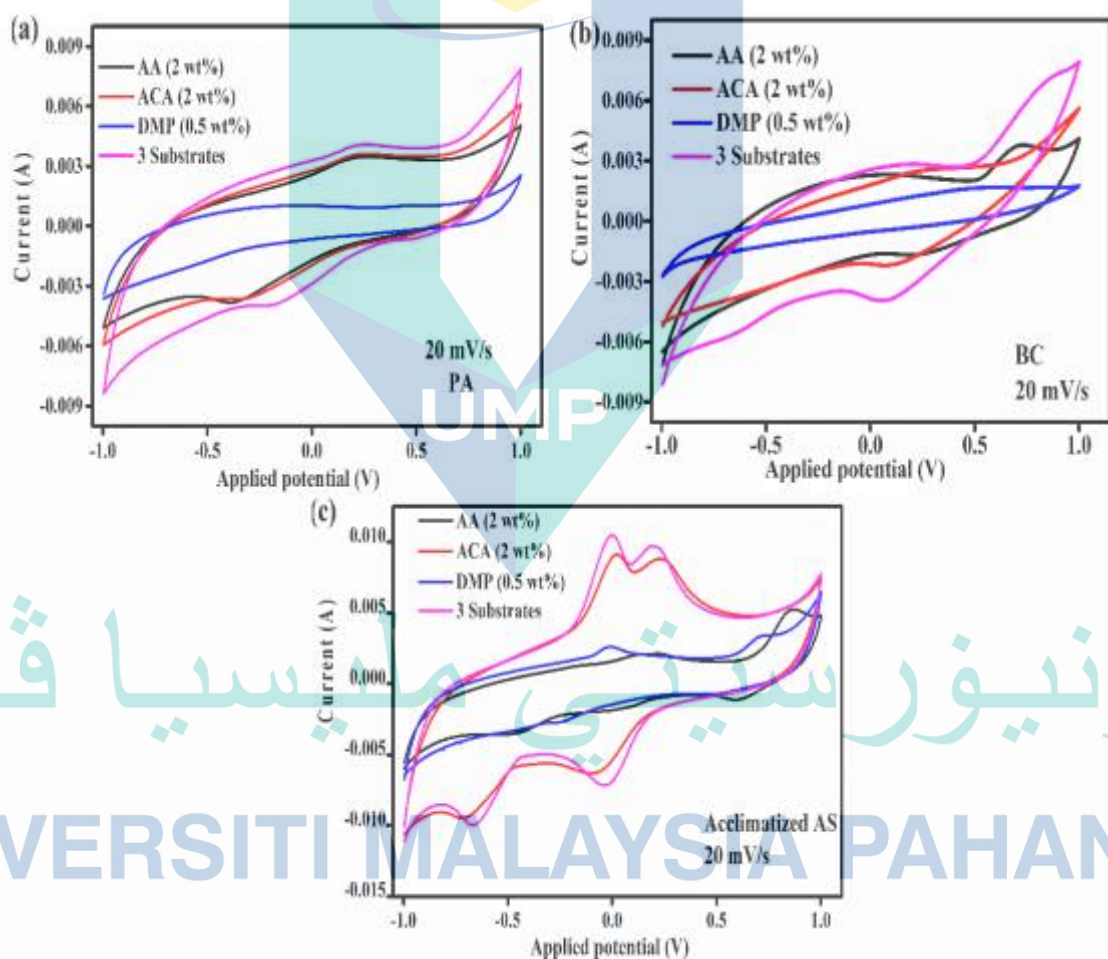


Figure 4.7 Cyclic voltammetry of a) AA (2 wt%), b) ACA (2 wt%), c) DMP (0.5 wt%) and d) 3 Substrates (AA:ACA:DMP=2:2:0.5 wt%) using PA, BC and acclimatized AS at day 11.

Besides, the CV was performed to characterize the electron transfer mechanism between the biofilm (biocatalyst) and the anode of the MFC using different microbes. The characteristics of CV rely on various factors, such as the chemical and biological species

present, the rate of the electron transfer reactions and the rates of diffusion of electroactive species (Modestra, Reddy, Krishna, Min, & Mohan, 2020). Moreover, it helps to elucidate the explicit role of redox mediators in the electrochemical reactions (Siu, Fu, & Lin, 2020). From Figure 4.7a-c, it can be seen that after 11th day of operation, redox peaks were observed at 0.47 V and 0.22 V, and 0.24, -0.34 V for BC and PA and acclimatized AS with different substrates respectively. The redox and oxidative current using different substrates with PA, BC and acclimatized AS is presented in Table 4.1.

Table 4.1 Oxidative and reductive peaks with oxidative and oxidative current using PA, BC and acclimatized AS with different substrates

Inoculum	Substrates	E _{ox} (V)	E _{red} (V)	I _{ox} (A)	I _{red} (A)
BC Day 11, 20 mV/s	AA	0.47	0.22	0.0035	-0.0011
	ACA	0.47	0.22	0.003	-0.0032
	DMP	0.47	0.22	0.0057	-0.0075
	3 Substrates	0.47	0.22	0.0039	-0.0045
Inoculum PA (20 mV/s), Day 11	Microbes	E _{ox} (V)	E _{red} (V)	I _{ox} (A)	I _{red} (A)
	AA	0.24	-0.390	0.0034	-0.0039
	ACA	0.24	-0.39	0.0037	-0.0037
	DMP	0.24	-0.39	0.0021	-0.002
Inoculum (Acclimatized AS)	3 Substrates	0.24	-0.39	0.0078	-0.0078
	Microbes	E _{ox} (V)	E _{red} (V)	I _{ox} (A)	I _{red} (A)
	AA	0.24	-0.47	0.0024	-0.0033
	ACA	0.24	-0.39	0.0043	-0.0057
PA	DMP	0.006	-0.39	0.0023	-0.003
	3 substrates	0.24	-0.56	0.009	-0.011
	AA	0.4	0.233	0.0018	-0.0037
	ACA	0.35	0.006	0.0033	-0.0063
BC	DMP	0.8	0.5	0.0041	-0.0083
	3 substrates	0.30	0.006	0.009	-0.0073

From Table 4.1, it can be seen that the acclimatized AS (PA and BC) using 3 substrates showed higher intense redox peak (maximum current of 0.009 and 0.009 A at 20 mV/s) compared to others also suggesting presence of higher concentration of electrogenic microbes (PA and BC) in acclimatized AS and higher electro-catalytic efficiency of electron shuttling mediators presented in acclimatized AS with 3 substrates driven MFC (Sarmin et al., 2020). Electron transfer from the biocatalyst to the anode can be distinguished between direct electron transfer (DET) and mediated electron transfer (MET) mechanisms which is helpful in avoiding electron losses between the biocatalyst and anode (Krishna et al., 2019). The documented mediator indicates electron transfer via

MET. Also, the additional soluble mediators present in mixed culture might also involved in the electron transfer in MFC. Moreover, the formation of reversible redox couples, revealed the presence of mediators that reversibly oxidized and reduced during CV tests (C. Zhang et al., 2020). Furthermore, on the basis of CV results, Zheng et al. also concluded that *Shewanella oneidensis* strains capable to secrete soluble mediators which help for the extracellular electron transfer between the biofilm and the anodes. Recent studies showed the capability of *Shewanella sp.* and *Geobacter sp.* to form filamentous pili as the third mechanism for extracellular electron transfer through biological nanowires (Zheng et al., 2020). *Shewanella sp.* have the capability to transfer electrons via DET (conductive bacterial pili) and MET (secondary metabolites) and MET (secondary metabolites) (Juping You et al., 2020). An electrochemically active strain can discharge electrons effectively into the exterior environment, while in the case of mixed culture, there are number of interferences resulting in the total electron losses (Velvizhi, 2019). The electron released might undergo neutralization prior to reaching the anode.

Electrochemical analysis enumerated higher electron transfer efficiencies with the acclimatized mixed culture with mixed substrates contributing for higher power output compared to single and mixed substrates with single cultures (Jiang & Zeng, 2019). The energy stored in the cell was higher than that of MFC-operated with mixed substrates with acclimatized AS. Furthermore, the multiple metabolic interactions occurring within the mixed culture and with the acclimatized strain might have helped in maintaining the redox power shuttling between metabolic intermediates leading to the high potential maintenance for longer periods (Lazaro, Sagir, & Hallenbeck, 2020).

4.2.4 Electrochemical impedance spectroscopy of synthetic wastewater

Electrochemical Impedance Spectroscopy is employed to understand the role of anodic capacitance and individual component resistance in the bioelectricity generation of microbial fuel cells. It also provides information to analyse the electrochemical reactions at electrode/electrolyte interface, bacterial metabolism, surface and material properties of the electrodes) (L. Shen et al., 2016). The EIS experiments were conducted using Biological Electrochemical Workstation as shown in Figure 4.8a-c.

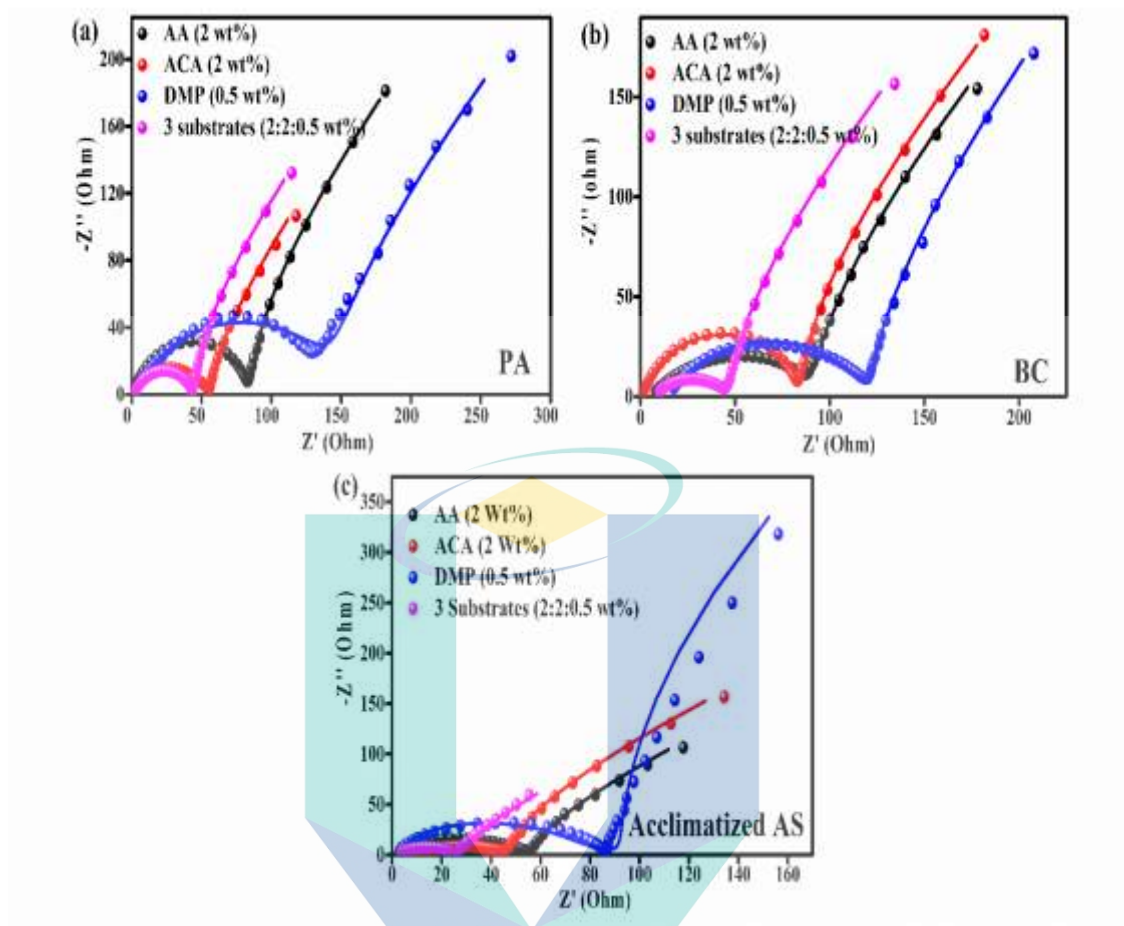


Figure 4.8 a) Nyquist plot of different substrates using PA , b) BC and c) Acclimatized AS at day 11

In Figure 4.8a-c, the Nyquist plot represents a complex plane plot for the anode of the MFC, expressing the real (X-axis) and imaginary part impedance (Y-axis) (Sarmin et al., 2019). The Nyquist plot formed a semicircle at higher frequency region followed by a tail between the medium to lower frequency region. Typically, the high-frequency impedance limit indicates the ohmic resistance (R_s) and the diameter of the semicircle arc represents the charge transfer resistance (R_{ct}) (Ter Heijne, Liu, Sulonen, Sleutels, & Fabregat-Santiago, 2018). In order to obtain the quantitative values of resistances, the anode impedance data was fitted by an equivalent circuit, $[R_s(R_{ct})(WQ)]$ which presents the complex behaviour of the bio-electrochemical reactions. The components of the equivalent circuit R_s , R_{ct} , Q (CPE) and W represent the ohmic resistance, charge transfer resistances (R_{ct}), constant phase elements (Q) and the Warburg element, respectively (Mandal & Mitra, 2020). The EIS data fitting parameters of PCW with other substrates at day 11 are presented in Table 4.2.

Table 4.2 EIS fitting parameters using different substrates at day 11

Name	R_s (Ohm)	R_{ct} (Ohm)	Q ((Y_0) (mMho))	Z_w ((Y_0) (mMho))	τ_b (μs)
AA, (PA)	4.58	82	37	5.9	0.002
ACA, (PA)	5.98	57	39.5	14.6	0.000952
DMP, (PA)	2.31	130	7.34	2.87	0.007
3 substrates, (PA)	8.09	47	44.9	17	0.000762
AA, (BC)	3.06	89	38	6.89	0.010
ACA, (BC)	3.87	88	36	6.65	0.008
DMP, (BC)	2.92	119	8	3.06	0.002
3 substrates, (BC)	8.78	45	41	15.5	0.0014
AA (acclimatized AS)	6.09	59	55.5	22.5	0.0009
ACA (acclimatized AS)	8.84	43	43.1	16.3	0.0007
DMP (Acclimatized AS)	3.87	85	40	7.02	0.001
3 Substrates (acclimatized AS)	9.9	27	75	26.8	0.00031

Using mixed substrates using mixed inoculum showed lower charge transfer resistance of 27 Ω from Table 4.2 which might be due to the presence of higher microbes, proper biofilm and higher concentration of naturally produced metabolites (Yousefi et al., 2020). Besides, the constant phase element (ω) is calculated by the following equation 4.1:

$$Q = Y_0(j\omega)^N \quad 4.1$$

where Y_0 = the value of the admittance, $\omega=1$ rad/s. If the value of the admittance increases, constant phase element also increases. From the Table 4.2, it can be seen that, on day 11, using 3 substrates with Acclimatized AS showed maximum admittance value (85.24 mMho) was achieved in comparison to other days indicating higher charge holding capacity and the highest concentration of the mediators. In addition to this, mass transfer resistance (Z_w) plays an important role in MFC which is calculated by the following equation 4.2. (Agostino et al., 2017).

$$Z_w = \frac{\sigma}{\sqrt{\omega}} + \frac{\sigma}{j\sqrt{\omega}} \quad 4.2$$

where, σ is the Warburg coefficient, and $\omega = 1$ rad/s. The Warburg coefficient σ depends on the magnitude of impedance Y_0 and is calculated by following equation 4.3 (Sarmin et al., 2019):

$$\sigma = \frac{1}{\sqrt{2Y_0}} \quad 4.3$$

where, Y_0 is the magnitude of impedance. From equation 4.3, it can be seen that Y_0 is inversely proportional to the Warburg coefficient. Hence, if the value of Y_0 increases, the Warburg resistance will decrease. From equivalent circuit, $([R(RQ)(WQ)])$ fitting the values of the Y_0 component were obtained and presented in Table 4.2. The Y_0 value sharply increased from single to mixed substrates using mixed culture 2.02 mMho to 25.1 mMho on day 11 indicating the drastic reduction in mass transfer resistance with higher microbial growth in the bulk leading to higher metabolite concentrations and biofilm formation (Sankaran et al., 2019). The result is consistent with the literature. Sanchez-Herrera et al. showed that the increased concentrations of mediators reduces the anode activation losses and facilitates the kinetics of the electrochemical reactions. reported that the synergism of bacteria could enhance the secretion of electron shuttling mediators (W. Shen et al., 2020). Moreover, in their study, the Acclimatized AS remarkably enhanced the mediator (pyocyanin) production and showed higher power generation compared to the monocultures. However, the higher R_{ct} for the monocultures ascribe that less mediator concentrations (using PA and BC) in MFCs. Another important point was aforementioned that both bacteria (PA and BC) produced soluble electron shuttle mediators thus facilitated electron transfer from microbes to electrodes. Even though the redox mediator facilitates rapid electron transfer, the charge transfer resistance of MFC still remains high due to its low concentration (Tahernia et al., 2020). Hence, comparing the monoculture, the Acclimatized AS with 3 substrates achieved lower charge transfer resistance possibly due to the presence of higher mediator concentration and availability of organic substrates in the anode compartment of MFC indicating higher electro-catalytic efficiency in the MFC. The presence of higher cell density in the vicinity of the electrode consequently reduced the diffusion path resulting in a lower diffusion resistance in co-culture inoculated MFC.

Apart from this, a shortcoming of the complex plane plot is that it does not show the values of the frequency of the applied ac signal and the phase angle. On the other hand, as a non-destructive technique, bode plot can provide charge transfer information of the electronic devices, in which the time constant τ_d is used to describe the charge transfer time, i.e., the average time interval from the charge generation to collection. The smaller the τ_d , the faster the charge transfer rate is, and the higher charge collection efficiency as well. For bode plot measurements, τ_d can be determined by the equation 4.4 (Y. Wang, Wang, Woldu, Zhang, & He, 2019).

$$\tau_b = \frac{1}{2\pi f_{max}} \quad 4.4$$

where, f_{max} is the frequency when the imaginary part of photocurrent reaches the highest value. The f_{max} value can be determined with the corresponding Bode plot is presented in Figure 4.9a-c and the value of τ_b as listed in Table 4.2.

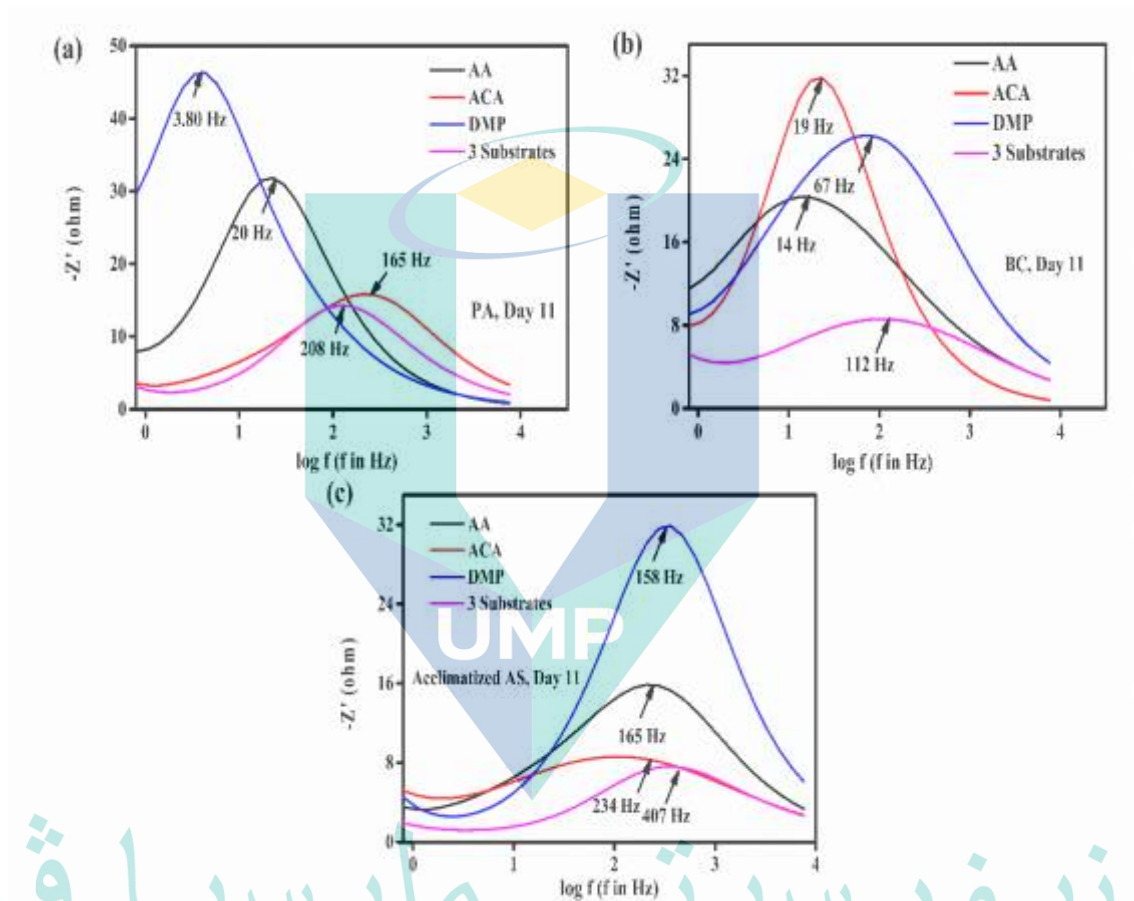


Figure 4.9 Bode plot of different substrates using different microbes, a) PA, b) BC and c) acclimatized AS.

From Figure 4.9a-c and Table 4.2, it can be seen that acclimatized AS with 3 substrates showed the shortest electron transfer time ($0.00031 \mu s$) compared to single substrates and microbes indicating the electrons generated using mixed culture can be readily injected into the electrolyte at a much faster speed. At the same time, the arc accumulated more favourably in the anode and then flow to the cathode. Moreover, electron transfer from anode to cathode will become low if the electron transfer rate to the solution is faster than the electron generation rate (Y. Wang et al., 2019). Therefore, such kinetic difference in the transfer of electrons and generation can have a great influence on the charge separation process, indicating that acclimatized AS has the

highest performance in charge transfer. However, the increment of biofilm thickness plays an opposite role in the charge generation and transfer (Zhuang et al., 2020). There will not be enough amount of electron transfer and charge carriers to be involved in the reduction reaction if the biofilm is too thin; while there will be plenty of multiple layers that can hinder the efficient charge transfer and separation if the multilayer biofilm forms (Angelaalincy et al., 2018). Hence, the acclimatized AS sample with a suitable film thickness shows the best MFC performance than the PA and BC due to the balance of charge generation and transfer (Nikhil, Chaitanya, Srikanth, Swamy, & Mohan, 2018). Besides, the information of frequency and phase angle presented in Figure 4.10a-c.

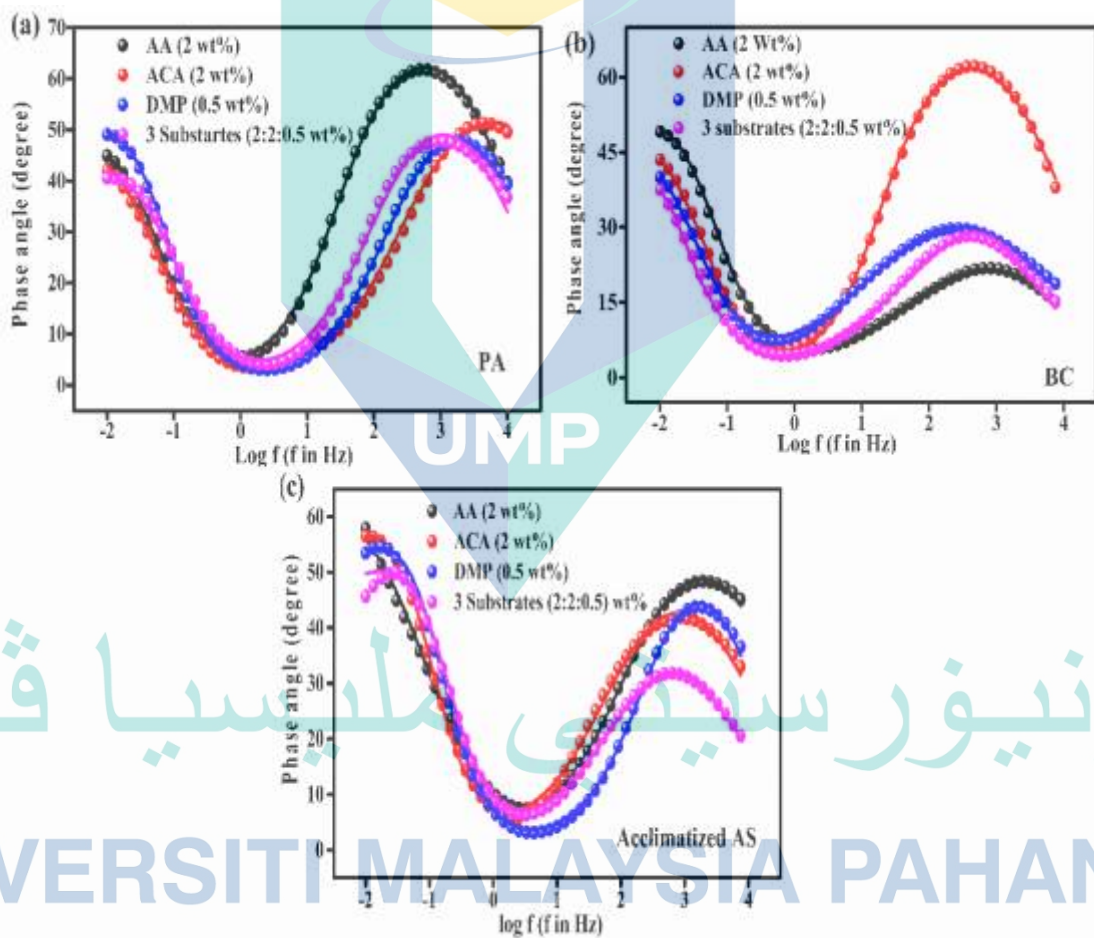


Figure 4.10 Bode plot of different substrates using different microbes, a) PA, b) BC and c) acclimatized AS.

From Figure 4.10a-c, it can be seen that both bode modulus and phase shifts from single to mixed substrates using single to mixed microbes. From Figure 4.10 a-c, it can also be seen that among all microbes, in the case of 3 substrates fed MFC with acclimatized AS, the bode modulus and phase shifts more than others indicating the lower

charge transfer and mass transfer capability of using mixed substrates with acclimatized AS (Sarmin et al., 2020).

4.3 Substrate analysis by HPLC

From Figure 4.11a-c., it can be seen that although AA and ACA fed MFCs were run using 2 wt%, their concentration and COD removal are not the same after 16 days of operation. For AA, initial COD was 21000 mg/L and after 16 days of operation (16 days was taken based on operational time), it was 4500 mg/L which was higher than ACA where COD removal was 21000 mg/L to 4000 mg/L. It is because of simple structure ACA than AA resulted in more COD in the system than AA. Generally, microbes choose the more simple substrates to degrade first than other substrates (Puentes-Télliez & Salles, 2020). So, the simple structure of ACA degraded more than AA in the system. Among 3 substrates, the COD removal was efficiency (82%) was higher in the case of DMP fed MFC where initial COD was 2500 mg/L and the final COD was 400 mg/L.

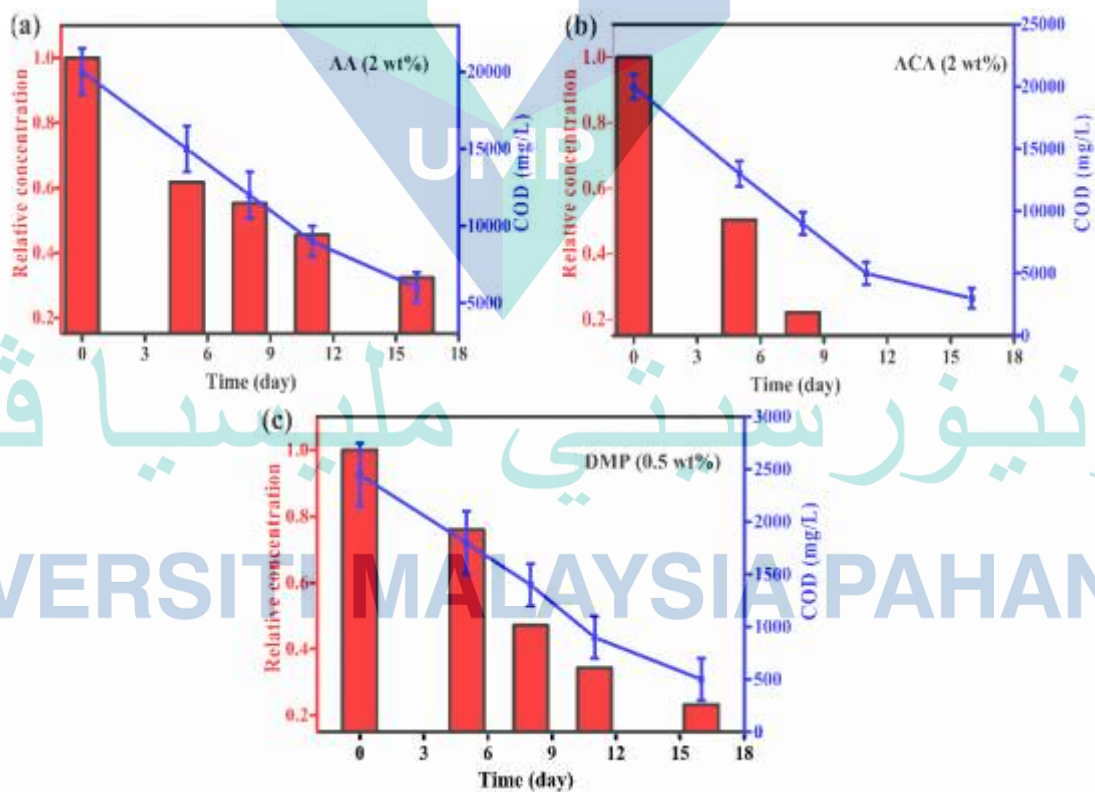


Figure 4.11 Relative concentration, COD vs time using a) Acrylic acid (AA), b) Acetic acid (ACA) and c) Dimethyl phthalate (DMP)

This can be due to the using of less amount of DMP. On the other hand, from Figure 4.11a-c, it can also be seen that COD removal was less than substrates

concentration. It is common for 3 substrates. It can be due to the production of new organic compounds and metabolites secreted by the microbes during the reaction which was responsible for less COD removal. The result is consistent with the literature (Soh, Kunacheva, Webster, & Stuckey, 2020). From the above all results and discussion (section 4.1-4.3), it can be said that synthetic wastewater can be treated by using PA, BC and acclimatized AS. Among all substrates, acclimatized AS showed better performance than the individual microbes. So, the next section will be based on performance using real PCW with acclimatized AS.

4.4 Treatment of industrial PCW by MFC

4.4.1 Effect of initial concentration

Four MFCs fed with different concentrations (initial COD of 100000, 75000, 45000 and 26000 mg/L) of PCW were operated for 16 days under an external resistance of 1 k Ω . The graph for the current generation with respect to time is represented in Figure 4.12a.

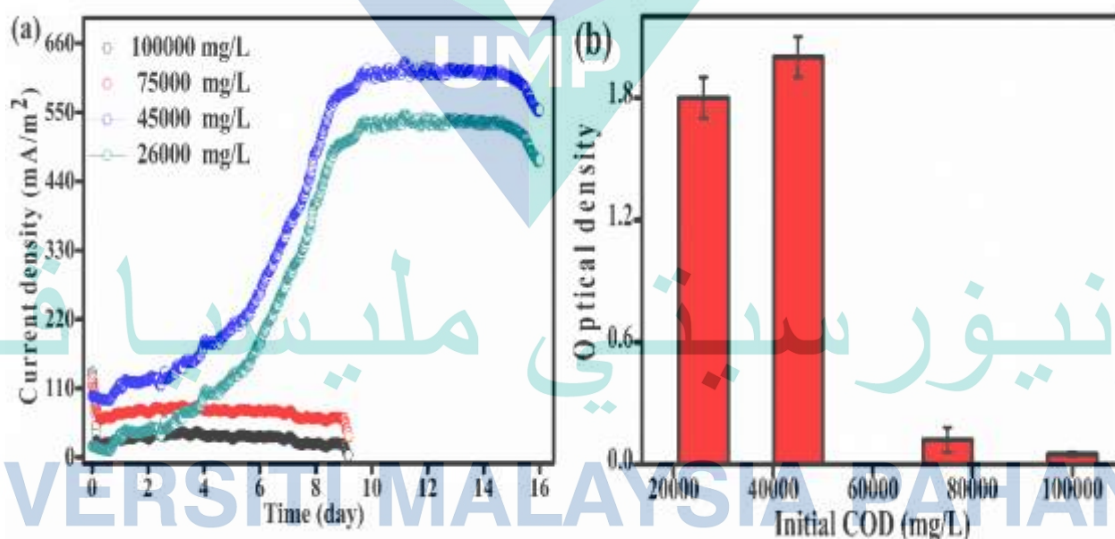


Figure 4.12 (a) The current vs. time curves at different initial COD, and (b) Effect of initial COD on microbial growth in MFCs (after 7 days of operation).

From Figure 4.12a., it can be seen that the current generation of the MFCs that operated within the range of 100000 and 75000 mg/L, COD was found to be very low which eventually decreased after 7 days of operation. However, the current generation exhibited an opposite trend with a further dilution of raw wastewater within the range of 26000-45000 mg/L of COD: a steady increase in current generation until 9 days of

operation, thereafter, the current started to decline. The low current generation for high initial COD (75000 and 100000 mg/L) might be attributed to less cell growth (0.06 and 0.01) in concentrated PCW as presented in Figure 4.12b. The cell growth was found as ~ 4 – 5 times higher when the initial COD was in the range of 26000 – 45000 mg/L. Several studies have shown that MFCs fed with higher COD attained lower cell growth due to the presence of higher amount of cell growth inhibitors (cyanide and azide) thus resulting in lower power generations (Cui, Lai, & Tang, 2019; Sevda et al., 2020). Santos et al. reported that when the MFC was operated with vinasses as substrate and AS as an inoculum, the higher CODs resulted in lower current generation (Santos et al., 2017). Additionally, from Figure 4.12a, it is evident that the current generation rate (calculated from the slope of the current generation profile) from 6 to 8 days of operation for the MFC run with 26000 mg/L COD (120 mA/m²/day) was slightly higher compared to the MFC operated with 45000 mg/L COD (115 mA/m²/day). However, the overall current generation was significantly higher at all times with 45000 mg/L of COD. Therefore, among the different concentrations of PCW, the 45000 mg/L COD containing PCW was considered as optimum substrate and was thus used for subsequent experiments as it allowed higher current generation along with maximum cell growth.

4.4.2 Polarization behaviour of the MFC

To evaluate the maximum power generation from MFC, the polarization curve was obtained at different days of operation as presented in Figure 4.13a-b. From Figure 4.13a-b, it can be seen that where a steady increase in power density until 11 days of operation was noticed. On 5th day of operation, the maximum power density of 500 ± 10 mW/m² with a current density of 1200 mA/m² was achieved which significantly increased to 850 ± 10 mW/m² delivering a current density of 1400 mA/m² after 11 days of operation. The low power density after 5 days of operation might be due to the lower abundance of microbial biofilm on the anode surface (Sarmin et al., 2019). Besides the maximum power density was declined after 16 days of operation (680 ± 20 mW/m² and 1200 mA/m²) which ascribed that the ineffective biofilm formation constituting a large percentage of dead cells (Islam, Ethiraj, et al., 2017; Islam et al., 2016). The trend of power generation is consistent with some of the recently reported wastewater fed MFC studies (Islam, Ehiraj, Cheng, Dubey, & Khan, 2019; Islam, Ethiraj, et al., 2017).

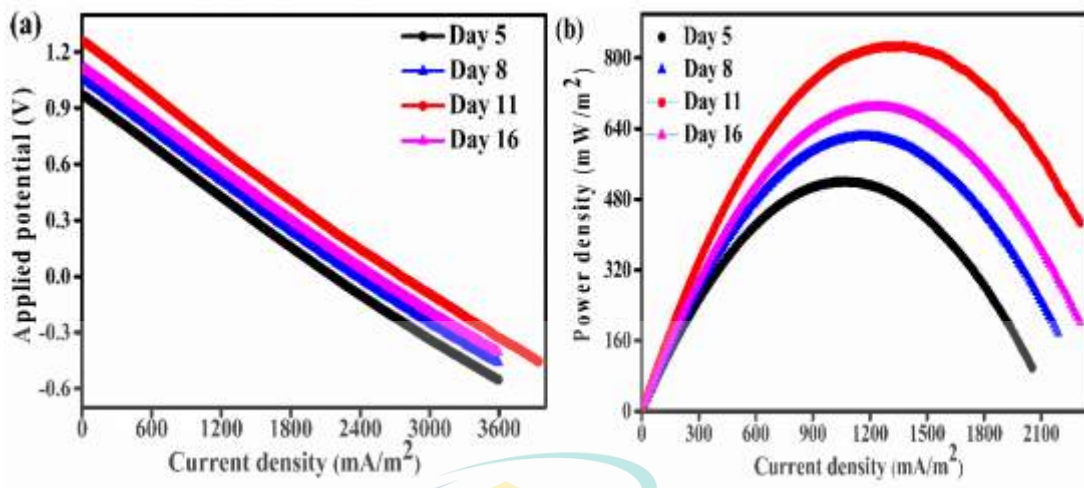


Figure 4.13 a) The polarization curve, and b) The power curves for MFC

4.4.3 Time course biofilm formation of PCW using SEM

The biofilm formation capability of acclimatized microbes using PCW (45000 mg/L) with acclimatized AS was visualized by SEM analysis as shown in Figure 4.14a-e.

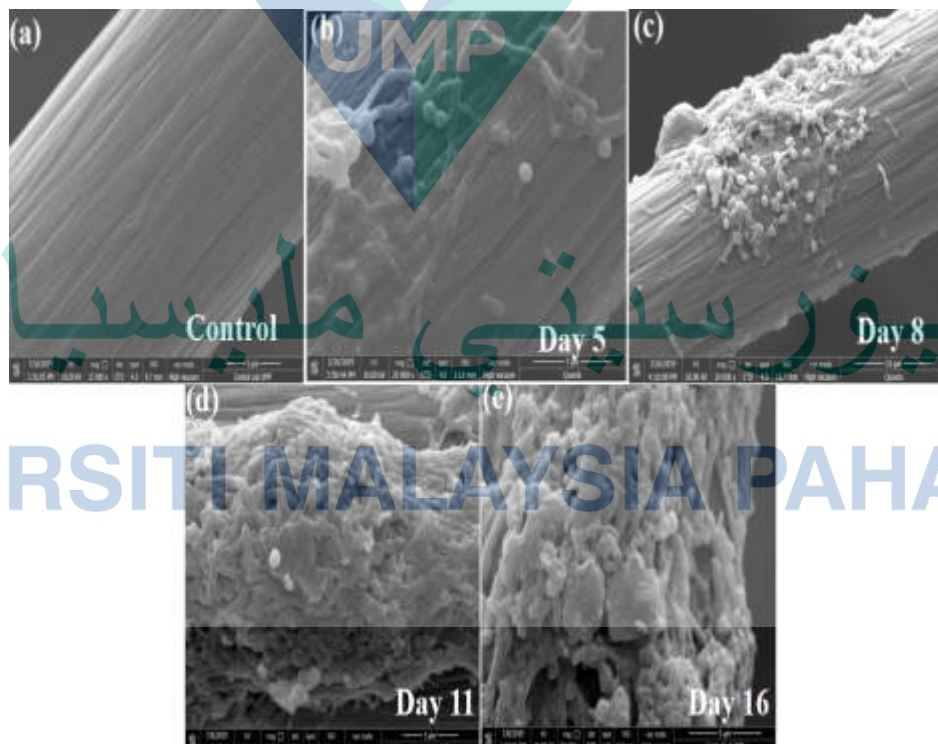


Figure 4.14 SEM images on anode electrode at a) Control, b) Day 5, c) Day 8, d) Day 11 and e) Day 16 using PCW (45000 mg/L) with acclimatized AS.

From Figure 4.14b, it can be seen that on the 5th day of operation, similar kind of biofilm (presence of fewer cells on the electrode surface) was observed for all microbes because during the initial period, bacteria started to colonize on the electrode surface thereby achieved lower performance (Koók, Rózsenszki, Nemestóthy, Bélafi-Bakó, & Bakonyi, 2016; Santoro, Lei, Li, & Cristiani, 2012). Initially, bacterial adherence can occur on either biotic or abiotic surfaces and their adherence to the surface by forces like electrostatic and hydrophobic interactions, Vander Waals forces and other physiochemical parameters (Elbourne et al., 2019). Surface proteins play a vital role in the initial attachment of the microorganisms to a solid surface under humidified or submerged conditions and they are also found as a floating mat on liquid surfaces (Girmaye, Abdeta, & Tamiru, 2018). But, thereafter, these cells adhere to each other and frequently embedded inside a self-produced matrix of extracellular polymeric substance (EPS) that can be transformed into effective biofilm (Melander & Melander, 2019) and exhibited higher performance after on the 11th day of operation (Figure 4.14d). Recent studies reported that the intracellular aggregation occurs through the proteolytic mechanism of cell wall-anchored accumulation-associated protein by means of host proteases (Foster, Geoghegan, Ganesh, & Höök, 2014; Ortega-Peña, Martínez-García, Rodríguez-Martínez, Cancino-Díaz, & Cancino-Díaz, 2020). However, the significance of biofilm-associated protein (Bap) and the biofilm-associated homolog protein (Bhp) cannot be denied as they favor the process of biofilm aggregation (Algharib, Dawood, & Xie, 2020). It is apparently observed that more effective biofilm on day 11 compares to other days. Effective biofilm meant the dense as well as compact biofilm consisting of a higher number of active cells on the electrode surface (Srinivasan, Nambi, & Senthilnathan, 2019). However, on the 16th day, it can be observed that bacteria started to form localized multilayer micro-colonies on the electrode surface and consequently those colonies are frequently embedded within EPS leading to the formation of multilayer biofilm (Azeredo et al., 2017). This result is consistent with the current and power density data (Figure 4.12a and Figure 4.13b) where it can be seen that maximum current and power density were obtained at day 11 (650 mA/m² and 850 mW/m²) compared to day 16 (530 mA/m² and 650 mW/m²).

4.5 Electron transfer mechanism in MFC

4.5.1 Cyclic voltammetry

The CV was performed to characterize the electron transfer mechanism between the biofilm (biocatalyst) and the anode of the MFC. The characteristics of CV rely on various factors, such as the chemical and biological species present, the rate of the electron transfer reactions and the rates of diffusion of electroactive species (Modestra et al., 2020). Moreover, it also helps to elucidate the explicit role of redox mediators in the electrochemical reactions (Y. Song et al., 2020). The CV was run before (control) and after inoculation of MFCs using PCW with acclimatized AS as presented in Figure 4.15a-d.

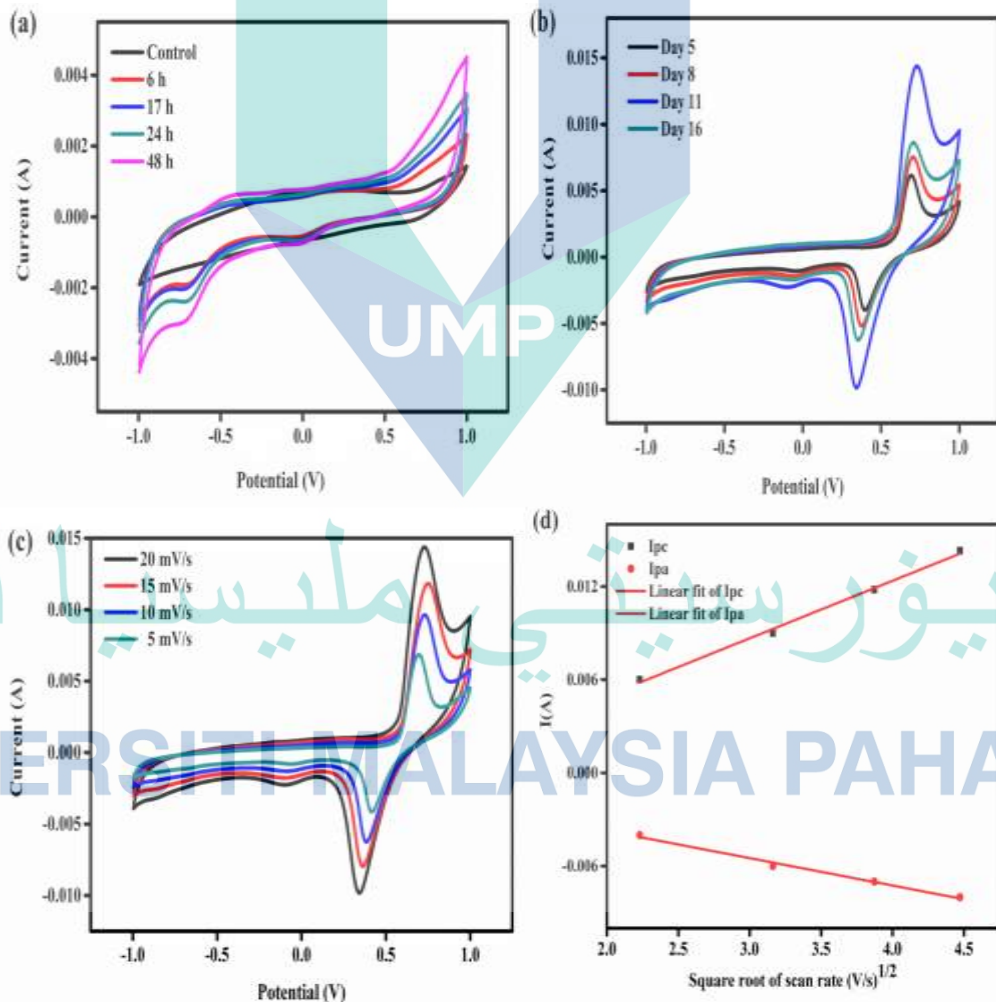


Figure 4.15 a) CV at 0 to 48 h (20 mV/s) b) CV at day 5, day 8 and day 11 and day 16 (20 mV/s), c) CV at different scan rates on day 11 and d) Peak current vs. square root of the scan rate on day 11.

Figure 4.15a represents the CV from 0 to 48 h of operation, and it can be noted that no oxidation and reduction speak was obtained for an un-inoculated (control) cell. In contrast, during the initial period (6 - 48 h), a weak redox peak was noticed during the forward and reverse scans indicating the presence of metabolites (Islam, Ethiraj, et al., 2017). However, the redox peak intensity was increased during 5-11 days of operation as shown in Figure 4.15b. Among the different days of CV operation, the sharp redox peak at 0.73V and 0.38V for forward and reverse scan respectively, was attained on 11th day of operation as presented in Figure 4.15c and Table 4.3. The sharp increase in the redox peak current indicates the presence of increased amount of natural mediators which facilitated the electron transfer from the bulk analyte and the biofilm to the anode leading to a high current generation (S. Lin, Hao, Li, Xiao, & Chen, 2020). *Pseudomonas aeruginosa* (PA) and *Bacillus cereus* (BC) predominantly present in the inoculum could produce natural metabolites functioning as electron shuttle as revealed by our previous works (Islam et al., 2018; Marsili et al., 2008). On the other hand, on day 16 the intensity of the redox peaks decreased. This might have occurred due to the blockage of the biofilm by the presence of large number of dead cells (Islam, Ehiraj, et al., 2019).

Table 4.3 Redox peaks and current (A) data on different days using PCW

Day	E _{ox} (V) Peak 1	E _{ox} (V) Peak 2	E _{red} (V) Peak 1	E _{red} (V) Peak 2	I _{ox} (A) Peak 1	I _{ox} (A) Peak 2	I _{red} (A) Peak 1	I _{red} (A) Peak 2
5	0.24	0.69	-0.32	0.40	0.002	0.005	0.0033	-0.003
8	0.24	0.70	-0.34	0.37	0.0021	0.006	0.0057	-0.005
11	0.006	0.73	-0.33	0.34	0.0026	0.0143	-0.003	-0.009
16	0.24	0.71	-0.33	0.35	0.0023	0.008	-0.011	-0.006

The CV on 11th day of operation at different scan rates is presented in Figure 4.15c while the oxidation and the reduction current as a function of the square root of the scan rate is presented in Figure 4.15d. The linear dependence for oxidation and reduction current on the square root of the scan rate suggests the occurrence of surface-confined redox process of the metabolite which is limited by diffusion (Oliveira Paiva et al., 2020).

4.5.1.1 Metabolite identification

To explore the presence of metabolites, after 11 days of operation, the media was removed from the MFC electrode chambers using PA, BC and acclimatized AS. Then samples were filtered and thereafter, the filtrate supernatant was then taken to a 1 cm cuvette and the UV-visible spectrum was measured. Peaks were observed in the UV-visible spectrum for media are presented in Figure 4.16a-b. From Figure 4.16a, it can be seen that the absorbance peaks was observed at 315 nm, 368 nm, 425 nm and 698 nm using acclimatized AS.

The corresponding absorbance peaks of PA (Figure 4.16a) were found at 313 nm, 366 nm, and 690 nm which is similar to the peak observed using pyocyanin (Figure 4.16b). On the other hand, the absorbance peak of BC was observed at 425 nm which is corresponded to the absorbance peak obtained by hydroquinone (Figure 4.16b).

The similar peak position of PA and BC with pyocyanin and hydroquinone indicated the presence of both pyocyanin and hydroquinone in PCW fed MFC using acclimatized AS as biocatalysts resulted in better performance. This might be due to the fact that both electron shuttle-like, hydroquinone, and pyocyanin are responsible for electron transfer (Bose, Dey, & Banerjee, 2020). When both electron shuttles were present in the system, they increased the electron transfer rate resulted in the higher current generation (Figure 4.12a).

This result is consistent with the literature where they also reported the higher current generation due to the presence of both pyocyanin and hydroquinone as metabolites using mixed culture (Farmer, Hines, Dowds, & Blumsack, 2010; Yu et al., 2019).

For further analysis, CV was done using the filtrate supernatant got during ultraviolet spectroscopy using PA, BC and acclimatized AS along with pyocanin and hydroquinone.

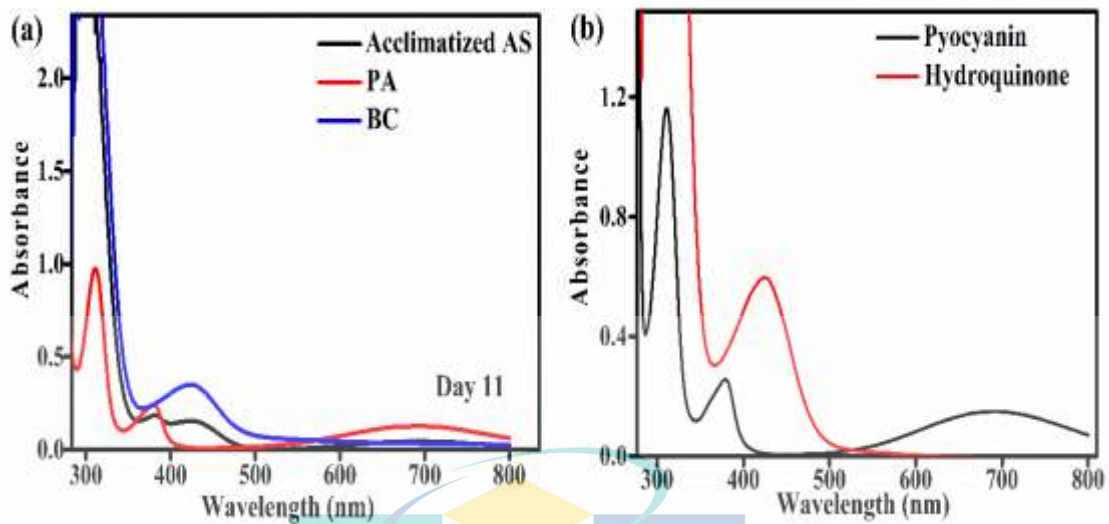


Figure 4.16 UV-vis of using a) Acclimatized AS, PA and BC with PCW (45000 mg/L), and b) UV-vis of pyocyanin and hydroquinone

The all CVs were done using glass setup which is presented in Figure 4.17a-b. As shown in Figure 4.17a, it can be seen that acclimatized AS with PCW gave two reduction peaks at -0.55 V and $\sim +0.37$ V respectively. These peaks are similar to the reduction peaks obtained from PA and BC (Figure 4.17a). From Figure 4.17a, it is clear that the reduction peaks were observed from PA and BC are the pyocyanin and hydroquinone (Figure 4.17b) because both of the compounds gave a peak at the same position. This result is consistent with the literature where they reported that the reduction peak of pyocyanin centered at ~ -0.55 V using PA inoculated MFCs and the reduction peak of hydroquinone at $\sim +0.37$ V using BC (Sarmin et al., 2019). According to the CV plots (Figure 4.17a) the MFC with naturally produced pyocyanin and hydroquinone from PA and BC showed much higher peak (0.010 A and 0.006 A) current than that of the control pyocyanin (0.0025 A) and hydroquinone (0.0022 A) from Figure 4.17b indicating the production of both pyocyanin and hydroquinone as metabolites in acclimatized AS. On the other hand, among all microbes acclimatized AS showed higher current intensity (0.012 A) compared to PA (0.010 A) and BC (0.006 A) indicating the good catalytic activity of acclimatized AS.

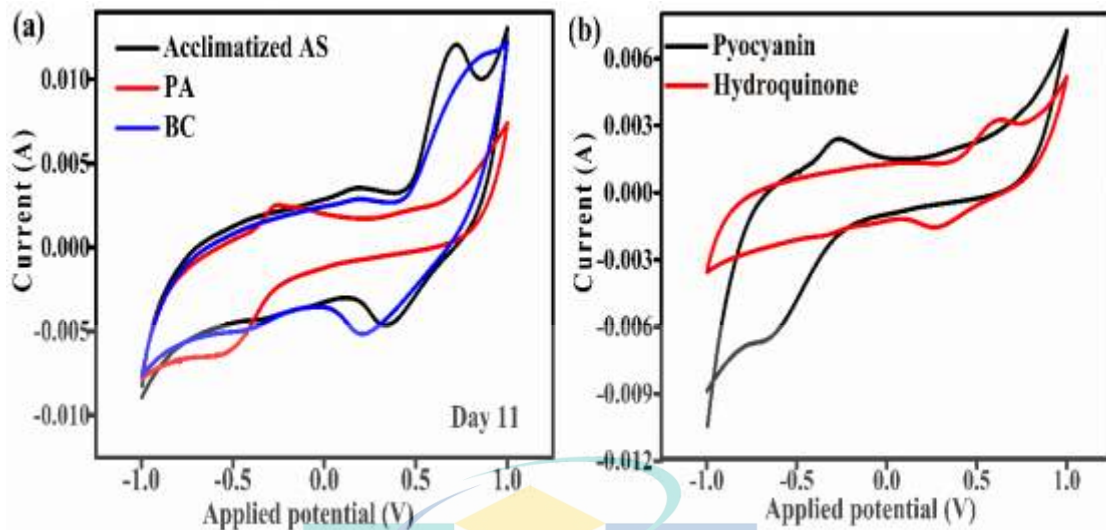


Figure 4.17 Cyclic voltammetry of supernatant from a) Acclimatized AS, PA and BC fed MFC after 11 days (PCW 45000 mg/L); (b) Cyclic voltammetry of pyocyanin and hydroquinone (CV in glass cell)

Apart from this, to check the charge transfer resistance of MFCs ran by using PA, BC, acclimatized AS, pyocyanin and hydroquinone compounds, EIS was done using the same filtrate supernatant used for CV. The changes in the Nyquist plot of 3 samples after treatment and chemical pyocyanin and hydroquinone were measured and presented in Figure 4.18a-b. From Figure 4.18a, it can be seen that in Nyquist plot obtained from acclimatized AS showed lower charge transfer resistance (15Ω) comparing to PA (22Ω) and BC (45Ω). It is an indication of the good catalytic activity of mixed microbe's presence in acclimatized AS than the single cultures. In contrast, while the comparison between PA and BC, PA showed lower charge transfer resistance (22Ω) than the BC (45Ω). It indicated that as pyocyanin is the major endogenous electron shuttle that directly involved in electron transfer from cells to the anode, the enhanced pyocyanin production usually resulted in bioelectricity improvement in PA-inoculated MFC with lower charge transfer resistance BC fed MFC where hydroquinone acts as metabolite.

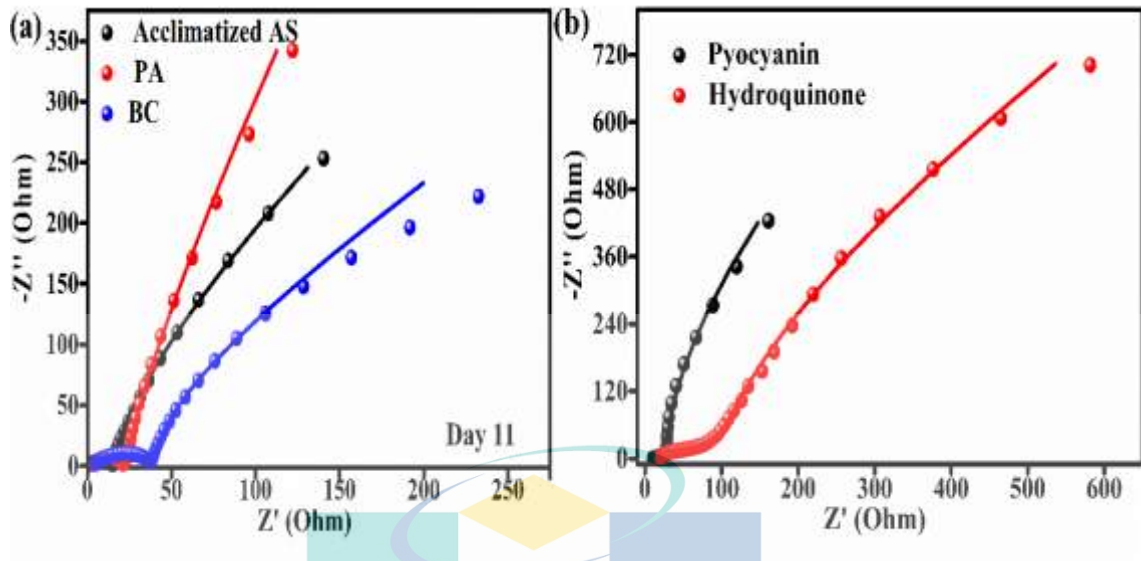


Figure 4.18 EIS of a) Acclimatized AS, PA, BC with PCW (45000 mg/L) and b) EIS of pyocyanin and hydrquinone

Apart from that from Figure 4.18b, there is no proper semicircle observed in case the of Nyquist plots using chemical pyocyanin and hydroquinone. Actually, Nyquist plot is a symbol of charge transfer resistance which is considered as one of the most important parameters in MFC (Goode, 2020). Without charge transfer, no electricity will generate. No proper semicircle formed means no charge transferred happened in case of both pyocyanin and hydroquinone suggesting that proper charge transferred happened when reaction happened in presence of catalyst and organic substrates. It is one of the proof of distinguish between the natural and artificial pyocyanin and hydroquinone. This result is consistent with the bode plot and phase angle which is presented in Figure 4.19a-d. From Figure 4.19a-b, it can be seen that the position of both maximum frequency and phase angle of acclimatized AS shifted its position (489 Hz and 45 degree for acclimatized AS, whereas for PA and BC, it was 363 HZ, 83 Hz, 74 degree and 60 degree) which proved more electron transfer efficiency with lower charge transfer resistance of acclimatized AS than the single substrates. It can be due to the presence of mixed microbes with multiple metabolites. Besides, in contrast among single microbes, PA showed lower bode modulus and phase angle than BC again proving the good catalytic activity of PA than the BC. Apart from this, Figure 4.19c-d represents the bode modulus and phase angle with respect to log f of both pyocyanin and hydroquinone.

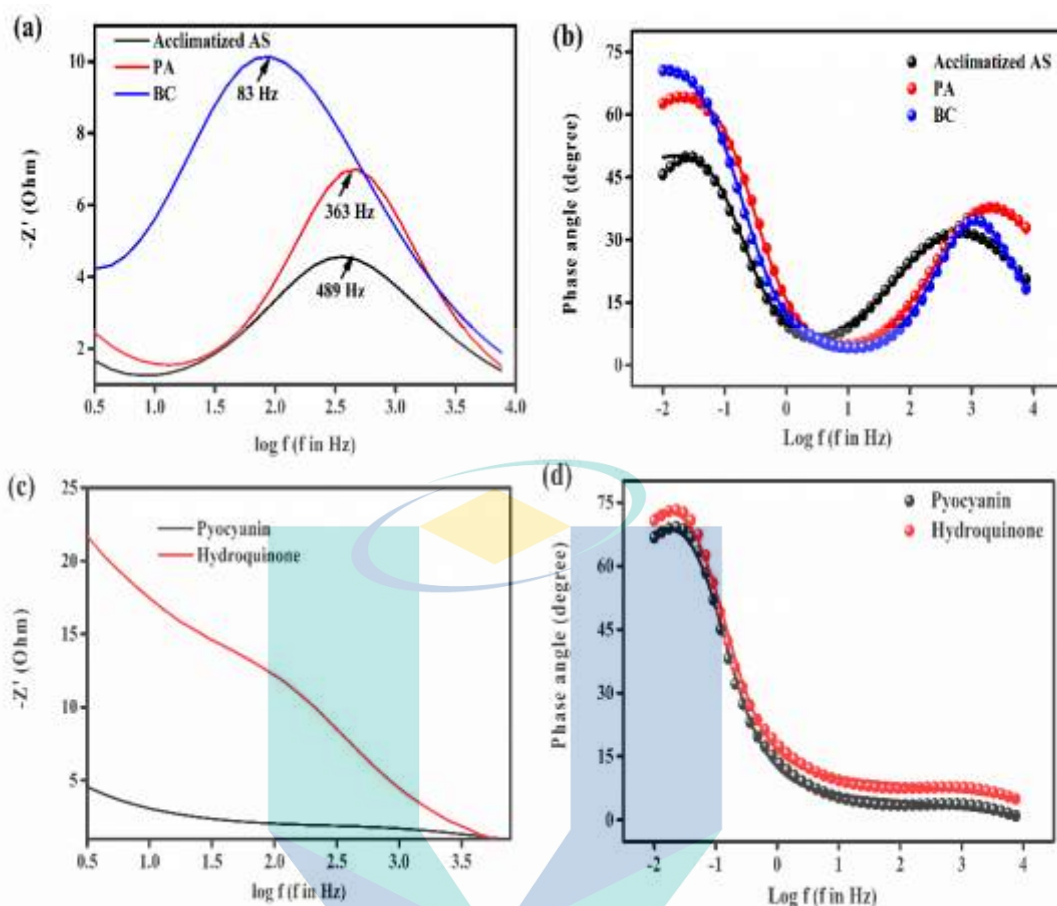


Figure 4.19 Bode modulus phase angle vs. $\log f$ using a) and b) acclimatized AS, PA, and BC (PCW= 45000 mg/L), c) and d) pyocyanin and hydroquinone

From Figure 4.19c-d, it can be seen that although the bode modulus and phase angle position of both pyocyanin and hydroquinone shifted but in the high frequency region the arc is absent. From literature, it can be seen that corresponding changes in bode modulus and phase angle are also observable in a complex plane plot, where an arc is evident at higher frequencies, indicative of the presence of a charge transfer resistance (M. M. Khan, Deen, Shabib, Asselin, & Haider, 2020).

Moreover, the impedance signature of the negative controls remains constant using artificial pyocyanin and hydroquinone, with no deviation from a capacitive interface (i.e. an interface where no electron transfer occurs). Besides, the evidence of charge transfer using acclimatized AS, PA and BC shows a full cycle than the artificial one which confirmed the charge transfer and mass diffusion of electroactive compounds of impedance processes (Chang, Kao, & Yu, 2020). From, above discussion it is confirmed that the pyocyanin and hydroquinone were present in acclimatized AS as

metabolites. Now, the role of metabolite and biofilm on MFC performance are given in the next section.

4.5.2 Role of both biofilm and metabolite and their effect on MFC performance

To further elucidate the mechanism of electron transfer, a control experiment was run, where after 16 days of operation, the anolyte was removed from the anode chamber and filtered. The filtrate was stored at 4 °C and the biofilm with electrode was kept in the setup under N₂ purging condition and again filled with fresh inoculum and substrate. CV of the anode was run at different scan rate (from 1 to 10 mV/s) with the same potential window and the data is presented in Figure 4.20a.

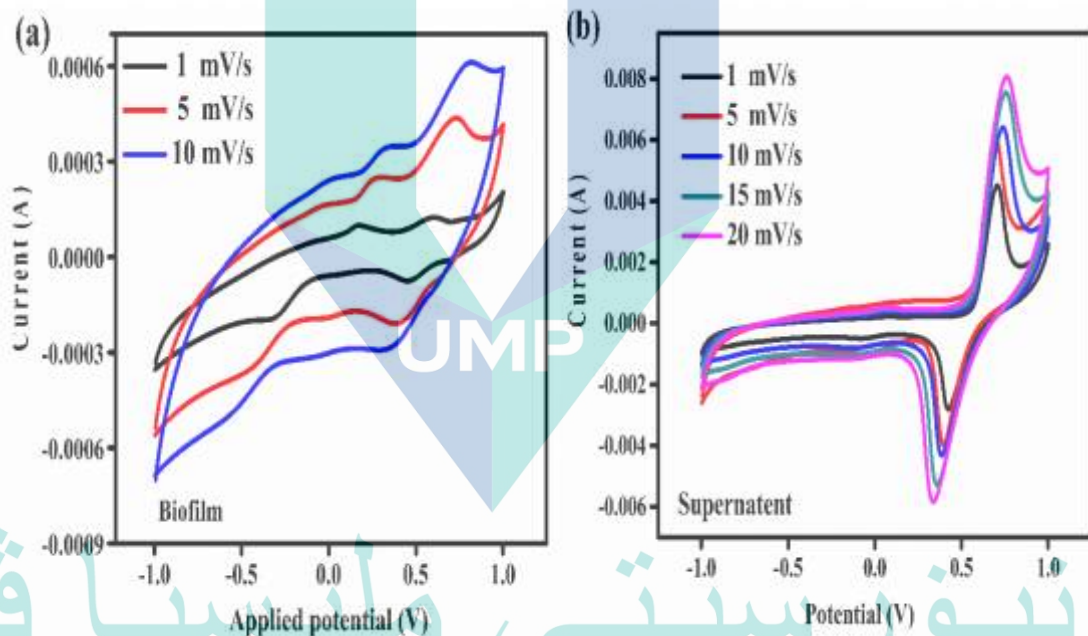


Figure 4.20 a) CV of biofilm in microbe-free medium and b) CV of microbe-free supernatant with fresh anode after 16 days of operation at different scan rates.

The appearance of reversible redox peaks at 0.8 to 0.3 V at different scan rates (1, 5 and 10 mV/s) evidenced the charge transfer process through the biofilm. Another MFC setup was constructed where the filtrate was used as anolyte and a fresh carbon felt with same dimension was used as electrode. The CV data are presented in Figure 4.20b where sharp oxidation and reduction peaks were observed and the redox peak intensity was many times higher compared to the biofilm. The result clearly demonstrates the role of the indirect electron transfer via natural mediators produced by the microbes. To further evaluate the role of biofilm, another MFC was operated and after 14 days of operation,

the bulk anolyte was removed followed by filling up the chamber with fresh substrate and inoculum. The current generation as a function of time is presented in Figure 4.21a. From Figure 4.21a, it can be seen that the current generation was dropped from ~ 600 to ~ 200 mA/m² after refilling the anolyte which was two times higher than the initial current generation. The difference in current generation might be due to the existence of the biofilm on the anode surface after 14 days of operation (Sarmin et al., 2019). The appearance of weak redox peak in CV after 18 days of operation (Figure 4.21b) supports the current generation data. The current generation from 15 to 20 days follows the trend of 5 to 10 days and after 20 days of operation current generation reached to ~ 650 mA/m² which was slightly higher compared to the current generation after 14 days of operation. When the bulk solution was removed from anode, the toxin along with metabolites were replaced with fresh inoculum and substrate which might give impetus to microbial growth in the bulk as well as on the electrode interface and the appearance of strong redox peak in CV on 24th day of operation supports the current generation profile. The electrochemical activity of microbes behaved distinctly different during different stages, suggesting that suspension cells were growing or adhering onto the anode to form biofilm in the MFC (Islam, Ehiraj, et al., 2019). These results of the present study suggest that, biofilm is a crucial component of MFC that allows considerable conversion capacity and opportunities for extracellular electron transfer. These results revealed that the CV data's were consistent with the MFC performance. Additionally, the performance of PCW wastewater fed MFCs severely depends on the substrate utilization capability and the electrogenic properties of microbes. Hence, in the present study, acclimatized AS was selected for PCW fed MFC on the basis of the above mentioned properties. Using acclimatized AS with PCW obtained the better power density (850 mW/m²) which was due to the higher electron transfer efficiency in MFCs. In MFCs, it is well known that acclimatized AS is a model organism for mediated electron transfer and electrogenic microbes presence inside this (Chatterjee, Dessì, Kokko, Lakaniemi, & Lens, 2019). These microbes can produce different types of electrochemically active metabolites which have the capability of higher electron transfer efficiency compare to other single microbes secreted mediators (H. Chen et al., 2020). Besides, the performance of PCW fed MFC with acclimatized AS was investigated with current vs. time and it was observed that initially (from day 1 to day 11), the performance gradually increased with the time and reached to a stable value; however, thereafter it drastically dropped and reached to the minimum value (Figure 4.12a). The drastic drop in the power generation of MFCs

after certain days of operation is very common and well known phenomenon in MFCs (Obata et al., 2020).

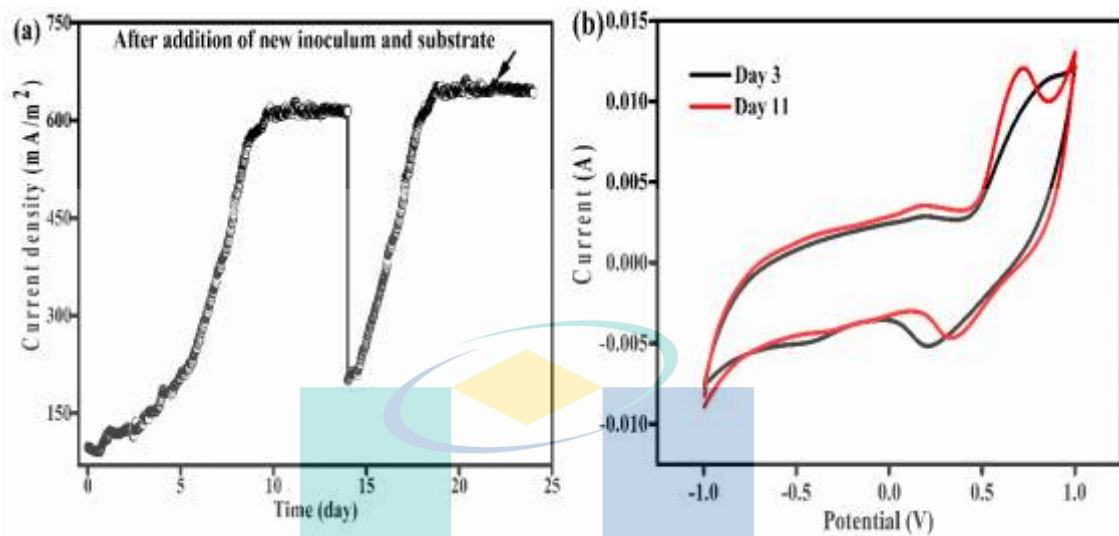


Figure 4.21 a) Current vs. time data, b) Cyclic voltammetry at day 18 and day 24 (20 mV/s)

Several reasons such as substrate depletion, catalyst inactivation, membrane fouling, electrode fouling etc. have been reported for this drastic drop of performance in MFCs (Hussain, Khan, & Gul, 2020). On the other hand, the secret of high power generation in PCW fed MFC can be due to the availability of the microbes, substrates, effective biofilm etc. Besides, in the present study, it was found that not only the above-mentioned factors but also the vital role of naturally produced metabolites (pyocyanin and hydroquinone) from microbes onto the surface of anode electrode also responsible for high power generation. If the percentage of metabolites increases there is a possibility to carry and pass the electron fast from anode to cathode resulted in high power generation (Modestra et al., 2020). Moreover, the vital role of biofilm with naturally produced metabolite architecture and the electron transfer mechanism have been illustrated in Figure 4.22. The initial biofilm comprising with live cells and metabolite transfer the less electron whereas after forming the good biofilm with large percentage of mediators, electron transfer process increased (Figure 4.22). The effect of biofilm formation with naturally produced metabolite on anode resistance over time was also evaluated and found that an effective biofilm with metabolite can produce high power corresponding to low charge transfer resistance. In MFCs, it is well known that the formation of biofilm on electrode provides large conductive surface that facilitate the electron transfer and reduces the charge transfer resistance (S. Luo et al., 2020).

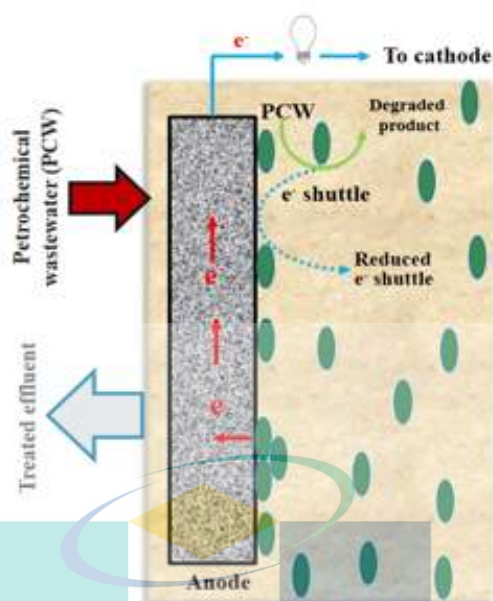


Figure 4.22 Schematic diagram of Electron transfer mechanism in PCW fed MFC

Besides, good correlation between the levels of metabolites relating to the organic compounds and current generation is corroborated by the previous study showing that the intracellular metabolites produced by the microbes in the anode are present at high concentration and activation of the organic compounds cycle supports higher electricity generation by a pure *Geobacter* culture (M. Hassan et al., 2020). Logan et al. reported that *S. oneidensis* produces flavins that can facilitate the electrode reduction and these electron mediators can also enhance the metabolic activity of *E. coli* in the mutualistic community resulted in lower charge transfer resistance (Logan et al., 2019). In another study, Kirchner demonstrated that high voltage generation produced due to important role of metabolites in the system (Kirchner, Dachet, & Loeb, 2019). These results of the present study suggest that, metabolite plays an important role in MFC that allows considerable conversion capacity and opportunities for extracellular electron transfer resulted in high power generation.

4.5.3 Electrochemical impedance spectroscopy

Electrochemical Impedance Spectroscopy is employed to analyse the electrochemical reactions at electrode/electrolyte interface, bacterial metabolism, surface and material properties of the electrodes (Caizán-Juanarena et al., 2020). The Nyquist plots for different days of operation using PCW (45000 mg/L) with acclimatized AS were recorded and presented in Figure 4.23.

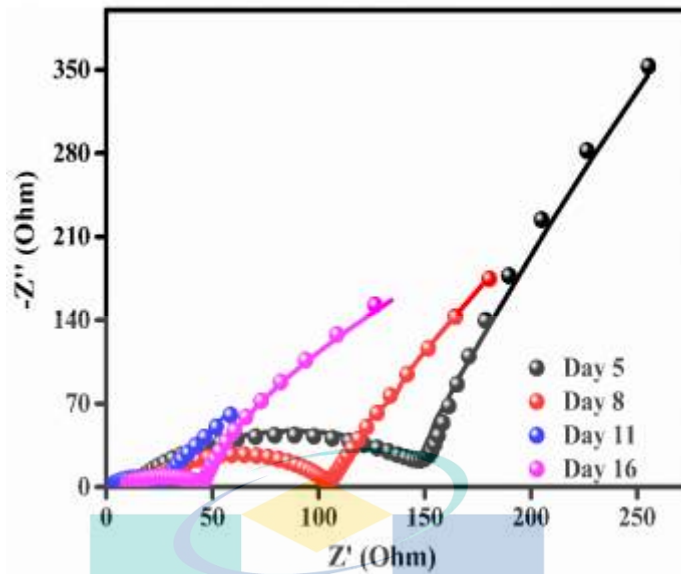


Figure 4.23 Nyquist of PCW 45000 mg/L and Acclimatized AS on different days of operation

From Figure 4.23, it can be seen that the Nyquist plot represents a complex plane plot for the anode of the MFC, expressing the real (X-axis) and imaginary part impedance (Y-axis). The EIS data fitting parameters are presented by an equivalent circuit $[R_s(R_{ct})(WQ)]$ and the fitted parameters are presented in Table 4.4. Table 4.4, it can be seen that the R_s value was increased from day 5 to day 11 and thereafter it again decreased on day 16. The highest R_s value obtained on day 11 (10.45Ω) comparing with different days of operation suggests the presence of increased concentration of protons in the anolyte generated by the microbial activities which in turn increased the solution conductivity (Islam, Karim, et al., 2017). Besides the anode R_{ct} values were found to be 145Ω , 87Ω , 24.4Ω and 41.4Ω on day 5, day 8, day 11 and day 16 respectively Table 4.4).

Table 4.4 EIS data fitting parameters for DC-MFC

Time (day)	R_s (Ω)	R_{ct} (Ω)	Q		τ_b (μs)
			Y0 (mMho)	Zw	
5	1.64	145	5.8	2.02	0.003
8	6.79	87	39.8	7.85	0.0012
11	11.6	24	88.1	35.1	0.000439
16	9.56	41	43	16.3	0.0015

On day 5, the higher R_{ct} values (145 Ω) were obtained which could be due to the lower concentration of the microbes and mediator, microbes started to form colonies on the anode surface after 5 days of operation as shown in Figure 4.14b. In contrast, on the day 11, the lower R_{ct} value (24.4 Ω) was obtained compared to other days indicating higher mediator concentration in the bulk and at the same time formation of effective biofilm (Figure 4.14d) that increased the abundance of the electron shuttle compound at the electrode/electrolyte interface (Baranitharan et al., 2015). The Y_0 value sharply increased from 2.02 mMho to 35.1 mMho on 5th and 11th day respectively indicating the drastic reduction in mass transfer resistance with the increase in operational time. Two major things can happen between 5th to 11th day of operation: microbial growth in the bulk leading to higher metabolite concentrations and biofilm formation facilitating the cytochrome based along with mediator-assisted electron transfer processes (Tahernia et al., 2020). The CV results clearly demonstrated the predominant role of metabolite assisted electron transfer process. Considering the fact that the mass transfer resistance does not depend on the concentration, but largely depends on the diffusion path, it seems that the presence of biofilm obviously could reduce the diffusion path leading to the significant reduction in mass transfer resistance after 11 days of operation (Avellaneda, Bataille, Toutant, & Flamant, 2020). On 16th day of operation, the Y_0 value was dropped by 50% compared to the 11th day of operation indicating the increase in mass transfer resistance. The increase in mass transfer resistance might be related to the formation of multilayer biofilm as evidenced from Figure 4.14e with a higher abundance of dead cells interfering the metabolite diffusion process (Islam et al., 2018). The inert biomass layer in the thick biofilm might have hindered the electron transfer process which resulted in increased charge transfer resistance. Besides, in case of thick biofilm formation, the inner layer might experience the lack of nutrient supply and eventually it forms a dead layer at the proximity of the surface, can be called as electrode fouling in MFC (H. Chen et al., 2020) which might have enhanced the anode R_{ct} . Some recent studies (D. Sun et al., 2016) reported that the highest electrochemical activity obtained in MFCs while thickness of biofilm reached to the ~20 mm, and thereafter the electrochemical activity decreased with increasing anode R_{ct} . The bode plot and phase angle with respect to frequency is presented in Figure 4.24a-d.

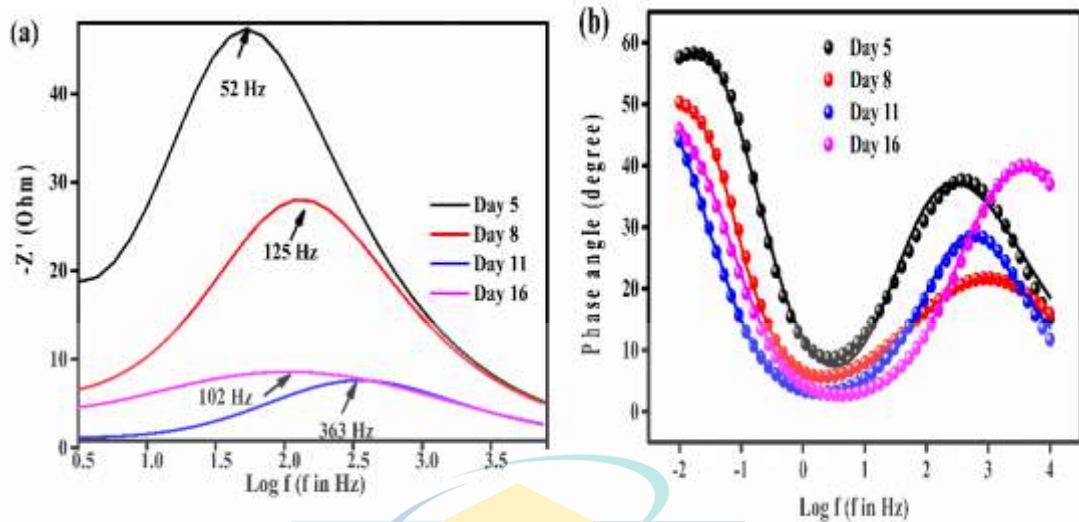


Figure 4.24 a) $-Z'$ vs. $\log f$, and b) phase angle vs. $\log f$ using PCW (45000 mg/L) after different days of operation

From Figure 4.24a, among different days of operation at day 11, the maximum frequency was higher (363 Hz) than other days. The higher maximum frequency is related with delay time τ_b from equation 4.4. From equation 4.4, it can be seen that delay time τ_b is inversely proportional to the maximum frequency (f_{max}). If maximum frequency increases, then delay time will decrease. From Figure 4.24 and Table 4.4, where, it can be seen that, among different days, the microbial charge transfer time (0.000439 μ s) with higher maximum frequency (363 Hz) for day 11 is less than the other days that indicating the efficient biofilm formation with higher metabolite in the bulk, that transfer the charge more efficiently or faster than the other days. On the other hand, phase angle is important factor for MFC performance. Lower phase angle indicates lower charge transfer resistance. From Figure 4.24b, it can be seen that the phase shift for day decreased from a peak of 55 degree (day 5) to 45 degree and then further increased to a minimum of 48 on day 16. This indicates that charge transfer resistance decreased on day 11 observed here. The EIS data is consistent with the CV and current generation.

4.6 HPLC analysis PCW fed MFC

To further understand the individual role of organic compounds in PCW, further HPLC was done using PCW supernatant at different days of operation. Although, different types of compounds present in PCW, here only three compounds AA, ACA, and DMP were selected for HPLC due to their presence of a higher percentage in PCW. The

relative concentration was calculated from the final and initial areas of each sample. The overall feature of the relative concentration vs. time is shown in Figure 4.25a-c.

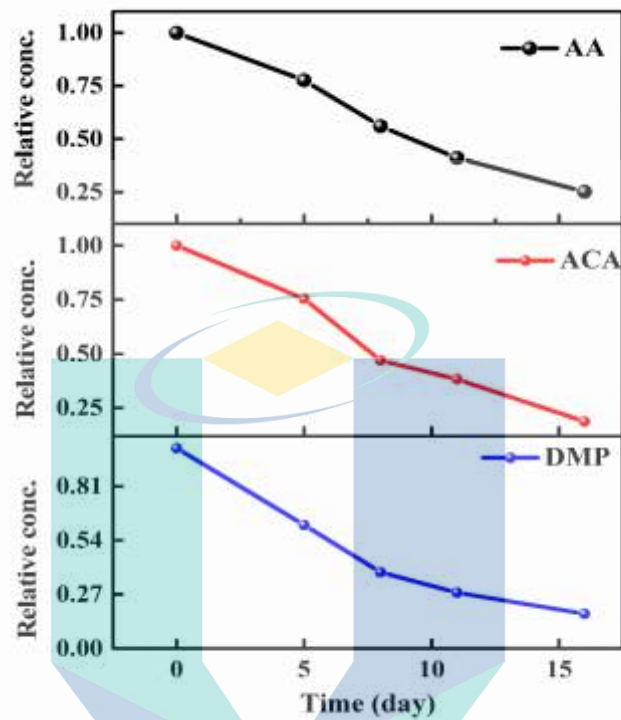


Figure 4.25 (a) Relative concentration vs. time of AA (2 wt%), ACA (2 wt%) and DMP (0.5 wt%) using PCW (45000 mg/L)

From Figure 4.25a-c, it can be seen that initially, the relative concentration was 1 for all substrates (HPLC data using PCW 45000 mg/L is presented in A3) AA and ACA degraded linearly until 16 days of operation. On the other hand, DMP degraded very fast until 9 days of operation and then degraded slowly. When comparing these three organic compounds, it can be seen that ACA degraded most than the AA and DMP. It can be due to the simple form of ACA than AA and DMP. The redox mediators and/or redox transfer enzymes involved in the metabolism of simple substrates like ACA proceed through very different pathways, which should reveal the efficiency of an MFC. While comparing with complex substrates, microbes first priority will be simple behavioural organic compounds because of hydrolysis and fermentation which is required for the complex substrate to break macromolecules to simpler ones and then convert them to other readily biodegradable substrates like acetate, which is then degraded by anode respiring bacteria (Do et al., 2020).

On the other hand, AA concentration was still higher than AA and ACA after 16 days of operation than ACA and DMP. Firstly, it can be due to the presence of a higher percentage of AA concentration (3-15 wt %) in PCW than ACA and DMP. Secondly, there is a possibility for AA to form an intermediates which are indirectly responsible for higher concentration of AA (Sarmin et al., 2019). Finally, the reason for the presence of a lower amount of DMP after treatment can be due to a reason of lower concentration of DMP than AA in PCW after treatment. The COD removal efficiency in the PCW is discussed in the following section.

4.7 PCW treatment efficiency and comparison of the MFC performance with literature

To correlate the COD removal efficiency and the power density with the initial COD, MFCs were run with different initial CODs (5000 - 100000 mg/L) and the maximum power density and the COD removal efficiency for each MFC after 11 days of operation were recorded and presented in Figure 4.26a. From this Figure 4.26a, it can be seen that around 82% COD removal efficiency could be achieved after 11 days of operation at lower initial COD (5000 mg/L).

However, the COD removal efficiency linearly dropped from 82% to 9% with the increase in initial COD from 5000 to 100000 mg/L. On the other hand, power density sharply increased from 150 to 850 mW/m² with the increase in initial COD from 5000 to 45000 mg/L and thereafter it drastically dropped. The MFCs using initial COD of 75000 and 100000 mg/L could not sustain beyond 8 days of operation which clearly demonstrated the inhibition of microbes due to the presence of high concentration of toxins (Abdulsalam, Che Man, Isma Idris, Faezah Yunos, & Zainal Abidin, 2018). The low COD removal efficiency (40 - 50%) at higher initial COD (45000 – 26000 mg/L) suggest that the metabolites or the intermediates produced by the microbes, predominantly electrogens as evidenced by Biolog GEN III analysis of the inoculum, caused for retaining high COD in the effluent that should be treated by aerobic processes in the downstream.

Hence, there is a trade-off between the power density and the COD removal efficiency in the treatment of AA containing PCW by MFC. Additionally, the performance of the MFC was further evaluated in terms of coulombic efficiency (CE) and COD removal efficiency as a function of time using initial COD of 45000 mg/L and the results are presented in Figure 4.26b from which, a steady increase in COD removal efficiency with time is evident. However, the CE increased until 11 days of operation reaching a value of 21% and thereafter slightly decreased to 17.8%.

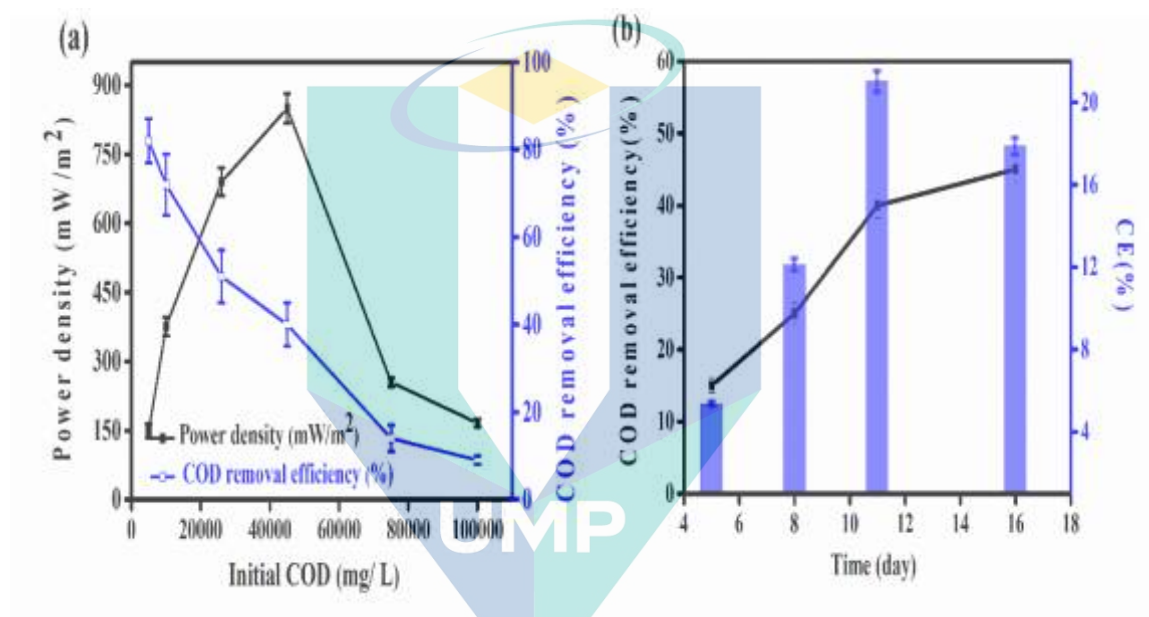


Figure 4.26 a) COD removal efficiency (%) and CE (%) with respect to time; b) Effect of initial COD on power generation and COD removal efficiency.

The maximum CE after 11 days of operation indicated the efficient degradation of the substrates in the bulk solution by the microbes leading to the generation of electrons which transferred to the anode surface with minimum charge transfer resistance as evidenced by EIS results (Sarmin et al., 2020). The drop of CE after 16 days of operation revealed the formation of inefficient biofilm, where the electrons generated by the metabolic pathway of the microbes were not able to reach the anode surface. Moreover, the COD removal efficiency was increased with time due to the efficient growth of the microbes in the bulk (Sarmin et al., 2020). The maximum power density, COD removal efficiency and CE obtained in the current study has been compared with other literature and presented in Table 4.5.

Table 4.5 Comparison the performance of PCW with literature

Substrate	Operational day	Initial COD (mg/ L)	Electrode	Microbes	Power density (mW/ m ²)	COD removal efficiency (%)	CE (%)	Ref.
PCW	16	45000	Carbon felt	AAS	850	43	21	This study
PCW	11	5000	Carbon felt	AAS	150	82	-	This study
SMWS	30	1632	Graphite plate electrode	Pure culture	189	82	28	(S. H. Hassan et al., 2019)
RSWS	30	-	Carbon paper	Mixed culture	145	-	45	(S. H. Hassan et al., 2014)
Domestic wastewaer	30	435	Graphite felts	AS	253.84	25	9	(Ye et al., 2019)
POME	15	34180	Carbon brush	AS	60.67 ^{*3}	35	12	(Islam, Ethiraj, et al., 2017)
Dairy wastewater	11	4500	Carbon paper	AS	161	75	-	(Sekar et al., 2019)
POME	70	15000	Stainless steel	AS	344	91	3	(Lee, Ng, Lo, & Bashir, 2019)

*Units was = W/m³, PCW= Petrochemical wastewater, SMWS= Sugercan molasses wastewater, RSWS= Rice straw wastewater

From Table 4.5, it can be found that AA containing PCW driven MFC with acclimatized inoculum as biocatalyst produced significantly higher power compared to the POME, rice straw (RS), sugarcane molasses (SM), domestic wastewater (DW) and dairy wastewater (DW) driven MFCs. Moreover, at lower initial COD, the performance of MFC, in term of power generation and COD removal efficiency is comparable with the literature values. The initial COD of the wastewater used in the MFCs as shown in Table 4.5 was significantly lower compared to the present study. The results of the work suggest that the PCW from the acrylic acid plant can be used as fuel in MFC with concurrent treatment of wastewater and power generation.

4.8 Kinetic study

Electrical energy can be obtained from fuel cell operation only when a reasonable current is drawn, but the actual cell potential is decreased from its equilibrium potential because of irreversible losses present in the fuel cell (Ren et al., 2020). Electron transfer from the biocatalyst to the anode is generally hampered by different losses which lower the conversion efficiency of the fuel cell (Ivase et al., 2020). Especially at lower current densities activation losses are considered to be crucial during MFC operation. As the flow of electrons increases in the circuit, activation losses show some decrement. Activation losses appear when the rate of an electrochemical reaction at an electrode surface is controlled by electrode kinetics (Anwer, Khan, Khan, & Joshi, 2020).

In other words, activation losses can be directly correlated to the rates of bio-electrochemical reactions. Electrons generated from the substrate degradation need to overcome various barriers to transfer from the biocatalyst to the anode and then to the cathode prior to getting reduced at the cathode, which incurs energy loss and can account under activation losses (I. Chakraborty, S. M. Sathe, C. N. Khuman, & M. M. Ghangrekar, 2020). There is a close similarity between bio-electrochemical and biochemical reactions wherein both encounter an activation barrier that must be overcome by the reacting species or biocatalyst. These losses result in a cell voltage (V) that is less than its ideal potential, E ($V = E - \text{Losses}$) (Juska, 2020). For a better understanding of the observation, the anode and cathode polarization curves were separately plotted as presented in Figure 4.27.

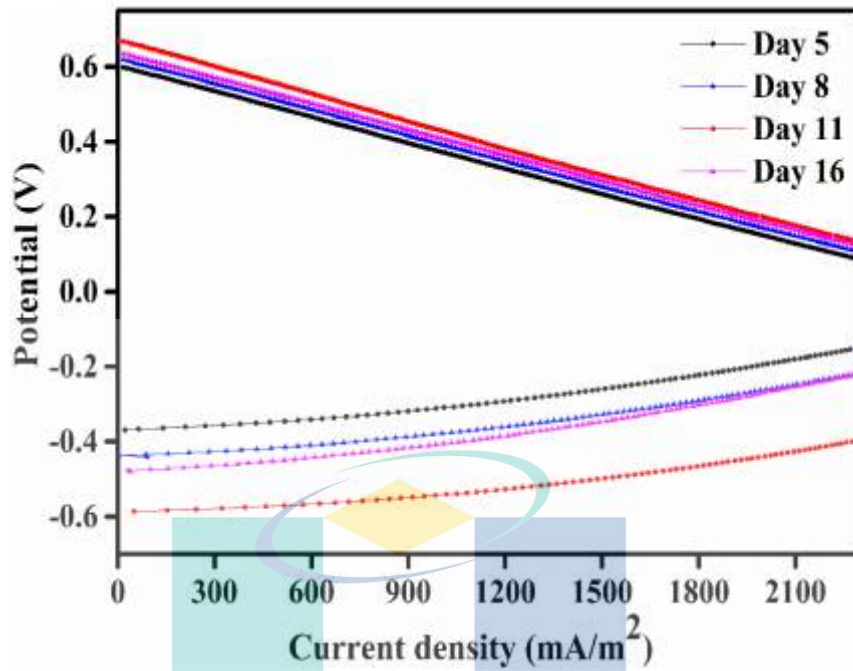


Figure 4.27 Anode and cathode polarization curve using PCW (45000 mg/L) on different days of operation

It can be seen that from Figure 4.27, the cathode performance was consistent over the duration of the experiment while the anode potential and current varied with time. In comparison to other days, on day 11, anode had the maximum negative open circuit voltage (-0.611 ± 0.10 V). The anodic polarization behaviour was further elucidated by fitting the data using the Tafel equation 4.5 (P. Singh, Chauhan, Chauhan, Singh, & Quraishi, 2020).

$$\ln i = \ln i_0 + \alpha_a \frac{nFE}{RT} \quad 4.5$$

where i is the current density (mA/m^2), E is the over potential (V), i_0 is the exchange current density (mA/m^2) and $\alpha_a \frac{nFE}{RT}$ is the Tafel slope $= \beta_a$. The values of β_a and i_0 depend on several factors such as electrochemical reaction, electrode and substrates concentration, furthermore β_a also helps to understand the activation losses of a fuel cell (Eid, Shaaban, & Shalabi, 2020) presented in Figure 4.28. From Figure 4.28, it can be seen that the Tafel slop was higher (1.93 V/decade) on day 5 followed by a significant decrease after 11 days of operation (0.65 V/decade).

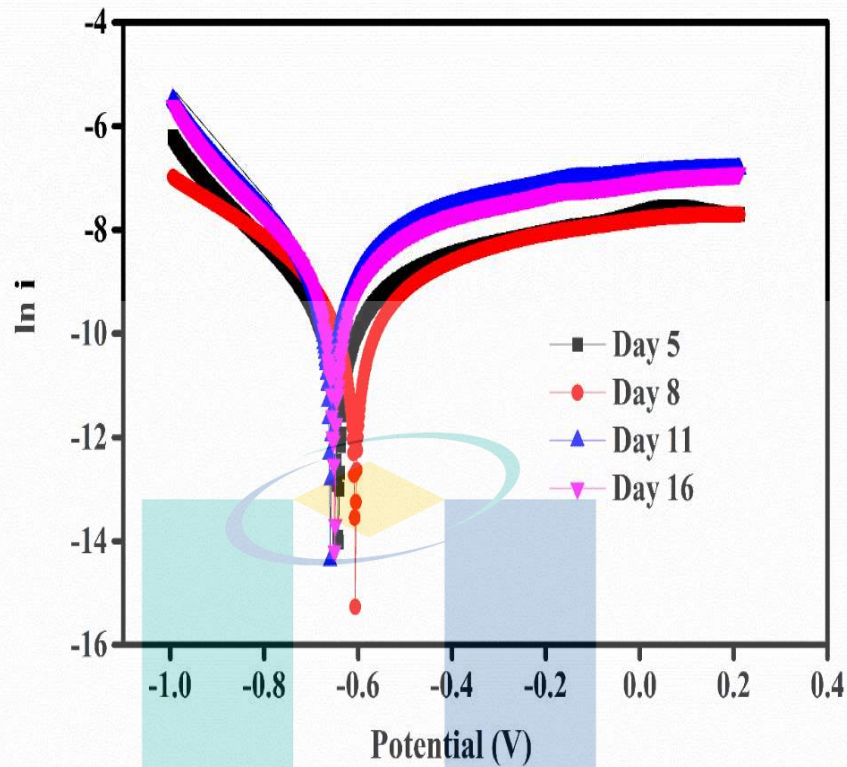


Figure 4.28 Tafel slope using PCW (45000 mg/L) on different days of operation

A similar range of the Tafel slope was found between the intervals from day the 5 to day 8 (Figure 4.29a). The higher Tafel slope indicated the lower electron transfer efficiency and catalytic activity (Ai et al., 2019). The higher electron transfer efficiency (low Tafel slope) after 11 days of operation (might be due to the formation of efficient biofilm and higher microbial density in the bulk producing metabolites which functioned as electron shuttles (T. s. Song, Zhou, Wang, Huang, & Xie, 2020). High charge transfer resistance and low anodic potential was observed on day 5 (R_{ct} , 145 Ohm, -300 mV) followed by 24 Ohm and -580 mV on day 11 (Figure 4.29b). This indicates the decrease in ohmic resistance and higher anodic potential for the electron discharge on day 11 the electrochemically active strain. The anodic potential and R_{ct} varied with time in each experiment, where R_{ct} was observed to be initially quite high and decreased with time prior to increase again at the end of the experiment. This pattern indicates the proportional variation of anodic potential and R_{ct} with the metabolic activities of the biocatalyst. There is no significant variation in the substrate conversion of the native mixed culture on day 5-16. The anodic potential also vary much (-300 to -598 mV) indicating a different electron generating capability on different days of operation (Pankan, Yunus, & Fisher, 2020).

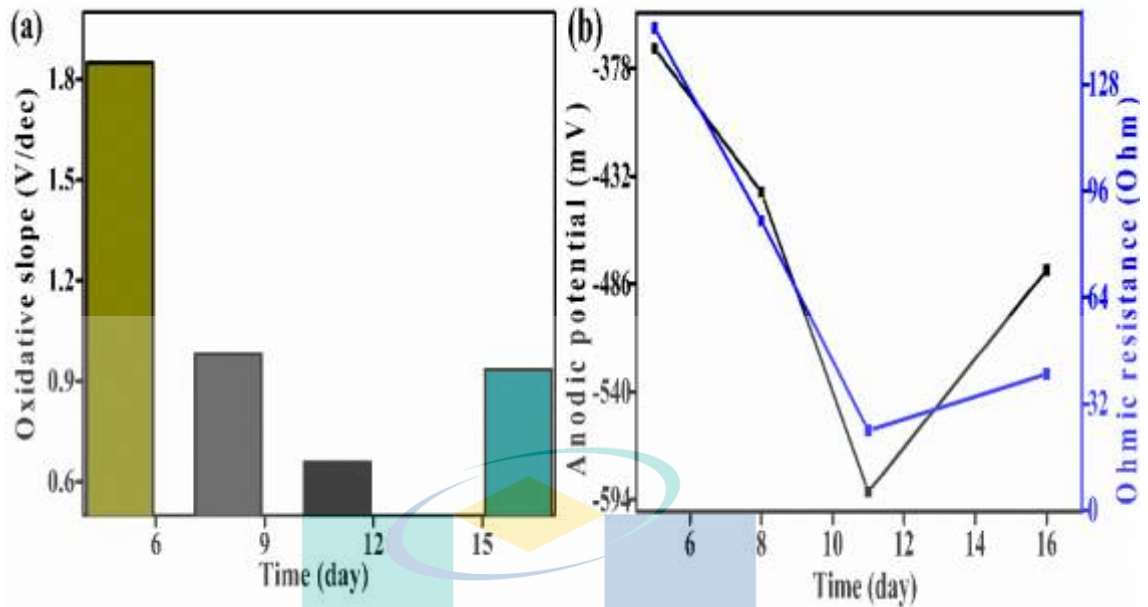


Figure 4.29 (a) Oxidative value vs time, and (b) Anodic potential and resistance vs time using PCW (45000 mg/L) on different days

However, a marked decrease in R_{ct} was noticed (from 145 to 24 Ohm) on day 11 with an electrochemically active strain which might be due to the syntrophic association of acclimatized AS with the anodic microflora in discharging the electrons efficiently along with overcoming the losses prior to reaching the anode (Pankan et al., 2020). A higher number of electrons generated during the substrate metabolism by the mixed culture might also have helped in the enhancement of power generation after augmenting with the electrochemically active strain (Jadhav, Chendake, Schievano, & Pant, 2018). Variation in the electron discharge observed on the voltammogram strongly supports the same. A significant increment in the electrogenesis was also observed after augmenting with an electrochemically active strain. A marked decrement observed in the electron losses strongly supports the reduction in the polarization resistance and increment in the power generation (Modestra, Reddy, Krishna, Min, & Mohan, 2019). Tafel analysis helped in understanding the variations in the number of electrons present as well as electron transfer resistance for correlating the overall performance (Modestra et al., 2020).

Apart from this, the dynamic model was developed based on the batch operated double chamber MFC consisting of anode and cathode, as described in Annie et al. literature (Modestra et al., 2020). The microbial population at the anode is represented using a simple two population model, clubbing the bacteria into two types, one that

consume the substrate (COD) and release electrons which are then transferred to the anode via intracellular mediators (primary microbial population) and second type that decompose the substrate but do not contribute to power generation (secondary microbial population). The important assumptions made in the model are as follows:

- i. Substrate in the MFC chamber is perfectly mixed.
- ii. Microbial population in the biofilm of the anode is uniformly distributed.
- iii. Any gases (CO₂, H₂, etc.) released during substrate oxidation at the anode remain dissolved in the bulk solution.
- iv. MFC is operated in fed-batch mode.
- v. Changes in pH and temperature are negligible
- vi. Electrons are transferred from the cells to the anode using intracellular mediators, as they undergo transformation between reduced and oxidized forms.

The governing equations described in sections Mass balance and Ohm's Law and voltage losses using equation 2.12-2.24, can be solved in an ODE solver to determine the influence of different parameters on the MFC performance. The final parameter values obtained from the curve fitting and other parameters that were directly obtained from literature are given in Table 4.6.

Table 4.6 Kinetics parameters

Parameter	Unit	Value	Notes
F	A. s/ mol	96485.4	Constant
R	J/ mol/ K	8.314	Constant
T	K	298	Constant
V	m ³	0.00004	Measured
$\frac{m}{k_m}$	$\frac{1}{1}$	$\frac{2}{0.919}$	Measured Estimated
R _{min}	Ohm	8	Estimated
R _{max}	Ohm	500	Estimated
q _{maxp}	Day ⁻¹	0.11	Estimated
q _{maxs}	Day ⁻¹	0.36	Estimated
μ _{maxp}	Day ⁻¹	0.253	Estimated
μ _{maxs}	Day-1	0.089	Estimated
K _{sp}	g/L	0.11	Estimated

Table 4.6 Continued

Parameter	Unit	Value	Notes
K_{r1}	L/g	0.0005	Estimated
K_{r2}	L/g	0.000004	Estimated
Y	1	0.96	Estimated
E_{min}	V	0.09	Estimated
E_{max}	V	0.67	Estimated
n	1	8	(Ward, Connolly, & Tucker, 2014)

From Table 4.6, it can be seen that most of the biological parameters such as the maximum substrate consumption rates, maximum microbial growth rates, yield coefficient, half saturation constants, etc., are specific to the microbial population and the substrate used in the experiment. Thus these parameters are estimated using best-fit regression analysis by comparing the numerical results with experimental values obtained from Liu and Logan (H. Liu & Logan, 2004).

In this analysis, the objective function was defined as the difference between theoretical and measured MFC current density. The simplex search method was used for minimizing the objective function. The dynamic model was used to study how the operating parameters, including the initial COD influence the MFC performance in terms of current density and COD removal rate, While COD removal rate is important when discussing MFC as a wastewater treatment technology, current density is useful when comparing MFC with standard fuel cells or other power generation technologies. For this analysis, S_{in} and R_{ext} are assumed to be 5-45 g/L and 1000 Ohm respectively.

4.8.1 The effect of initial COD

Figure 4.30a-d shows the experimental and fitted values of COD vs. time, COD removal rate vs. time, and MFC current density (experimental and theoretical) as a function of time. As can be seen from Figure 4.30a-b, the initial COD ((experimental and theoretical) and COD removal rate decreased linearly with time using initial COD of 5-45 g/L. As has been shown, while increasing S_{in} helps in increasing COD removal rate. In terms of percentage, increasing the initial COD concentration from 5 to 45 g/L, results in 75% increase in COD removal rate, for the MFC system studied in this analysis. The experiment and predicted result (Figure 4.30a) of COD from the simulation is also fully consistent with that observed in previous experimental studies (Gadkari & Sadhukhan,

2020; Nouri & Najafpour Darzi, 2017). On the other hand, this improvement in COD removal rate at higher S_{in} values is ascribed to the enhanced hydroxyl radical (OH) formation, which helps in further oxidative degradation of the COD adsorbed on the surface of the electrode (Lam et al., 2020). Thus, depending on the focus of MFC end-use, optimum initial COD concentration can be selected by performing a parametric analysis using the current model. Additionally, the experimental and theoretical value of current density with respect time at different initial COD is presented in Figure 4.30c. As can be seen Figure 4.30c, the current density (experimental and theoretical) increases linearly with an increase in initial COD concentration of 5-45 g/L until 11 days of operation and then decreased. Among all COD (5-45 g/L), the current density reaches a maximum value and plateaus using 45 g/L after 11 days of operation.

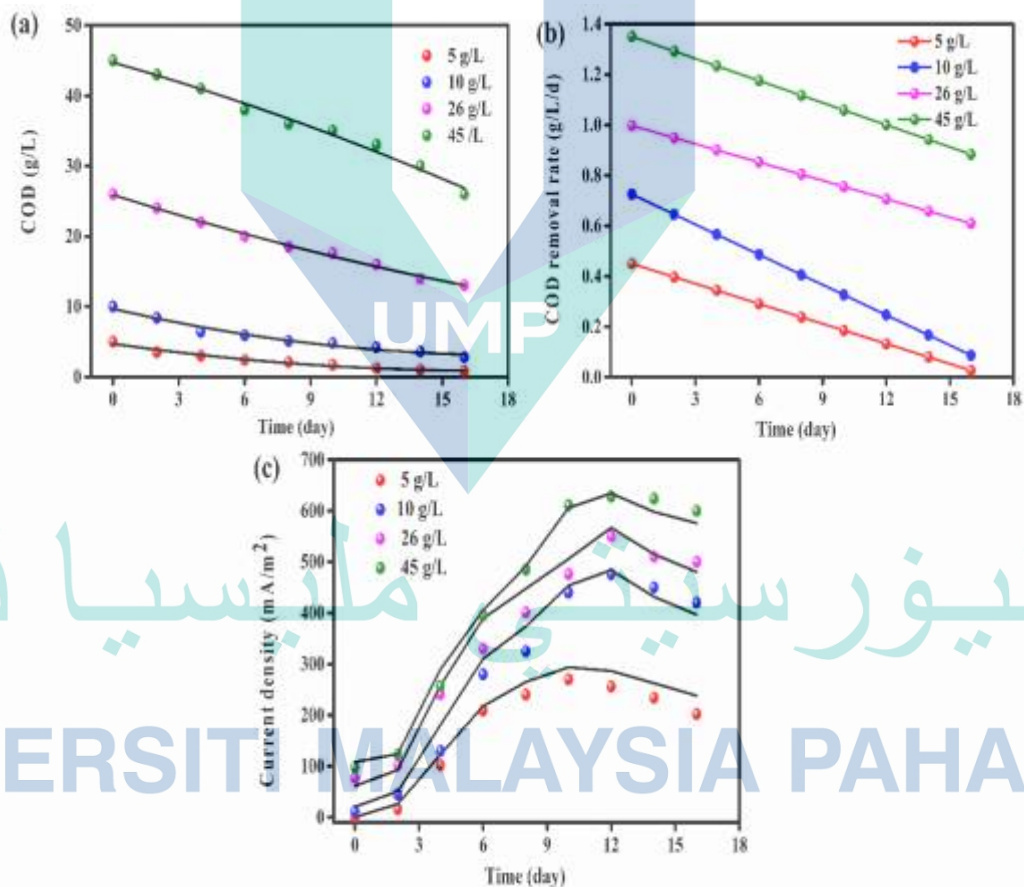


Figure 4.30 a) Initial COD vs. time (experimental and simulated), b) COD removal rate vs. time, and c) Current density vs. time (experimental and simulated).

A similar relationship between current density and initial COD concentration has been reported in previous works (G. Yang et al., 2019). As can also be seen from Figure 4.30d, there is close agreement between current density values obtained from model

predictions and those measured in the experiment. Actually, the mathematical model accurately captures the trends similar to that observed in the vast majority of studies, showing the influence of initial COD concentration on important MFC performance indices, such as the coulombic efficiency, COD removal rate, and the power density (S. Luo, Sun, Ping, Jin, & He, 2016). However, some experimental studies that have observed either no change or a reverse relationship (Gorgin, Luo, & Wu, 2020; R. C. O. Tang et al., 2020). The factors responsible for such variations could be very specific to the design and operational conditions of the particular MFC and will need to be studied individually. The proposed mathematical model can be easily implemented by experimentalists and used to run a parametric analysis of important operating parameters using basic computational resources, to determine the optimum range of operation of a given MFC system. The optimum range required depends on the targeted end-use of the MFC, which can be focused on just current generation or wastewater treatment alone, or have a dual goal with improving the efficiency of both outputs. As seen from Figure 4.30a-c, increasing initial substrate concentration of 5-45 g/L, the current density of the MFC (90-650 mA/m²) and substrate (COD) removal rate (0.1-1.2 g/L/d) also increase. As the substrate concentration (COD) at the anode is consumed by both primary and secondary microbial populations, an increase in substrate concentration also leads to increased competition between the two populations. Thus, while the primary microbial population consumes more substrate and results in higher current generation as S_{in} is increased from 5-45 g/L, the corresponding increment in substrate consumption by secondary microbial population leads to decrease in the current density of the cell (Gadkari, Shemfe, Modestra, Mohan, & Sadhukhan, 2019). Several experimental studies that have studied the influence of initial COD concentration have also observed a similar increasing trend of current density with increase in initial COD concentration until fixed level (Abbasi et al., 2020; Sleutels, Darus, Hamelers, & Buisman, 2011). Thus, even though the current generated increases initially with an increase in substrate concentration, the total energy that could be extracted from the substrate is getting reduced. It is important to choose the initial substrate concentration judiciously considering all factors such that the MFC system could be operated at optimum efficiency. Similarly the optimum range of operation of other important system parameters, like the external resistance, electrode surface area, volume of the MFC chamber, choice of substrate and microbial population (which determine the maximum substrate consumption rate, maximum growth rate, and half-saturation coefficient), can also be studied using the proposed modelling framework. The model is robust, therefore it is useful for MFC system optimization.

4.9 Summary

In summary, the performance was evaluated using single, mixed substrates and inoculum. The present study demonstrates that the individual components of the wastewater such as AA, ACA, and DMP can be used as fuel in microbial fuel cell. Among the single and mixed substrates, the mixed substrates (AA: ACA: DMP = 2: 2: 0.5 wt %) showed the maximum performance in terms of power generation. Compared to the individual inoculum such as PA and BC, the acclimatized AS shows the highest performance which might be due to the mutualistic interaction between the microbes. When the PCW was run in this MFC with the acclimatized AS, the power generation was higher than the synthetic wastewater which can be due to few reasons. Firstly, the morphology of the biofilm was visualized by SEM and it was observed that an effective biofilm with the discrete distribution of single layer microorganisms can produce high power corresponding to low charge transfer resistance. However, the growth of biofilm in multilayers consisting of outnumbered dead cells in the vicinity of the electrode surface caused the polarization resistance and diffusion resistance resulting in a sharp drop in the current generation. Secondly, the presence of some other compounds and the mutualistic interaction within the microbes. Finally, the metabolites (pyocyanin and hydroquinone) produced PA and BC inoculated MFC leading to the enhancement in the performance of acclimatized AS MFC fed with PCW. Based on the cyclic voltammetry results and EIS, it was found that the MFC can achieve the best performance with lower charge transfer resistance when the metabolite played an important role. So, not only biofilm but also naturally produced metabolite plays an important role to achieve simultaneous wastewater treatment and electricity generation in acclimatized inoculated MFCs. Besides, initial concentration was an important factor for power generation and COD removal efficiency in the case of PCW. Apart from this, the role of the initial COD of PCW also optimized by the kinetic model using polymath software. The predicted results were in good agreement with the experimental results. Moreover, the interaction between initial COD and their effect on the performance of MFC was analysed and correlated with the cell current density. The result of the present study reveals that the performance of MFC can be predicted through Nernst-Monod-Butler –Volmer model for COD range of 5 – 45 g/L and for 0 – 16 days of operation.

CHAPTER 5

CONCLUSION

5.1 Conclusion

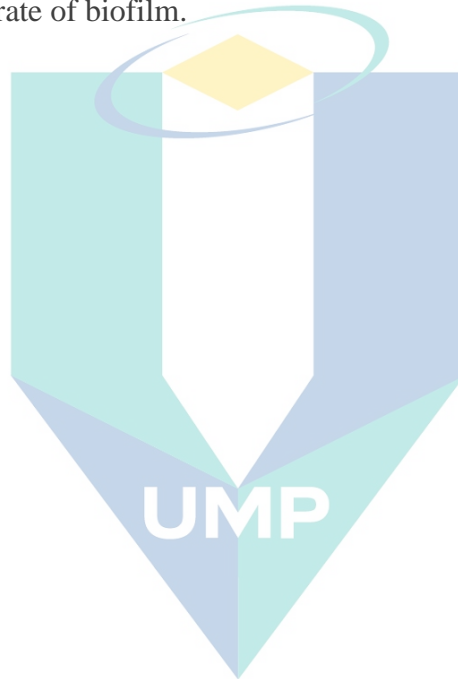
The effect of substrate-inoculum interaction on power generation was evaluated using pure (*Pseudomonas aeruginosa*, *Bacillus cereus*) and mixed cultures (acclimatized AS) with single (AA, ACA and DMP) and their mixed substrates (AA: ACA: DMP). The results revealed that the mixed substrates with acclimatized AS can produce high power (0.78 W/m^3) compared to AA with PA (0.24 W/m^3), AA with BC (0.22 W/m^3), ACA with PA (0.39 W/m^3), ACA with BC (0.32 W/m^3), DMP with PA (0.24 W/m^3) and DMP with BC (0.21 W/m^3) respectively suggesting the inoculum-substrates based synergy with high microbial growth while using mixed substrates. On the other hand, while exploring the effect of inoculum using synthetic wastewater, the maximum power generation of 0.78 W/m^3 was attained using acclimatized AS compared to PA (0.60 W/m^3) and BC (0.48 W/m^3) respectively demonstrating the mutualistic interaction between the microbes along with proper degradation capability in a wide diversity of substrates with concurrent power generation. On the other hand, acclimatized AS showed higher current intensity (0.012 A) compared to PA (0.010 A) and BC (0.006 A) indicating the good catalytic activity of acclimatized AS. The study also evaluated the potentiality of MFC in treating PCW from the acrylic acid plant using the acclimatized mixed culture inoculum as a biocatalyst. The PCW with initial COD of $\leq 45000 \text{ mg/L}$ was found feasible to be used as fuel in the MFC with concomitant high power generation and partial COD removal. The COD removal efficiency and CE were found to be 45% and ~18% respectively after 16 days of operation using PCW with an initial COD of 45000 mg/L . However, the maximum power generation (850 mW/m^2) was achieved after 11 days of operation owing to the presence of a high concentration of microbes along with the formation of an efficient biofilm as evidenced by SEM analysis. Despite the high power generation, this study embarks the problem of low COD removal efficiency (45%) at high initial COD (45000 mg/L) where the COD removal efficiency was found to be inversely related to the initial COD and the power generation was linearly increased with the increase of initial

COD. Moreover, the electron transfer mechanism was elucidated using the CV and EIS. Control experiments on supernatant and biofilm after two weeks of operation clearly demonstrated the predominant role of natural metabolites whereas direct electron transfer through the microbes in the biofilm was found to be insignificant as revealed by CV; however, the formation of biofilm was crucial that significantly reduced the interfacial charge transfer resistance leading to high electricity generation (850 mW/m^2). The presence of mediators such as pyocyanin and hydroquinone was identified by UV-vis, CV and EIS. The result of the present study also indicates that MFC with naturally produced pyocyanin and hydroquinone from PA and BC showed much higher peak current (0.010 A and 0.006 A) than that of the control pyocyanin (0.0025 A) and hydroquinone (0.0022 A). Additionally, the anodic polarization behaviour was further elucidated by fitting the data using the Tafel equation. From Tafel equation, it can be seen that the Tafel slope was higher (1.93 V/decade) on day 5 followed by a significant decrease after 11 days of operation (0.65 V/decade) indicating the higher electron transfer efficiency at day 11. Finally, the Nernst-Monod-Butler-Volmer model was employed to fit the MFC data to extract the kinetic parameters. It was shown that the model can be used to predict the performance of the PCW driven MFC for the COD range of 5 – 45 g/L. The model can further be used for optimization of the MFC performance for wide range of parameters.

5.2 RECOMMENDATION

In the present work, the role of initial COD, metabolite interaction with biofilm for power generation was studied for, however, in acclimatized AS system; the important role of methanogenic bacteria for the production of methane and their adverse effect on power generation was not properly identified due to time limit. Further studies are needed to identify an inter-microbial relationship with methanogenic bacteria with electrogenic bacteria to develop an efficient inoculum for PCW treatment along with power generation. In this study, the role of biofilm, metabolite were elucidated using polarization, CV, EIS, and SEM techniques. More precise and sophisticated techniques such as denaturing gel gradient electrophoresis (DGGE), fluorescence in situ hybridization (FISH), terminal restriction fragment length polymorphism (T-RFLP), DNA microarray and pyrosequencing techniques need to be studied in order to get more insight of synergistic and antagonistic mechanisms among microbes. The individual

components of synthetic wastewater were analyzed. However, the analysis of the full component in the PCW was not done. Detailed investigation needed to observe the change of individual components during the reaction and the product analysis. The study demonstrated the kinetic study using petrochemical wastewater. However, the detailed kinetic study using individual substrates was not done. Again studies needed to observe the changing effect of individual substrates concentration on power generation. The kinetics of biofilm is directly correlated with the performance of MFC which was not broadly investigated due to the time limit. Further studies are required to measure the thickness and growth rate of biofilm.



اونيورسيتي ملايسيا قهغ

UNIVERSITI MALAYSIA PAHANG

REFERENCES

- Aarthy, M., Rajesh, T., & Thirunavoukkarasu, M. (2020). Critical review on microbial fuel cells for concomitant reduction of hexavalent chromium and bioelectricity generation. *Journal of Chemical Technology Biotechnology*, 95(5), 1298-1307.
- Abbasi, S., Mirghorayshi, M., Zinadini, S., & Zinatizadeh, A. (2020). A novel single continuous electrocoagulation process for treatment of licorice processing wastewater: optimization of operating factors using RSM. *Process Safety Environmental Protection*, 134, 323-332.
- Abdulsalam, M., Che Man, H., Isma Idris, A., Faezah Yunos, K., & Zainal Abidin, Z. (2018). Treatment of palm oil mill effluent using membrane bioreactor: Novel processes and their major drawbacks. *Water*, 10(9), 1165.
- Abo-Zahhad, E. M., Ookawara, S., Radwan, A., El-Shazly, A., El-Kady, M., & Esmail, M. F. (2020). Performance, limits, and thermal stress analysis of high concentrator multijunction solar cell under passive cooling conditions. *Applied Thermal Engineering*, 164, 114497.
- Abuabdou, S. M., Ahmad, W., Aun, N. C., & Bashir, M. J. (2020). A review of anaerobic membrane bioreactors (AnMBR) for the treatment of highly contaminated landfill leachate and biogas production: effectiveness, limitations and future perspectives. *Journal of Cleaner Production*, 255, 120215.
- Adeel, M., Rahman, M. M., Caligiuri, I., Canzonieri, V., Rizzolio, F., & Daniele, S. (2020). Recent advances of electrochemical and optical enzyme-free glucose sensors operating at physiological conditions. *Biosensors Bioelectronics*, 112331.
- Ağbulut, Ü., Ceylan, İ., Gürel, A. E., & Ergün, A. (2019). The history of greenhouse gas emissions and relation with the nuclear energy policy for Turkey. *International Journal of Ambient Energy*, 1-9.
- Agostino, V., Ahmed, D., Sacco, A., Margaria, V., Armato, C., & Quaglio, M. (2017). Electrochemical analysis of microbial fuel cells based on enriched biofilm communities from freshwater sediment. *Electrochimica Acta*, 237, 133-143.
- Ahmad, M., Kamaruzzaman, M., & Chin, S. (2014). New method for acrylic acid recovery from industrial waste water via esterification with 2-ethyl hexanol. *Process Safety Environmental Protection*, 92(6), 522-531.
- Ahmad, N., Sultana, S., Khan, M. Z., & Sabir, S. (2020). Chitosan Based Nanocomposites as Efficient Adsorbents for Water Treatment. In *Modern Age Waste Water Problems* (pp. 69-83): Springer.
- Ai, J., Jin, R., Liu, Z., Jiang, J., Yuan, S., Huang, G., . . . Li, X. (2019). Three-dimensionally ordered macroporous FeP self-supported structure for high-efficiency hydrogen evolution reaction. *International Journal of Hydrogen Energy*, 44(12), 5854-5862. doi:<https://doi.org/10.1016/j.ijhydene.2018.12.202>

- Aiyer, K. S. (2020a). How does electron transfer occur in microbial fuel cells? *World Journal of Microbiology Biotechnology*, 36(2), 19.
- Aiyer, K. S. (2020b). How does electron transfer occur in microbial fuel cells? *World Journal of Microbiology Biotechnology*, 36(2), 19.
- Algharib, S. A., Dawood, A., & Xie, S. (2020). Nanoparticles for treatment of bovine *Staphylococcus aureus* mastitis. *Drug delivery*, 27(1), 292-308.
- Aljuboury, D., Palaniandy, P., Abdul Aziz, H., & Feroz, S. (2017). Treatment of petroleum wastewater by conventional and new technologies-A review. *Glob. Nest J*, 19, 439-452.
- Allam, F., Elnouby, M., El-Khatib, K., El-Badan, D. E., & Sabry, S. A. (2020). Water hyacinth (*Eichhornia crassipes*) biochar as an alternative cathode electrocatalyst in an air-cathode single chamber microbial fuel cell. *International Journal of Hydrogen Energy*, 45(10), 5911-5927.
- Alvarado, A., Behrens, W., & Josenhans, C. (2020). Protein Activity Sensing in Bacteria in Regulating Metabolism and Motility. *Frontiers in microbiology*, 10, 3055.
- Ameen, F., Alshehri, W. A., & Nadhari, S. A. (2019). Effect of Electroactive Biofilm Formation on Acetic Acid Production in Anaerobic Sludge Driven Microbial Electrosynthesis. *ACS Sustainable Chemistry Engineering*.
- An, B.-M., Seo, S.-j., Hidayat, S., & Park, J.-Y. (2020). Treatment of ethanolamine and electricity generation using a scaled-up single-chamber microbial fuel cell. *Journal of Industrial Engineering Chemistry*, 81, 1-6.
- An, Q., Cheng, J.-R., Wang, Y.-T., & Zhu, M.-J. (2020). Performance and energy recovery of single and two stage biogas production from paper sludge: *Clostridium thermocellum* augmentation and microbial community analysis. *Renewable Energy*, 148, 214-222.
- Anawar, H. M., & Strezov, V. (2019). Microbial Fuel Cells to Produce Renewable Energy from Organic Matter-Rich Wastewater and Solid Wastes Focusing on Economic Benefits and Sustainability. *Sustainable Economic Waste Management: Resource Recovery Techniques*, 197.
- Angelaalincy, M. J., Navanietha Krishnaraj, R., Shakambari, G., Ashokkumar, B., Kathiresan, S., & Varalakshmi, P. (2018). Biofilm Engineering Approaches for Improving the Performance of Microbial Fuel Cells and Bioelectrochemical Systems. *Frontiers in Energy Research*, 6, 63.
- Ansari, F. A. (2019). *Application of lipid extracted algae in feed and energy production*.
- Anwer, A. H., Khan, M. D., Khan, M. Z., & Joshi, R. (2020). Microbial Electrochemical Cell: An Emerging Technology for Waste Water Treatment and Carbon Sequestration. In *Modern Age Waste Water Problems* (pp. 339-360): Springer.
- Aquino, S. F., Araújo, J. C., Passos, F., Curtis, T. P., & Foresti, E. (2019). Fundamentals of anaerobic sewage treatment.

- Arends, J. (2013). *Optimizing the plant microbial fuel cell: Diversifying applications and product outputs*. Ghent University,
- Arvin, A., Hosseini, M., Amin, M. M., Darzi, G. N., & Ghasemi, Y. (2019). A comparative study of the anaerobic baffled reactor and an integrated anaerobic baffled reactor and microbial electrolysis cell for treatment of petrochemical wastewater. *Biochemical Engineering Journal*, 144, 157-165.
- Asensio, Y., Montes, I., Fernandez-Marchante, C., Lobato, J., Cañizares, P., & Rodrigo, M. (2017). Selection of cheap electrodes for two-compartment microbial fuel cells. *Journal of Electroanalytical Chemistry*, 785, 235-240.
- Atiénzar Fernández, C. (2020). Microorganismos marinos en la producción de corriente eléctrica. Celdas de combustible y posibles aplicaciones en generadores de corriente.
- Avellaneda, J., Bataille, F., Toutant, A., & Flamant, G. (2020). Entropy generation minimization in a channel flow: application to different advection-diffusion processes and boundary conditions. *Chemical Engineering Science*, 115601.
- Azeredo, J., Azevedo, N. F., Briandet, R., Cerca, N., Coenye, T., Costa, A. R., . . . Jaglic, Z. (2017). Critical review on biofilm methods. *Critical reviews in microbiology*, 43(3), 313-351.
- Azeumo, M. F., Germana, C., Ippolito, N. M., Franco, M., Luigi, P., & Settimio, S. (2019). Photovoltaic module recycling, a physical and a chemical recovery process. *Solar Energy Materials*, 193, 314-319.
- Babanova, S., Jones, J., Phadke, S., Lu, M., Angulo, C., Garcia, J., . . . Phan, T. (2020). Continuous flow, large-scale, microbial fuel cell system for the sustained treatment of swine waste. *Water Environment Research*, 92(1), 60-72.
- Bagchi, S., & Behera, M. (2020). Assessment of Heavy Metal Removal in Different Bioelectrochemical Systems: A Review. *Journal of Hazardous, Toxic, Radioactive Waste*, 24(3), 04020010.
- Bagetta, G., Cosentino, M., Corasaniti, M. T., & Sakurada, S. (2016). *Herbal medicines: development and validation of plant-derived medicines for human health*: CRC Press.
- Bahri, M., Mahdavi, A., Mirzaei, A., Mansouri, A., & Haghghat, F. (2018). Integrated oxidation process and biological treatment for highly concentrated petrochemical effluents: A review. *Chemical Engineering Processing-Process Intensification*, 125, 183-196.
- Bajpai, P. (2019). *Third Generation Biofuels*: Springer.
- Baker, B. R., Mohamed, R., Al-Gheethi, A., & Aziz, H. A. (2020). Advanced technologies for poultry slaughterhouse wastewater treatment: A systematic review. *Journal of Dispersion Science Technology*, 1-20.

- Bakraoui, M., Karouach, F., Ouhammou, B., Aggour, M., Essamri, A., & El Bari, H. (2020). Biogas production from recycled paper mill wastewater by UASB digester: Optimal and mesophilic conditions. *Biotechnology Reports*, 25, e00402.
- Banu, J. R., Kavitha, S., Kannah, R. Y., Bhosale, R. R., & Kumar, G. (2020). Industrial wastewater to biohydrogen: Possibilities towards successful biorefinery route. *Bioresource technology*, 298, 122378.
- Baranitharan, E., Khan, M. R., Prasad, D., Teo, W. F. A., Tan, G. Y. A., & Jose, R. (2015). Effect of biofilm formation on the performance of microbial fuel cell for the treatment of palm oil mill effluent. *Bioprocess biosystems engineering*, 38(1), 15-24.
- Barhoumi, N., Olvera-Vargas, H., Oturan, N., Huguenot, D., Gadri, A., Ammar, S., . . . Oturan, M. A. (2017). Kinetics of oxidative degradation/mineralization pathways of the antibiotic tetracycline by the novel heterogeneous electro-Fenton process with solid catalyst chalcopyrite. *Applied Catalysis B: Environmental*, 209, 637-647.
- Basile, A., & Ghasemzadeh, K. (2020). *Current Trends and Future Developments on (Bio-) Membranes: Recent Achievements in Wastewater and Water Treatments*: Elsevier.
- Behnami, A., Benis, K. Z., Shakerkhatibi, M., Derafshi, S., & Chavoshbashi, M. M. (2019). A systematic approach for selecting an optimal strategy for controlling VOCs emissions in a petrochemical wastewater treatment plant. *Stochastic environmental research risk assessment*, 33(1), 13-29.
- Beran, F., Köllner, T. G., Gershenzon, J., & Tholl, D. (2019). Chemical convergence between plants and insects: biosynthetic origins and functions of common secondary metabolites. *New Phytologist*.
- Bharagava, R. N., Saxena, G., & Mulla, S. I. (2020). Introduction to industrial wastes containing organic and inorganic pollutants and bioremediation approaches for environmental management. In *Bioremediation of industrial waste for environmental safety* (pp. 1-18): Springer.
- Birjandi, N., Younesi, H., Ghoreyshi, A. A., & Rahimnejad, M. (2020). Enhanced medicinal herbs wastewater treatment in continuous flow bio-electro-Fenton operations along with power generation. *Renewable Energy*.
- Bolognesi, S., Cecconet, D., & Capodaglio, A. G. (2020). Agro-industrial wastewater treatment in microbial fuel cells. In *Integrated Microbial Fuel Cells for Wastewater Treatment* (pp. 93-133): Elsevier.
- Borciani, G., Montalbano, G., Baldini, N., Cerqueni, G., Vitale-Brovarone, C., & Ciapetti, G. (2020). Co-culture systems of osteoblasts and osteoclasts: Simulating in vitro bone remodeling in regenerative approaches. *Acta Biomaterialia*.
- Bose, D., Dey, A., & Banerjee, T. (2020). Aspects of Bioeconomy and Microbial Fuel Cell Technologies for Sustainable Development. *Sustainability*, 13(3), 107-118. doi:10.1089/sus.2019.0048

- Bratby, J. (2016). *Coagulation and flocculation in water and wastewater treatment*: IWA publishing.
- Brocker, J. H. L. (2020). *Comparative study for the transformation of emerging contaminants and endocrine disrupting compounds: electrochemical oxidation and biological metabolism*.
- Cai, Q., Wu, M., Li, R., Deng, S., Lee, B., Ong, S., & Hu, J. (2020). Potential of combined advanced oxidation–Biological process for cost-effective organic matters removal in reverse osmosis concentrate produced from industrial wastewater reclamation: Screening of AOP pre-treatment technologies. *Chemical Engineering Journal*, 389, 123419.
- Caizán-Juanarena, L., Borsje, C., Sleutels, T., Yntema, D., Santoro, C., Ieropoulos, I., . . . ter Heijne, A. (2020). Combination of bioelectrochemical systems and electrochemical capacitors: Principles, analysis and opportunities. *Biotechnology advances*, 39, 107456.
- Can, O. T., Gengec, E., & Kobya, M. (2019). TOC and COD removal from instant coffee and coffee products production wastewater by chemical coagulation assisted electrooxidation. *Journal of Water Process Engineering*, 28, 28-35.
- Cao, T. N.-D., Chen, S.-S., Ray, S. S., Le, H. Q., & Chang, H.-M. (2019). Application of Microbial Fuel Cell in Wastewater Treatment and Simultaneous Bioelectricity Generation. In *Water and Wastewater Treatment Technologies* (pp. 501-526): Springer.
- Cao, Y., Mu, H., Liu, W., Zhang, R., Guo, J., Xian, M., & Liu, H. (2019a). Electricigens in the anode of microbial fuel cells: pure cultures versus mixed communities. *Microbial cell factories*, 18(1), 39.
- Cao, Y., Mu, H., Liu, W., Zhang, R., Guo, J., Xian, M., & Liu, H. (2019b). Electricigens in the anode of microbial fuel cells: pure cultures versus mixed communities. *Microbial cell factories*, 18(1), 39.
- Cao, Y., Mu, H., Liu, W., Zhang, R., Guo, J., Xian, M., & Liu, H. (2019c). Electricigens in the anode of microbial fuel cells: pure cultures versus mixed communities. *Microbial cell factories*, 18(1), 1-14.
- Caruso, G. (2020). Microbial Colonization in Marine Environments: Overview of Current Knowledge and Emerging Research Topics. *Journal of Marine Science Engineering*, 8(2), 78.
- Celenza, G. (2019). *Industrial Waste Treatment Process Engineering: Biological Processes, Volume II*: CRC Press.
- Chakraborty, I., Das, S., Dubey, B., Ghangrekar, M., & Physics. (2020). Novel low cost proton exchange membrane made from sulphonated biochar for application in microbial fuel cells. *Materials Chemistry*, 239, 122025.
- Chakraborty, I., Sathe, S., Khuman, C., & Ghangrekar, M. (2020). Bioelectrochemically powered remediation of xenobiotic compounds and heavy metal toxicity using

microbial fuel cell and microbial electrolysis cell. *Materials Science for Energy Technologies*, 3, 104-115.

Chakraborty, I., Sathe, S. M., Khuman, C. N., & Ghangrekar, M. M. (2020). Bioelectrochemically powered remediation of xenobiotic compounds and heavy metal toxicity using microbial fuel cell and microbial electrolysis cell. *Materials Science for Energy Technologies*, 3, 104-115. doi:<https://doi.org/10.1016/j.mset.2019.09.011>

Chang, C.-C., Kao, W., & Yu, C.-P. (2020). Assessment of voltage reversal effects in the serially connected biocathode-based microbial fuel cells through treatment performance, electrochemical and microbial community analysis. *Chemical Engineering Journal*, 125368.

Chatterjee, P., Dessì, P., Kokko, M., Lakaniemi, A.-M., & Lens, P. (2019). Selective enrichment of biocatalysts for bioelectrochemical systems: A critical review. *Renewable Sustainable Energy Reviews*, 109, 10-23.

Cheeseman, S., Christofferson, A. J., Kariuki, R., Cozzolino, D., Daeneke, T., Crawford, R. J., . . . Elbourne, A. (2020). Antimicrobial Metal Nanomaterials: From Passive to Stimuli-Activated Applications. *Advanced Science*, 7(10), 1902913.

Chen, C., Yoza, B. A., Wang, Y., Wang, P., Li, Q. X., Guo, S., & Yan, G. (2015). Catalytic ozonation of petroleum refinery wastewater utilizing Mn-Fe-Cu/Al₂O₃ catalyst. *Environmental Science Pollution Research*, 22(7), 5552-5562.

Chen, H., Dong, F., & Minteer, S. D. (2020). The progress and outlook of bioelectrocatalysis for the production of chemicals, fuels and materials. *Nature Catalysis*, 1-20.

Chen, J. Y., Xie, P., & Zhang, Z. P. (2019). Reduced graphene oxide/polyacrylamide composite hydrogel scaffold as biocompatible anode for microbial fuel cell. *Chemical Engineering Journal*, 361, 615-624.

Chen, X. (2020). Graphene and biomass-based carbocatalysts as high-performance peroxydisulfate activator for the removal of recalcitrant pollutants in water.

Chevrette, M. G., Gutiérrez-García, K., Selem-Mojica, N., Aguilar-Martínez, C., Yañez-Olvera, A., Ramos-Aboites, H. E., . . . Barona-Gómez, F. (2020). Evolutionary dynamics of natural product biosynthesis in bacteria. *Natural Product Reports*, 37(4), 566-599.

Chiranjeevi, P., & Patil, S. A. (2020). Strategies for improving the electroactivity and specific metabolic functionality of microorganisms for various microbial electrochemical technologies. *Biotechnology advances*, 39, 107468.

Chiranjeevi, P., Yeruva, D. K., Kumar, A. K., Mohan, S. V., & Varjani, S. (2019). Plant-Microbial Fuel Cell Technology. In *Microbial Electrochemical Technology* (pp. 549-564): Elsevier.

Chmielowiec, B. J. (2019). *Electrochemical engineering considerations for gas evolution in molten sulfide electrolytes*. Massachusetts Institute of Technology,

- Choi, O., & Sang, B.-I. (2016). Extracellular electron transfer from cathode to microbes: application for biofuel production. *Biotechnology for biofuels*, 9(1), 11.
- Chomel, M., Guittonny-Larchevêque, M., Fernandez, C., Gallet, C., DesRochers, A., Paré, D., . . . Baldy, V. (2016). Plant secondary metabolites: a key driver of litter decomposition and soil nutrient cycling. *Journal of Ecology*, 104(6), 1527-1541.
- Choudhury, P., Ray, R. N., Bandyopadhyay, T. K., & Bhunia, B. (2020). Fed batch approach for stable generation of power from dairy wastewater using microbial fuel cell and its kinetic study. *Fuel*, 266, 117073.
- Christensen, M. L., Keiding, K., Nielsen, P. H., & Jørgensen, M. K. (2015). Dewatering in biological wastewater treatment: a review. *Water research*, 82, 14-24.
- Chung, Y. W., Gwak, H.-J., Moon, S., Rho, M., & Ryu, J.-H. (2020). Functional dynamics of bacterial species in the mouse gut microbiome revealed by metagenomic and metatranscriptomic analyses. *PLOS one*, 15(1), e0227886.
- Coenen, J., Martin, A., & Dahl, O. (2020). Performance assessment of chemical mechanical planarization wastewater treatment in nano-electronics industries using membrane distillation. *Separation Purification Technology*, 235, 116201.
- Cong, B., Liu, C., Wang, L., & Chai, Y. (2020). The Impact on Antioxidant Enzyme Activity and Related Gene Expression Following Adult Zebrafish (*Danio rerio*) Exposure to Dimethyl Phthalate. *Animals*, 10(4), 717.
- Conley, B., & Gralnick, J. (2019). Anaerobic Bacteria: Solving a shuttle mystery. *eLife*, 8, e49831.
- Corbella, C., Hartl, M., Fernandez-Gatell, M., & Puigagut, J. (2019). MFC-based biosensor for domestic wastewater COD assessment in constructed wetlands. *Science of the total environment*, 660, 218-226.
- Crini, G., & Lichtfouse, E. (2019). Advantages and disadvantages of techniques used for wastewater treatment. *Environmental Chemistry Letters*, 17(1), 145-155.
- Crini, G., Lichtfouse, E., Wilson, L. D., & Morin-Crini, N. (2019). Conventional and non-conventional adsorbents for wastewater treatment. *Environmental Chemistry Letters*, 17(1), 195-213.
- Cui, Y., Lai, B., & Tang, X. (2019). Microbial fuel cell-based biosensors. *Biosensors*, 9(3), 92.
- Cullen, C. M., Aneja, K. K., Beyhan, S., Cho, C. E., Woloszynek, S., Convertino, M., . . . Alvarez-Ponce, D. (2020). Emerging Priorities for Microbiome Research. *Frontiers in microbiology*, 11, 136.
- Czerwińska-Główka, D., & Krukiewicz, K. (2020). A journey in the complex interactions between electrochemistry and bacteriology: From electroactivity to electromodulation of bacterial biofilms. *Bioelectrochemistry*, 131, 107401.

- Dai, K., Zhang, W., Zeng, R. J., & Zhang, F. (2020). Production of chemicals in thermophilic mixed culture fermentation: mechanism and strategy. *Critical Reviews in Environmental Science Technology*, 50(1), 1-30.
- Dai, Q., Zhang, S., Liu, H., Huang, J., & Li, L. (2020). Sulfide-mediated azo dye degradation and microbial community analysis in a single-chamber air cathode microbial fuel cell. *Bioelectrochemistry*, 131, 107349.
- Dai, X., Chen, C., Yan, G., Chen, Y., & Guo, S. (2016). A comprehensive evaluation of re-circulated bio-filter as a pretreatment process for petroleum refinery wastewater. *Journal of Environmental Sciences*, 50, 49-55.
- De Corato, U. (2020). Disease-suppressive compost enhances natural soil suppressiveness against soil-borne plant pathogens: A critical review. *Rhizosphere*, 13, 100192.
- De Natale, A., Mele, B. H., Cennamo, P., Del Mondo, A., Petrarretti, M., & Pollio, A. (2020). Microbial biofilm community structure and composition on the lithic substrates of Herculaneum Suburban Baths. *PLOS one*, 15(5), e0232512.
- de Oliveira, C. P. M., Viana, M. M., & Amaral, M. C. S. (2020). Coupling photocatalytic degradation using a green TiO₂ catalyst to membrane bioreactor for petroleum refinery wastewater reclamation. *Journal of Water Process Engineering*, 34, 101093.
- De Schampelaere, L., Rabaey, K., Boeckx, P., Boon, N., & Verstraete, W. (2008). Outlook for benefits of sediment microbial fuel cells with two bio-electrodes. *Microbial biotechnology*, 1(6), 446-462.
- Deng, C., Lin, R., Cheng, J., & Murphy, J. D. (2019). Can acid pre-treatment enhance biohydrogen and biomethane production from grass silage in single-stage and two-stage fermentation processes? *Energy Conversion Management*, 195, 738-747.
- Do, M. H., Ngo, H. H., Guo, W., Chang, S. W., Nguyen, D. D., Liu, Y., . . . Kumar, M. (2020). Microbial fuel cell-based biosensor for online monitoring wastewater quality: A critical review. *Science of the total environment*, 712, 135612. doi:https://doi.org/10.1016/j.scitotenv.2019.135612
- Dong, Q., Guo, X., Huang, X., Liu, L., Tallon, R., Taylor, B., & Chen, J. (2019). Selective removal of lead ions through capacitive deionization: Role of ion-exchange membrane. *Chemical Engineering Journal*, 361, 1535-1542.
- Du, C.-M., Gao, X., Ueda, S., & Kitamura, S.-Y. (2019). Separation and recovery of phosphorus from steelmaking slag via a selective leaching–chemical precipitation process. *Hydrometallurgy*, 189, 105109.
- Ebenau-Jehle, C., Soon, C. I., Fuchs, J., Geiger, R., & Boll, M. (2020). An aerobic hybrid phthalate degradation pathway via phthaloyl-coenzyme A in denitrifying bacteria. *Applied Environmental Microbiology*, 86(11).

- Eid, A. M., Shaaban, S., & Shalabi, K. (2020). Tetrazole-based organoselenium bi-functionalized corrosion inhibitors during oil well acidizing: Experimental, computational studies, and SRB bioassay. *Journal of Molecular Liquids*, 298, 111980. doi:https://doi.org/10.1016/j.molliq.2019.111980
- El-Mokadem, E. A., El-Leboudy, A. A., & Amer, A. A. (2020). Occurrence of Enterobacteriaceae in Dairy Farm Milk. *Alexandria Journal for Veterinary Sciences*, 64(2).
- El Chakhtoura, J. R. (2011). *Harvesting Electricity from the Organic Fraction of Municipal Solid Waste Using Microbial Fuel Cells*. American University of Beirut, Interfaculty Graduate Environmental Sciences ...
- Elbourne, A., Chapman, J., Gelmi, A., Cozzolino, D., Crawford, R. J., & Truong, V. K. (2019). Bacterial-nanostructure interactions: The role of cell elasticity and adhesion forces. *Journal of colloid interface science*, 546, 192-210.
- Elbourne, A., Cheeseman, S., Atkin, P., Truong, N. P., Syed, N., Zavabeti, A., . . . McConville, C. F. (2020). Antibacterial Liquid Metals: Biofilm Treatment via Magnetic Activation. *ACS nano*, 14(1), 802-817.
- Eljamal, R., Kahraman, I., Eljamal, O., Thompson, I. P., Maamoun, I., & Yilmaz, G. (2020). Impact of nZVI on the formation of aerobic granules, bacterial growth and nutrient removal using aerobic sequencing batch reactor. *Environmental technology innovation*, 100911.
- Elmaadawy, K., Hu, J., Guo, S., Hou, H., Xu, J., Wang, D., . . . Liu, B. (2020). Enhanced treatment of landfill leachate with cathodic algal biofilm and oxygen-consuming unit in a hybrid microbial fuel cell system. *Bioresource technology*, 123420.
- Farmer, C., Hines, P., Dowds, J., & Blumsack, S. (2010). *Modeling the impact of increasing PHEV loads on the distribution infrastructure*. Paper presented at the 2010 43rd Hawaii International Conference on System Sciences.
- Fei, C., Mao, S., Yan, J., Alert, R., Stone, H. A., Bassler, B. L., . . . Košmrlj, A. (2020). Nonuniform growth and surface friction determine bacterial biofilm morphology on soft substrates. *Proceedings of the National Academy of Sciences*, 117(14), 7622-7632.
- Feng, L., Liu, Y., Zhang, J., Li, C., & Wu, H. (2020). Dynamic variation in nitrogen removal of constructed wetlands modified by biochar for treating secondary livestock effluent under varying oxygen supplying conditions. *Journal of environmental management*, 260, 110152.
- Feng, Y., Wang, X., Logan, B. E., & Lee, H. (2008). Brewery wastewater treatment using air-cathode microbial fuel cells. *Applied microbiology biotechnology*, 78(5), 873-880.
- Figueroa, I. A., Barnum, T. P., Somasekhar, P. Y., Carlström, C. I., Engelbrekton, A. L., & Coates, J. D. (2018). Metagenomics-guided analysis of microbial chemolithoautotrophic phosphite oxidation yields evidence of a seventh natural

CO₂ fixation pathway. *Proceedings of the National Academy of Sciences*, 115(1), E92-E101.

- Foster, T. J., Geoghegan, J. A., Ganesh, V. K., & Höök, M. (2014). Adhesion, invasion and evasion: the many functions of the surface proteins of *Staphylococcus aureus*. *Nature Reviews Microbiology*, 12(1), 49.
- Fu, T., Tang, X., Cai, Z., Zuo, Y., Tang, Y., & Zhao, X. (2020). Correlation research of phase angle variation and coating performance by means of Pearson's correlation coefficient. *Progress in Organic Coatings*, 139, 105459.
- Fuqua, C., Filloux, A., Ghigo, J.-M., & Visick, K. L. (2019). Biofilms 2018: A diversity of microbes and mechanisms. *Journal of bacteriology*, JB. 00118-00119.
- Gadkari, S., & Sadhukhan, J. (2020). A robust correlation based on dimensional analysis to characterize microbial fuel cells. *Scientific reports*, 10(1), 1-5.
- Gadkari, S., Shemfe, M., Modestra, J. A., Mohan, S. V., & Sadhukhan, J. (2019). Understanding the interdependence of operating parameters in microbial electrosynthesis: a numerical investigation. *Physical Chemistry Chemical Physics*.
- Gadkari, S., Shemfe, M., & Sadhukhan, J. (2019). Microbial fuel cells: A fast converging dynamic model for assessing system performance based on bioanode kinetics. *International Journal of Hydrogen Energy*, 44(29), 15377-15386.
- Gajda, I., Greenman, J., & Ieropoulos, I. (2018). Recent advancements in real-world microbial fuel cells applications. *Current opinion in electrochemistry*.
- Gallego-Cartagena, E., Morillas, H., Maguregui, M., Patiño-Camelo, K., Marcaida, I., Morgado-Gamero, W., . . . Madariaga, J. M. (2020). A comprehensive study of biofilms growing on the built heritage of a Caribbean industrial city in correlation with construction materials. *International Biodeterioration Biodegradation*, 147, 104874.
- Gao, N., Fan, Y., Long, F., Qiu, Y., Geier, W., & Liu, H. (2020). Novel trickling microbial fuel cells for electricity generation from wastewater. *Chemosphere*, 248, 126058.
- Garba, N., Sa'adu, L., & Dambatta, M. (2017). An overview of the substrates used in microbial fuel cells. *Greener J. Biochem. Biotechnol*, 4, 7-26.
- Garcia-Segura, S., Qu, X., Alvarez, P., Chaplin, B. P., Chen, W., Crittenden, J., . . . Hou, C.-H. (2020). Opportunities for Nanotechnology to Enhance Electrochemical Treatment of Pollutants in Potable Water and Industrial Wastewater-A perspective. *Environmental Science: Nano*.
- Garcia, D., Laurens, S., & Panin, S. (2019). A comprehensive study of the spatial distribution of the galvanic protection current supplied by zinc layer anodes applied to steel-reinforced concrete structures. *Corrosion Science*, 158, 108108.

- Gautam, P., Kumar, S., & Lokhandwala, S. (2019). Advanced oxidation processes for treatment of leachate from hazardous waste landfill: A critical review. *Journal of Cleaner Production*, 117639.
- Geng, B.-Y., Cao, L.-Y., Li, F., Song, H., Liu, C.-G., Zhao, X.-Q., & Bai, F.-W. (2020). Potential of *Zymomonas mobilis* as an electricity producer in ethanol production. *Biotechnology for biofuels*, 13(1), 1-11.
- Ghangrekar, M., & Neethu, B. (2020). Bioelectrochemical System for Bioremediation and Energy Generation. In *Microbial Bioremediation & Biodegradation* (pp. 365-391): Springer.
- Ghimire, N., & Wang, S. (2018). Biological Treatment of Petrochemical Wastewater. In *Petroleum Chemicals-Recent Insight: IntechOpen*.
- Girmaye, D., Abdeta, D., & Tamiru, Y. (2018). Review on Bacterial Biofilms and its impact. *Int. J. Adv. Microbiol. Health. Res*, 2(3), 22-30.
- Giwa, A., Dindi, A., & Kujawa, J. (2019). Membrane bioreactors and electrochemical processes for treatment of wastewaters containing heavy metal ions, organics, micropollutants and dyes: Recent developments. *Journal of hazardous materials*, 370, 172-195.
- Goel, K., & Soni, S. (2019). Physio-Chemical Analysis of Water Collected From Villages Adopted Under Unnat Bharat Abhiyan.
- Goode, J. F. (2020). *The Turkish Arms Embargo: Drugs, Ethnic Lobbies, and US Domestic Politics*: University Press of Kentucky.
- Gorgin, R., Luo, Y., & Wu, Z. (2020). Environmental and operational conditions effects on Lamb wave based structural health monitoring systems: A review. *Ultrasonics*, 106114.
- Gounden, A. N., & Jonnalagadda, S. B. (2019). Advances in Treatment of Brominated Hydrocarbons by Heterogeneous Catalytic Ozonation and Bromate Minimization. *Molecules*, 24(19), 3450.
- Gupta, G. K., & Shukla, P. (2020). Insights into the resources generation from pulp and paper industry wastes: challenges, perspectives and innovations. *Bioresour technology*, 297, 122496.
- Haavisto, J., Dessi, P., Chatterjee, P., Honkanen, M., Noori, M., Kokko, M., & Puhakka, J. (2019). Selection of an efficient anode electrode for treatment of thermomechanical pulping wastewater in an up-flow microbial fuel cell. *Manuscript submitted for publication*.
- Hacker, V., & Sumereder, C. (2020). *Electrical Engineering: Fundamentals*: Walter de Gruyter GmbH & Co KG.
- Haldar, D., Manna, M. S., Sen, D., Bhowmick, T. K., & Gayen, K. (2019). Microbial Fuel Cell for the Treatment of Wastewater. *Microbial Fuel Cells: Materials Applications*, 46, 289-306.

- Halim, M. (2019). *Effect of Various Operating Parameters on Power Generation from Mediator Less Microbial Fuel Cell*. Khulna University of Engineering & Technology (KUET), Khulna, Bangladesh,
- Hanchi, H., Mottawea, W., Sebei, K., & Hammami, R. (2018). The genus *Enterococcus*: Between probiotic potential and safety concerns—An update. *Frontiers in microbiology*, 9, 1791.
- Haq, I., & Raj, A. (2020). Pulp and Paper Mill Wastewater: Ecotoxicological Effects and Bioremediation Approaches for Environmental Safety. In *Bioremediation of Industrial Waste for Environmental Safety* (pp. 333-356): Springer.
- Harder, J., Marmulla, R., & Lipids. (2020). Catabolic pathways and enzymes involved in the anaerobic degradation of terpenes. *Anaerobic Utilization of Hydrocarbons, Oils, Lipids*, 151-164.
- Hassan, H., Jin, B., Donner, E., Vasileiadis, S., Saint, C., & Dai, S. (2018). Microbial community and bioelectrochemical activities in MFC for degrading phenol and producing electricity: microbial consortia could make differences. *Chemical Engineering Journal*, 332, 647-657.
- Hassan, M., Ashraf, G. A., Zhang, B., He, Y., Shen, G., & Hu, S. (2020). Energy-efficient degradation of antibiotics in microbial electro-Fenton system catalysed by M-type strontium hexaferrite nanoparticles. *Chemical Engineering Journal*, 380, 122483.
- Hassan, S. H., Abd el Nasser, A. Z., & Kassim, R. M. (2019). Electricity generation from sugarcane molasses using microbial fuel cell technologies. *Energy*, 178, 538-543.
- Hassan, S. H., El-Rab, S. M. G., Rahimnejad, M., Ghasemi, M., Joo, J.-H., Sik-Ok, Y., . . . Oh, S.-E. (2014). Electricity generation from rice straw using a microbial fuel cell. *International Journal of Hydrogen Energy*, 39(17), 9490-9496.
- He, L., Du, P., Chen, Y., Lu, H., Cheng, X., Chang, B., & Wang, Z. (2017). Advances in microbial fuel cells for wastewater treatment. *Renewable Sustainable Energy Reviews*, 71, 388-403.
- He, Z., Wagner, N., Minteer, S. D., & Angenent, L. T. (2006). An upflow microbial fuel cell with an interior cathode: assessment of the internal resistance by impedance spectroscopy. *Environmental science technology*, 40(17), 5212-5217.
- Hernandez, C. A., & Osma, J. F. (2020). Microbial electrochemical systems: deriving future trends from historical perspectives and characterization strategies. *Frontiers in Environmental Science*.
- Hitam, C. N. C., & Jalil, A. A. (2020). A review on exploration of Fe₂O₃ photocatalyst towards degradation of dyes and organic contaminants. *Journal of environmental management*, 258, 110050. doi:<https://doi.org/10.1016/j.jenvman.2019.110050>
- Höflinger, J., Hofmann, P., & Geringer, B. (2019). Dynamic multi-parameter sensitive modeling of a PEM fuel cell system for BEV range extender applications. In *Der Antrieb von morgen 2019* (pp. 171-190): Springer.

- Hou, R., Luo, C., Zhou, S., Wang, Y., Yuan, Y., & Zhou, S. (2020). Anode potential-dependent protection of electroactive biofilms against metal ion shock via regulating extracellular polymeric substances. *Water research*, 115845.
- Hu, L., Zhang, M., Komini Babu, S., Kongkanand, A., & Litster, S. (2019). Ionic Conductivity over Metal/Water Interfaces in Ionomer-Free Fuel Cell Electrodes. *ChemElectroChem*, 6(10), 2659-2666.
- Huppmann, D., Gidden, M., Fricko, O., Kolp, P., Orthofer, C., Pimmer, M., . . . Riahi, K. (2019). The MESSAGEix Integrated Assessment Model and the ix modeling platform (ixmp): An open framework for integrated and cross-cutting analysis of energy, climate, the environment, and sustainable development. *Environmental modelling*, 112, 143-156.
- Hussain, S., Khan, S. U., & Gul, S. (2020). Electrochemical Treatment of Antibiotics in Wastewater. In *Antibiotics and Antimicrobial Resistance Genes* (pp. 355-394): Springer.
- Inohana, Y., Katsuya, S., Koga, R., Kouzuma, A., & Watanabe, K. (2020). Shewanella algae Relatives Capable of Generating Electricity from Acetate Contribute to Coastal-Sediment Microbial Fuel Cells Treating Complex Organic Matter. *Microbes environments*, 35(2), ME19161.
- Islam, M. A., Ehiraj, B., Cheng, C. K., Dubey, B. N., & Khan, M. M. R. (2019). Biofilm re-vitalization using hydrodynamic shear stress for stable power generation in microbial fuel cell. *Journal of Electroanalytical Chemistry*, 844, 14-22.
- Islam, M. A., Ehiraj, B., Cheng, C. K., Yousuf, A., & Khan, M. M. R. (2017). Electrogenic and antimethanogenic properties of Bacillus cereus for enhanced power generation in anaerobic sludge-driven microbial fuel cells. *Energy Fuels*, 31(6), 6132-6139.
- Islam, M. A., Ehiraj, B., Cheng, C. K., Yousuf, A., & Khan, M. M. R. (2018). An insight of synergy between Pseudomonas aeruginosa and Klebsiella variicola in a microbial fuel cell. *ACS Sustainable Chemistry Engineering*, 6(3), 4130-4137.
- Islam, M. A., Karim, A., Mishra, P., Dubowski, J. J., Yousuf, A., Sarmin, S., & Khan, M. M. R. (2020). Microbial synergistic interactions enhanced power generation in co-culture driven microbial fuel cell. *Science of the total environment*, 140138.
- Islam, M. A., Karim, A., Mishra, P., Mohammad, C. K., Faizal, M., Khan, M. R., & Yousuf, A. (2019). Role of Biocatalyst in Microbial Fuel Cell Performance. *Waste to Sustainable Energy: MFCs—Prospects through Prognosis*.
- Islam, M. A., Karim, A., Woon, C. W., Ehiraj, B., Cheng, C. K., Yousuf, A., & Khan, M. M. R. (2017). Augmentation of air cathode microbial fuel cell performance using wild type Klebsiella variicola. *RSC Advances*, 7(8), 4798-4805.
- Islam, M. A., Woon, C. W., Ehiraj, B., Cheng, C. K., Yousuf, A., & Khan, M. M. R. (2016). Ultrasound driven biofilm removal for stable power generation in microbial fuel cell. *Energy Fuels*, 31(1), 968-976.

- Ivase, T. J. P., Nyakuma, B. B., Oladokun, O., Abu, P. T., & Hassan, M. N. (2020). Review of the principal mechanisms, prospects, and challenges of bioelectrochemical systems. *Environmental Progress Sustainable Energy*, 39(1), 13298.
- Jadhav, D. A., Chendake, A. D., Schievano, A., & Pant, D. (2018). Suppressing methanogens and enriching electrogens in bioelectrochemical systems. *Bioresource technology*.
- Jamaly, S., Giwa, A., & Hasan, S. W. (2015). Recent improvements in oily wastewater treatment: Progress, challenges, and future opportunities. *Journal of Environmental Sciences*, 37, 15-30.
- Jawad, S. S., & Abbar, A. H. (2019). Treatment of petroleum refinery wastewater by electrochemical oxidation using graphite anodes. *Al-Qadisiyah Journal for Engineering Sciences*, 12(3), 144-150.
- Jiang, Y., & Zeng, R. J. (2019). Bidirectional extracellular electron transfers of electrode-biofilm: Mechanism and application. *Bioresource technology*, 271, 439-448.
- Jung, S., Lee, J., Park, Y.-K., & Kwon, E. E. (2020). Bioelectrochemical systems for a circular bioeconomy. *Bioresource technology*, 300, 122748.
- Juska, V. B. (2020). *Design, development and characterization of nanostructured electrochemical sensors*. University College Cork,
- Karatayev, M., Movkebayeva, G., & Bimagambetova, Z. (2019). Increasing Utilisation of Renewable Energy Sources: Comparative Analysis of Scenarios Until 2050. In *Energy Security* (pp. 37-68): Springer.
- Karekar, S. C., Srinivas, K., & Ahring, B. K. (2019). Kinetic Study on Heterotrophic Growth of *Acetobacterium woodii* on Lignocellulosic Substrates for Acetic Acid Production. *Fermentation*, 5(1), 17.
- Karygianni, L., Ren, Z., Koo, H., & Thurnheer, T. (2020). Biofilm Matrixome: Extracellular Components in Structured Microbial Communities. *TRENDS in Microbiology*.
- Kaur, R., Marwaha, A., Chhabra, V. A., Kim, K.-H., & Tripathi, S. (2020). Recent developments on functional nanomaterial-based electrodes for microbial fuel cells. *Renewable Sustainable Energy Reviews*, 119, 109551.
- Khan, M. M., Deen, K. M., Shabib, I., Asselin, E., & Haider, W. (2020). Controlling the dissolution of Iron through the development of nanostructured Fe-Mg for biomedical applications. *Acta Biomaterialia*.
- Khan, N., Anwer, A. H., Ahmad, A., Sabir, S., & Khan, M. Z. (2020). Investigating microbial fuel cell aided bio-remediation of mixed phenolic contaminants under oxic and anoxic environments. *Biochemical Engineering Journal*, 155, 107485.
- Khaneghah, A. M., Abhari, K., Eş, I., Soares, M. B., Oliveira, R. B., Hosseini, H., . . . Cruz, A. G. (2020). Interactions between probiotics and pathogenic

microorganisms in hosts and foods: A review. *Trends in Food Science Technology*, 95, 205-218.

Khater, D. Z., El-Khatib, K., & Hassan, R. Y. (2018). Exploring the bioelectrochemical characteristics of activated sludge using cyclic voltammetry. *Applied biochemistry biotechnology*, 184(1), 92-101.

Khurul, M. A., Wang, Z., & Lim, B. (2020). Submission of "Electric power generation from sediment microbial fuel cells with graphite rod array anode". *Environmental Engineering Research*, 25(2), 238-242.

Kirchner, A., Dachet, F., & Loeb, J. A. (2019). Identifying targets for preventing epilepsy using systems biology of the human brain. *Neuropharmacology*, 107757.

Kitzinger, K., Padilla, C. C., Marchant, H. K., Hach, P. F., Herbold, C. W., Kidane, A. T., . . . Niggemann, J. (2019). Cyanate and urea are substrates for nitrification by Thaumarchaeota in the marine environment. *Nature microbiology*, 4(2), 234-243.

Koo, B., & Jung, S. P. (2019). Recent Trends of Oxygen Reduction Catalysts in Microbial Fuel Cells: A Review. *J. Korean Soc. Environ. Eng*, 41(11), 657-675.

Koók, L., Desmond-Le Quéméner, E., Bakonyi, P., Zitka, J., Trably, E., Tóth, G., . . . Bélafi-Bakó, K. (2019). Behavior of two-chamber microbial electrochemical systems started-up with different ion-exchange membrane separators. *Bioresource technology*, 278, 279-286.

Koók, L., Rózsenszki, T., Nemestóthy, N., Bélafi-Bakó, K., & Bakonyi, P. (2016). Bioelectrochemical treatment of municipal waste liquor in microbial fuel cells for energy valorization. *Journal of Cleaner Production*, 112, 4406-4412.

Korshunov, S., Imlay, K. R. C., & Imlay, J. A. (2020). Cystine import is a valuable but risky process whose hazards *Escherichia coli* minimizes by inducing a cysteine exporter. *Molecular Microbiology*, 113(1), 22-39.

Krishna, K. V., Swathi, K., Hemalatha, M., & Mohan, S. V. (2019). Bioelectrocatalyst in Microbial Electrochemical Systems and Extracellular Electron Transport. In *Microbial Electrochemical Technology* (pp. 117-141): Elsevier.

Krishnaraj, R. N., & Sani, R. K. (2019). Bioelectrochemical Interface Engineering. In: Wiley Online Library.

Kubota, K., Watanabe, T., Maki, H., Kanaya, G., Higashi, H., & Syutsubo, K. (2019). Operation of sediment microbial fuel cells in Tokyo Bay, an extremely eutrophicated coastal sea. *Bioresource Technology Reports*, 6, 39-45.

Kul, S., & Nuhoğlu, A. (2020). Removal Kinetics of Olive-Mill Wastewater in a Batch-Operated Aerobic Bioreactor. *Journal of Environmental Engineering*, 146(3), 04019122.

Kumar, A., & Samadder, S. (2020). Performance evaluation of anaerobic digestion technology for energy recovery from organic fraction of municipal solid waste: A review. *Energy*, 117253.

- Kumar, V. (2015). *Process Assessment of Bio-Energy Options (Hydrogen and Methane) Using Microbes with Industrial Waste Water*. Department of Environmental Science, School for Environmental Sciences ... ,
- Kundu, P. P., & Dutta, K. (2018). *Progress and recent trends in microbial fuel cells*: Elsevier.
- La, J. A., Jeon, J.-M., Sang, B.-I., Yang, Y.-H., & Cho, E. C. (2017). A hierarchically modified graphite cathode with Au nanoislands, cysteamine, and Au nanocolloids for increased electricity-assisted production of isobutanol by engineered *Shewanella oneidensis* MR-1. *ACS applied materials interfaces*, 9(50), 43563-43574.
- Lam, S.-M., Sin, J.-C., Hua, L., Haixiang, L., Wei, L. J., & Zeng, H. (2020). A Z-scheme WO₃ loaded-hexagonal rod-like ZnO/Zn photocatalytic fuel cell for chemical energy recuperation from food wastewater treatment. *Applied Surface Science*, 145945.
- Lazaro, C. Z., Sagir, E., & Hallenbeck, P. C. (2020). Biotechnological Production of Fuel Hydrogen and Its Market Deployment. *Green Energy to Sustainability: Strategies for Global Industries*, 355-394.
- Le, N. L., & Nunes, S. P. (2016). Materials and membrane technologies for water and energy sustainability. *Sustainable Materials Technologies*, 7, 1-28.
- Lee, J., Ng, C. A., Lo, P. K., & Bashir, M. J. (2019). Enhancement of renewable electrical energy recovery from palm oil mill effluent by microbial fuel cell with activated carbon. *Energy Sources, Part A: Recovery, Utilization, Environmental Effects*, 1-13.
- Leyva-Díaz, J., Monteoliva, A., Martín-Pascual, J., Munio, M., García-Mesa, J., & Poyatos, J. (2019). Moving bed biofilm reactor as an alternative wastewater treatment process for nutrient removal and recovery in the circular economy model. *Bioresour. Technol.*, 122631.
- Li, F., Li, Y., Sun, L., Li, X., Yin, C., An, X., . . . Song, H. (2017). Engineering *Shewanella oneidensis* enables xylose-fed microbial fuel cell. *Biotechnology for biofuels*, 10(1), 196.
- Li, J., Ziara, R. M., Li, S., Subbiah, J., & Dvorak, B. I. (2020). Understanding the sustainability niche of continuous flow tubular microbial fuel cells on beef packing wastewater treatment. *Journal of Cleaner Production*, 257, 120555.
- Li, M., Zhou, M., Luo, J., Tan, C., Tian, X., Su, P., & Gu, T. (2019). Carbon dioxide sequestration accompanied by bioenergy generation using a bubbling-type photosynthetic algae microbial fuel cell. *Bioresour. Technol.*, 280, 95-103.
- Li, S.-W., Zeng, R. J., & Sheng, G.-P. (2017). An excellent anaerobic respiration mode for chitin degradation by *Shewanella oneidensis* MR-1 in microbial fuel cells. *Biochemical Engineering Journal*, 118, 20-24.

- Li, S., & Chen, G. (2018). Factors affecting the effectiveness of bioelectrochemical system applications: Data synthesis and meta-analysis. *Batteries*, 4(3), 34.
- Li, X. M., Cheng, K. Y., Selvam, A., & Wong, J. W. (2013). Bioelectricity production from acidic food waste leachate using microbial fuel cells: effect of microbial inocula. *Process Biochemistry*, 48(2), 283-288.
- Li, Y., Sim, L. N., Ho, J. S., Chong, T. H., Wu, B., & Liu, Y. (2020). Integration of an anaerobic fluidized-bed membrane bioreactor (MBR) with zeolite adsorption and reverse osmosis (RO) for municipal wastewater reclamation: Comparison with an anoxic-aerobic MBR coupled with RO. *Chemosphere*, 245, 125569.
- Liang, D.-W., Zhang, T., Fang, H. H., & He, J. (2008). Phthalates biodegradation in the environment. *Applied microbiology biotechnology*, 80(2), 183.
- Liao, C., Li, Y., & Tjong, S. C. (2020). Visible-light active titanium dioxide nanomaterials with bactericidal properties. *Nanomaterials*, 10(1), 124.
- Licandro, H., Ho, P. H., Nguyen, T. K. C., Petchkongkaew, A., Van Nguyen, H., Chu-Ky, S., . . . Waché, Y. (2020). How fermentation by lactic acid bacteria can address safety issues in legumes food products? *Food control*, 110, 106957.
- Lin, S., Hao, T., Li, X., Xiao, Y., & Chen, G. (2020). Pin-point denitrification for groundwater purification without direct chemical dosing: Demonstration of a two-chamber sulfide-driven denitrifying microbial electrochemical system. *Water research*, 115918.
- Lin, X.-Q., Li, Z.-L., Liang, B., Nan, J., & Wang, A.-J. (2019). Identification of biofilm formation and exoelectrogenic population structure and function with graphene/polyaniline modified anode in microbial fuel cell. *Chemosphere*, 219, 358-364.
- Liu, D., Chang, Q., Gao, Y., Huang, W., Sun, Z., Yan, M., & Guo, C. (2020). High performance of microbial fuel cell afforded by metallic tungsten carbide decorated carbon cloth anode. *Electrochimica Acta*, 330, 135243.
- Liu, E., Lee, L. Y., Ong, S. L., & Ng, H. Y. (2020). Treatment of industrial brine using Capacitive Deionization (CDI) towards zero liquid discharge – Challenges and optimization. *Water research*, 116059. doi:<https://doi.org/10.1016/j.watres.2020.116059>
- Liu, H., & Logan, B. E. (2004). Electricity generation using an air-cathode single chamber microbial fuel cell in the presence and absence of a proton exchange membrane. *Environmental science technology*, 38(14), 4040-4046.
- Liu, J., Liu, T., Chen, S., Yu, H., Zhang, Y., & Quan, X. (2020). Enhancing anaerobic digestion in anaerobic integrated floating fixed-film activated sludge (An-IFFAS) system using novel electron mediator suspended biofilm carriers. *Water research*, 115697.

- Liu, J., Vipulanandan, C., & Yang, M. (2019). Biosurfactant production from used vegetable oil in the anode chamber of a microbial electrosynthesizing fuel cell. *Waste Biomass Valorization*, *10*(10), 2925-2931.
- Liu, T. (2020). *Practical applications of microbial fuel cell technology in winery wastewater treatment*. University of British Columbia,
- Liu, X., Ye, Y., Xiao, K., Rensing, C., & Zhou, S. (2020). Molecular evidence for the adaptive evolution of *Geobacter sulfurreducens* to perform dissimilatory iron reduction in natural environments. *Molecular Microbiology*, *113*(4), 783-793.
- Logan, B. E., Rossi, R., & Saikaly, P. E. (2019). Electroactive microorganisms in bioelectrochemical systems. *Nature Reviews Microbiology*, *17*(5), 307-319.
- Logan, B. E., Zikmund, E., Yang, W., Rossi, R., Kim, K.-Y., Saikaly, P. E., & Zhang, F. (2018). Impact of ohmic resistance on measured electrode potentials and maximum power production in microbial fuel cells. *Environmental science technology*, *52*(15), 8977-8985.
- Louro, R. O., Costa, N. L., Fernandes, A. P., Silva, A. V., Trindade, I. B., Fonseca, B. M., & Paquete, C. M. (2019). Exploring the Molecular Mechanisms of Extracellular Electron Transfer for Harnessing Reducing Power in METs: Methodologies and Approaches. In *Microbial Electrochemical Technology* (pp. 261-293): Elsevier.
- Lovley, D. R., & Walker, D. (2019). *Geobacter* protein nanowires. *Frontiers in microbiology*, *10*, 2078.
- Luo, Q., An, A., & Wang, M. (2019). *Model Reference Adaptive Control for Microbial Fuel Cell (MFC)*. Paper presented at the Proceedings of the 2019 4th International Conference on Robotics, Control and Automation.
- Luo, S., Fu, B., Liu, F., He, K., Yang, H., Ma, J., . . . Huang, X. (2020). Construction of innovative 3D-weaved carbon mesh anode network to boost electron transfer and microbial activity in bioelectrochemical system. *Water research*, *172*, 115493.
- Luo, S., Sun, H., Ping, Q., Jin, R., & He, Z. (2016). A review of modeling bioelectrochemical systems: engineering and statistical aspects. *Energies*, *9*(2), 111.
- Ma, H., Peng, C., Jia, Y., Wang, Q., Tu, M., & Gao, M. (2018). Effect of fermentation stillage of food waste on bioelectricity production and microbial community structure in microbial fuel cells. *Royal Society open science*, *5*(9), 180457.
- Macarie, H., & technology. (2000). Overview of the application of anaerobic treatment to chemical and petrochemical wastewaters. *Water science*, *42*(5-6), 201-214.
- Magwaza, S. T., Magwaza, L. S., Odindo, A. O., & Mditshwa, A. (2020). Hydroponic technology as decentralised system for domestic wastewater treatment and vegetable production in urban agriculture: A review. *Science of the total environment*, *698*, 134154.

- Mahadevan, A., Gunawardena, D. A., & Fernando, S. (2014). Biochemical and electrochemical perspectives of the anode of a microbial fuel cell. In *Technology and Application of Microbial Fuel Cells*: IntechOpen.
- Mahamuni-Badiger, P. P., Patil, P. M., Badiger, M. V., Patel, P. R., Thorat-Gadgil, B. S., Pandit, A., & Bohara, R. A. (2020). Biofilm formation to inhibition: Role of zinc oxide-based nanoparticles. *Materials Science Engineering: C*, *108*, 110319.
- Mahmoudi, A., Mousavi, S. A., & Darvishi, P. (2020). Effect of ammonium and COD concentrations on the performance of fixed-bed air-cathode microbial fuel cells treating reject water. *International Journal of Hydrogen Energy*, *45*(7), 4887-4896.
- Mai, Q., Yang, G., Cao, J., Zhang, X., & Zhuang, L. (2020). Stratified microbial structure and activity within anode biofilm during electrochemically assisted brewery wastewater treatment. *Biotechnology bioengineering*.
- Mancilio, L. B. K., Ribeiro, G. A., Lopes, E. M., Kishi, L. T., Martins-Santana, L., de Siqueira, G. M. V., . . . Reginatto, V. (2020). Unusual microbial community and impact of iron and sulfate on microbial fuel cell ecology and performance. *Current Research in Biotechnology*.
- Mandal, B., & Mitra, P. (2020). Interpretation of electrical conduction mechanism by Godet's VRH model in TiO₂ incorporated MnCo₂O₄ host matrix. *Journal of Alloys Compounds*, *812*, 152129.
- Mani, P. (2019). Development of a biocathode system in microbial fuel cells for treatment of azo dyes.
- Marassi, R. J., Queiroz, L. G., Silva, D. C., dos Santos, F. S., Silva, G. C., & de Paiva, T. C. (2020). Long-term performance and acute toxicity assessment of scaled-up air-cathode microbial fuel cell fed by dairy wastewater. *Bioprocess biosystems engineering*, 1-11.
- Marsili, E., Baron, D. B., Shikhare, I. D., Coursolle, D., Gralnick, J. A., & Bond, D. R. (2008). *Shewanella* secretes flavins that mediate extracellular electron transfer. *Proceedings of the National Academy of Sciences*, *105*(10), 3968-3973.
- Mathuriya, A. S., Hiloidhari, M., Gware, P., Singh, A., & Pant, D. (2020). Development and life cycle assessment of an auto circulating bio-electrochemical reactor for energy positive continuous wastewater treatment. *Bioresource technology*, *304*, 122959.
- McQuillan, R. V., Stevens, G. W., & Mumford, K. A. (2020). Electrochemical removal of naphthalene from contaminated waters using carbon electrodes, and viability for environmental deployment. *Journal of hazardous materials*, *383*, 121244.
- Melander, R. J., & Melander, C. (2019). Strategies for the Eradication of Biofilm-Based Bacterial Infections. In *Antibacterial Drug Discovery to Combat MDR* (pp. 499-526): Springer.

- Michelson, K., Alcalde, R. E., Sanford, R. A., Valocchi, A. J., & Werth, C. (2019). Diffusion-Based Recycling of Flavins Allows *Shewanella oneidensis* MR-1 To Yield Energy from Metal Reduction Across Physical Separations. *Environmental science technology*, 53(7), 3480-3487.
- Michelson, K., Alcalde, R. E., Sanford, R. A., Valocchi, A. J., Werth, C. J. J. E. s., & technology. (2019). Diffusion-Based Recycling of Flavins Allows *Shewanella oneidensis* MR-1 To Yield Energy from Metal Reduction Across Physical Separations. 53(7), 3480-3487.
- Modestra, J. A., & Mohan, S. V. (2019). Capacitive biocathodes driving electrotrophy towards enhanced CO₂ reduction for microbial electrosynthesis of fatty acids. *Bioresource technology*, 294, 122181.
- Modestra, J. A., Reddy, C. N., Krishna, K. V., Min, B., & Mohan, S. V. (2019). Regulated surface potential impacts bioelectrogenic activity, interfacial electron transfer and microbial dynamics in microbial fuel cell. *Renewable Energy*.
- Modestra, J. A., Reddy, C. N., Krishna, K. V., Min, B., & Mohan, S. V. (2020). Regulated surface potential impacts bioelectrogenic activity, interfacial electron transfer and microbial dynamics in microbial fuel cell. *Renewable Energy*, 149, 424-434.
- Mohanakrishna, G., Abu-Reesh, I. M., & Al-Raoush, R. I. J. J. o. c. p. (2018). Biological anodic oxidation and cathodic reduction reactions for improved bioelectrochemical treatment of petroleum refinery wastewater. 190, 44-52.
- Momayez, F., Karimi, K., & Taherzadeh, M. J. (2019). Energy recovery from industrial crop wastes by dry anaerobic digestion: A review. *Industrial crops products*, 129, 673-687.
- Moradi, M., Vasseghian, Y., Khataee, A., Kobya, M., Arabzade, H., & Dragoi, E.-N. (2020). Service life and stability of electrodes applied in electrochemical advanced oxidation processes: A comprehensive review. *Journal of Industrial Engineering Chemistry*.
- Moscoviz, R., Quémener, E. D.-L., Trably, E., Bernet, N., & Hamelin, J. (2020). Novel Outlook in Microbial Ecology: Nonmutualistic Interspecies Electron Transfer. *TRENDS in Microbiology*, 28(4), 245-253. doi:<https://doi.org/10.1016/j.tim.2020.01.008>
- Mudhoo, A., Ramasamy, D. L., Bhatnagar, A., Usman, M., & Sillanpää, M. (2020). An analysis of the versatility and effectiveness of composts for sequestering heavy metal ions, dyes and xenobiotics from soils and aqueous milieus. *Ecotoxicology Environmental Safety*, 197, 110587.
- Munjal, M., Tiwari, B., Lalwani, S., Sharma, M., Singh, G., & Sharma, R. K. (2020). An insight of bioelectricity production in mediator less microbial fuel cell using mesoporous Cobalt Ferrite anode. *International Journal of Hydrogen Energy*.
- Nassani, A. A., Aldakhil, A. M., Abro, M. M. Q., Zaman, K., & Kabbani, A. (2019). Resource management for green growth: Ensure environment sustainability

agenda for mutual exclusive global gain. *Environmental Progress Sustainable Energy*, 38(4).

Nguyen, L. N., Nguyen, A. Q., & Nghiem, L. D. (2019). Microbial community in anaerobic digestion system: Progression in microbial ecology. In *Water and Wastewater Treatment Technologies* (pp. 331-355): Springer.

Nguyen, T. H. T., Lee, J., Kim, H.-Y., Nam, K. M., & Kim, B.-K. (2020). Current research on single-entity electrochemistry for soft nanoparticle detection: Introduction to detection methods and applications. *Biosensors*, 151, 111999.

Nikhil, G., Chaitanya, D. K., Srikanth, S., Swamy, Y., & Mohan, S. V. (2018). Applied resistance for power generation and energy distribution in microbial fuel cells with rationale for maximum power point. *Chemical Engineering Journal*, 335, 267-274.

Noori, M. T., Bhowmick, G., Tiwari, B., Das, I., Ghangrekar, M., & Mukherjee, C. (2020). Utilisation of waste medicine wrappers as an efficient low-cost electrode material for microbial fuel cell. *Environmental technology*, 41(10), 1209-1218.

Noori, M. T., Vu, M. T., Ali, R. B., & Min, B. (2020). Recent advances in cathode materials and configurations for upgrading methane in bioelectrochemical systems integrated with anaerobic digestion. *Chemical Engineering Journal*, 392, 123689.

Nouri, P., & Najafpour Darzi, G. (2017). Impacts of process parameters optimization on the performance of the annular single chamber microbial fuel cell in wastewater treatment. *Engineering in Life Sciences*, 17(5), 545-551.

Nozhevnikova, A., Russkova, Y. I., Litt, Y. V., Parshina, S., Zhuravleva, E., & Nikitina, A. (2020). Syntrophy and Interspecies Electron Transfer in Methanogenic Microbial Communities. *Microbiology*, 89, 129-147.

Obata, O., Salar-Garcia, M. J., Greenman, J., Kurt, H., Chandran, K., & Ieropoulos, I. (2020). Development of efficient electroactive biofilm in urine-fed microbial fuel cell cascades for bioelectricity generation. *Journal of environmental management*, 258, 109992.

Ohki, A., & Rich, W. (2020). System for wastewater treatment through controlling microorganism purification functions. In: Google Patents.

Olajire, A. A. (2020). The brewing industry and environmental challenges. *Journal of Cleaner Production*, 256, 102817.

Oliveira Paiva, T. M., Torbensen, K., Patel, A., Anne, A., Chovin, A., Demaille, C., . . . Michon, T. (2020). Probing the Enzymatic Activity of Individual Biocatalytic fd-Viral Particles by Electrochemical-Atomic Force Microscopy. *ACS Catalysis*.

Oliveira, V., Simões, M., Melo, L., & Pinto, A. (2013). Overview on the developments of microbial fuel cells. *Biochemical Engineering Journal*, 73, 53-64.

- Ortega-Peña, S., Martínez-García, S., Rodríguez-Martínez, S., Cancino-Díaz, M. E., & Cancino-Díaz, J. C. (2020). Overview of Staphylococcus epidermidis cell wall-anchored proteins: Potential targets to inhibit biofilm formation. *Molecular biology reports*, 1-14.
- Pandey, P., Shinde, V. N., Deopurkar, R. L., Kale, S. P., Patil, S. A., & Pant, D. (2016). Recent advances in the use of different substrates in microbial fuel cells toward wastewater treatment and simultaneous energy recovery. *Applied energy*, 168, 706-723.
- Pandit, S., Chandrasekhar, K., Jadhav, D. A., & Madhao, M. (2019). Contaminant Removal and Energy Recovery in Microbial Fuel Cells. *Microbial Biodegradation of Xenobiotic Compounds*, 76.
- Pankan, A. O., Yunus, K., & Fisher, A. C. (2020). Mechanistic evaluation of the exoelectrogenic activity of Rhodospseudomonas palustris under different nitrogen regimes. *Bioresource technology*, 300, 122637. doi:https://doi.org/10.1016/j.biortech.2019.122637
- Pasternak, G., Greenman, J., & Ieropoulos, I. (2018). Dynamic evolution of anodic biofilm when maturing under different external resistive loads in microbial fuel cells. Electrochemical perspective. *Journal of Power Sources*, 400, 392-401.
- Patel, R., Deb, D., Dey, R., & Balas, V. E. (2020a). Exact Linearization of Two Chamber Microbial Fuel Cell. In *Adaptive and Intelligent Control of Microbial Fuel Cells* (pp. 91-98): Springer.
- Patel, R., Deb, D., Dey, R., & Balas, V. E. (2020b). Mathematical Modelling. In *Adaptive and Intelligent Control of Microbial Fuel Cells* (pp. 11-28): Springer.
- Patel, S. K., Kumar, P., Mehariya, S., Purohit, H. J., Lee, J.-K., & Kalia, V. C. (2014). Enhancement in hydrogen production by co-cultures of Bacillus and Enterobacter. *International Journal of Hydrogen Energy*, 39(27), 14663-14668.
- Pedersen, M. K. (2019). *Fundamentals of Positrodes for Proton Ceramic Electrochemical Cells*.
- Peng, X., Cao, J., Xie, B., Duan, M., & Zhao, J. (2020). Evaluation of degradation behavior over tetracycline hydrochloride by microbial electrochemical technology: Performance, kinetics, and microbial communities. *Ecotoxicology Environmental Safety*, 188, 109869.
- Pinto, R., Srinivasan, B., Escapa, A., & Tartakovsky, B. (2011). Multi-population model of a microbial electrolysis cell. *Environmental science technology*, 45(11), 5039-5046.
- Pinto, R., Srinivasan, B., Manuel, M.-F., & Tartakovsky, B. (2010). A two-population bio-electrochemical model of a microbial fuel cell. *Bioresource technology*, 101(14), 5256-5265.

- Ploetz, E., Engelke, H., Lächelt, U., & Wuttke, S. (2020). The Chemistry of Reticular Framework Nanoparticles: MOF, ZIF, and COF Materials. *Advanced Functional Materials*, 1909062.
- Prakasham, R., & Kumar, B. S. (2019). Bacterial Metabolism–Coupled Energetics. In *Microbial Electrochemical Technology* (pp. 227-260): Elsevier.
- PrévotEAU, A., Carvajal-Arroyo, J. M., Ganigué, R., & Rabaey, K. (2020). Microbial electrosynthesis from CO₂: forever a promise? *Current opinion in biotechnology*, 62, 48-57. doi:https://doi.org/10.1016/j.copbio.2019.08.014
- Puentes-Téllez, P. E., & Salles, J. F. (2020). Dynamics of Abundant and Rare Bacteria During Degradation of Lignocellulose from Sugarcane Biomass. *Microbial ecology*, 79(2), 312-325. doi:10.1007/s00248-019-01403-w
- Pushkar, P., & Mungray, A. K. (2020). Exploring the use of 3 dimensional low-cost sugar-urea carbon foam electrode in the benthic microbial fuel cell. *Renewable Energy*, 147, 2032-2042.
- Qazi, A., Hussain, F., Rahim, N. A., Hardaker, G., Alghazzawi, D., Shaban, K., & Haruna, K. (2019). Towards Sustainable Energy: A Systematic Review of Renewable Energy Sources, Technologies, and Public Opinions. *IEEE Access*, 7, 63837-63851.
- Qin, R. (2019). Fractionation of oil sands process water and fractions influence and degradation by advanced oxidation processes.
- Qin, S., Yu, L., Yang, Z., Li, M., Clough, T., Wrage-Mönnig, N., . . . Zhou, S. (2019). Electrodes Donate Electrons for Nitrate Reduction in a Soil Matrix via DNRA and Denitrification. *Environmental science technology*, 53(4), 2002-2012.
- Radeef, A. Y., & Ismail, Z. Z. (2019). Polarization model of microbial fuel cell for treatment of actual potato chips processing wastewater associated with power generation. *Journal of Electroanalytical Chemistry*, 836, 176-181.
- Radwan, L. M., & Mahrous, M. Y. (2019). Genetic selection for growth performance and thermal tolerance under high ambient temperature after two generations using heat shock protein 90 expression as an index. *Animal Production Science*, 59(4), 628-633.
- Ragab, M., Elawwad, A., & Abdel-Halim, H. (2019). Evaluating the performance of Microbial Desalination Cells subjected to different operating temperatures. *Desalination*, 462, 56-66.
- Raghavulu, S. V., Babu, P. S., Goud, R. K., Subhash, G. V., Srikanth, S., & Mohan, S. V. (2012). Bioaugmentation of an electrochemically active strain to enhance the electron discharge of mixed culture: process evaluation through electro-kinetic analysis. *RSC Advances*, 2(2), 677-688.
- Ram, M., Aghahosseini, A., & Breyer, C. (2020). Job creation during the global energy transition towards 100% renewable power system by 2050. *Technological Forecasting Social Change*, 151, 119682.

- Ramadan, M. A., Abd-Alla, M. H., & Abdul-Raouf, U. M. (2020). Bioelectricity generation from agro-industrial waste water using dual-chambered microbial fuel cell.
- Rana, K. L., Kour, D., Yadav, A. N., Yadav, N., & Saxena, A. K. (2020). Agriculturally important microbial biofilms: Biodiversity, ecological significances, and biotechnological applications. In *New and Future Developments in Microbial Biotechnology and Bioengineering: Microbial Biofilms* (pp. 221-265): Elsevier.
- Rana, S., Singh, L., & bin ab Wahid, Z. (2019). Electrotroph as an Emerging Biocommodity Producer in a Biocatalyzed Bioelectrochemical System. *Waste to Sustainable Energy: MFCs–Prospects through Prognosis*.
- Rani, R., Sharma, D., & Kumar, S. (2019). Optimization of operating conditions of miniaturize single chambered microbial fuel cell using NiWO₄/graphene oxide modified anode for performance improvement and microbial communities dynamics. *Bioresource technology*, 285, 121337.
- Raychaudhuri, A., & Behera, M. (2020a). Comparative evaluation of methanogenesis suppression methods in microbial fuel cell during rice mill wastewater treatment. *Environmental technology*, 17, 100509.
- Raychaudhuri, A., & Behera, M. (2020b). Comparative evaluation of methanogenesis suppression methods in microbial fuel cell during rice mill wastewater treatment. *Environmental technology innovation*, 17, 100509.
- Ren, P., Pei, P., Li, Y., Wu, Z., Chen, D., & Huang, S. (2020). Degradation mechanisms of proton exchange membrane fuel cell under typical automotive operating conditions. *Progress in Energy Combustion Science*, 80, 100859.
- Rivett, M., & Sweeney, R. (2019). An introduction to natural source zone depletion at LNAPL sites.
- Rodrigues, D. R., Olivieri, A. C., Frago, W. D., & Lemos, S. G. (2019). Complex numbers-partial least-squares applied to the treatment of electrochemical impedance spectroscopy data. *Analytica chimica acta*, 1080, 1-11.
- Rodrigues, L. C., Puig-Ventosa, I., López, M., Martínez, F. X., Ruiz, A. G., & Bertrán, T. G. (2020). The impact of improper materials in biowaste on the quality of compost. *Journal of Cleaner Production*, 251, 119601.
- Ruiz, Y., Baeza, J. A., Montpart, N., Moral-Vico, J., Baeza, M., & Guisasola, A. (2020). Repeatability of low scan rate cyclic voltammetry in bioelectrochemical systems and effects on their performance. *Journal of Chemical Technology Biotechnology*, 95(5), 1533-1541.
- Saien, J., & Nejati, H. (2007). Enhanced photocatalytic degradation of pollutants in petroleum refinery wastewater under mild conditions. *Journal of hazardous materials*, 148(1-2), 491-495.

- Sala-Garrido, R., & Molinos-Senante, M. (2020). Benchmarking energy efficiency of water treatment plants: Effects of data variability. *Science of the total environment*, 701, 134960.
- Samer, M. (2015). Biological and chemical wastewater treatment processes. *Wastewater Treatment Engineering*, 1-50.
- Sankaran, J., Tan, N. J., But, K. P., Cohen, Y., Rice, S. A., & Wohland, T. (2019). Single microcolony diffusion analysis in *Pseudomonas aeruginosa* biofilms. *NPJ biofilms microbiomes*, 5(1), 1-10.
- Santoro, C., Lei, Y., Li, B., & Cristiani, P. (2012). Power generation from wastewater using single chamber microbial fuel cells (MFCs) with platinum-free cathodes and pre-colonized anodes. *Biochemical Engineering Journal*, 62, 8-16.
- Santos, M. L. V., Valadéz, F. J. R., Solís, V. M., Nava, C. G., Martell, A. J. C., & Hensel, O. (2017). Performance of a microbial fuel cell operated with vinasses using different COD concentrations. *Revista Internacional de Contaminación Ambiental*, 33(3), 521-528.
- Saputra, E., Amri, A., Marshall, A., & Gostomski, P. (2019). *Reaction kinetics for microbial-reduced mediator in an ethanol-fed microbial fuel cell*. Paper presented at the MATEC Web of Conferences.
- Saratale, G. D., Saratale, R. G., Banu, J. R., & Chang, J.-S. (2019). Biohydrogen Production From Renewable Biomass Resources. In *Biohydrogen* (pp. 247-277): Elsevier.
- Saratale, R. G., Saratale, G. D., Pugazhendhi, A., Zhen, G., Kumar, G., Kadier, A., & Sivagurunathan, P. (2017). Microbiome involved in microbial electrochemical systems (MESs): a review. *Chemosphere*, 177, 176-188.
- Sarkar, D., Poddar, K., Verma, N., Biswas, S., & Sarkar, A. (2020). Bacterial quorum sensing in environmental biotechnology: a new approach for the detection and remediation of emerging pollutants. In *Emerging Technologies in Environmental Bioremediation* (pp. 151-164): Elsevier.
- Sarkar, S. (2020). Release mechanisms and molecular interactions of *Pseudomonas aeruginosa* extracellular DNA. *Applied microbiology biotechnology*.
- Sarmin, S., Ethiraj, B., Islam, M. A., Ideris, A., Yee, C. S., & Khan, M. M. R. (2019). Bio-electrochemical power generation in petrochemical wastewater fed microbial fuel cell. *Science of the total environment*, 695, 133820.
- Sarmin, S., Ideris, A. B., Ethiraj, B., Amirul, M., Islam, C. S. Y., & Khan, M. M. R. (2020). Potentiality of petrochemical wastewater as substrate in microbial fuel cell. *MS*, 736(3), 032015.
- Sarode, S., Upadhyay, P., Khosa, M., Mak, T., Shakir, A., Song, S., & Ullah, A. (2019). Overview of wastewater treatment methods with special focus on biopolymer chitin-chitosan. *International journal of biological macromolecules*, 121, 1086-1100.

- Sawalha, H., Maghalseh, M., Qutaina, J., Junaidi, K., & Rene, E. R. (2020). Removal of hydrogen sulfide from biogas using activated carbon synthesized from different locally available biomass wastes-a case study from Palestine. *Bioengineered*, *11*(1), 607-618.
- Schneider, W. D. H., Fontana, R. C., Baudel, H. M., de Siqueira, F. G., Rencoret, J., Gutiérrez, A., . . . Martínez, Á. T. (2020). Lignin degradation and detoxification of eucalyptus wastes by on-site manufacturing fungal enzymes to enhance second-generation ethanol yield. *Applied energy*, *262*, 114493.
- Segundo, I. D. B., Silva, T. F., Moreira, F. C., Silva, G. V., Boaventura, R. A., & Vilar, V. J. (2019). Sulphur compounds removal from an industrial landfill leachate by catalytic oxidation and chemical precipitation: From a hazardous effluent to a value-added product. *Science of the total environment*, *655*, 1249-1260.
- Sekar, A. D., Jayabalan, T., Muthukumar, H., Chandrasekaran, N. I., Mohamed, S. N., & Matheswaran, M. (2019). Enhancing power generation and treatment of dairy waste water in microbial fuel cell using Cu-doped iron oxide nanoparticles decorated anode. *Energy*, *172*, 173-180.
- Semkiw, I. P., Brown, S. D., & Wall, J. D. (2014). New Model for Electron Flow for Sulfate.
- Sevda, S., Abu-Reesh, I. M., Yuan, H., & He, Z. (2017). Bioelectricity generation from treatment of petroleum refinery wastewater with simultaneous seawater desalination in microbial desalination cells. *Energy Conversion Management*, *141*, 101-107.
- Sevda, S., Garlapati, V. K., Naha, S., Sharma, M., Ray, S. G., Sreekrishnan, T. R., & Goswami, P. (2020). Biosensing capabilities of bioelectrochemical systems towards sustainable water streams: Technological implications and future prospects. *Journal of bioscience bioengineering*, *129*(6), 647-656.
- Shabani, M., Younesi, H., Pontié, M., Rahimpour, A., Rahimnejad, M., & Zinatizadeh, A. A. (2020). A critical review on recent proton exchange membranes applied in microbial fuel cells for renewable energy recovery. *Journal of Cleaner Production*, 121446.
- Shankar, Y. S., Ankur, K., Bhushan, P., & Mohan, D. (2019). Utilization of Water Treatment Plant (WTP) Sludge for Pretreatment of Dye Wastewater Using Coagulation/Flocculation. In *Advances in Waste Management* (pp. 107-121): Springer.
- Shaw, D. R., Ali, M., Katuri, K. P., Gralnick, J. A., Reimann, J., Mesman, R., . . . Saikaly, P. E. (2020). Extracellular electron transfer-dependent anaerobic oxidation of ammonium by anammox bacteria. *Nature communications*, *11*(1), 1-12.
- Sheldon, R. A., & Brady, D. (2019). Broadening the Scope of Biocatalysis in Sustainable Organic Synthesis. *ChemSusChem*.

- Shen, L., Ma, J., Song, P., Lu, Z., Yin, Y., Liu, Y., . . . Zhang, L. (2016). Anodic concentration loss and impedance characteristics in rotating disk electrode microbial fuel cells. *Bioprocess biosystems engineering*, 39(10), 1627-1634.
- Shen, W., Zhao, X., Wang, X., Yang, S., Jia, X., Yu, X., . . . Zhao, H. (2020). Improving the power generation performances of Gram-positive electricigens by regulating the peptidoglycan layer with lysozyme. *Environmental Research*, 109463.
- Sheng, Y., Tan, X., Zhou, X., & Xu, Y. (2020). Bioconversion of 5-Hydroxymethylfurfural (HMF) to 2, 5-Furandicarboxylic Acid (FDCA) by a Native Obligate Aerobic Bacterium, *Acinetobacter calcoaceticus* NL14. *Applied biochemistry biotechnology*.
- Sima, N. A. K., Ebadi, A., Reiahisamani, N., & Rasekh, B. (2019). Bio-based remediation of petroleum-contaminated saline soils: Challenges, the current state-of-the-art and future prospects. *Journal of environmental management*, 250, 109476.
- Singh, P., Chauhan, D. S., Chauhan, S. S., Singh, G., & Quraishi, M. A. (2020). Bioinspired synergistic formulation from dihydropyrimidinones and iodide ions for corrosion inhibition of carbon steel in sulphuric acid. *Journal of Molecular Liquids*, 298, 112051. doi:https://doi.org/10.1016/j.molliq.2019.112051
- Singh, S., & Chakraborty, S. (2020). Performance of organic substrate amended constructed wetland treating acid mine drainage (AMD) of North-Eastern India. *Journal of hazardous materials*, 122719.
- Siu, J. C., Fu, N., & Lin, S. (2020). Catalyzing Electrosynthesis: A Homogeneous Electrocatalytic Approach to Reaction Discovery. *Accounts of chemical research*, 53(3), 547-560.
- Sleutels, T. H., Darus, L., Hamelers, H. V., & Buisman, C. J. (2011). Effect of operational parameters on Coulombic efficiency in bioelectrochemical systems. *Bioresource technology*, 102(24), 11172-11176.
- Smith, R. T. (1981). *Environmental aspects of alternative wet technologies for producing energy/fuel from peat. Final report*. Retrieved from
- Sobczyk, M. (2019). *Analysis of the possibility of using protozoa inhabiting activated sludge to evaluate the efficiency of wastewater treatment*.
- Soh, Y. N. A., Kunacheva, C., Webster, R. D., & Stuckey, D. C. (2020). Identification of the production and biotransformational changes of soluble microbial products (SMP) in wastewater treatment processes: A short review. *Chemosphere*, 126391.
- Song, H.-T., Gao, Y., Yang, Y.-M., Xiao, W.-J., Liu, S.-H., Xia, W.-C., . . . Jiang, Z.-B. (2016). Synergistic effect of cellulase and xylanase during hydrolysis of natural lignocellulosic substrates. *Bioresource technology*, 219, 710-715.
- Song, J., Zhang, W., Gao, J., Hu, X., Zhang, C., He, Q., . . . Zhan, X. (2020). A pilot-scale study on the treatment of landfill leachate by a composite biological system under low dissolved oxygen conditions: Performance and microbial community.

- Sun, D., Chen, J., Huang, H., Liu, W., Ye, Y., & Cheng, S. (2016). The effect of biofilm thickness on electrochemical activity of *Geobacter sulfurreducens*. *International Journal of Hydrogen Energy*, *41*(37), 16523-16528.
- Sun, J.-Z., Peter Kingori, G., Si, R.-W., Zhai, D.-D., Liao, Z.-H., Sun, D.-Z., . . . Yong, Y.-C. (2015). Microbial fuel cell-based biosensors for environmental monitoring: a review. *Water science*, *71*(6), 801-809.
- Sun, M., Ren, G., Li, Y., Lu, A., & Ding, H. (2019). Extracellular Electron Transfer Between Birnessite and Electrochemically Active Bacteria Community from Red Soil in Hainan, China. *Geomicrobiology journal*, *36*(2), 169-178.
- Sun, M., Zhai, L.-F., Mu, Y., & Yu, H.-Q. (2020). Bioelectrochemical element conversion reactions towards generation of energy and value-added chemicals. *Progress in Energy Combustion Science*, *77*, 100814.
- Sundarraman, D., Hay, E. A., Martins, D. M., Shields, D. S., Pettinari, N. L., & Parthasarathy, R. (2020). Quantifying multi-species microbial interactions in the larval zebrafish gut. *BioRxiv*.
- Tahernia, M., Mohammadifar, M., Gao, Y., Panmanee, W., Hassett, D. J., & Choi, S. (2020). A 96-well high-throughput, rapid-screening platform of extracellular electron transfer in microbial fuel cells. *Biosensors Bioelectronics*, 112259.
- Tahir, K., Miran, W., Jang, J., Shahzad, A., Moztahida, M., Kim, B., & Lee, D. S. (2020). A novel MXene-coated biocathode for enhanced microbial electrosynthesis performance. *Chemical Engineering Journal*, *381*, 122687.
- Tahir, K., Miran, W., Nawaz, M., Jang, J., Shahzad, A., Moztahida, M., . . . Jeon, C. O. (2019). Investigating the role of anodic potential in the biodegradation of carbamazepine in bioelectrochemical systems. *Science of the total environment*, *688*, 56-64.
- Tan, Y., Zheng, C., Cai, T., Niu, C., Wang, S., Pan, Y., . . . Zhao, Y. (2020). Anaerobic bioconversion of petrochemical wastewater to biomethane in a semi-continuous bioreactor: Biodegradability, mineralization behaviors and methane productivity. *Bioresource technology*, *304*, 123005.
- Tang, J., Zhang, C., Shi, X., Sun, J., & Cunningham, J. A. (2019). Municipal wastewater treatment plants coupled with electrochemical, biological and bio-electrochemical technologies: Opportunities and challenge toward energy self-sufficiency. *Journal of environmental management*, *234*, 396-403.
- Tang, R. C. O., Jang, J.-H., Lan, T.-H., Wu, J.-C., Yan, W.-M., Sangeetha, T., . . . Ong, Z. C. (2020). Review on design factors of microbial fuel cells using Buckingham's Pi Theorem. *Renewable Sustainable Energy Reviews*, *130*, 109878.
- Temple, S. M., & O'Donnell, T. J. (2020). Influencing Culture Condition for Promotion of Enhanced Growth and Increased Sustainability for Laboratory Maintenance of Fastidious Organisms: *Pseudomonas aeruginosa*, *Lactococcus lactis*, and *Serratia marcescens*.

- Ter Heijne, A., Liu, D., Sulonen, M., Sleutels, T., & Fabregat-Santiago, F. (2018). Quantification of bio-anode capacitance in bioelectrochemical systems using Electrochemical Impedance Spectroscopy. *Journal of Power Sources*, 400, 533-538.
- Toghyani, S., Afshari, E., & Baniasadi, E. (2019). Performance evaluation of an integrated proton exchange membrane fuel cell system with ejector absorption refrigeration cycle. *Energy Conversion Management*, 185, 666-677.
- Trifonov, A. (2020). *Novel Approaches for Direct Electron Transfer of Redox Enzymes and their Implementation in Biosensors and Biofuel Cells*. ETH Zurich,
- Tyagi, V. K., Liu, J., Poh, L. S., & Ng, W. J. (2019). Anaerobic-aerobic system for beverage effluent treatment: Performance evaluation and microbial community dynamics. *Bioresource Technology Reports*, 7, 100309. doi:https://doi.org/10.1016/j.biteb.2019.100309
- Uniyal, S., Paliwal, R., Kaphaliya, B., & Sharma, R. (2020). Human Overpopulation: Impact on Environment. In *Megacities and Rapid Urbanization: Breakthroughs in Research and Practice* (pp. 20-30): IGI Global.
- Utesch, T., Sabra, W., Prescher, C., Baur, J., Arbter, P., & Zeng, A. P. (2019). Enhanced electron transfer of different mediators for strictly opposite shifting of metabolism in *Clostridium pasteurianum* grown on glycerol in a new electrochemical bioreactor. *Biotechnology bioengineering*, 116(7), 1627-1643.
- Varjani, S., Joshi, R., Srivastava, V. K., Ngo, H. H., & Guo, W. (2019). Treatment of wastewater from petroleum industry: current practices and perspectives. *Environmental Science Pollution Research*, 1-9.
- Velvizhi, G. (2019). Overview of Bioelectrochemical Treatment Systems for Wastewater Remediation. In *Microbial Electrochemical Technology* (pp. 587-612): Elsevier.
- Velvizhi, G., & Mohan, S. V. (2012). Electrogenic activity and electron losses under increasing organic load of recalcitrant pharmaceutical wastewater. *International Journal of Hydrogen Energy*, 37(7), 5969-5978.
- Velvizhi, G., Shanthakumar, S., Das, B., Pugazhendhi, A., Priya, T. S., Ashok, B., . . . Karthick, C. (2020). Biodegradable and non-biodegradable fraction of municipal solid waste for multifaceted applications through a closed loop integrated refinery platform: Paving a path towards circular economy. *Science of the total environment*, 138049.
- Vrancken, G., Gregory, A. C., Huys, G. R., Faust, K., & Raes, J. (2019). Synthetic ecology of the human gut microbiota. *Nature Reviews Microbiology*, 17(12), 754-763.
- Wang, B., Liu, W., Zhang, Y., & Wang, A. (2020). Bioenergy recovery from wastewater accelerated by solar power: Intermittent electro-driving regulation and capacitive storage in biomass. *Water research*, 115696.

- Wang, D., Zeng, H., Xiong, X., Wu, M.-F., Xia, M., Xie, M., . . . Luo, S.-L. (2020). Highly efficient charge transfer in CdS-covalent organic framework nanocomposites for stable photocatalytic hydrogen evolution under visible light. *Science Bulletin*, 65(2), 113-122.
- Wang, H., Fu, B., Xi, J., Hu, H.-Y., Liang, P., Huang, X., & Zhang, X. (2019). Remediation of simulated malodorous surface water by columnar air-cathode microbial fuel cells. *Science of the total environment*, 687, 287-296.
- Wang, S.-S., Sharif, H. M. A., Cheng, H.-Y., & Wang, A.-J. (2019). Bioelectrochemical System Integrated with Photocatalysis: Principle and Prospect in Wastewater Treatment. In *Bioelectrochemistry Stimulated Environmental Remediation* (pp. 227-244): Springer.
- Wang, T., Zhu, G., Li, C., Zhou, M., Wang, R., & Li, J. (2020). Anaerobic digestion of sludge filtrate using anaerobic baffled reactor assisted by symbionts of short chain fatty acid-oxidation syntrophs and exoelectrogens: Pilot-scale verification. *Water research*, 170, 115329.
- Wang, V. B., Sivakumar, K., Yang, L., Zhang, Q., Kjelleberg, S., Loo, S. C. J., & Cao, B. (2015). Metabolite-enabled mutualistic interaction between *Shewanella oneidensis* and *Escherichia coli* in a co-culture using an electrode as electron acceptor. *Scientific reports*, 5, 11222.
- Wang, W., Yao, H., & Yue, L. (2020). Supported-catalyst CuO/AC with reduced cost and enhanced activity for the degradation of heavy oil refinery wastewater by catalytic ozonation process. *Environmental Science Pollution Research*, 27(7), 7199-7210.
- Wang, Y., Wang, H., Woldu, A. R., Zhang, X., & He, T. (2019). Optimization of charge behavior in nanoporous CuBi₂O₄ photocathode for photoelectrochemical reduction of CO₂. *Catalysis Today*, 335, 388-394.
- Ward, A. C., Connolly, P., & Tucker, N. P. (2014). *Pseudomonas aeruginosa* can be detected in a polymicrobial competition model using impedance spectroscopy with a novel biosensor. *PLoS one*, 9(3), e91732.
- Wei, Y., Jin, Y., & Zhang, W. (2020). Treatment of High-Concentration Wastewater from an Oil and Gas Field via a Paired Sequencing Batch and Ceramic Membrane Reactor. *International journal of environmental research public health*, 17(6), 1953.
- Werkneh, A. A., Beyene, H. D., & Osunkunle, A. A. (2019). Recent advances in brewery wastewater treatment; approaches for water reuse and energy recovery: a review. *Environmental Sustainability*, 1-11.
- Williams, E. A., Raimi, M., Yarwamara, E. I., & Modupe, O. (2019). Renewable Energy Sources for the Present and Future: An Alternative Power Supply for Nigeria. *Ebuefe Abinotami Williams, Raimi Morufu Olalekan, Ebuefe Ibim Yarwamara Oshatunberu Modupe Renewable Energy Sources for the Present Future: An Alternative Power Supply for Nigeria. Energy Earth Science*, 2(2).

- Wu, D., Sun, F., Chua, F. J. D., Lu, D., Stuckey, D. C., & Zhou, Y. (2019). In-situ power generation and nutrients recovery from waste activated sludge—Long-term performance and system optimization. *Chemical Engineering Journal*, *361*, 1207-1214.
- Wu, D., Sun, F., Chua, F. J. D., & Zhou, Y. (2020). Enhanced power generation in microbial fuel cell by an agonist of electroactive biofilm—Sulfamethoxazole. *Chemical Engineering Journal*, *384*, 123238.
- Xia, T., Zhang, X., Wang, H., Zhang, Y., Gao, Y., Bian, C., . . . Xu, P. (2019). Power generation and microbial community analysis in microbial fuel cells: A promising system to treat organic acid fermentation wastewater. *Bioresource technology*, *284*, 72-79.
- Xiao, N., Wu, R., Huang, J. J., & Selvaganapathy, P. R. (2020). Anode surface modification regulates biofilm community population and the performance of micro-MFC based biochemical oxygen demand sensor. *Chemical Engineering Science*, 115691.
- Xin, S., Shen, J., Liu, G., Chen, Q., Xiao, Z., Zhang, G., & Xin, Y. (2020). Electricity generation and microbial community of single-chamber microbial fuel cells in response to Cu₂O nanoparticles/reduced graphene oxide as cathode catalyst. *Chemical Engineering Journal*, *380*, 122446.
- Xu, H., Ithisuphalap, K., Li, Y., Mukherjee, S., Lattimer, J., Soloveichik, G., & Wu, G. (2020). Electrochemical ammonia synthesis through N₂ and H₂O under ambient conditions: Theory, practices, and challenges for catalysts and electrolytes. *Nano Energy*, *69*, 104469.
- Xu, P. (2020). Analytical solution for a hybrid Logistic-Monod cell growth model in batch and continuous stirred tank reactor culture. *Biotechnology bioengineering*, *117*(3), 873-878.
- Xue, S., Song, J., Wang, X., Shang, Z., Sheng, C., Li, C., . . . Liu, J. (2020). A systematic comparison of biogas development and related policies between China and Europe and corresponding insights. *Renewable Sustainable Energy Reviews*, *117*, 109474.
- Yadav, S., & Chandra, R. (2015). Syntrophic co-culture of *Bacillus subtilis* and *Klebsiella pneumoniae* for degradation of kraft lignin discharged from rayon grade pulp industry. *Journal of Environmental Sciences*, *33*, 229-238.
- Yan, Y., Li, T., Zhou, L., Tian, L., Yan, X., Liao, C., . . . Wang, X. (2020). Spatially heterogeneous propionate conversion towards electricity in bioelectrochemical systems. *Journal of Power Sources*, *449*, 227557.
- Yang, G., Wang, J., Zhang, H., Jia, H., Zhang, Y., Cui, Z., & Gao, F. (2019). Maximizing energy recovery from homeostasis in microbial fuel cell by synergistic conversion of short-chain volatile fatty acid. *Bioresource Technology Reports*, *7*, 100200.

- Yang, Y., Jiang, J., Liu, X., & Si, Y. (2020). Effect of sulfonamides on the electricity generation by *Shewanella putrefaciens* in microbial fuel cells. *Environmental Progress Sustainable Energy*, e13436.
- Yang, Z., & Yang, A. (2020). Modelling the impact of operating mode and electron transfer mechanism in microbial fuel cells with two-species anodic biofilm. *Biochemical Engineering Journal*, 107560.
- Yao, Y., Huang, G., An, C., Chen, X., Zhang, P., Xin, X., . . . Agnew, J. (2020). Anaerobic digestion of livestock manure in cold regions: Technological advancements and global impacts. *Renewable Sustainable Energy Reviews*, 119, 109494.
- Yasri, N., Roberts, E. P., & Gunasekaran, S. (2019). The electrochemical perspective of bioelectrocatalytic activities in microbial electrolysis and microbial fuel cells. *Energy Reports*, 5, 1116-1136.
- Yasri, N., Roberts, E. P., & Gunasekaran, S. (2019). *Energy Reports*.
- Ye, Y., Ngo, H. H., Guo, W., Chang, S. W., Nguyen, D. D., Liu, Y., . . . Wang, J. (2019). Effect of organic loading rate on the recovery of nutrients and energy in a dual-chamber microbial fuel cell. *Bioresource technology*, 281, 367-373.
- Yin, Z., Zhu, L., Li, S., Hu, T., Chu, R., Mo, F., . . . Li, B. (2020). A comprehensive review on cultivation and harvesting of microalgae for biodiesel production: Environmental pollution control and future directions. *Bioresource technology*, 301, 122804.
- You, J. (2016). *Waste and wastewater clean-up using microbial fuel cells*. University of the West of England,
- You, J., Deng, Y., Chen, H., Ye, J., Zhang, S., & Zhao, J. (2020). Enhancement of gaseous o-xylene degradation in a microbial fuel cell by adding *Shewanella oneidensis* MR-1. *Chemosphere*, 126571.
- Yousefi, V., Mohebbi-Kalhari, D., & Samimi, A. (2019). Equivalent Electrical Circuit Modeling of Ceramic-Based Microbial Fuel Cells Using the Electrochemical Impedance Spectroscopy (EIS) Analysis. *Journal of Renewable Energy Environment*, 6(1), 21-28.
- Yousefi, V., Mohebbi-Kalhari, D., & Samimi, A. (2020). Start-up investigation of the self-assembled chitosan/montmorillonite nanocomposite over the ceramic support as a low-cost membrane for microbial fuel cell application. *International Journal of Hydrogen Energy*, 45(7), 4804-4820.
- Yu, B., Liu, C., Wang, S., Wang, W., Zhao, S., & Zhu, G. (2020). Applying constructed wetland-microbial electrochemical system to enhance NH₄⁺ removal at low temperature. *Science of the total environment*, 138017.
- Yu, J., Feng, H., Tang, L., Pang, Y., Zeng, G., Lu, Y., . . . Ye, S. (2020). Metal-free carbon materials for persulfate-based advanced oxidation process: Microstructure, property and tailoring. *Progress in Materials Science*, 111, 100654. doi:<https://doi.org/10.1016/j.pmatsci.2020.100654>

- Yu, L., Wang, P.-t., Xu, Q.-t., He, T., Oduro, G., & Lu, Y. (2019). Enhanced decolorization of methyl orange by *Bacillus* sp. strain with magnetic humic acid nanoparticles under high salt conditions. *Bioresource technology*, 288, 121535.
- Yuan, Q., Liu, B.-B., & Song, X.-L. (2020). The influences of monosaccharide structure on power generation performance. *Journal of Electroanalytical Chemistry*, 857, 113753.
- Yuan, Y., Wang, S., Liu, Y., Li, B., Wang, B., & Peng, Y. (2015). Long-term effect of pH on short-chain fatty acids accumulation and microbial community in sludge fermentation systems. *Bioresource technology*, 197, 56-63.
- Zago, M., Baricci, A., Bisello, A., Jahnke, T., Yu, H., Maric, R., . . . Casalegno, A. (2020). Experimental analysis of recoverable performance loss induced by platinum oxide formation at the polymer electrolyte membrane fuel cell cathode. *Journal of Power Sources*, 455, 227990. doi:https://doi.org/10.1016/j.jpowsour.2020.227990
- Zeppilli, M., Chouchane, H., Scardigno, L., Mahjoubi, M., Gacitua, M., Askri, R., . . . Majone, M. (2020). Bioelectrochemical vs hydrogenophilic approach for CO₂ reduction into methane and acetate. *Chemical Engineering Journal*, 125243.
- Zhang, B., Li, W., Guo, Y., Zhang, Z., Shi, W., Cui, F., . . . Tay, J. H. (2020). Microalgal-bacterial consortia: From interspecies interactions to biotechnological applications. *Renewable Sustainable Energy Reviews*, 118, 109563.
- Zhang, C., Dandu, N., Rastegar, S., Misal, S. N., Hemmat, Z., Ngo, A. T., . . . Salehi-Khojin, A. (2020). A Comparative Study of Redox Mediators for Improved Performance of Li–Oxygen Batteries. *Advanced Energy Materials*, 2000201.
- Zhang, L., Fu, G., & Zhang, Z. (2019). Electricity generation and microbial community in long-running microbial fuel cell for high-salinity mustard tuber wastewater treatment. *Bioelectrochemistry*, 126, 20-28.
- Zhang, L., Tang, S., He, F., Liu, Y., Mao, W., & Guan, Y. (2019). Highly efficient and selective capture of heavy metals by poly (acrylic acid) grafted chitosan and biochar composite for wastewater treatment. *Chemical Engineering Journal*, 378, 122215.
- Zhang, S., You, J., Chen, H., Ye, J., Cheng, Z., & Chen, J. (2020). Gaseous toluene, ethylbenzene, and xylene mixture removal in a microbial fuel cell: Performance, biofilm characteristics, and mechanisms. *Chemical Engineering Journal*, 386, 123916.
- Zhang, X.-C., & Halme, A. (1995). Modelling of a microbial fuel cell process. *Biotechnology letters*, 17(8), 809-814.
- Zhang, Y., Guo, B., Zhang, L., & Liu, Y. (2020). Key Syntrophic Partnerships Identified in a Granular Activated Carbon Amended UASB Treating Municipal Sewage under Low Temperature Conditions. *Bioresource technology*, 123556.

- Zhang, Y., Yang, W., Fu, Q., Li, J., Zhu, X., & Liao, Q. (2019). Performance optimization of microbial fuel cells using carbonaceous monolithic air-cathodes. *International Journal of Hydrogen Energy*, 44(6), 3425-3431.
- Zhao, C., Ge, R., Zhen, Y., Wang, Y., Li, Z., Shi, Y., & Chen, X. (2019). A hybrid process of coprecipitation-induced crystallization-capacitive deionization-ion exchange process for heavy metals removal from hypersaline ternary precursor wastewater. *Chemical Engineering Journal*, 378, 122136.
- Zhao, F., Heidrich, E. S., Curtis, T. P., & Dolfing, J. (2020). Understanding the complexity of wastewater: The combined impacts of carbohydrates and sulphate on the performance of bioelectrochemical systems. *Water research*, 115737.
- Zhao, J., Feng, K., Liu, S.-H., Lin, C.-W., Zhang, S., Li, S., . . . Chen, J. (2020). Kinetics of biocathodic electron transfer in a bioelectrochemical system coupled with chemical absorption for NO removal. *Chemosphere*, 249, 126095.
- Zhao, N., Ma, Z., Song, H., Xie, Y., & Wang, D. (2019). The Interaction between Electricigens and Carbon Nanotube Forest and Electricity Generation Performance in MFC. *Energy Technology*, 7(2), 188-192.
- Zhao, N., Treu, L., Angelidaki, I., & Zhang, Y. (2019). Exoelectrogenic anaerobic granular sludge for simultaneous electricity generation and wastewater treatment. *Environmental science technology*, 53(20), 12130-12140.
- Zhao, Y., Meng, L., & Shen, X. (2020). Study on ultrasonic-electrochemical treatment for difficult-to-settle slime water. *Ultrasonics Sonochemistry*, 64, 104978.
- Zheng, T., Li, J., Ji, Y., Zhang, W., Fang, Y., Xin, F., . . . Jiang, M. (2020). Progress and Prospects of Bioelectrochemical Systems: Electron Transfer and Its Applications in the Microbial Metabolism. *Frontiers in Bioengineering Biotechnology*, 8, 10.
- Zhu, J., Song, X., Tan, W. K., Wen, Y., Gao, Z., Ong, C. N., . . . Li, J. (2020). Chemical Modification of Biomass Okara Using Poly (acrylic acid) through Free-radical Graft Polymerization. *Journal of Agricultural Food Chemistry*.
- Zhuang, Z., Yang, G., Mai, Q., Guo, J., Liu, X., & Zhuang, L. (2020). Physiological potential of extracellular polysaccharide in promoting *Geobacter* biofilm formation and extracellular electron transfer. *Science of the total environment*, 140365.
- Zou, L., Qiao, Y., Zhong, C., & Li, C. M. (2017). Enabling fast electron transfer through both bacterial outer-membrane redox centers and endogenous electron mediators by polyaniline hybridized large-mesoporous carbon anode for high-performance microbial fuel cells. *Electrochimica Acta*, 229, 31-38.

APPENDIX A
COLONY FORMING UNIT AND SEM

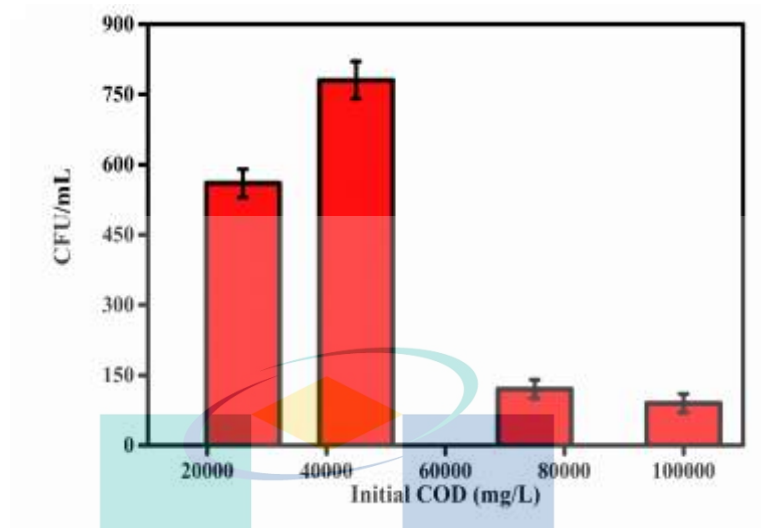


Figure A1 CFU/mL vs. initial COD (mg/L) of PCW at day 7

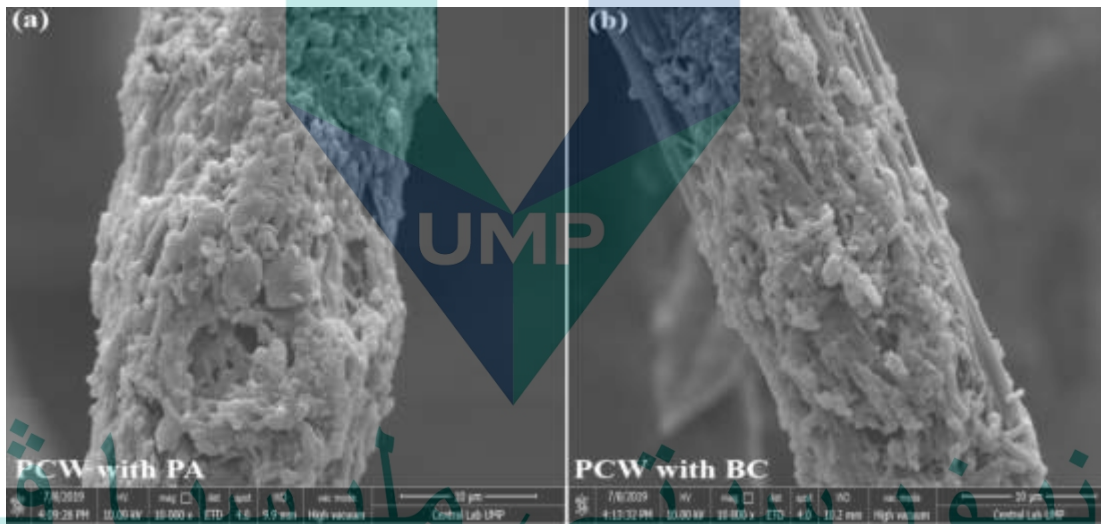


Figure A2 SEM of a) PCW with PA, and b) PCW with BC

**APPENDIX B
PHYLOGENETIC TREE**

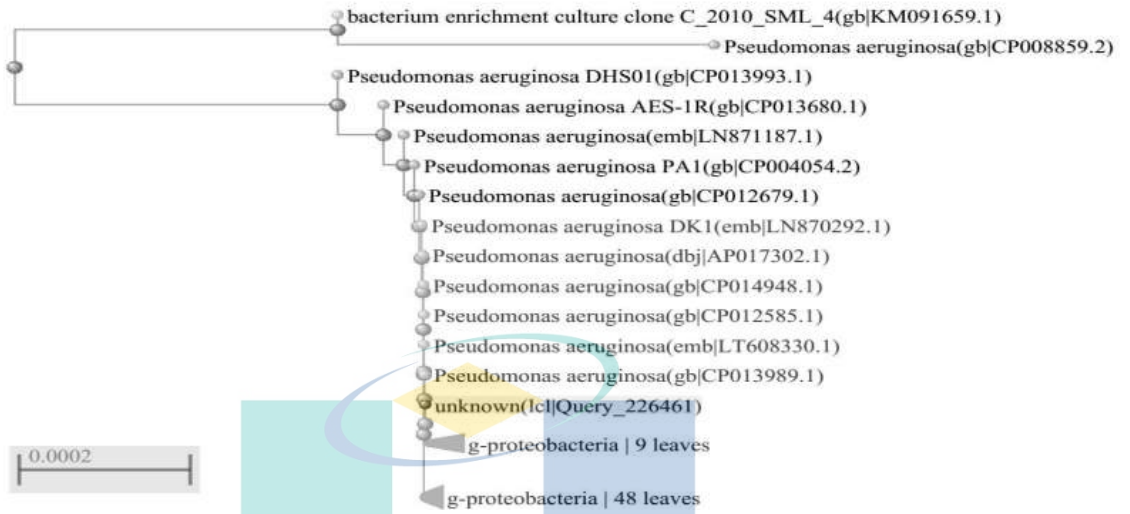


Figure B1 Phylogenetic tree of PA (*Pseudomonas aeruginosa*)

Source: Islam et al., (2018)

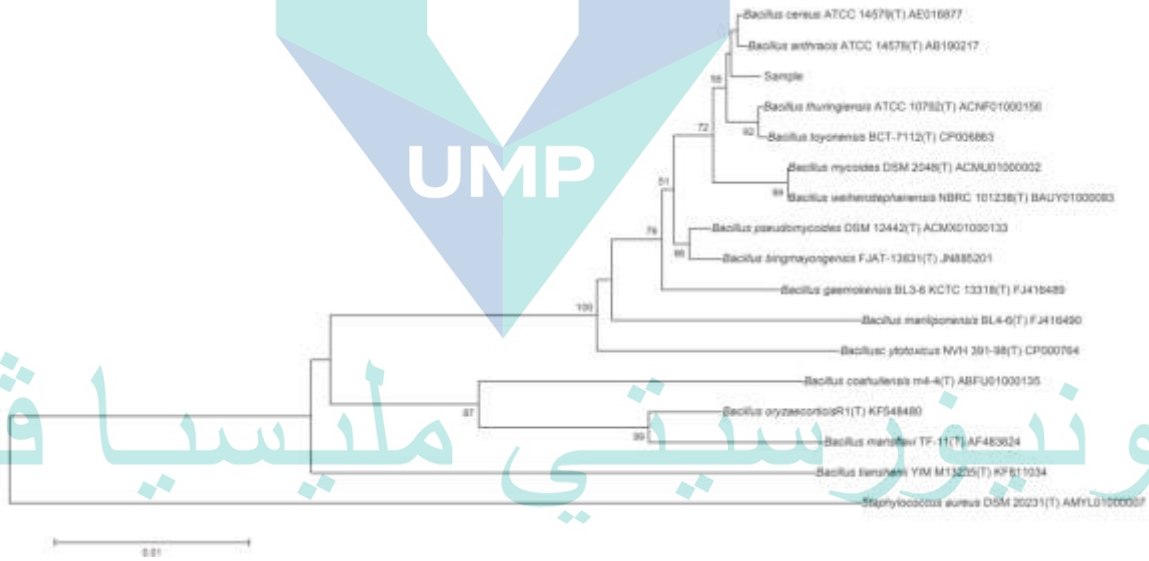


Figure B2 Phylogenetic tree of BC (*Bacillus cereus*)

Source: Islam, Ethiraj, et al., (2017)

**APPENDIX C
EIS AND BODE PLOT**

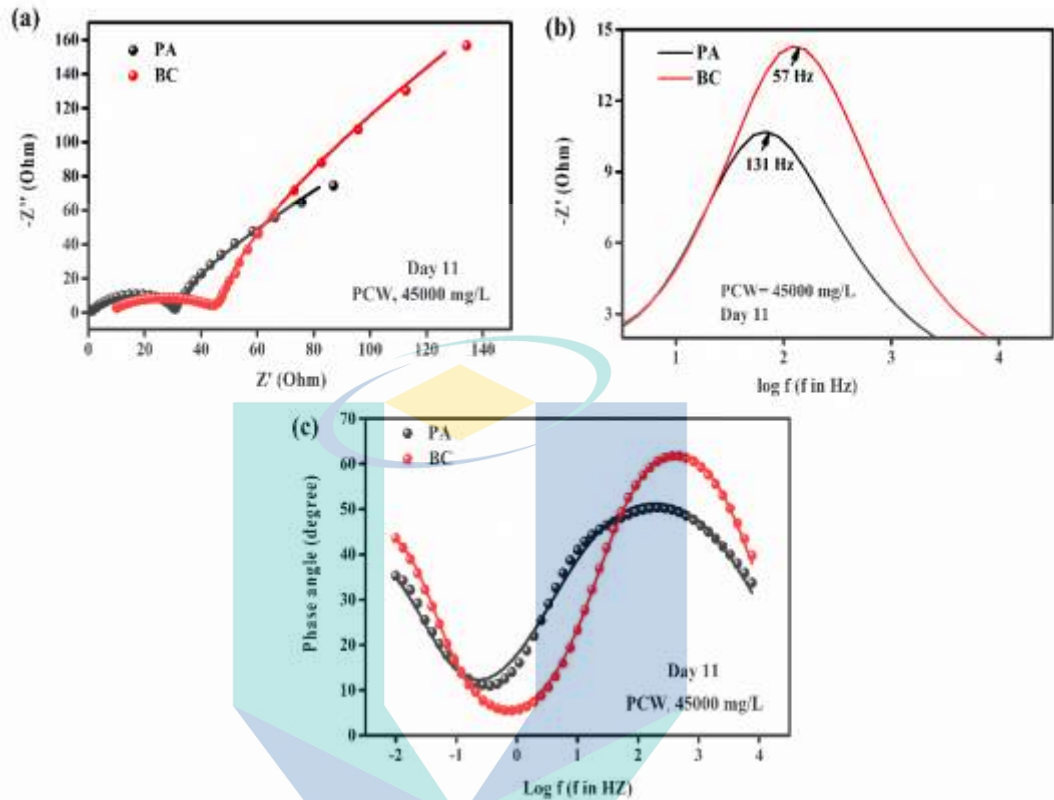


Figure C1 11 a) EIS, b) log vs. $-Z'$ and c) log f vs. phase angle using PA and BC at day 11

اونيورسيتي ملايسيا قهغ
UNIVERSITI MALAYSIA PAHANG

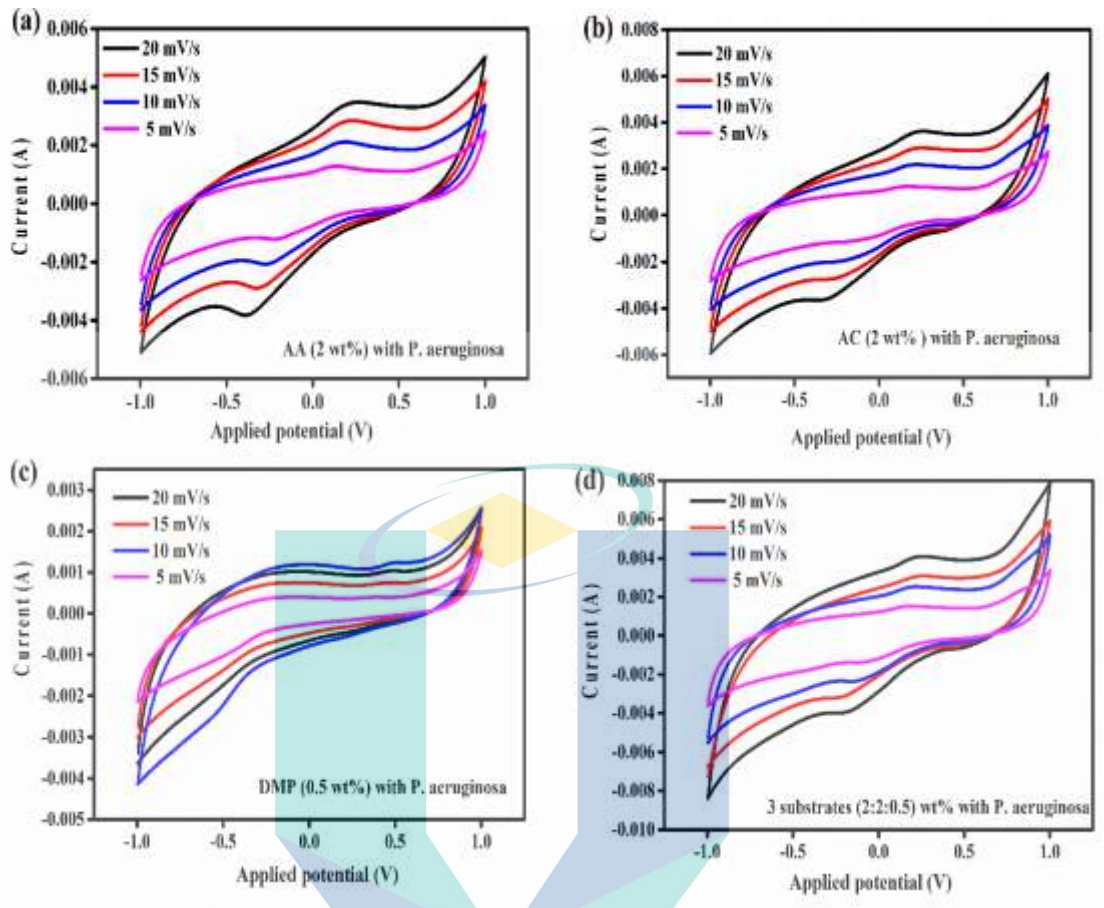


Figure C2 Cyclic voltammetry using different substrates and PA

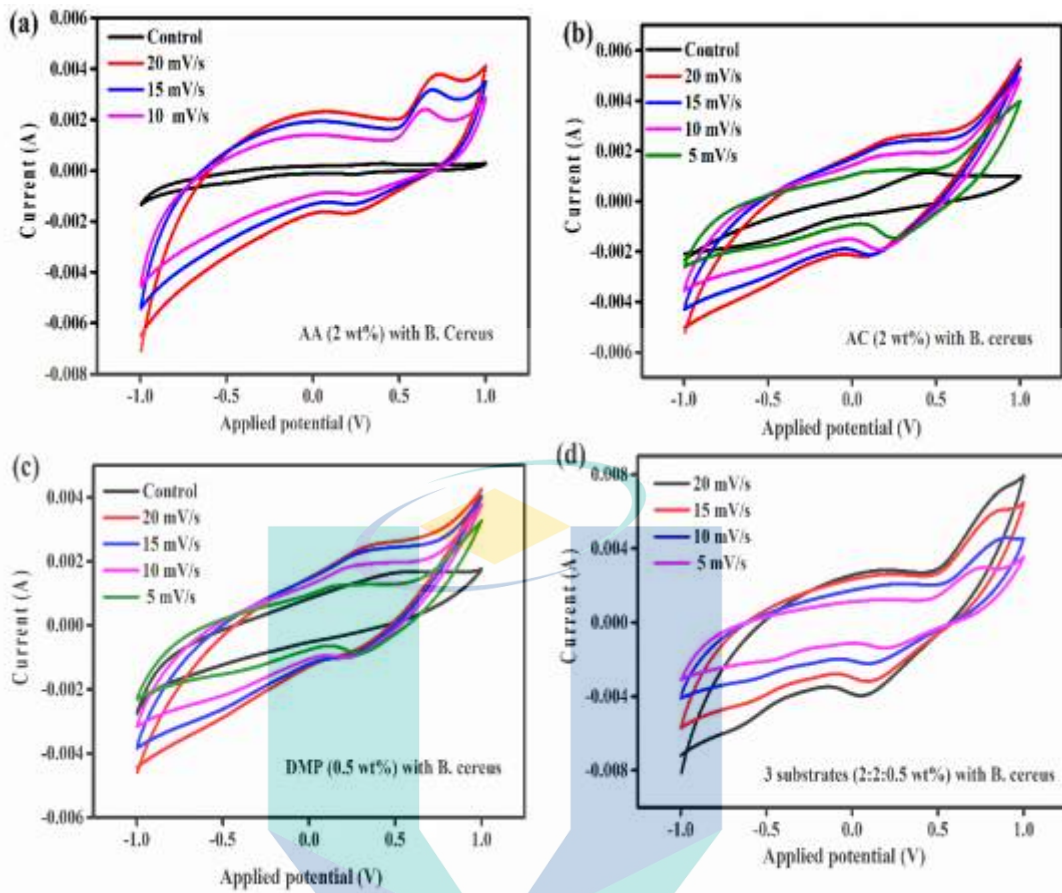


Figure C3 Cyclic voltammetry using different substrates and BC

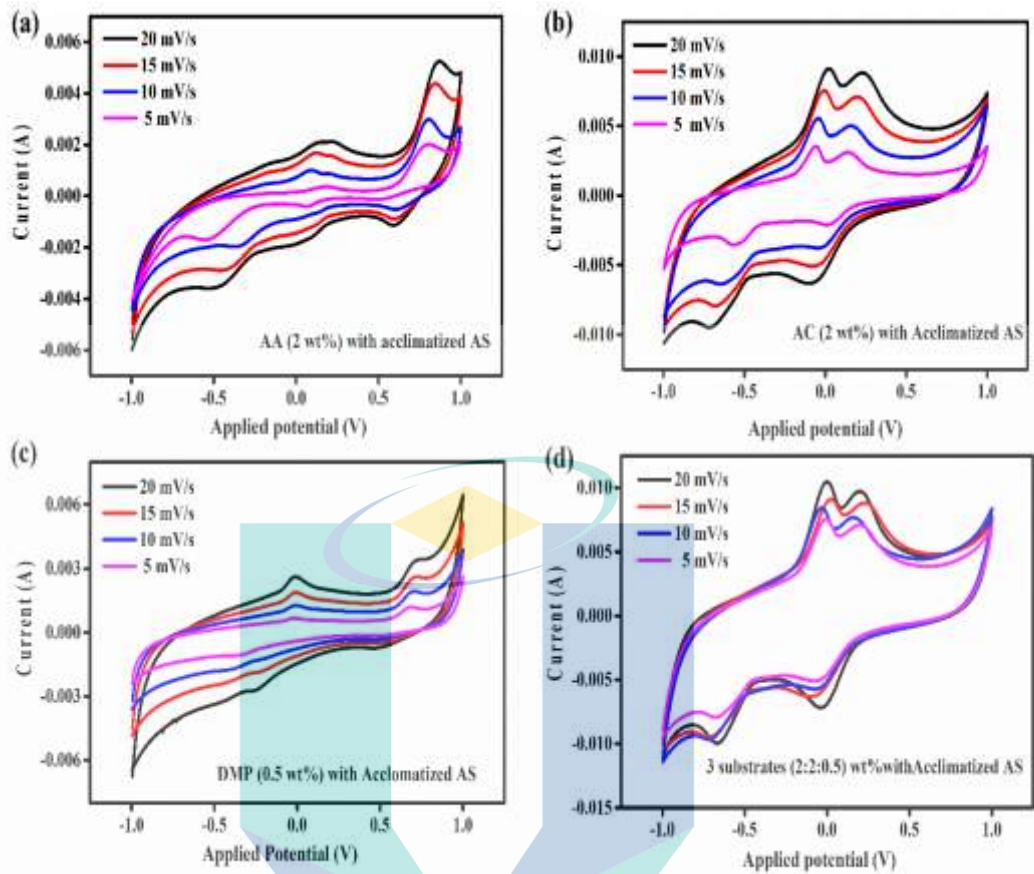


Figure C4 Cyclic voltammetry of PCW (45000 mg/L) using PA and BC

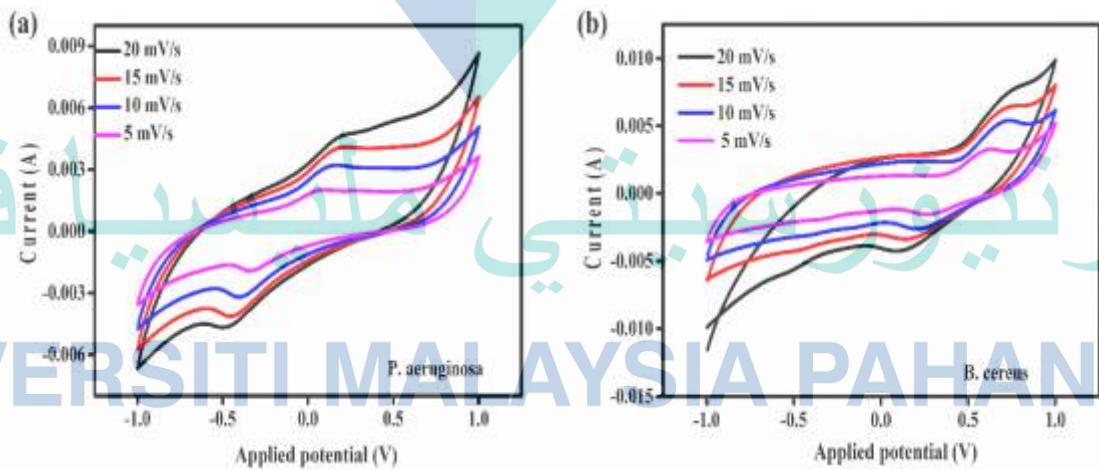


Figure C5 Cyclic voltammetry of PCW (45000 mg/L) using PA and BC

APPENDIX D
HPLC OF DIFFERENT SUBSTRATES

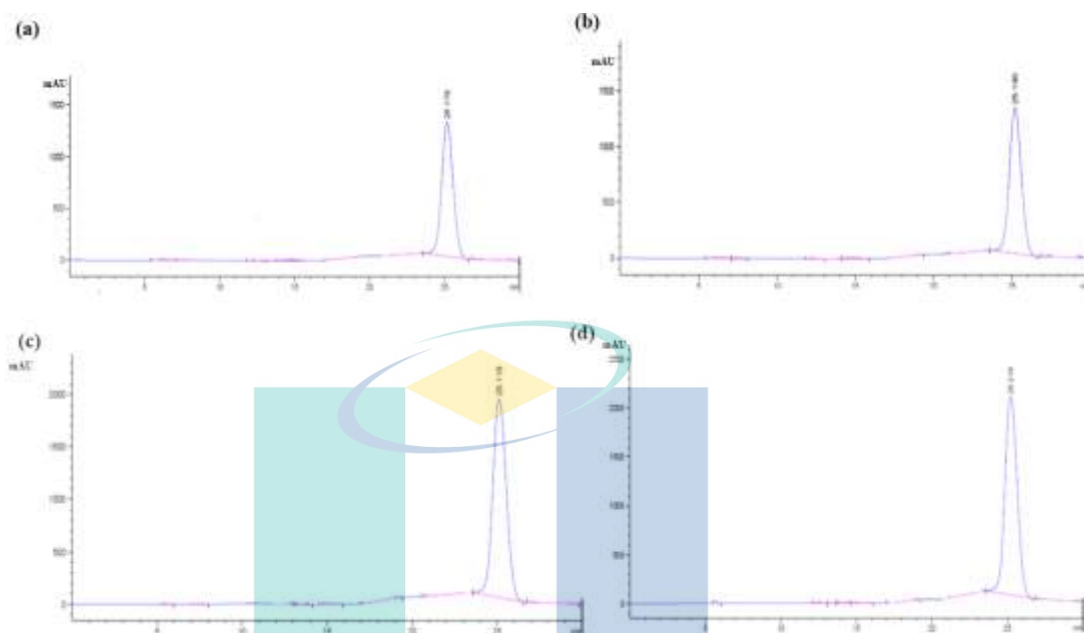


Figure D1 HPLC of AA using a concentration of a) 0.4 μL , b) 0.6 μL , c) 0.8 μL and d) 1 mL.

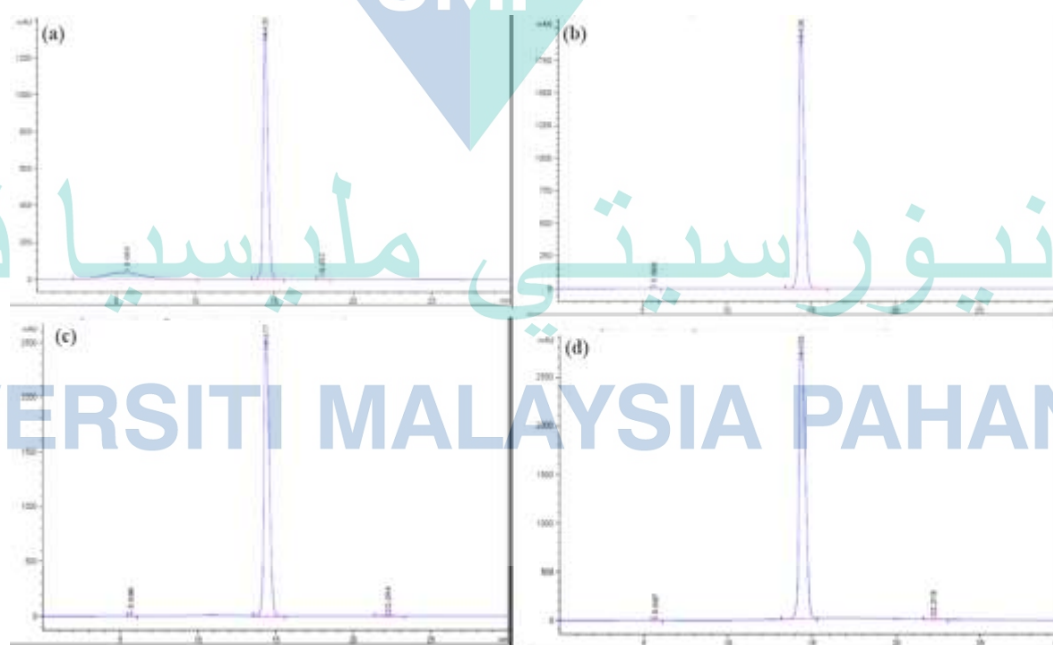


Figure D2 HPLC of ACA using a concentration of a) 0.4 μL , b) 0.6 μL , c) 0.8 μL and d) 1 mL.

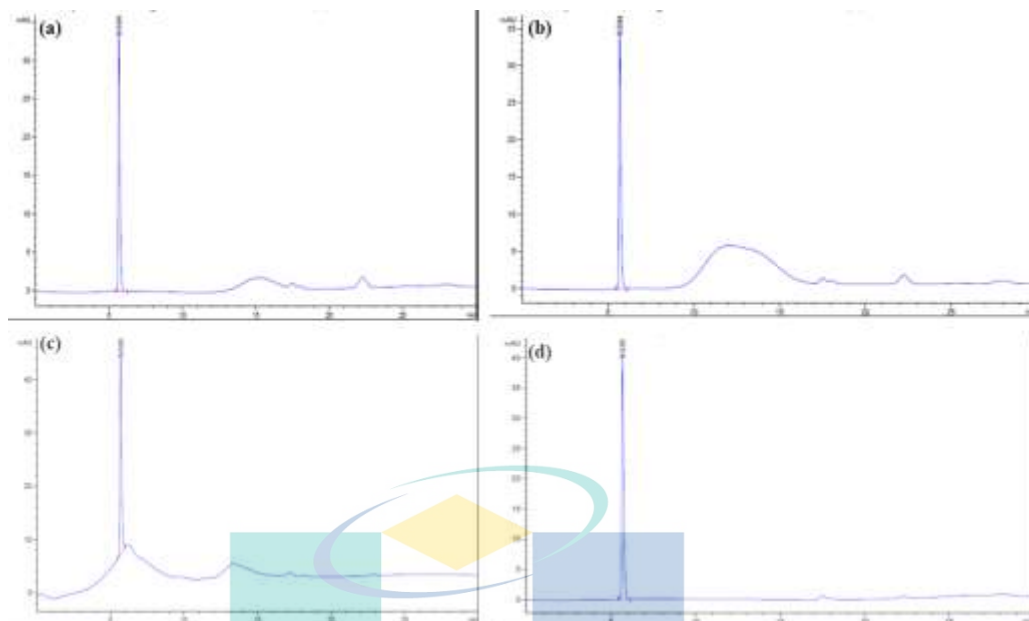


Figure D3 HPLC of DMP using a concentration of a) 0.4 μ L, b) 0.6 μ L, c) 0.8 μ L and d) 1 mL.

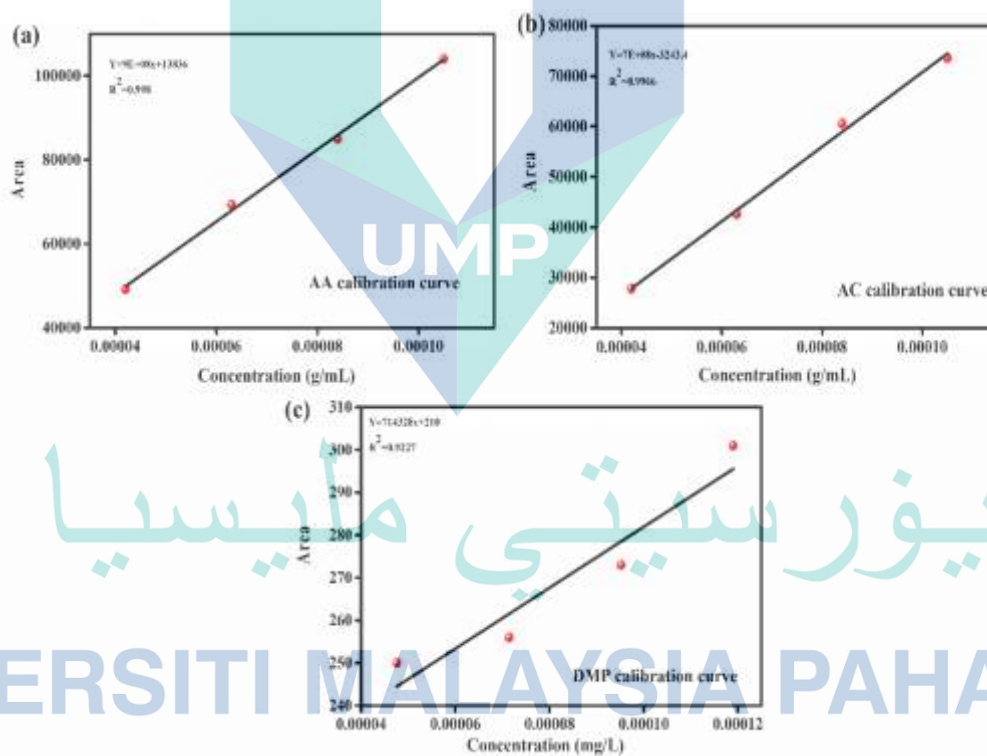


Figure D4 Calibration curve from HPLC using a) AA, b) ACA, and c) DMP.

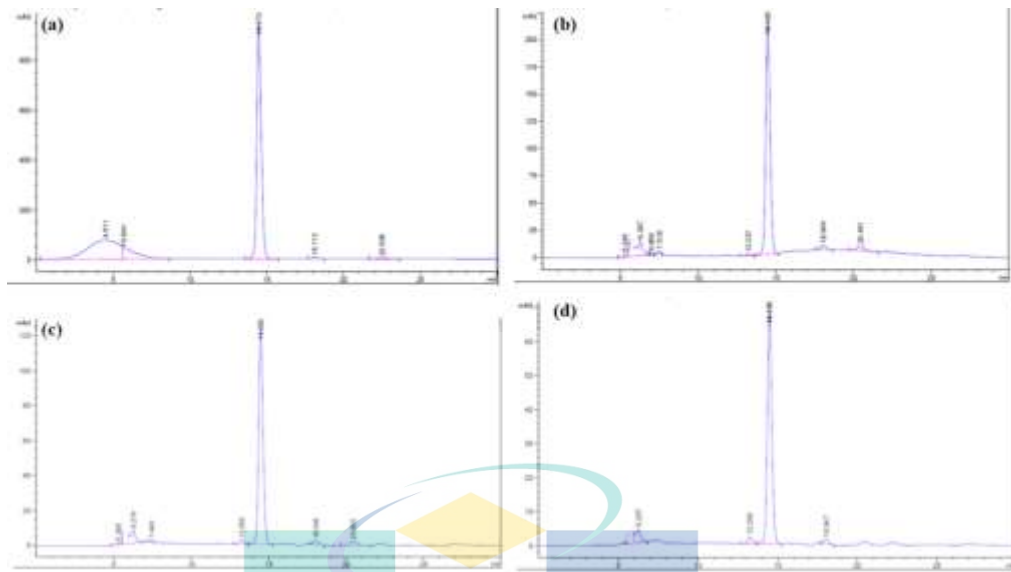


Figure D5 HPLC of Acetic acid (ACA) fed MFC at a) day 5, b) day 8, c) day 11 and d) day 16 respectively.

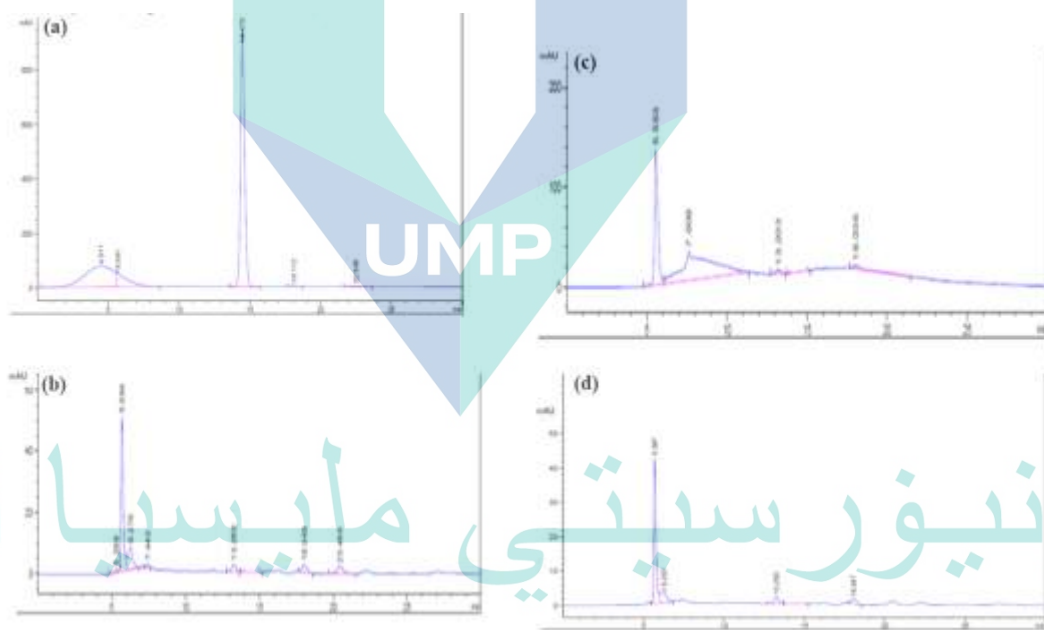


Figure D6 HPLC of dimethyl pthalate (DMP) fed MFC at a) day 5, b) day 8, c) day 11 and d) day 16 respectively.

اونیورسیتی ملیسیا قهق
 UNIVERSITI MALAYSIA PAHANG

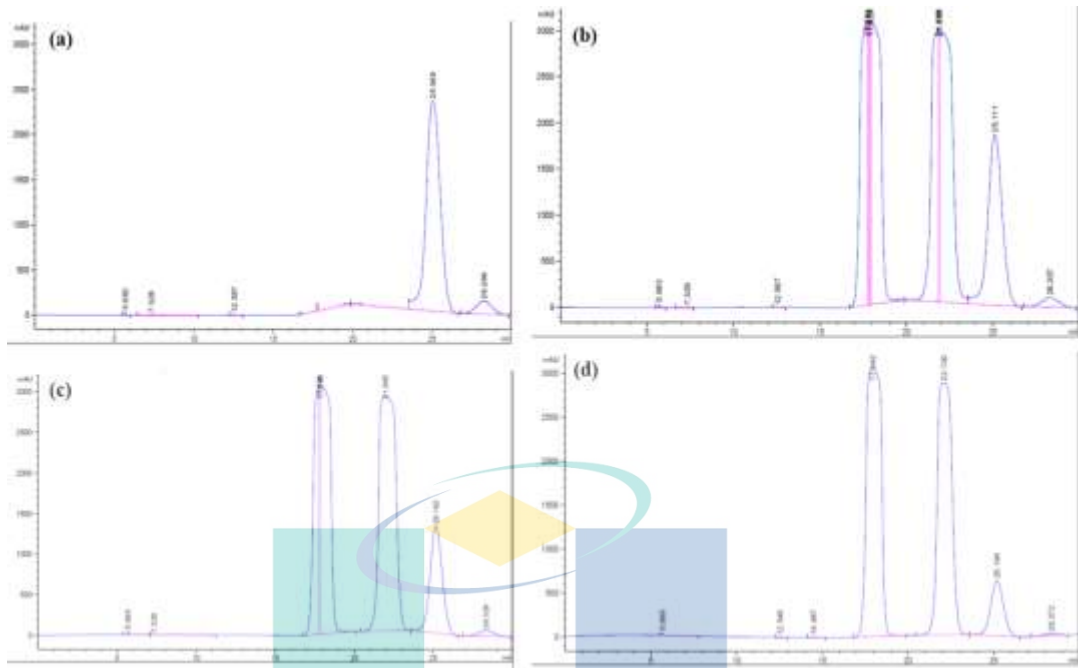


Figure D7 HPLC of Acrylic acid (AA) fed MFC at a) day 5, b) day 8, c) day 11 and d) day 16 respectively.

UMP

اونيورسيتي ملايسيا قهغ

UNIVERSITI MALAYSIA PAHANG

LIST OF PUBLICATIONS

1. **Sumaya Sarmin**, Baranitharan Ethiraj, M. Amirul Islam, Asmida Ideris, Chin Sim Yee, Md. Maksudur Rahman Khan: Bio-electrochemical power generation in petrochemical wastewater fed microbial fuel cell. *Science of the Total Environment*. 2019, 695, 133820
 2. **Sumaya Sarmin**, Asmida Binti Ideris, Chin Sim Yee, Chin Kui Cheng, Md. Maksudur Rahman Khan. Performance evaluation of petrochemical wastewater fed air-cathode microbial fuel cells using yeast biocatalysts. *Journal of Chemical Engineering and Industrial Biotechnology*. 2018, V (4), 32-42.
 3. Turga Devi Munusamy, **Sumaya Sarmin**, Huei Ruey Ong, Wei Teng Gan, Chi Shein Hong, Maksudur R. Khan. Catalytic performance and antimicrobial activity of $Mg(OH)_2/MgO$ colloidal nanoparticles in alkyl resin nanocomposite derived from palm oil. *Polymer Bulletin*, 2019, 1-16.
 4. **Sumaya Sarmin**, Asmida Ideris, Baranitharan Ethiraj. M. Amirul Islam, Chin Sim Yee and Md. Maksudur Rahman Khan. Potentiality of petrochemical wastewater as substrate in microbial fuel cell. *IOP Conference Series: Materials Science and Engineering*. Revised Version submitted.
 5. Mostafa Tarek, Kaykobad Md. Rezaul Karim, **Sumaya Sarmin**, Huei Ruey Ong, Hamidah Abdullah and Md. Maksudur Rahman Khan. Photoelectrochemical activity of $CuO-CdS$ heterostructured catalyst for CO_2 reduction. *IOP Conference Series: Materials Science and Engineering*. Revised Version Submitted.
-
1. **Silver Medal** from ITEX-2018 Organized by 29th International Invention, Innovation and Technology Exhibition 2018, Kuala Lumpur, Malaysia for invention title: Bioresin from crude palm oil.